A framework for assessing the CO_2 mitigation options for the electricity generation sub-sector

by

Colin F. Alie

A thesis
presented to the University of Waterloo
in fulfilment of the
thesis requirement for the degree of
Doctor of Philosophy
in
Chemical Engineering

Waterloo, Ontario, Canada, 2013

I hereby declare that I am the sole author of this thesis. This is a true copy of the thesis, including any required final revisions, as accepted by my examiners.

I understand that my thesis may be made electronically available to the public.

Abstract

Carbon capture and storage is a key technology for limiting global warming to 2C above historical levels and, thereby, avoiding the worst impacts of climate change.[24, 5] In particular, CCS (Carbon Capture and Storage) is one of the few alternatives for large-scale reductions within the power generating sector. The pace of CCS deployment in the electricity generation sector is slower than would be dictated by environmental concerns and this is attributed to CCS's relatively high capital and operating costs and the impact that this has on the *CoE* (Cost of Electricity). CCS is an active area of research with most of the focus being on reducing the capture costs with *CoE* and *CCA* (Cost of CO_2 Avoided) being the metric of choice.

Techno-economic assessments of CCS normally disregard the operation of the electricity system in which CCS is targeted. Generic assumptions are made with respect to the performance (*e.g.*, heat rate, capacity factor) of units fitted with CCS with little or no validation and despite the fact that *CCA* is highly sensitive to the values selected for these parameters. Additionally, the use of *CoE* as a key performance metric may lead to suboptimal conclusions since the average electricity *price* is likely of greater interest to electricity market participants and it is not certain that cost is a good proxy for price. It is proposed that in order to effectively assess the performance of GHG (Greenhouse Gas) mitigation strategies in general, and CCS in particular, one needs to explicitly consider the operation of the target electricity system. The primary objective of this work is to develop and describe an approach for evaluating GHG mitigation strategies that considers the detailed operation of the electricity system in question and to ascertain whether considering the detailed operation of the electricity system affects the assessment of the effectiveness of the GHG mitigation strategy.

It is also typically assumed that generating units with CCS operate at full load with a constant CO_2 recovery. It is normal for the dispatch of generating units to vary with time in an effort on the part of system operators to optimally meet electricity demand. It may be the case that generating units with flexible CO_2 capture may be able experience better performance than units without this flexibility by independently varying production electricity and CO_2 to match the instantaneous demand for these commodities. A secondary objective of this work is to evaluate the potential benefit of flexible CO_2 capture and storage.

An electricity system simulator is developed; it is based upon a deregulated electricity system containing markets for both real and reserve power, with consumers that are price-insensitive, generators that bid their units' power at the marginal cost of generating, and a system operator that provides hourly dispatch instructions seeking to maximize social welfare while respecting the physical constraints of the units and transmission system. Using the IEEE RTS '96 (IEEE One-Area Reliability Test System — 1996) as a test case, the performance of the electricity system is benchmarked with GHG regulation in the form of a carbon tax at \$15, \$40, and \$100/tonne CO_2. Two different implementations of CO_2

capture are added to the electricity system — with fixed CO_2 capture and with flexible CO_2 capture — and the impact of having CCS is assessed.

In techno-economic assessments of generating units with CCS, it is typical to use the design heat rate at 100% load and a constant capacity factor of 0.85 or greater. In contrast, the average heat rate observed changes from scenario to scenario and also varied, in each scenario, depending upon the stringency of GHG regulation. Variations of 2% in thermal efficiency are observed from one case to another. Additionally, capacity factor varies from one generating unit to the other, changes as a function of CO_2 price, and is often found to be considerably less than 0.85. Capacity factor also is also significantly different between the scenario with fixed CO_2 capture versus the one where the generating unit with CCS is flexible. Finally, while directionally the response of cost of electricity and price to, for example, increasing GHG regulation are (mostly, but not always) in sync, the relative magnitude of the response can be significantly different.

The results of this work, some of which is noted above, support the notion that the assessment of GHG mitigation strategies for the electricity generation subsector should consider the detailed operation of the electricity system in question. Historical performance of a generating unit is not necessarily a good indicator of future performance once GHG mitigation is imposed or GHG mitigation strategies introduced. Cost of generation alone is not necessarily a good indicator of economic impact; obtaining an estimate of the impact on electricity price is important to ensure that the economic impact on consumers and producers is properly understood.

The scenarios with CCS reveal that CCS is an effective GHG mitigation strategy: adding CCS at a single generating unit reduced GHG emissions and moderated the economic impact of GHG regulation relative to the cases where CCS is not present. When the generating unit's CCS process is flexible, the generating unit participates preferentially in the reserve market enabling it to increase its net energy benefit. The conclusion is that there is a significant potential advantage to generating units with flexible CCS processes and the flexibility of existing and novel CCS process should be an assessment and design criterion, respectively.

Understanding the impact of CCS on the operation of an electricity system triggered the development of a reduced-order model of a coal-fired generating unit with flexible CO_2 capture and the integration of this into the MINLP (Mixed-Interger Non-Linear Programming) formulation of an economic dispatch model. Both of these efforts, not observed previously in the literature, constitute an important contribution of the work as the methodology provides a template for future assessment of CCS and other electricity mitigation strategies in the electricity generation sector. The demonstration that a reduced-order model representing the the Pareto optimal frontier of the generating unit — as opposed to the entire feasible operating space — is sufficient for assessing the performance of CCS will reduce the effort required to undertake similar technology assessments in the future.

Regulation of GHG emissions coupled with the deployment of CCS can effectively reduce the emissions of an electricity system. From an economic perspective, CCS moderated the economic impact of GHG regulation to electricity consumers while increasing the net energy benefit of the unit at which CCS is deployed. In particular, generating units with CCS that are *flexible* seem to accrue additional benefits as compared to those units that aren't flexible and the development of novel CCS processes with optimal operability is a suggested area of future research activity.

Contents

List of Tables

List of Figures

List of Acronyms and Abbreviations

AC	Alternating Current
AMP	2-amino-2-methyl-1-propanol
ANOVA	Analysis of Variance
BARON	Brand And Reduce Optimization Navigator
BAU	Business As Usual
CCA	Cost of CO_2 Avoided
CCS	Carbon Capture and Storage
CoE	Cost of Electricity
DC	Direct Current
DEA	Diethanolamine
DG	Distributed Generation
DICOPT	DIscrete and Continuous OPTimizer
ECBM	Enhanced Coal-Bed Methane
EOR	Enhanced Oil Recovery
FGD	Flue Gas Desulphurization
FOM	Fixed Operating and Maintenance
GAMS	General Algebraic Modelling System
GHG	Greenhouse Gas

GT .... Gas Turbine

HEP .... Hourly Electricity Price

IEA .... International Energy Agency

IESO .... Independent Electricity System Operator

IGCC .... Integrated Gasification Combined Cycle

IHR .... Incremental Heat Rate

IP/LP .... Intermediate Pressure/Low Pressure

KEPCO ...... Kansai Electric Power Company Inc.

KP .... Kansai packing

KS .... Kansai solvent

LFE .... Large Final Emitter

LP .... Linear Programming

LULUCF ..... Land Use, Land Use Change, and Forestry

MARKAL .... MARKet ALlocation

MCR .... Maximum Continuous Rating

MDEA .... methyldiethanolamine

MEA .... monoethanolamine

MEA .... monoethanolamine

MHI .... Mitsubishi Heavy Industries Ltd.

MILP .... Mixed-Interger Linear Programming

MINLP .... Mixed-Interger Non-Linear Programming

MIP .... Mixed-Interger Programming

N/A .... Not Applicable/Available

NEM .... National Electricity Market

NERC .... North American Electric Reliability Corporation

NGCC .... Natural Gas Combined Cycle

NLP .... Non-Linear Programming

OPF .... Optimal Power Flow

OPG .... Ontario Power Generation

PC .... Pulverized Coal

PCC .... Post-Combustion Capture

PSAT .... Power System Analysis Toolbox

RHS .... Right-Hand Side

RMINLP ..... Relaxed Mixed-Interger Non-Linear Programming

IEEE RTS '96 IEEE One-Area Reliability Test System — 1996

SGER......... Specified Gas Emitters Regulation

SQP .... Sequential Quadratic Programming

SRMC .... Short-Run Marginal Cost

UOM .... Unit Operation Model

VOM .... Variable Operating and Maintenance

Nomenclature

Variables

a	unit availability factor
B/F	liquid ratio of "bottoms" stream to "feed" stream in a distillation column
B	susceptance
$\dot{C}$	annual cost, \$/year
CCC	Cost of CO_2 Capture, \$/tonne CO_2
C	cost, *e.g.*, \$, \$/MWh$_e$
$CAPEX$	capital cost per unit capacity, \$/MW$_e$
CCA	cost of CO_2 avoided, \$/tonne CO_2
CEI	CO_2 emissions intensity, tonne CO_2/MWh$_e$
CF	capacity factor
CoE	cost of electricity, \$/MWh$_e$
d	diameter, *e.g.*, metres
$\dot{E}$	rate of energy inflow, *e.g.*, MMBtu/h
E	electric energy, MWh$_e$
FA	approach to flooding
F	molar flow rate
FCF	for a given interest rate, i, and total number of payments, N, the annuity as fraction of the present value that must be paid to reduce the future value to zero, \$/year

G	conductance
g	annual rate of decline
HR	heat rate, But/kWh$_e$
h	height, *e.g.*, metres
HV	energy content of fuel, kJ/kg
IHR	incremental heat rate, Btu/kWh$_e$
I	current, *e.g.*, A
L_1/D	reflux ratio in a distillation column
$\dot{m}$	mass flow rate
MCR	Maximum continuous rating of a transmission line, *e.g.*, MVA
m	power system reserve margin
N	number
n	transformer off-nominal voltage ratio
ΔP	pressure drop, *e.g.*, kPa
ΔP^S	ramp rate for discrete units, *e.g.*, MW$_e$/min
P	pressure, *e.g.*, kPa
P	real power
P_{out}/P_{in}	ratio of outlet pressure to inlet pressure across the turbine
$\Delta\dot{q}$	ramp rate for continuous units, *e.g.*, MW$_{th}$/min
$\dot{Q}$	heat duty, *e.g.*, MW$_{th}$
$\dot{q}$	heat input to boiler, MMBtu/h
Q	reactive power, *e.g.*, MVAr
RM	reserve market power, *e.g.*, MW$_e$
R	resistance
r	discount rate

S	apparent power flow, *e.g.*, MVA
TAX	emissions levy, \$ per unit mass emitted
TCR	total capital recovery, \$
TS	tray spacing, *e.g.*, metres
T	temperature, *e.g.*, °C
u	state of generating unit with respect to start-up (*i.e.*, one if the unit started-up in the time period and zero otherwise
UHR	unit heat rate, Btu/kWh$_e$
$import$	pertaining to electricity imported from outside the grid
VOM_e	generator variable operating and maintenance costs (excluding fuel), \$/MWh$_e$
V	voltage, *e.g.*, V
x^{off}	number of time periods that generating unit has been off
x^{on}	number of time periods that generating unit has been on
X	installed capacity, MW$_e$
X	reactance
x	fraction recovered or extracted
x	load factor
y	power plant de-rate as a fraction of plant capacity
y	quantity of bid that is accepted into the market, MWh$_e$
Y	admittance, *e.g.*, Ω
z	value of objective function
Z	impedance

Greek

α	lean solvent loading, mol solute/mol solvent
η	efficiency

ρ	dummy variable used in the exact linearization of constraints with terms $P^R \cdot \omega$
ρ	price of electricity, \$/MWh$_e$
τ	length of time, hours
θ	length of power demand block, hours
θ	phase angle, *e.g.*, rad
ω	state of generating unit (*i.e.*, one if the unit is off and zero otherwise)
χ, ψ	dummy variables used in the exact linearization of constraints with terms $x \cdot \omega$

Parameters

EI	fuel emissions intensity, lb/MMBtu
FC	fuel cost, \$/MMBtu
HI	heat input required to cold-start a unit, MMBtu
HPY	hours per year, *e.g.*, $8760h/year$
L	time period duration, *e.g.*, hours
M	parameter used for the exact linearization of terms that are the product of a binary variable and a continuous variable
MEA	unit cost of make-up solvent, \$/tonne CO_2
N_b	number of bids per generating unit
P	number of power demand blocks
P^{bid}	quantity of power bid into the market
RM_r^D	reserve power requirements
τ^{off}	minimum downtime, hours
τ^{on}	minimum uptime, hours
T	number of time periods
TS	unit cost of CO_2 transportation and storage, \$/tonne CO_2
V	vintage of the oldest operating unit in the system at $t = 0$

Superscripts

$*$	denotes complex conjugate
$*$	denotes optimal value
$*$	denotes set-point
$\circ$	pertaining to initial state
B	pertaining to imaginary part of admittance
CO_2	pertaining to CO_2
cap	pertaining to case with CO_2 capture
C	pertaining to line-charging
nocap	pertaining to generator with no CO_2 capture
D	pertaining to demand
d	pertaining to day
e	pertaining to energy
FOM	pertaining to fixed operating and maintenance component of the cost
fuel	pertaining to fuel
non-fuel	excluding fuel
G	pertaining to real part of admittance
H	pertaining to hydroelectric units
h	pertaining to hour
max	indicates maximum value
OM	pertaining to operating and maintenance component of the cost
$\prime$	pertaining to a situation where a contingency has occurred
R	pertaining to reserve market
slack	pertaining to the slack bus
start-up	pertaining to unit start-up

S	pertaining to supply
TS	pertaining to transportation and storage
up	pertaining to uptime
VOM	pertaining to variable operating and maintenance component of the cost
w	pertaining to week

Subscripts

10^{ns}	pertaining to ten-minute, non-spinning reserve market
10^{sp}	pertaining to ten-minute, spinning reserve market
30	pertaining to 30-minute, non-spinning reserve market
aux	pertaining to auxiliary turbine
CO_2	pertaining to CO_2
C	pertaining to continuous units
D	pertaining to discrete units
IM	denotes imaginary part of complex variable
k,m	index of bus
$grid$	pertaining to electricity injected into grid
net	pertaining to electricity generated net of station service
n	index of generating units
p	index of power demand block
Re	denotes real part of complex variable
r	index of reserve markets
ref	pertaining to reference case
$steam$	pertaining to Intermediate Pressure/Low Pressure extraction point
th	pertaining to heat
t	index of time period

v index of generator vintage (*i.e.*, time period corresponding to capacity addition)

Sets

j_{km} set of branches that connect buses k and m

j_{k} set of branches that terminate at bus k

N^{shunt} set of buses with shunt admittance to ground

N_k set of buses adjacent to bus k

NG set of generating units

N^{ST} set of buses with energy storage

N set of buses in the electricity system

RM set of reserve markets

Chapter 1

Introduction

1.1 Context

1.1.1 Global warming and climate change

"Global warming" describes the enhancement of the greenhouse effect due to anthropogenic emissions of greenhouse gases. The greenhouse effect is the phenomena through which the ambient temperature of the earth is maintained at comfortable levels. Solar energy is absorbed by the earth and re-emitted as infrared radiation. Greenhouse gases in the atmosphere prevent this energy from escaping into space thereby raising the terrestrial temperature above what it would otherwise be (it is estimated that the greenhouse effect is 33°C [14, p 7]).

Industrializing western civilizations demanded ever increasing quantities of energy and carbon-based fuels — wood, coal, oil, and natural gas — were, and remain, the primary sources. The harvesting and/or extraction of these fuels and their subsequent consumption have increased the abundance of greenhouse gases in the atmosphere causing global warming. There is near consensus that global warming is leading to global climate change and, unabated, could have disastrous impacts for humanity and the other inhabitants of the biosphere.

The Kyoto Protocol is a 1997 treaty[1] in which developed countries agreed to collectively reduce their annual emissions of greenhouse gases to 5.2% below the 1990 level by the first commitment period of 2008–2012.

1.1.2 GHG emissions in Canada

The Kyoto Protocol was signed by Canada's Prime Minister on April 29, 1998 and it was ratified by parliament December 12, 2002 thereby officially committing Canada to reduce

[1] The treaty didn't actually come into force until February 16th, 2005.

its GHG emissions by 6% below the emissions in 1990.[2] Under the Copenhagen Accord, Canada made a commitment in January 2010 to reduce its GHG emissions to 17% below 2005 levels by 2020.

Figure 1.1 shows Canada's actual GHG emissions from 1990 through 2011, the most recent year for which data is available. Also shown is the emissions trajectory based upon the emissions during the 1990 to 2002 time period. Since 2002, there has been a change in the rate of emissions growth and this is attributed to:[35]

- a decrease in the share of coal-fired generation,
- increased fuel efficiency in the transportation sector, and
- a structural shift in the economy away from manufacturing and toward the service sector.

Despite the change in trajectory, closing the 'gap' between 2011 emissions and the Copenhagen Accord target requires additional CO_2 mitigation of 90 Mt CO_2 eq/year.

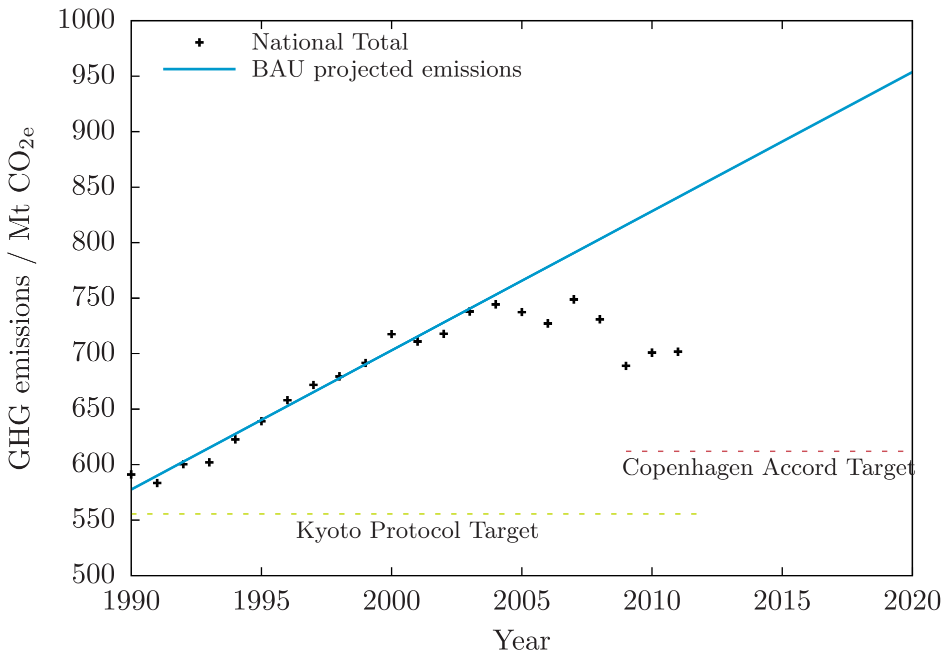

Figure 1.1: Canada's GHG emissions 1990–2011 (Source: Environment Canada [35])

[2]The Government of Canada announced its intention to withdraw from the Kyoto Protocol on December 15, 2011 and this became effective December 31, 2012.

Figure 1.2 indicates Canada's GHG emissions for the period 1990–2011, disaggregated by source type. The majority of Canada's emissions results from the combustion, flaring, or venting of fossil fuels and the relative contribution from each source to the total has remained relatively constant. Figure 1.3 shows Canada's GHG emissions in 2011 by economic sector.

- *Fuel Combustion — Energy Industries* from Figure 1.2 is broken out in Figure 1.3 into Public Electricity and Heat Production, Petroleum Refining, and Manufacture of Solid Fuels and Other Energy Industries.
- *Fuel Combustion — Other Sectors* is essential GHG emissions by the commercial, institutional, and residential sectors for space heating and small scale power generation.
- *All other sources* is a mix of 40% industrial processes, 40% waste, and 20% agriculture.

28% of the emissions are from mobile sources, 9% is from fugitive emissions (mostly methane), and about 22% is from a large number of diffuse sources. The remaining 41% shown in Figure 1.3 is emitted by LFEs (Large Final Emitters) and nearly a third of these is attributable to the electricity generation sub-sector.

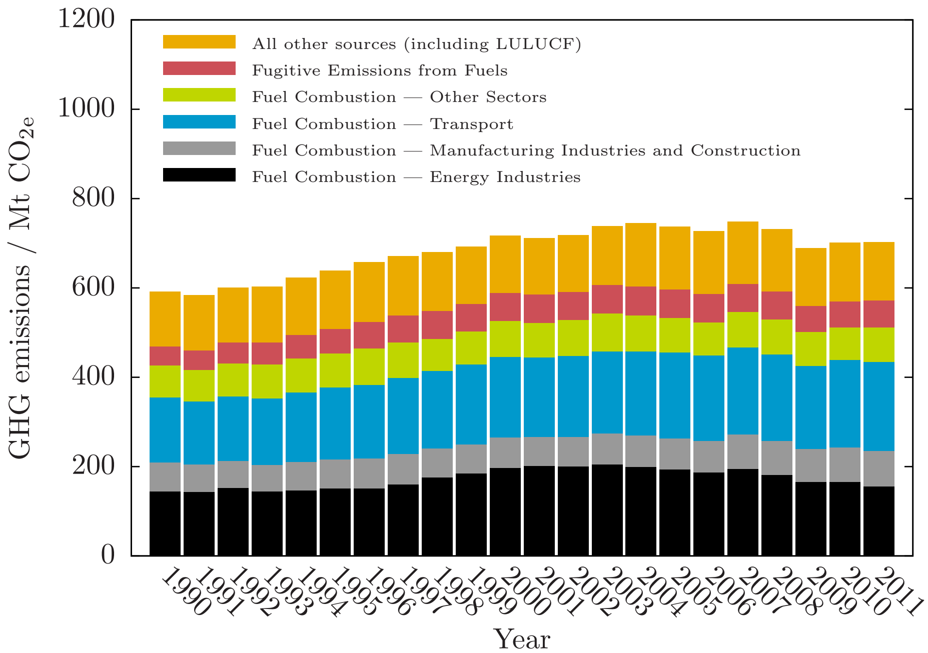

Figure 1.2: Canada's GHG emissions by source (Source: Environment Canada)

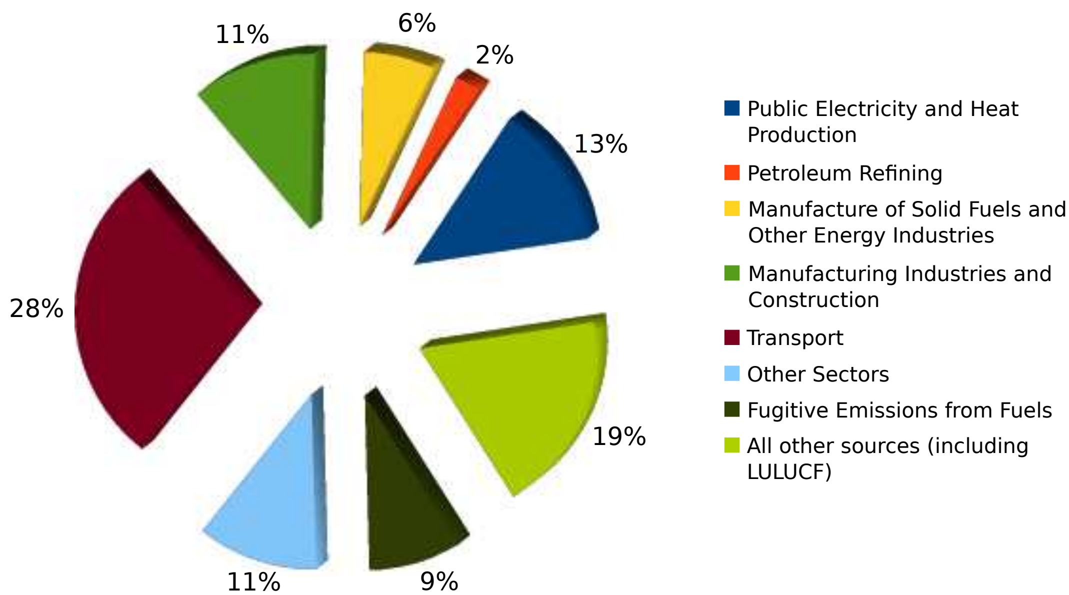

Figure 1.3: Canada's GHG emissions by sector, 2011 (Source: Environment Canada)

1.1.3 Strategies for GHG mitigation in electricity sub-sector

In Canada, each provincial government has the authority to make laws, within its borders, respecting the generation and transmission of electricity. Not surprisingly, each province has its own *electricity system*: a collection of elements (*e.g.*, loads and generators), connected via transmission lines, whose operation is managed by a central authority with the objective of satisfying the demand for electricity securely, reliably, and economically.

Overall, the electricity sub-sector is an attractive target for mitigation action:

- GHG emissions in this sub-sector are almost entirely in the form of CO_2 released by coal-fired electricity generating stations. So, in a perfect world, only a single mitigation solution needs be developed.
- Coal-fired power plants are stationary.
- The number of coal-fired generating stations is small relative to the total number of power stations across the country. So, any mitigation solution need only be applied to a small number of sites.
- Canada has a 'diversified portfolio' in terms of primary energy sources used to generate electricity. This should dampen negative effects associated with transitioning away from current coal technology and/or coal in general.

There are several different strategies for reducing the GHG emissions of the electricity generation sub-sector. These, listed in increasing impact to the existing electricity system, are:

1. Produce less electricity (*i.e.*, reduce demand).
2. Preferentially use generating units with lower carbon intensity. These could be existing units or new ones.
3. Using alternative energy sources (*e.g.*, wind, solar, tidal, geothermal)
4. Use electricity more efficiently (*e.g.*, compact fluorescent light-bulbs vs incandescent ones)
5. Use electricity more intelligently (*e.g.*, peak-shaving which could result in using fossil fuel generating units less)
6. Improve energy efficiency of existing generators (*e.g.*, raising steam pressures, combined-cycle units versus versus single-cycle ones)
7. Use lower carbon intensity fuels at existing power plants (*e.g.*, *fuel switching*).
8. Capture and store CO_2.

Ideally, the optimal mix of strategies would be deployed.

1.2 Literature survery of the evaluation of GHG mitigation strategies

Given the plethora of existing CO_2 mitigation actions, there is a need for robust means to compare one mitigation option to another. Currently, there are two methodologies for estimating the relative effectiveness of CO_2 mitigation actions: techno-economic study of individual plants and medium- to long-term electricity system planning.

1.2.1 Techno-economic study of individual plants

This methodology entails calculating a performance metric for each mitigation action. The better the value of the metric, the better the mitigation strategy. In the earlier literature, CO_2 capture options are frequently compared using the associated *CCC* (Cost of CO_2 Capture):

$$CCC = \frac{\begin{pmatrix} \textit{annualized} \\ \textit{capital cost} \end{pmatrix} + \dot{C}^{FOM}}{\textit{mass } CO_2 \textit{ recovered per year}} + \begin{pmatrix} \textit{fuel cost per} \\ \textit{unit mass} \\ CO_2 \textit{ recovered} \end{pmatrix} + CCC^{VOM,\textit{non-fuel}} \tag{1.1}$$

- Mariz *et al.* [36] compares the cost associated with retrofitting Shand Power Station in Saskatchewan, Canada to capture approximately 8000 tonne/day of CO_2 using two similar processes: Fluor Daniel's Econamine FG and MHI-KEPCO's KS-1/KP-1. The principal results are summarized in Table 1.1.

Table 1.1: *CCC* at Shand Power Station using amine-based absorption [36]

Process	CO_2 capture cost \$/tonne
Econamine FG	26
KS-1/KP-1	28

- David Singh [43] calculates the *CCC* using MEA (monoethanolamine) absorption and O_2/CO_2-recycle based CO_2 capture processes.

In the later literature, *CCA*, is used more often than *CCC* because, unlike *CCC*, it refers to the CO_2 emissions that are actually mitigated as a result of the mitigation action. This is often less than the CO_2 which is strictly captured. *CCA* is given by:

$$CCA = \frac{(CoE) - (CoE)_{ref}}{(CEI)_{ref} - (CEI)} \tag{1.2}$$

with cost of electricity given by:

$$CoE = \frac{\begin{pmatrix} annualized \\ capital\ cost \end{pmatrix} + \dot{C}^{FOM}}{annual\ net\ power\ output} + \begin{pmatrix} fuel\ cost\ per \\ unit\ energy \end{pmatrix} + CoE^{VOM,non\text{-}fuel} \tag{1.3}$$

and *CEI* (CO_2 Emissions Intensity) expressed as:

$$CEI = \frac{CO_2\ emissions\ rate}{net\ plant\ output} \tag{1.4}$$

- Paitoon *et al.* [46] investigate different scenarios for capturing 8000 tonne/day from a 300 MW_e power plant in Saskatchewan for use in EOR (Enhanced Oil Recovery). For the amine solvents MEA and AMP (2-amino-2-methyl-1-propanol), Paitoon *et al.* provide the supplemental energy via a new coal-fired co-generation plant sized in in one of four different ways:

  max Maximum size plant deemed feasible (230 MW_e net output).

80–120 MW_e Producing just enough steam such that cooling towers can be replaced with capture plant reboilers (80–120 MW_e net output).

null Producing just enough electricity for the capture plant (± 10 MW_e net output).

buy-back Steam is provided by utility boiler and electricity is purchased from the grid.

Table 1.2 shows the costs of CO_2 capture reported by Paitoon *et al.* as well as the corresponding cost of CO_2 avoided.

Table 1.2: *CCC* and *CCA* for cases studied by Paitoon *et al.*[46]

Case	x^{CO_2} mass basis	*CCC* \$/tonne CO_2	*CCA* \$/tonne CO_2
MEA: max	0.58	9.07	17.92
MEA: 80–120 MW	0.71	18.13	4.32
MEA: null	0.81	31.17	-4.29
MEA: buy-back	0.86	33.62	-21.07
AMP: max	0.58	6.61	17.81
AMP: 80–120 MW	0.77	18.89	-0.51
AMP: null	0.86	28.71	-8.35
AMP: buy-back	0.91	27.20	-21.52

Key assumptions are that the 8000 tonne/day of CO_2 captured is purchased at a price of \$28.30/tonneCO_2 CO_2 (2002 CAN\$), the existing power plant and capture facility operate 24 hours a day, 365 days a year, and that any surplus electricity produced by the co-generation plant is purchased at a price of 6¢/kWh. Paitoon *et al.* state that a CO_2 cost of \$28.30/tonneCO_2 is required for EOR to be economically feasible. Therefore, the viability of the project depends almost completely upon the assumption that there is strong demand for additional electricity. It is also interesting to note that the mitigation options which produce CO_2 at the lowest cost are the worst investments for mitigation purposes and *vice versa*. This supports the belief that cost of CO_2 avoided is a better means for evaluating CO_2 mitigation actions than cost of CO_2 capture.

- Guillermo Ordorica-Garcia [40] reports the cost of CO_2 avoided for IGCC (Integrated Gasification Combined Cycle) power plants with and without CO_2 capture. The base IGCC generator has a net power output of 583 MW_e. The principal results are repeated in Table 1.3.

  Ordorica-Garcia's reference plants are new IGCC and NGCC (Natural Gas Combined Cycle) power plants. This implies the situation that an IGCC or NGCC power plant, respectively, is intended to be installed but then a different, lower-CO_2 emitting unit

Table 1.3: *CCA* for IGCC power plants with integrated CO_2 capture [40]

Plant	Reference	*CCA* US$/kWh$_e$
IGCC w/ 80% capture	IGCC w/o capture	24
IGCC w/ 59% capture	IGCC w/o capture	27
IGCC w/ 80% capture	NGCC w/o capture	127

is considered in its stead. If this is the context, using IGCC as the reference plant needs further justification as its *CoE* is substantially higher than that of the NGCC and with a higher CO_2 emissions intensity.

- Rao and Rubin [42] estimate *CCA* for a 500 MW$_e$ coal-fired power plant deterministically and stochastically. It is worth noting that the functional form of the model and the nominal values for its inputs are obtained from published reports, a survey of experts, and detailed process simulations. It is the variability in the model inputs — CO_2 capture process parameters, CO_2 capture cost model parameters, and power plant performance parameters — that are 'uncertain' in the stochastic case. The probabilistic results give the range of *CCA* that one would expect to see if amine-based CO_2 capture were implemented 'across the board' and does not refer to any particular scenario.

  In the deterministic case, *CCA* is estimated to be \$51/tonne CO_2. Table 1.4 shows the 95% confidence interval for the *CCA* in each of the stochastic runs and gives the parameter to which the result is most sensitive.

Table 1.4: Effect of increasingly probabilistic input parameters of range of cost of CO_2 avoided

Variable	Nominal	Dist. type	Dist.	*CCA* \$/tonne CO_2
1. Variable CO_2 capture process parameters				43–72
α^{CO_2}	0.22	triangular	$(0.17, 0.22, 0.25)$	
y^{CO_2}	0.14	uniform	$(0.09, 0.19)$	
2. Variable CO_2 capture cost model parameters				33–73
TS	\$5/tonne CO_2	triangular	$(-10, 5, 8)$	
3. Variable power plant performance, w/o different than w/				21–79
UHR (Unit Heat Rate)	9600	uniform	$(9230, 9600)$	
CF (Capacity Factor)	75%	triangular	$(65, 75, 85)$	
FCF (Fixed Charge Factor)	0.15	uniform	$(0.10, 0.20)$	

Of these parameters, most often α^{CO_2}, y^{CO_2}, TS, and FCF are fixed at values obtained as a result of a detailed process design or specified in the terms of reference for the study. In contrast, values for UHR and CF are left to the discretion of the researcher. A conclusion of the work of Rao and Rubin is that selection of different feasible sets of values for these parameters could lead to strikingly different estimates of CCA.[3]

1.2.2 Medium- to long-term electricity system planning

Electricity system planning identifies the investments that will best satisfy electricity demand and other system constraints over a given planning horizon. The models used for this purpose are extended with CO_2 mitigation strategies and a CO_2 emission constraint (or, equivalently, a CO_2 tax). The greater the activity of a mitigation technology in the optimal solution, the better the mitigation strategy.

- Turvey and Anderson [47], in the context of expected growth in Turkish electricity demand beginning in 1977, present the prototypical LP formulation of an electricity system planning model. The objective function is:

$$\begin{array}{lrcl} \min\limits_{X_{jv},P^S_{jtvp}} & \multicolumn{3}{l}{\overbrace{\sum_{n\in NG1}\sum_{v=1}^{T} CAPEX_{nv}X_{nv}}^{\substack{\textit{present value of}\\ \textit{capacity additions}}} + \overbrace{\sum_{n\in NG}\sum_{t=1}^{T}\sum_{v=-V}^{t}\sum_{p=1}^{P} CoE^{OM}_{ntv}\,P^S_{ntvp}\,\theta_p}^{\substack{\textit{present value of}\\ \textit{future operating costs}}}} \\ \text{s.t.} & CAPEX_{nv} & = & CAPEX_n\cdot(1+r)^{-v}(1+g^{-v}) \\ & CoE^{OM}_{ntv} & = & CoE^{OM}_n\cdot(1+r)^{-t}(1+g^{-v}) \end{array} \tag{1.5}$$

  and the constraints are as follows:

  1. $CAPEX_{nv} = CAPEX_n\cdot(1+r)^{-v}(1+g^{-v})$ and $CoE^{OM}_{ntv} = CoE^{OM}_n\cdot(1+r)^{-t}(1+g^{-v})$[4]
  2. Available installed capacity must be equal to peak demand plus some reserve margin in every power demand block.

[3]It can be argued that the probability distribution assigned to these parameters by Rao and Rubin is unrealistically narrow. Had a broader range of values been permitted, the observed 95% confidence interval for CCA in the third scenario of Table 1.4 would have been even greater.

[4]For capital cost, g can be thought to represent cost decreases resulting from economies of scale and technological learning. For the operating cost factor, g can be thought of as representing changes in fuel price and plant thermal efficiency.

3. Generator power output must be equal to or greater than demand in every power demand block.
4. Generator output cannot exceed product of capacity and availability factor.
5. Energy balance on generators with storage (*e.g.*, hydroelectric facilities with reservoirs).
6. Temporal dependence of generator capacity (*e.g.*, photovoltaic generators would have zero capacity at night) must be respected.
7. New installed capacity is restricted by resource availability (*e.g.*, new hydroelectric capacity is limited by availability of flowing water).
8. Minimum and maximum amounts of particular types of capacity, perhaps as a fraction of total installed capacity, must be respected (*e.g.*, accommodating public policy reasons for not having electricity generation too heavily dependent upon any one resource).

The solid line in Figure 1.4 is the 2005 load duration curve for Ontario. To use this data in the model formulation of Turvey and Anderson, the load is divided into power demand blocks — four of these are shown in the figure. Each block has a different length θ_p and peak demand P_p^D. The corresponding values for the demand power blocks shown in Figure 1.4 are given in Table 1.5.

Table 1.5: Ontario demand power block length and peak demand, 2005

Period	θ_p hours	P_p^D 10^3 MW_e
1	282	24.3
2	2722	20.7
3	2721	18.2
4	3035	15.2

Creating a framework with which to evaluate CO_2 mitigation strategies requires simply constraining the CO_2 emissions by imposing, for example,

– a limit of the system-wide CO_2 emissions intensity,
– a limit on the aggregate CO_2 emissions in each time period, or
– a tax on CO_2 emissions.

By default, the second mitigation strategy from Section 1.1.3 — to use generators with lower carbon intensity — is always enabled. Other mitigation actions require the addition of new technological and economic parameters, variables, and constraints but the general model structure remains the same. The optimal solution provides

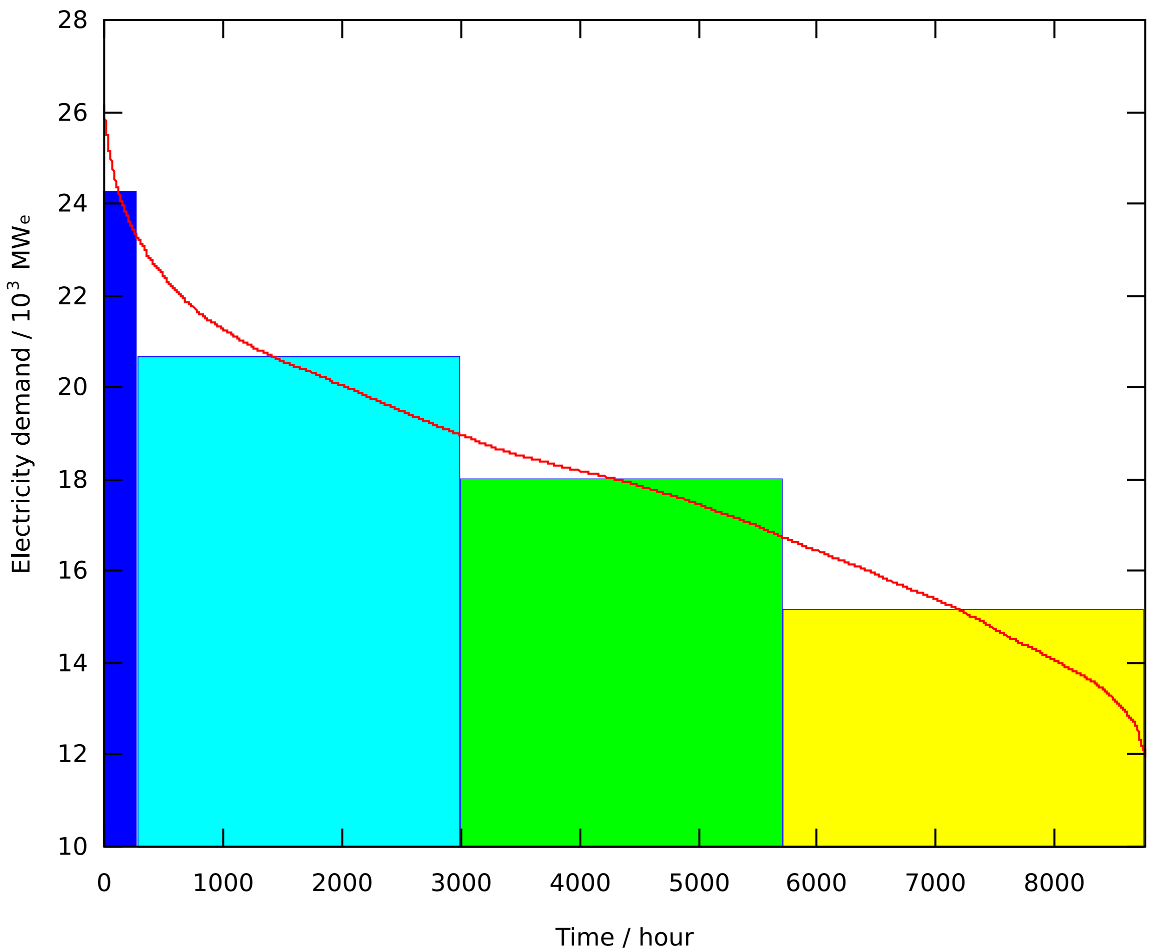

Figure 1.4: "Vertical" stepwise linear approximation of load duration curve: Ontario, 2005 (Source: IESO)

information regarding the relative usefulness of the different mitigation actions in fulfilling the CO_2 emission reduction agenda.

- Johnson and Keith's 'electricity system planning with CO_2 mitigation' model [25] extends the framework of Turvey and Anderson [47] by allowing for CO_2 capture as a technology option for retrofits and for newly-installed plants.

  The only other noteworthy item, from a modelling perspective, is the manner in which energy demand is allocated to the different generation classes: PC (Pulverized Coal), GT (Gas Turbine), NGCC, oil, nuclear, hydroelectric, and wind. Like Turvey and Anderson, Johnson and Keith create power demand blocks from the load duration curve but these are delineated 'horizontally' as opposed to 'vertically'. Figure 1.5 gives an example of how Johnson and Keith power demand blocks might look for Ontario in 2005.

  Normally, when load duration curves are partitioned in this manner, each class of generation can only serve a specified subset of the power demand blocks. For example, nuclear and GT would only be able to serve off-peak (also referred to as base-load) and peak-load demand, respectively. However, not enough information is provided to definitively state whether Johnson and Keith constrain generation in this manner.

  Johnson and Keith imply that system scheduling is critical for a correct assessment of different CO_2 mitigation strategies:

  > The cost of CO_2 mitigation via CCS varies directly with the utilization of carbon capture plants, where the dispatch of the individual plants is a function of the marginal costs of all the plants in the system. *p 369*

  But, the model does not take system scheduling into account.

- Haslenda Hashim [21] developed a model to predict, given a CO_2 reduction target, the optimal strategy for OPG (Ontario Power Generation) to pursue.[5] Hashim's model is simpler than that of Turvey and Anderson's [47] in some ways and yet more complex in others. In terms of simplicity,

  – Hashim's modelling horizon is on par with others seen in the literature but has only a single period.
  – Hashim uses a single power-demand block. This implicitly assumes that power demand is constant throughout the entire period.
  – Hashim assumes that all non-fossil fuel power plants operate at their maximum capability.

[5] OPG owns about 70% of the installed generation capacity in the province of Ontario.

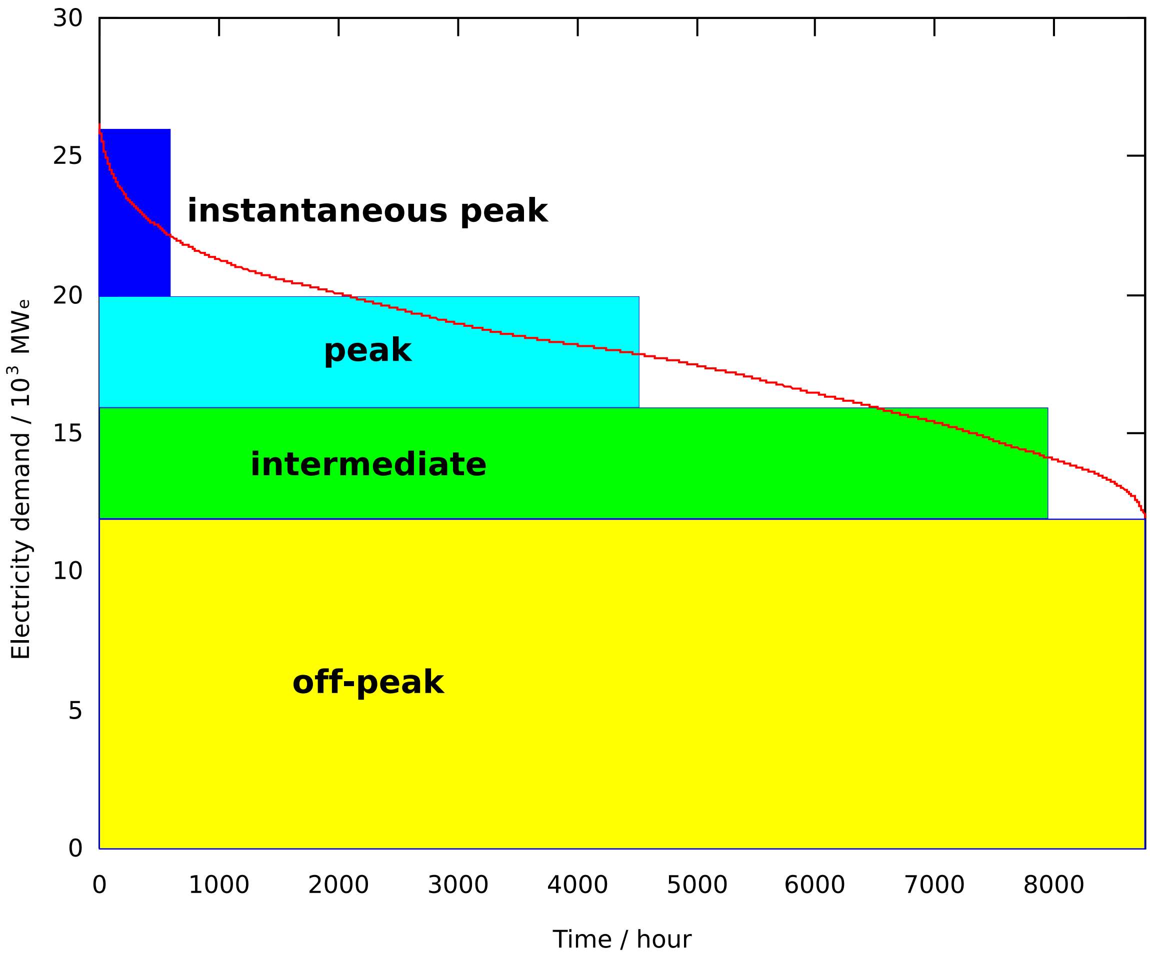

Figure 1.5: "Horizontal" stepwise linear approximation of load duration curve: Ontario, 2005 (Source: IESO)

However, unlike the models of Turvey and Anderson [47], Sparrow and Bowen [44], and Johnson and Keith [25], Hashim's model is implemented as a MILP (Mixed-Interger Linear Programming) problem. In addition, the electricity system and mitigation options are modelled in more detail (*e.g.*, generators are represented at the unit level). Because of these two enhancements, her model solution contains additional information:

  - The solution specifies the activity level for each unit and not just for the class of generation.
  - If a PC power plant is to be retrofitted for CO_2 capture, the optimal unit for this retrofit is singled out and, the solution indicates which of the possible sequestration locations is preferred.
  - New capacity can only be added in discrete quantities. The models listed above unrealistically allow for capacity addition in continuous amounts.

- Akimoto *et al.* [2] developed an electricity system planning model for Japan. The article only provides an overview of the model and highlights of the technological and economic parameters that are used. That being said, the degree of sophistication appears to exceed that of Turvey and Anderson [47] in several respects:

  - The model includes processes pertaining to the production of fuels for power generation (*e.g.*, oil refineries, hydrolysis plants)
  - The model is multi-regional: there are twenty on-shore regions and twenty off-shore sites. Akimoto *et al.* specify the supply-demand energy balance for four power demand blocks using load duration curves as a basis.[6] Like David and Keith [25], these are horizontally aligned.
  - The model includes CCS. All the potential for CO_2 sequestration resides in the off-shore sites either in the ocean or in aquifers beneath the ocean floor. The geographical disposition of the CO_2 sources and sequestration opportunities figures into the decision of where to capture CO_2 and to which site(s) it should be transported.

- Sparrow and Bowen [44] have developed a model to examine the potential benefits of 'pooling' among nine countries in southern Africa. CO_2 emissions are not included in the model but it deserves mention anyway because it contains some novel extensions to the model of Turvey and Anderson [47]:

  - Inter-regional transmission line capacity can be increased.

[6] It is not clear whether there is one load duration curve for the entire country or one for each on-shore region.

– It is possible to increase the capacity of existing generators above their initial rating.

– The capacity of existing generators tends to decrease over time.

and because the authors state that they've attempted to integrate system scheduling within the larger system planning effort. However, with computational difficulties listed as the reason, none of the features normally associated with system scheduling are present in the system planning mathematical programming problem. The scheduling features omitted by Sparrow and Bowen are as follows:

– Each utility is modelled as a single node. A parameter, independent of electricity flow is used to adjust for transmission losses. *No Optimal Power Flow.*

– Each day is broken up into six time periods of different duration as opposed to the normal 24, one-hour increments. *No Economic Dispatch*

– Ramping, minimum up-time, and minimum down-time generator constraints are not included; all units of a power plant are dispatched collectively; and start-up and shutdown costs are ignored. *No Unit Commitment.*

The 'scheduling' that Sparrow and Bowen assert is a part of the south African power pool model can be achieved using the formulation of Turvey and Anderson merely by changing the number of and the manner in which power demand blocks are determined:

– use an electricity demand profile instead of a load duration curve as a basis and

– define six power demand blocks using the time intervals shown in Table 1.6.

Table 1.6: Sparrow and Bowen demand power block structure

Period	Hours	Description
1	6 a.m.–9 a.m. 10 a.m.–7 p.m.	average day
2	9 a.m.–10 a.m.	off-peak
3	7 p.m.–8 p.m.	1^{st} peak hour
4	8 p.m.–9 p.m.	2^{nd} peak hour
5	9 p.m.–10 p.m.	3^{rd} peak hour
6	10 p.m.–6 a.m.	average night

- MARKAL (MARKet ALlocation) is an economic model originally developed by the IEA (International Energy Agency) for long-term analysis of national and international energy markets. The most striking difference between MARKAL and the models presented thus far is the breadth of its scope:

  - MARKAL considers all energy carriers and not just electricity: from extraction of the raw material, through its initial processing, conversion and/or blending, right through to final consumption.
  - The final demand categories are structured such that multiple energy carriers could suffice (*e.g.*, space heating could be provided by electricity, natural gas, coal, wood, kerosene, *etc.*). Thus, substitution among energy carriers is endogenous to the model.

  Over the years, a 'Canadian' version of MARKAL, Extended-MARKAL, has been extended in other ways that further set it apart from the other planning models that have been reviewed:

  - Extended-MARKAL is multi-regional [26, 27, 28, 33]
  - Extended-MARKAL can operate stochastically. [26, 29, 32]
  - Extended-MARKAL can accommodate price elasticities of demand. [29]
  - Extended-MARKAL can accommodate international trade in CO_2 emission permits. [31]
  - Extended-MARKAL is multi-pollutant (*i.e.*, it calculates emissions of SO_x, NO_x, CH_4, and SF_6 in addition to CO_2. [33]

1.3 Critique of evaluation methodologies

With either methodology, there comes a point in the implementation where a non-obvious decision is required in regards to the value of a critical parameter:

- To calculate CoE, the annual energy output of the new[7] power plant is required (see Equation 1.3). This is often calculated using the following expression:

$$net\ power\ output = CF \cdot 8760 \frac{\text{hours}}{\text{year}} \cdot P^{max} \tag{1.6}$$

[7] In this context, *new* refers to green-field plants as well as existing power plants that have been retrofitted.

- Using typical expressions for the numerator and denominator of Equation 1.4 gives:

$$CEI = \frac{P^{max} \cdot CF \cdot 8760 \frac{\text{hours}}{\text{year}} \cdot UHR \cdot 1.055 \frac{\text{kJ}}{\text{Btu}} \cdot HV^{-1} \cdot EI^{CO_2} \cdot \left(1 - x^{CO_2}\right)}{P^{max} \cdot CF \cdot 8760 \frac{\text{hours}}{\text{year}}}$$

  which simplifies to:

$$CEI = \frac{UHR \cdot 1.055 \frac{\text{kJ}}{\text{Btu}} \cdot EI^{CO_2} \cdot \left(1 - x^{CO_2}\right)}{HV} \tag{1.7}$$

- The generator operating cost per unit energy output in the planning model formulation (1.5), is calculated along the lines of:

$$CoE_j^{OM} = CoE_j^{\text{VOM,non-fuel}} + UHR_j \cdot C_j^{fuel} \tag{1.8}$$

- CO_2 capture is extremely energy intensive process and integrating CO_2 capture with an existing power plant design significantly de-rates the unit. One of the implications is in the peak-demand constraint of planning models:

$$\sum_{n \in NG^{nocap}} \sum_{v=1}^{T} a_{nv} X_{nv} + \sum_{n \in NG^{cap}} \sum_{v=1}^{T} a_{nv} X_{nv} (1 - y^{CO_2}) \geq Q_{t,p=1}(1+m), \; \forall t = 1, 2, \ldots, T \tag{1.9}$$

In these expressions, it is the selection of values for parameters *CF*, *UHR*, x^{CO_2}, and y^{CO_2}, which is problematic.

In addition to the parameter selection issue, neither methodology speaks to the effect of CO_2 mitigation on the electricity price and, to at least one significant set of stakeholders — the consumers — it is the electricity price which is most relevant.

In the next four sections, the preceding points will be further developed.

1.3.1 Predicting the utilization of new power plant

Capacity factor is a measure of plant utilization. It is defined as the fraction of electrical energy produced relative to what could have been produced had the power plant been operated at its MCR (Maximum Continuous Rating). Usually, the time frame considered is at least a year. While MCR is easily calculated for an existing facility, predicting the value for a new generator can be nigh impossible. To understand the reasons requires thinking about the manner in which electricity generators are operated.

Firstly, there are technical reasons why a generator may not operate at its MCR or even run at all.

- Like most, if not all industrial processes, the generating equipment must periodically be taken off-line for routine maintenance. For example, a unit of a nuclear power station will typically require six weeks of such scheduled maintenance per year.[20] Assuming that it achieves its MCR the rest of the year, it would have a capacity factor of about 0.88.

- Again, like most industrial processes, generating equipment does not respond immediately to changes in set point. So, the nuclear generator which has been idle for six weeks of maintenance cannot immediately begin producing power at its MCR. A typical nuclear station will have a ramping limit of 20 MW_e/min [20] which nudges downward its maximum possible capacity factor.

All things considered, when a generator is not at its MCR, it is usually because the generating capability within the system exceeds the instantaneous demand and the economics dictate that the generator in question should operate at part-load or be shutdown.

Figure 1.6 shows the hourly peak demand for electricity and the average monthly aggregate planned capability for the Ontario system in 2005.[8] The vast majority of the time, there is more generating capability than required which means that many plants are not required to be at base-load.

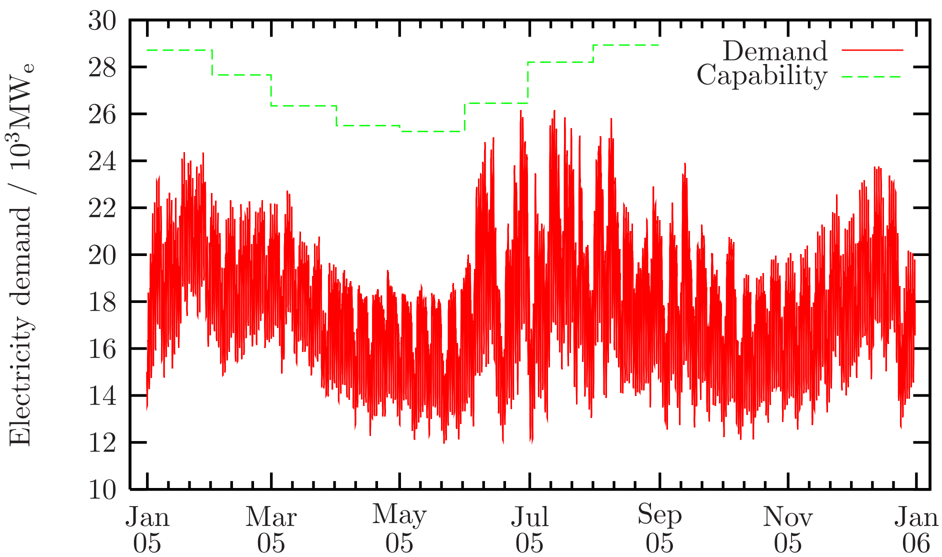

Figure 1.6: Ontario electricity demand profile, 2005 (Source: IESO)

The system operator decides how much electricity each generator should inject into

[8]The most recent monthly generator disclosure report that the IESO has made available is for August of that year which is why the average monthly aggregate planned capability is only shown up to that month.

the grid. In making this decision, system security, reliability, and economics are taken into account. The economics will change depending upon the regulatory environment in place. Locally, since the inception of Ontario Hydro in 1974, there have been two different economic operational objectives:

- Prior to 2002, the electricity system operator sought to minimize the average cost of electricity. The electricity tariff was designed to recover the cost of producing power from consumers.

- With the creation of an electricity market in April 2002, the system is said to have become 'deregulated'. The electricity system operator seeks to maximize the system 'social welfare' (*i.e.*, the sum of the producers' and consumers' surpluses). The hourly electricity price is nominally set to the marginal generation cost of the marginal unit (*i.e.*, the most expensive unit called upon to produce power).

As an example of how this decision making process plays out, Figures 1.7 and 1.8 show the power output from each of the eight nominally-500 MW_e units at the Nanticoke Generating Station for one late spring and one mid-summer day in 2005. The demand peaks for these days are the lowest and highest, respectively, observed in that year. Note that the performance of Unit 8 is not shown in Figure 1.7; this unit was out of service for scheduled maintenance that day.

Keeping in mind that the power plants are nominally all the same:

- Even during the 'summer peak', not all the units operate at their full capability. When loads are light, unit loads go up and down throughout the day with units even potentially shutting down.

- The units are not operated in unison. Even as some unit loads are increased others diminish.

- The dispatch order of the units seems to change. Unit 5, which is the lightest dispatched unit in Figure 1.8 starts the day June 17^{th}, 2005 more fully utilized than four other units.

So, if one were to add an additional 500 MW_e to the Ontario electricity system, making an educated guess of its future utilization would be non-trivial. In addition, Rao and Rubin demonstrate [42] that *CCA* is highly sensitive to this number so one would want to make sure to get this parameter value 'right'. To complicate matters even further, the new power plant is being situated within an environment for which there is no history: one in which the CO_2 emissions must be avoided. So, any lessons, if any, learned from a cursory review of the past utilization of generators (like the one above), wouldn't help the would-be modeller select a reasonable value for *CF*.

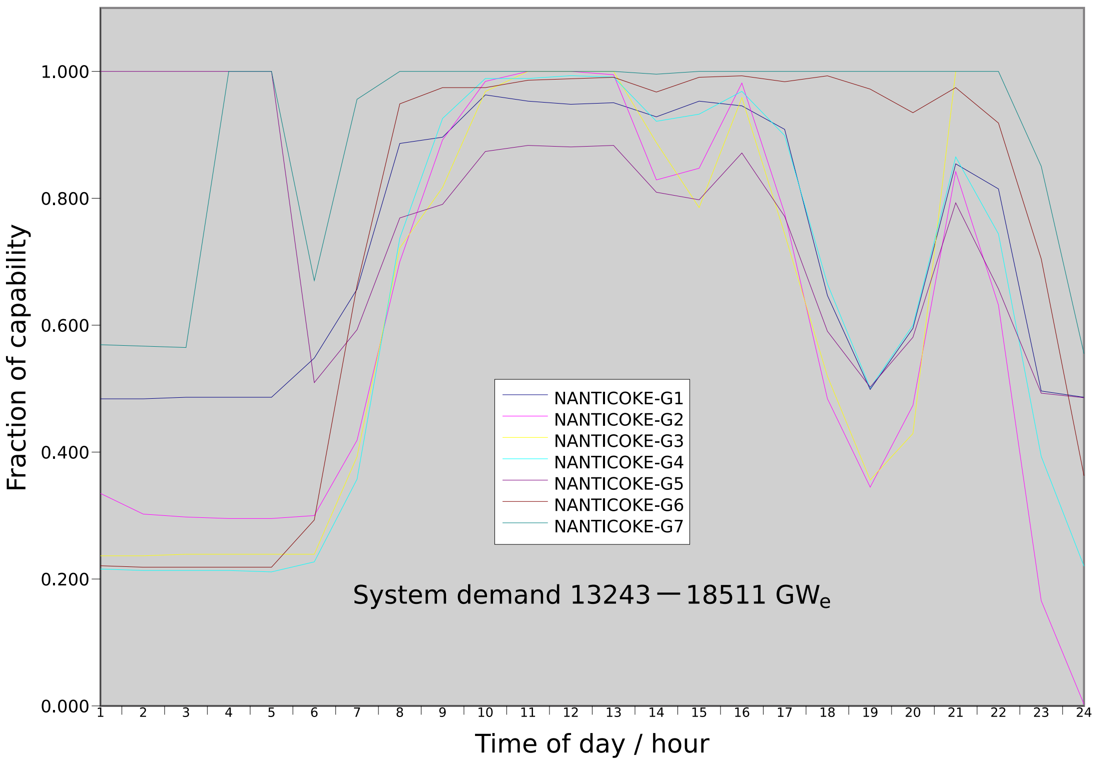

Figure 1.7: Output of Nanticoke Generating Station units 1–8, fraction of unit capability — June 17$^{\text{th}}$, 2005 (Source: Independent Electricity System Operator)

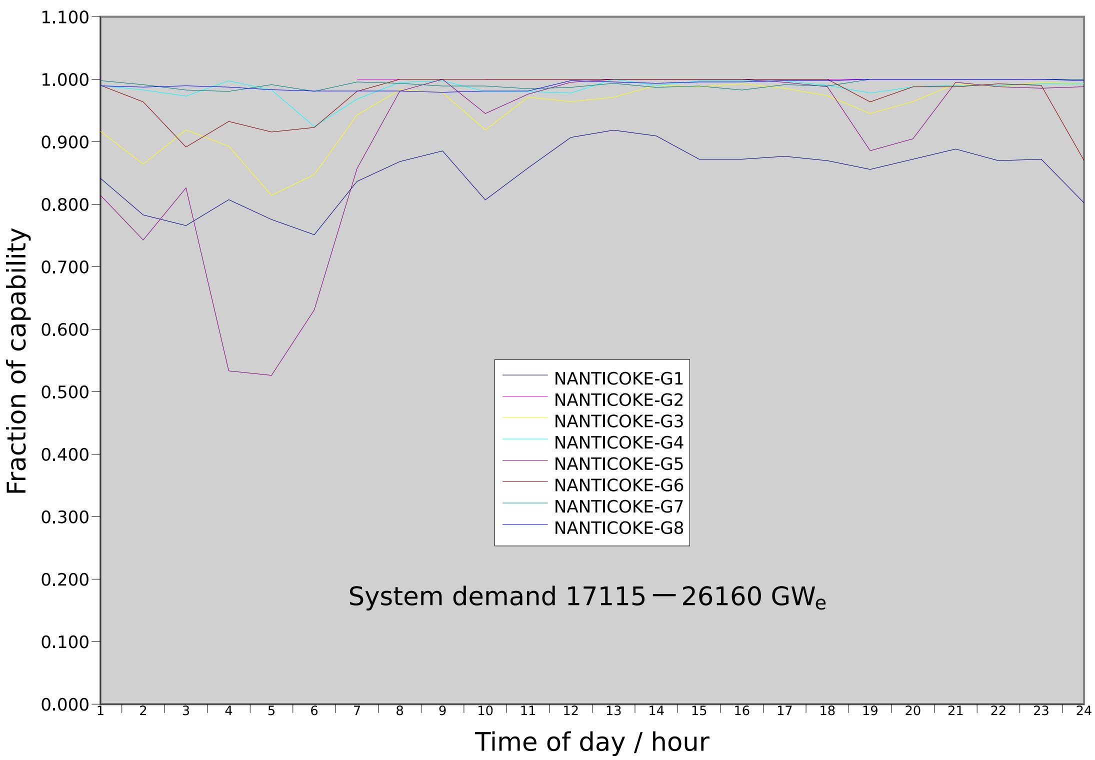

Figure 1.8: Output of Nanticoke Generating Station units 1–8, fraction of unit capability — July 13$^{\text{th}}$, 2005 (Source: Independent Electricity System Operator)

How, then, should one go about selecting a value for *CF* of a new power plant? Irrespective of the regulatory regime, a new plant's utilization will depend, in a complicated way, upon:

- the hourly electricity demand
- its marginal generation cost relative to all other generators
- the CO_2 emissions limit or, equivalently, the CO_2 emissions tax
- the CO_2 emissions intensity of the generator relative to that of all other generators
- its technical operating characteristics (*e.g.*, maintenance requirements, ramping capability, minimum up- and down-times)
- the proximity of the generator to load centres
- the transmission line capacities
- *etc.*

Coming up with a reasonable prediction of plant utilization requires consideration of how the generator would be called upon to produce power given the above dependencies.

1.3.2 Predicting the unit heat rate of a new power plant

Unit heat rate is an expression of the efficiency of a power plant. It is the quantity of thermal energy required per unit of net electrical energy generated. Using the steam cycle design heat balance for the Nanticoke units, a model of a boiler and steam cycle is developed using Aspen Plus®.[9] This model is then used to calculate the unit rate as a function of unit output and the results are shown in Figure 1.9.

The unit heat rate decreases by about 15% as its output increases from minimum load to maximum load. The range of *UHR* observed signifies that the thermal efficiency is in the interval $0.33 \leq \eta_{th} \leq 0.39$.This is a very broad spectrum of values as, in the context of power generation, even a change of $(\Delta\eta_{th}) = 0.01$ is significant.[10]

Given the possible variability in plant load as evinced by Figures 1.7 and 1.8, the effect that changes in load have on unit efficiency (shown by Figure 1.9), and the fact that the utilization of a new plant is uncertain (discussed in Section 1.3.1), selecting a reasonable value of *UHR* for a new plant without explicit consideration of how it will be dispatched seems unlikely.

[9] See [6] for a description of the Aspen Plus® software system and [3, Chapter 3] for a complete description of the boiler and steam cycle models.

[10] Two units at Nanticoke were recently shutdown to replace their turbine blades at considerable overall expense with the expectation that the unit efficiency would increase by 1%.

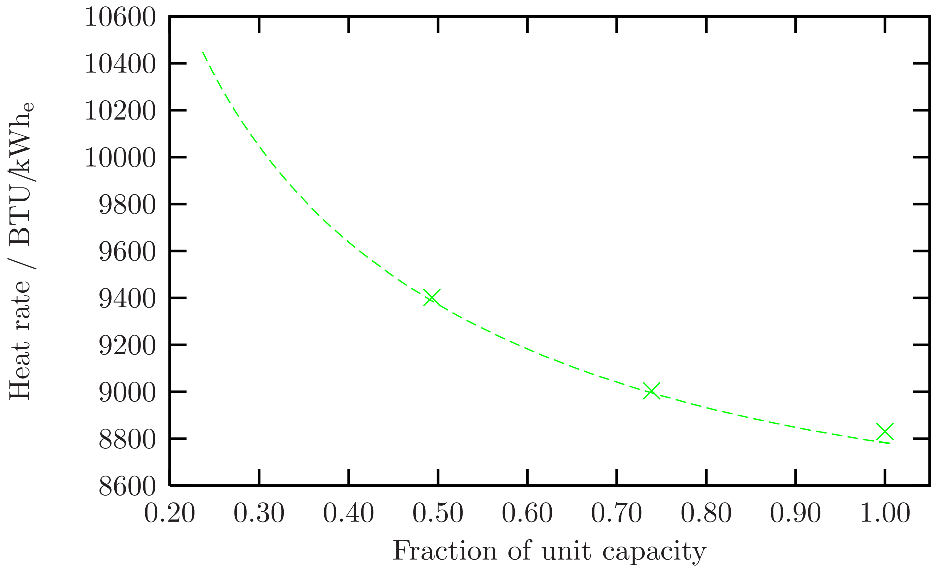

Figure 1.9: Unit heat rate as a function of plant output at Nanticoke Generating Station

1.3.3 Predicting the fraction of CO_2 captured and power plant de-rate

Every study reviewed thus far in which CO_2 capture is considered, whether the methodology has been that of the techno-economic study or electricity system planning, has had the fraction of CO_2 captured fixed, usually at $x^{CO_2} = 0.90$. The selection of a value close to unity seems to make sense; one would not go through the trouble of installing CO_2 capture equipment only to let most of the CO_2 generated flow unfettered into the atmosphere. However, in the real world, one can imagine there periodically being incentives to turn-down the CO_2 capture plant.

CO_2 capture is an energy intensive process. MEA absorption is a commercially-proven process for removing CO_2 from dilute vapour streams (*e.g.*, flue gas of coal-fired power plants). A well designed MEA absorption process recovering 85% of the CO_2 in the flue gas of a nominally 500 MW$_e$ unit at Nanticoke is estimated to cause $P^{S,max}$ to drop from 497 MW$_e$ to 342 MW$_e$ — a de-rate of $y^{CO_2} = 0.31$.[3].

On average, to achieve the CO_2 mitigation target, this energy penalty may be tolerable. However, during periods of high demand, perhaps shutting down the lights in downtown Toronto may be too high price to pay. In general, from an economic viewpoint, there are times when the value of electricity would exceed the value of CO_2 and one would want to produce more power (*i.e.*, increase P^S) by reducing the fraction of CO_2 captured. Conversely, after a long CO_2-emitting period, the value of CO_2 will exceed that of electricity and the CO_2 recovery should go up. Fixing x^{CO_2} at a single value biases mitigation option evaluation in the following manner:

- *Not all CO_2 capture process designs lend themselves to varying x^{CO_2}.* Thus, fixing x^{CO_2} fails to properly reward those designs that offer flexibility.

- In planning studies, a CO_2 capture process with flexibility is modelled such that the de-rate associated with capture (given the high values of x^{CO_2} chosen, this is usually on the order of at least 20% of the plant's initial MCR) is a persistent reduction in the plant's capability. In reality, it would be expected that the ability of the system to meet peak loads would not be affected.

- The second constraint in Turvey and Anderson's planning formulation [47] is intended to guarantee that there is sufficient available capacity to meet demand plus an amount for contingencies. Well, as a dispatchable load, a CO_2 capture process would be able to help meet this security constraint but by making x^{CO_2} a parameter as opposed to a decision variable, this benefit of flexible CO_2 capture processes is overlooked.

If flexible operation of a CO_2 capture process is as valuable a feature as it has thus far been proposed, then one would not be able to assign x^{CO_2} for a new plant with CO_2 capture without explicitly considering how the capture process would be called upon to operate as the entire system seeks to meet its electricity and CO_2 emission obligations. And, since y^{CO_2} is a strong function of x^{CO_2}, choosing a value for this parameter without undertaking such a study is equally as daunting.

1.3.4 Estimating the effect of CO_2 mitigation on the price of electricity

Cost of CO_2 Capture, Cost of CO_2 Avoided, present value of capital and operating costs. When it comes to evaluating CO_2 mitigation strategies, the methodologies all seek to estimate some *cost* — the amount of some thing such as time or labour, necessary for the achievement of a goal.[16] The cost of a project is an important datum for a business but only insofar as it enables the enterprise to predict the potential to make a profit. In a free market, the business owner is a profit maximizing entity and cost is only part of the equation. In order to estimate profit, the sale *price* — the amount as of money or goods, asked for in exchange for something else — is also necessary.

$$Net\ Profit = (quantity) \times (price) - (Cost\ of\ goods\ sold) - (Overhead)$$

By construction, a market has two types of participants: producers and consumers.[11] Does the consumer care about the cost to the producer of bringing a good to the market? No, the consumer is interested only in the price. Economists will talk about the demand-price elasticity but not production-cost elasticity. The homogeneity of existing methodologies in terms of their focus on cost for evaluating mitigation actions means that

[11] There is often a third participant, the *regulator*, who is charged with ensuring the smooth functioning of the market but, for the sake of argument, assume that the world is perfect.

the impact of these actions on consumers is not being explicitly considered. In addition, as cost is only one part of the profit equation for businesses, the existing methodologies are not fully addressing their concerns either.

The above statements are not always true. Consider a hypothetical electricity market with five consumers (A, B, C, D, E) and five producers (1, 2, 3, 4, 5) whose demand and generating capability, respectively, are shown in Table 1.7.

Table 1.7: Consumer demand and generator capability for Colinland

Producers			Consumers	
ID	$\frac{dC}{dP}$	Quantity	ID	Quantity
	$/MWh$_e$	MWh$_e$		MWh$_e$
1	45	61	A	32
2	7	99	B	84
3	13	64	C	58
4	4	87	D	66
5	36	80	E	64
Total		391		304

- As a first example, assume that the generators are owned by the public utility which is a vertically-integrated monopoly, operating on a cost-recovery basis, and is mandated to produce power to satisfy the regional demand. Under ideal circumstances, the utility will dispatch generators in order of increasing marginal cost until the supply of electricity equals the demand. This is shown in Figure 1.10.

  The entire demand of 304 MW$_e$ is satisfied; Generators 2, 3, and 4 are fully dispatched, Generator 5 operates at about 75%-load, and Generator 1 is idle. The price charged to consumers is given by:

  $$\rho = \frac{C}{P^D}$$

  assuming that the capital is fully amortized. In this example, the price works out to $12.56/MWh$_e$. If the capital has not been fully paid for, there would be a debt repayment charge and the price would be given by:

  $$\rho = \frac{C + TCR \cdot FCF}{P^D}$$

  In a situation like this, the cost of CO_2 mitigation is a relatively useful metric for all parties. Firstly, the utility is a *cost centre* and is driven by cost minimization rather

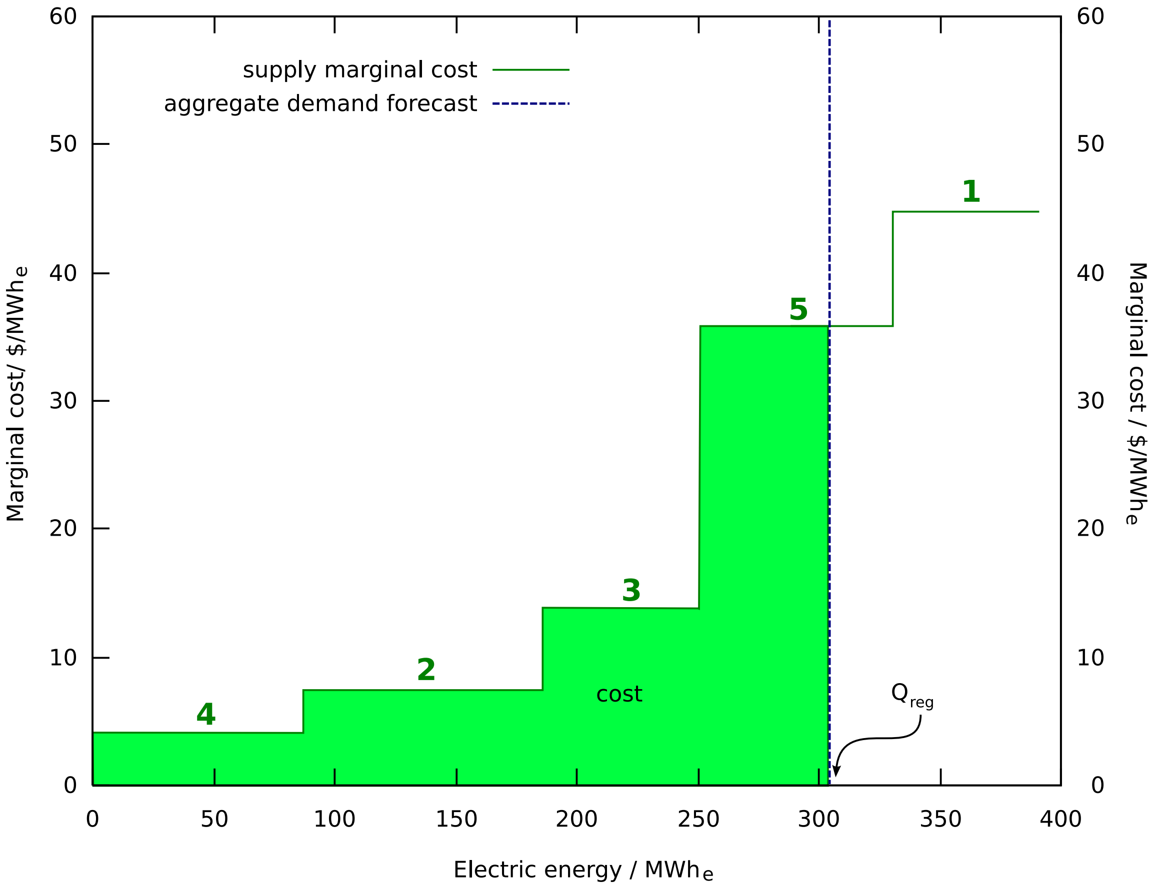

Figure 1.10: Supply-demand curve for regulated electricity market

than profit maximization. Therefore, it will be most interested in the cost aspect of various mitigation alternatives. Secondly, the consumer is still only interested in price but, as the present relationship between cost and price is simple, cost is a suitable proxy.

- As a second example, assume that the electricity system is deregulated and bilateral transactions are not allowed; dispatch of generation and load is performed exclusively by the system operator. Each generator is individually owned and operated and submits bids describing the amount of electricity it is willing to produce and at what minimum price. Assuming that generators are not gaming, they will be satisfied to produce power up to their full capability at their marginal cost. Consumers will also submit bids to the system operator. These bids outline the quantity of power desired and the maximum price they are willing to pay for it. The system operator will dispatch generators and loads such that social welfare is maximized. Table 1.8 shows the producer and consumer characteristics updated for the deregulated scenario. Figure 1.11 illustrates the system dispatch.

Table 1.8: Consumer and generator bids for Alieville

Producers			Consumers		
ID	Buy bid	Quantity	ID	Sell bid	Quantity
	$/MWh$_e$	MWh$_e$		$/MWh$_e$	MWh$_e$
1	45	61	A	13	32
2	7	99	B	57	84
3	13	64	C	53	58
4	4	87	D	31	66
5	36	80	E	27	64
Total		391		304	

The significance of Figure 1.11 is explained below.

  - The supply bids are sorted in order of increasing price and the demand bids are sorted in order of decreasing price (see Appendix A on why this is important).
  - Collectively, the bids form aggregate supply and demand curves for the market. The market equilibrium occurs where these two curves intersect. The total supply, at 250 MWh$_e$, is less than that observed in the regulated scenario. Loads B, C, and D are fully satisfied, Load E receives about two-thirds of the power it was willing to accept, and Load A is dark. Generators 2, 3, and 4 are fully utilized while Generators 1 and 5 are idle.
  - The price for electricity is set equal to the bid price of the marginal generator or load, depending upon which one is limiting. In this case, it is Load E that sets the market price of $27/MWh$_e$.

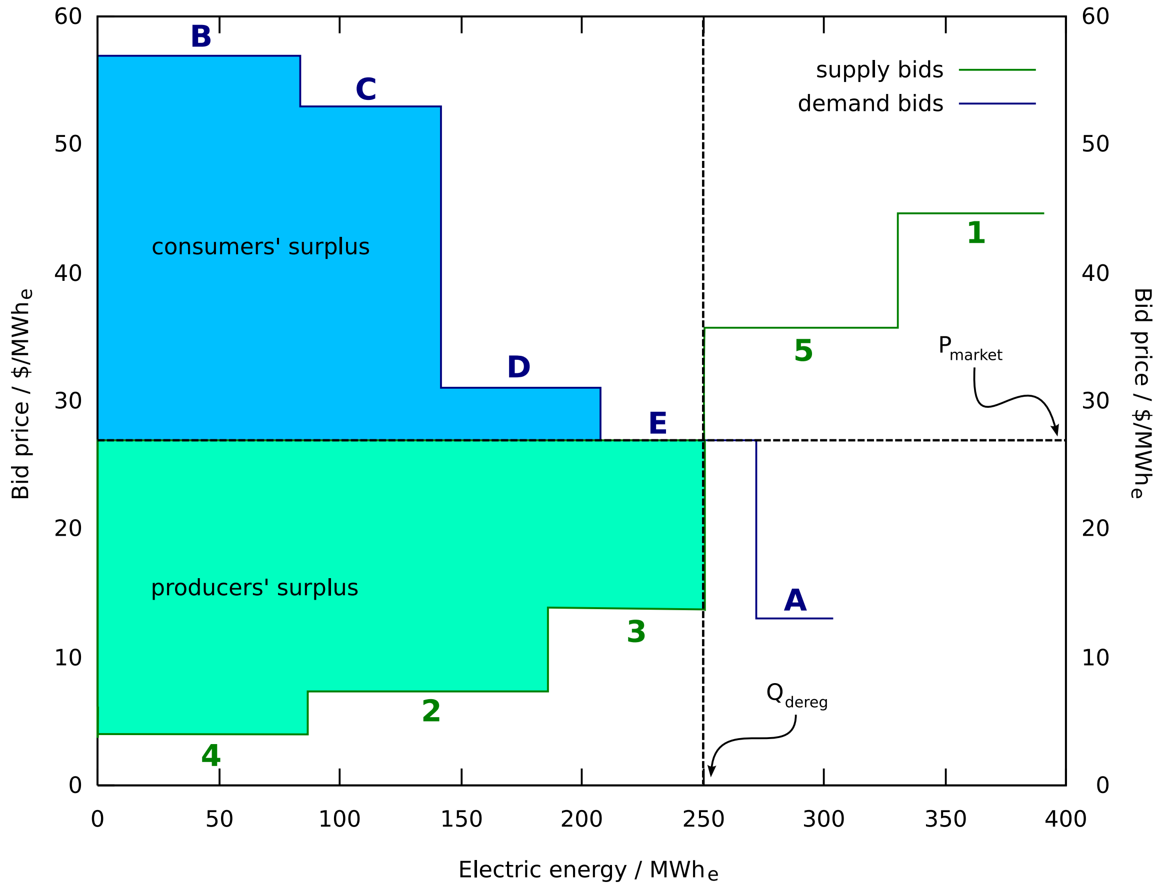

Figure 1.11: Supply-demand curve for deregulated electricity market

- The consumer's surplus represents the perceived extra value received by Generators B, C, and D. For example, Load B would have been willing to pay \$57/MWh$_e$ but is only charged \$27/MWh$_e$. Its surplus is the product of the difference in its bid price and the market price and the quantity of electricity it consumed. The producer's surplus is defined similarly. The sum of the consumers' and producers' surpluses is the social welfare.

Faced with this operating paradigm, how is the generator owner to assess the impact that CO_2 mitigation will have on its bottom line given the outcome of a cost-based methodology? Unlike the utility in the previous scenario, the generator owner has no assurance that it will recover its capital expenditures:

- Without market power, it does not make sense for a generator to bid greater than its marginal cost (*i.e.*, cannot simply add $TCR \cdot FCF$ to its supply bid). Doing so will not increase its revenue but increases the probability of being priced out of the market. Assuming non-zero FOM (Fixed Operating and Maintenance) costs, the generator losses money if it sits idle.
- However, by being the marginal generator, revenue is insufficient for debt repayment; revenue will just meet the cost of producing electricity. So, to be running is a necessary but not sufficient condition for debt financing.

In order to predict its revenue, the generator owner will need to know the effect of the CO_2 mitigation action on its generator's marginal operating cost as a function of generator output. This information has not yet been provided in any techno-economic or electricity system planning study of which the author is aware.

1.4 Research objective

The pre-assessment of the effectiveness of GHG mitigation strategies for the electricity sector is routinely undertaken in the context of:

- the development of GHG policy and regulation,
- the selection of technologies for deployment, and
- the prioritization of research and development of novel mitigation approaches.

Typical methodologies for evaluating GHG mitigation strategies are presented and critiqued in Sections 1.2 and 1.3, respectively. These methodologies are flawed in that:

- The existing methodologies require key parameters to be specified exogenously — parameters for which credible estimates are often not available *a priori*. Due to this lack of rigour, these methodologies can suggest investments that are suboptimal or even infeasible.

- The outputs of the existing methodologies (CCC, CCA, discounted cost of electricity system with CO_2 constraints) lack relevancy in the context of deregulated markets.

It is proposed that *to understand the effectiveness of GHG mitigation strategies on electricity systems requires detailed consideration of the operation of the electricity system in question.* Such an approach is not reported in the literature and the objective of this work is, first and foremost:

1. To develop and describe an approach for evaluating GHG mitigation strategies that considers the detailed operation of the electricity system in question.

2. To ascertain whether considering the detailed operation of the electricity system affects the assessment of the effectiveness of the GHG mitigation strategy.

Conventional designs of CCS capture processes focus on optimizing and assessing performance at a operating point (*e.g.*, 100% power plant load with 85% CO_2 capture). It is proposed that a generating unit with integrated CO_2 capture that is designed for flexible operation could provide greater benefit(s). A secondary objective of this work is to assess the potential advantage(s) that flexibility in the CO_2 capture process could confer.

Organization of thesis

This thesis is organized as follows:

- Chapter 2 describes the development of the electricity system simulator that is the tool used to understand the impact of GHG regulation and GHG mitigation strategies on the operation of an electricity system.

- Chapter 3 examines the impact of GHG regulation on the operation of an electricity system.

- CCS is a key GHG mitigation strategy for the electricity system sub-sector. Chapter 4 presents the design of a CO_2 capture process, the integration of CO_2 capture with a coal-fired power plant, and the development of a reduced-order model a generating unit with CO_2 capture suitable for inclusion in the electricity system simulator.

- Chapter 5 walks one through the process of adding the generating unit with CCS to the electricity system simulator and examines the impact of CCS on the performance of the electricity system.

- Typically, a generating unit with CCS is assumed to operate in an 'all-or-nothing' manner: either the unit is at full-load and capturing nearly all of the CO_2 it generates or the unit is shutdown. Chapter 6 considers the impact of *flexible* CCS on the performance of the electricity system.

- Chapter 7 summarizes the key findings of this work, reiterates the contributions, and suggests further avenues of investigation.

Chapter 2

Modelling the operation of an electricity system

2.1 Introduction

Electricity systems consist of four components:

1. Generation units.

   Supply is predominantly provided by large, centralized, dispatchable generators using either fossil fuels, uranium, or moving water as their primary energy source.

2. Loads.

   Demand, in contrast, occurs in small increments by loads that are spatially distributed within the region and are typically non-dispatchable.

3. Transmission and distribution networks.

   A large transmission and distribution network exists providing the necessary connectivity between the sources — where power is generated — and sinks — where power is consumed.

4. System operator.

   Electricity systems are demand-driven and have limited ability to store energy. The system operator role is critical; it orchestrates the generators and loads such that the supply of electricity matches demand in every time period. In doing so, it seeks to maximize the total benefit accrued by the stakeholders while satisfying requirements for security and reliability.

It is typical for system operation to be divided into three phases: pre-dispatch, real-time operation, and market settlement. These phases occur either before, during, or after, respectively, of a particular time period.

- The *pre-dispatch* phase occurs a minimum of a day in advance of the period in question. The system operator solicits firm offers to sell power from generators and, in the case of a double-sided auction, receives firm offers (or bids) to buy power from consumers.[1] Using this data and considerations around system reliability and energy availability the system operator commits power from selected units to satisfy anticipated demand. The time horizon considered is typically 24 hours broken up into 30 minute or one hour intervals.

- During the *real-time operation* phase, the system operator provides generators with dispatch instructions in order to balance electricity supply and demand. Important distinctions from pre-dispatch are that the output of energy-constrained units is fixed, that power flow is rigorously considered, and that the time horizon is shorter (*e.g.*, five minutes).

- In the *market-settlement* phase, a composite supply curve is created from the offer bids of units — and sell bids of consumers in the case of a double-sided auction — that were committed during the time period in question. The intersection of the composite supply and demand curves yields the price for electricity in the time period and, hence, the energy benefit of the generators and cost to consumers.

Successful simulation of an electricity system requires progressing through each of these phases and the development of such a simulator is the overall focus of this chapter. The '1-area' IEEE RTS '96 [20] is the electricity system selected as the basis for evaluating GHG mitigation strategies and a one-line diagram of the IEEE RTS '96 is shown in Figure 2.1. Reasons for selecting the IEEE RTS '96 include:

1. The IEEE RTS '96 has several desirable features:

   (a) Parameters describing the technical and economic performance of the generation units is provided and there is a variety with respect to the types of generating units that are represented.

   There are many ways of producing electricity and electricity systems have a variety of different types of units. Differences between units can exist with respect to:

   - sustainability (*e.g.*, fossil fuel vs. renewable)
   - technology (*e.g.*, steam generation vs. combustion turbine)
   - emissions intensity (*e.g.*, fossil fuel vs. nuclear)
   - dispatchability (*e.g.*, hydroelectric dam vs. wind)
   - waste (*e.g.*, natural gas vs nuclear)

[1] In this work, it is assumed that the consumers are price insensitive and do not submit offers to buy electricity.

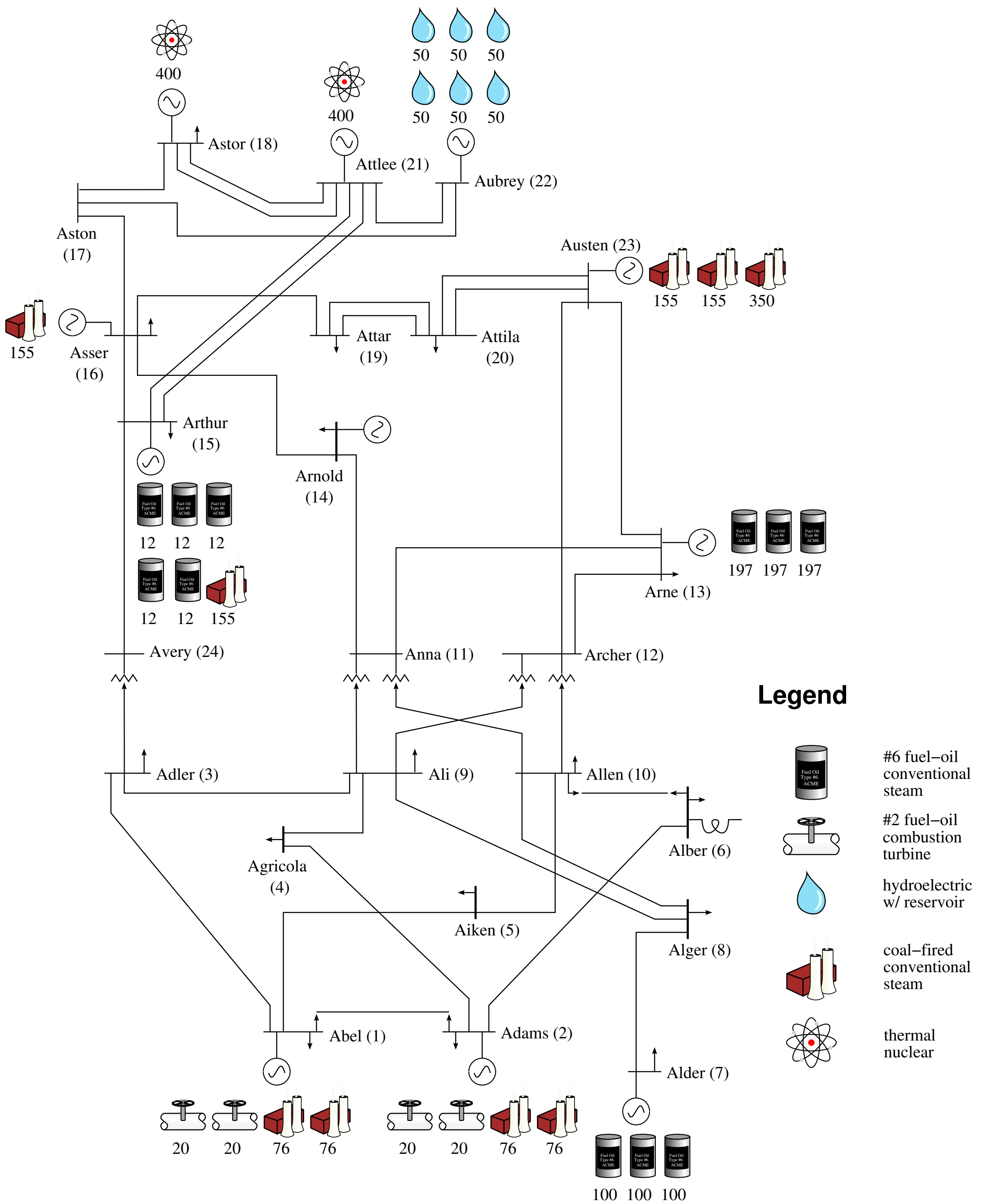

Figure 2.1: One-line diagram of IEEE RTS '96[a]

[a] "Abel (1)" specifies the name of the bus (*i.e.*, *Abel*) and the bus ID (*i.e.*, *1*); numbers below the generating unit symbols indicate the units capacity in MW_e.

- proximity to loads (*e.g.*, centralized vs distributed)

  Electricity systems in Alberta and Ontario are examples of Canadian electricity systems in which generating units cross the gamut.

  In the IEEE RTS '96, supply is provided by large, centralized, and dispatchable generating units using either fossil fuels, uranium, or moving water as their primary energy source. Except for distributed and non-dispatchable generation, all of the different 'types' of generating units are explicitly represented. And, as it is straightforward to represent distributed and/or non-dispatchable generation by manipulating demand, all types of generating units can be included in the analysis.

(b) Sources and sinks are spatially disaggregated and the physical properties of the transmission system are specified.

  Transmission lines provide the necessary connectivity between the sources and sinks. The IEEE RTS '96 is separated into high- and low-voltage regions. The regions are separated by transformers situated between the buses Adler, Ali, and Allen on the high-voltage side and Avery, Anna, and Archer on the low-voltage region.

2. The necessary parameters for an existing electricity system in a jurisdiction of interest (*e.g.*, the province of Ontario) were not readily available and the relative cost of estimating all the necessary parameters was deemed to outweigh the benefits of using a real system as the basis.

3. The IEEE RTS '96 has been used in many other electricity system studies including many focused specifically on DG (Distributed Generation) [13, 17, 52]. This allows the results from this effort to be easily compared with the work of others.

Section 2.4 walks through the execution of the electricity system simulator and Section 2.5 contrasts the approach taken with this electricity system simulator against approaches taken in other work.

Each phase has in common the need to solve an optimization problem seeking to maximize the economic benefit to producers and consumers subject to a set of constraints. The formulation of the *economic dispatch* problem is described in Section 2.3.

Conceptually, finding an economic dispatch requires evaluating several *loadflow* problems. That is, for a given demand and fixed output from the generating units, determining the power flows — and hence, losses — that occur within the transmission network. Since the loadflow problem is conceptually at the core of electricity system simulator, it is with the solution of the loadflow problem in Section 2.2 that the development of the electricity system simulator begins.

2.2 Solving the loadflow problem

As indicated in Section 2.1, the electricity system simulator is developed in a step-wise fashion with the first step being the development of a power flow model. As a precursor to developing a power flow model for the IEEE RTS '96, a power flow model is implemented in GAMS for a simpler system taken from literature. The objective is to validate the approach for implementing power flow problems in GAMS (see Section 2.2.1).

For the same simple problem, a loadflow model is implemented using PSAT (Power System Analysis Toolbox), commercial power flow analysis software (see Section 2.2.2). The intention is to use PSAT to validate the GAMS implementation of a power flow model for the IEEE RTS '96 and it is important to validate the use of PSAT (*i.e.*, demonstrate the capability to correctly specify electricity systems in PSAT's syntax).

Finally, a loadflow model for the IEEE RTS '96 is implemented both in GAMS and PSAT and the results are compared (see Section 2.2.3). To reiterate, finding an economic dispatch requires evaluating several loadflow problems and the loadflow model of the IEEE RTS '96 is at the core of the electricity system simulator. A comparison of loadflow results obtained from the GAMS and PSAT implementations is part of assuring that the GAMS implementation of the loadflow model and, hence, the economic dispatch models underlying the electricity system simulator are correct.

2.2.1 Solving simple loadflow problem with GAMS

Ward and Hale describe a computational method for solving loadflow problems and, in the paper, apply the methodology to a six-bus network.[50] The one-line diagram of Ward and Hale's network is reproduced in Figure 2.2 and the bus and transmission line specifications are given in Tables 2.2 and 2.1, respectively. The off-nominal transformer ratios are $n_{65} = 1.025$ and $n_{43} = 1.100$.

Table 2.1: Bus specifications of sample electricity system

Bus	$\|V\|$	θ	P^S	Q^S
	pu	pu	pu	pu
1	1.05	0		
2	1.10		0.50	
3			-0.55	-0.13
4			0.00	0.00
5			-0.30	-0.18
6			-0.50	-0.05

The power flow model is based upon three fundamental relationships:

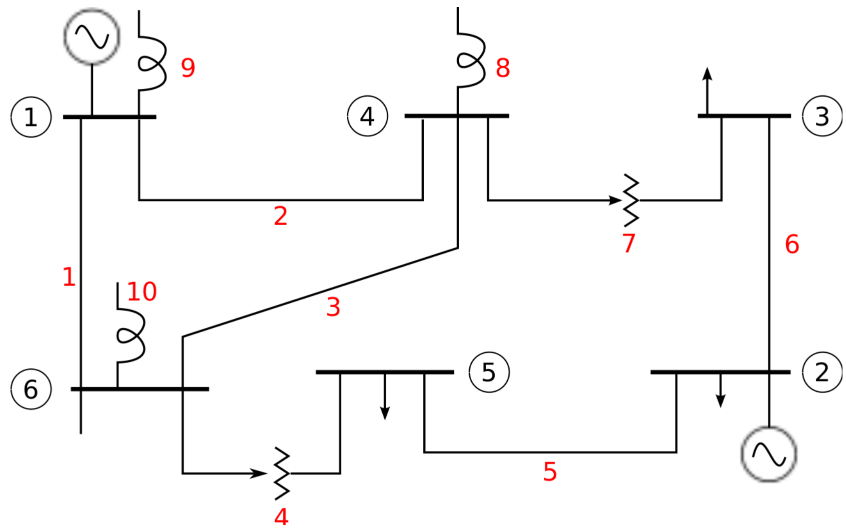

Figure 2.2: One-line diagram of sample electricity system (Source: Ward and Hale [50])

Table 2.2: Transmission line parameters of sample electricity system

Transmission line Branch	Number	Resistance pu	Reactance pu
1–4	2	0.080	0.370
1–6	1	0.123	0.518
1–7	9	0.000	-29.500
2–3	6	0.723	1.050
2–5	5	0.282	0.640
3–4	7	0.000	0.133
4–6	3	0.097	0.407
4–7	8	0.000	-34.100
5–6	4	0.000	0.300
6–7	10	0.000	-28.500

1. The relationship between voltage, current, and admittance is given by:

$$I = YV \tag{2.1}$$

The current flowing at bus k is equal to the sum of the current flowing from that bus to the adjacent nodes:

$$I_k = \sum_{m \in N_k} I_{km}$$

Substituting the expression for I from (2.1) into the above equation yields:

$$I_k = \sum_{m \in N_k} Y_{km} V_m \tag{2.2}$$

Rewriting the above using, for each term, expressions with the real and imaginary parts explicitly stated gives:

$$I_k^{Re} + \jmath I_k^{Im} = \sum_{m \in N_k} (G_{mk} + \jmath B_{mk}) \left(V_m^{Re} + \jmath V_m^{Im}\right) \tag{2.3}$$

In the above, complex voltage and current are expressed in terms of their real and imaginary parts as follows:

$$I = I^{Re} + \jmath I^{Im} \tag{2.4}$$

$$V = V^{Re} + \jmath V^{Im} \tag{2.5}$$

Expanding the RHS (Right-Hand Side) of (2.3) and collecting the real and imaginary parts yields the following expressions for the power flow at bus k:

$$I_k^{Re} = \sum_{m \in N_k} \left(G_{km} V_m^{Re} - B_{km} V_m^{Im}\right)$$

$$I_k^{Im} = \sum_{m \in N_k} \left(G_{km} V_m^{Im} + B_{km} V_m^{Re}\right)$$

The following equivalent expressions make use of the bus self- and mutual-admittance matrices in lieu of the branch admittances:

$$I_k^{Re} = \sum_{m \in N_k} \left(Y_{km}^{G} V_m^{Re} - Y_{km}^{Im} V_m^{Im}\right) \tag{2.6}$$

$$I_k^{Im} = \sum_{m \in N_k} \left(Y_{km}^{G} V_m^{Im} + Y_{km}^{Im} V_m^{Re}\right) \tag{2.7}$$

2. The apparent power flow at bus k is given by:

$$S_k = V_k I_k^*$$

It is convenient to express S_k in terms of its real and imaginary components P_k and Q_k.

$$P_k^S + \jmath Q_k^S = \left(V_k^{Re} + \jmath V_k^{Im}\right)\left(I_k^{Re} - \jmath I_k^{Im}\right) \tag{2.8}$$

Expanding the RHS of (2.8) and collecting the real and imaginary parts yields the following expressions for the power flow at bus k:

$$P_k^S = I_k^{Re} V_k^{Re} + I_k^{Im} V_k^{Im} \tag{2.9}$$
$$Q_k^S = I_k^{Re} V_k^{Im} - I_k^{Im} V_k^{Re} \tag{2.10}$$

3. The magnitude of the voltage is given by:

$$|V_k|^2 = \left(V_k^{Re}\right)^2 + \left(V_k^{Im}\right)^2 \tag{2.11}$$

The power flow model is obtained by writing out (2.6), (2.7), (2.9), (2.10), and (2.11) for each bus. The complete model is as follows:

$$\begin{aligned}
I_k^{Re} &= \sum_{m \in N_k} \left(Y_{km}^G V_m^{Re} - Y_{km}^{Im} V_m^{Im}\right) && \forall\, k \in N \\
I_k^{Im} &= \sum_{m \in N_k} \left(Y_{km}^G V_m^{Im} + Y_{km}^{Im} V_m^{Re}\right) && \forall\, k \in N \\
P_k^S/100 &= I_k^{Re} V_k^{Re} + I_k^{Im} V_k^{Im} && \forall\, k \in N \\
Q_k^S/100 &= I_k^{Re} V_k^{Im} - I_k^{Im} V_k^{Re} && \forall\, k \in N \\
|V|^2 &= {V_k^{Re}}^2 + {V_k^{Im}}^2 && \forall\, k \in N
\end{aligned} \tag{2.12}$$

Dividing P_k^S and Q_k^S by a factor of 100 is required to convert these quantities from a *per-unit* to a MW and MVAr basis, respectively. The loadflow problem implemented in

GAMS is shown in (2.13).

$$
\begin{aligned}
&\underset{\substack{P_k, Q_k, I_k^{Re}, I_k^{Im} \\ V_k^{Re}, V_k^{Im}, |V_k|}}{\text{minimize}} && z = \sum_{k \in K} (|V_k|)^2 \\
&\text{subject to} && I_k^{Re} = \sum_{m \in N_k} \left(Y_{km}^{G} V_m^{Re} - Y_{km}^{Im} V_m^{Im} \right) \quad \forall\, k \in N \\
& && I_k^{Im} = \sum_{m \in N_k} \left(Y_{km}^{G} V_m^{Im} + Y_{km}^{Im} V_m^{Re} \right) \quad \forall\, k \in N \\
& && P_k^S/100 = I_k^{Re} V_k^{Re} + I_k^{Im} V_k^{Im} \quad \forall\, k \in N \\
& && Q_k^S/100 = I_k^{Re} V_k^{Im} - I_k^{Im} V_k^{Re} \quad \forall\, k \in N \\
& && |V|^2 = {V_k^{Re}}^2 + {V_k^{Im}}^2 \quad \forall\, k \in N \\
&\text{variable bounds} && \\
& && \begin{array}{ccccc}
-\infty & \leq & P_k^S & \leq & +\infty \\
-\infty & \leq & Q_k^S & \leq & +\infty \\
-\infty & \leq & I_k^{Re} & \leq & +\infty \\
-\infty & \leq & I_k^{Im} & \leq & +\infty \\
-\infty & \leq & V_k^{Re} & \leq & +\infty \\
-\infty & \leq & V_k^{Im} & \leq & +\infty \\
-\infty & \leq & |V_k| & \leq & +\infty
\end{array}
\end{aligned}
\tag{2.13}
$$

To complete the implementation of the problem in GAMS requires:

- specifying the terminal conditions and
- calculating the self- and mutual-admittances.

Specifying terminal conditions

The terminal conditions, as given in [50], are reproduced in Table 2.2. There are several points worth noting:

- The phase angle of Bus No. 1 is set to zero. This is the *slack* bus. With respect to power flow along a line, it is the difference in phase angle between adjacent buses that is important and not the magnitude of the phase angles themselves. To that end, the phase angle of the slack bus is fixed at zero and the net real and reactive power injected at this bus, as well as the phase angles of the other buses, are part of the solution to the loadflow problem.

- The voltage magnitude of Buses No. 1 and 2 are specified. These are buses with *voltage regulation*, as is typically the case with buses that have generating units. The voltage magnitude and real power output will be fixed for these buses (except in the case of the slack bus — see above) and the voltage magnitude of the other buses is part of the solution to the loadflow problem.

- For the remaining buses — that is, non-slack buses and buses without voltage regulation — the net real and reactive power injected at the buses is specified.

Note that the loadflow problem is fully specified (*i.e.*, has zero degrees of freedom): there are $5|N|$ equations and $7|N|$ variables of which $2|N|$ of the variables have been specified (see Table 2.1). Hence, any arbitrary objective function can be used.

Calculating self- and mutual-admittances

Implementing the model in GAMS requires that the elements of the admittance matrix, Y, be calculated. From the omission of additional data, it is implicit in Ward and Hale's electricity system the transmission lines are 'short' and that only the series impedance, Z, needs to be considered. The impedance of a circuit is defined as [41, p 65]:

$$Z = R + \jmath X \tag{2.14}$$

The reciprocal of the of the impedance is known as the admittance, Y, an expression for which is can be readily derived from (2.14).

$$\begin{aligned}
Y &= \frac{1}{Z} \\
&= \frac{1}{R + \jmath X} \\
&= \frac{1}{R + \jmath X} \times \frac{R - \jmath X}{R - \jmath X} \\
Y &= \frac{R}{R^2 + X^2} - \jmath \frac{X}{R^2 + X^2} \qquad (2.15)
\end{aligned}$$

(2.15) is simplified by first defining conductance, G, and susceptance, B, such that:

$$G = \frac{R}{R^2 + X^2} \tag{2.16}$$

$$B = \frac{-X}{R^2 + X^2} \tag{2.17}$$

and substituting these expressions in (2.15). Thus:

$$Y = G + \jmath B \tag{2.18}$$

By inspecting the above, one sees that the conductance and the susceptance are the real and imaginary components, respectively, of the admittance.

In the GAMS program, parameters are declared to represent the conductance and susceptance of each branch and the self- and mutual-admittance matrices of each bus.

For convenience, separate variables — Y^{Re} and Y^{Im} — are used for the real and imaginary parts of the admittance matrices.

Conductance and susceptance are calculated using (2.16) and (2.17), respectively, and the values for R and X shown in Table 2.2. The self-admittance of bus k is the sum of the admittance of all branches that terminate at the node:

$$\begin{aligned} Y_{kk}^{Re} &= \sum_{m \in j_k} G_{mk} \\ Y_{kk}^{Im} &= \sum_{m \in j_k} B_{mk} \end{aligned} \tag{2.19}$$

The mutual-admittance between buses k and m is the negative sum of the admittance of all branches that connect nodes k and m:

$$\begin{aligned} Y_{km}^{Re} &= -\sum_{m \in j_{km}} G_{km} \\ Y_{km}^{Im} &= -\sum_{m \in j_{km}} B_{km} \end{aligned} \tag{2.20}$$

Adjustment for off-nominal transformer ratios: (2.19) and (2.20) assume unity transformer ratios at buses k and m but there are two off-nominal transformer ratios in [50]: $n_{65} = 1.025$ and $n_{43} = 1.100$. For branches km with turn ratio $n_{km} \neq 1$, adjustments to the values calculated above are required.

- For self-admittance, the term $\sum_{m \in j_{km}} \left(n_{km}^2 - 1\right) Y_k$ is added to the value calculated via (2.19):

$$\begin{aligned} Y_{kk}^{Re} &= \left(Y_{kk}^{Re}\right)' + \sum_{m \in j_{km}} \left(n_{km}^2 - 1\right) G_{km} \\ Y_{kk}^{Im} &= \left(Y_{kk}^{Im}\right)' + \sum_{m \in j_{km}} \left(n_{km}^2 - 1\right) B_{km} \end{aligned}$$

- For mutual-admittance, the term $-\sum_{m \in j_{km}} (n_{km} - 1) Y_k$ is added to the value calculated via (2.20):

$$\begin{aligned} Y_{km}^{Re} &= \left(Y_{km}^{Re}\right)' - \sum_{m \in j_{km}} (n_{km} - 1) G_{km} \\ Y_{km}^{Im} &= \left(Y_{km}^{Im}\right)' - \sum_{m \in j_{km}} (n_{km} - 1) B_{km} \end{aligned}$$

A program to solve this model is implemented in GAMS (see Appendix E.1 for a listing of the source code). The model is solved using the NLP (Non-Linear Programming) solver MINOS [38] and the GAMS program executes successfully in 0.003 seconds on an Intel Core 2 Duo commodity personal computer. The results obtained using GAMS are identical to those provided in [50].

2.2.2 Solving simple loadflow problem with PSAT

PSAT[37] is commercial-grade software for analyzing power flows developed by the Power Systems group at the University of Waterloo.

The loadflow problem from [50] is implemented in PSAT (see Appendix E.2). The results are identical to those provided in the literature and calculated using GAMS.

Implementing the example from Ward and Hale in GAMS and PSAT serves two purposes. Firstly, a loadflow problem is embedded within the economic dispatch problem and solving an economic dispatch problem is required to simulate the pre-dispatch and real-time phases of electricity system operation. The above exercise demonstrates that the capability exists to properly specify and solve loadflow problems in GAMS.

Secondly, PSAT is to be used to validate the GAMS implementation of the loadflow problem for the IEEE RTS '96. The above exercise also demonstrates the capability to properly specify electricity systems in the input format required by PSAT.

2.2.3 Solving IEEE RTS '96 loadflow problem

A loadflow problem for the IEEE RTS '96 (see Figure 2.1 in Section 1 for the one-line diagram) is implemented in both GAMS using the model above and PSAT. The development of each will be discussed in turn.

In GAMS, the procedure for specifying the loadflow problem for the IEEE RTS '96 is analogous to what was done for the electricity system described by Ward and Hale. The ensuing section focuses on the aspects of the development of the loadflow problem that are unique to the IEEE RTS '96 and the reader is encouraged to revisit Section 2.2.1 for supplemental information.

Specifying terminal conditions

As before, there are three classes of buses that need to be specified: slack, voltage-regulated, and other.

1. Recall that the net real and reactive power injected of the slack are part of the solution to the loadflow problem. Although not strictly required, a bus with a single generator and no demand makes a good slack bus and, thus, *Attlee* is selected.

2. Table 2.3 lists the busses in the IEEE RTS '96 with voltage regulation, with values of voltage magnitude as reported in [20, Table 7]. The buses are those with generating units and Arnold (bus #14).[2]

Table 2.3: Buses with voltage regulation in IEEE RTS '96

Bus	$\lvert V_k \rvert^*$
Abel	1.035
Adams	1.035
Alder	1.025
Arne	1.020
Arnold	0.980
Arthur	1.014
Asser	1.017
Astor	1.050
Attlee	1.050
Aubrey	1.050
Austen	1.050

3. Nominal values of the real and reactive power supply for each bus and output of each generator are provided [20, Tables 1 and 7] and these are reproduced in Table 2.4. Using these values, the net real and reactive power injected at each bus — with the exception of the slack bus and buses without voltage regulation — is specified.

The above leads to the following terminal conditions for the IEEE RTS '96 shown in Table 2.5.

Calculate self- and mutual-admittances

Two kinds of branches exist in the IEEE RTS '96: transmission lines and a 100 MVAr reactor at Alber (bus #6). For the former, resistance, reactance, and line-charging susceptance are given in Table 2.6.

[2] A synchronous condenser is present at Arnold and these are regulated to hold constant terminal voltage.

Table 2.4: Real and reactive power demand in IEEE RTS '96

	Demand		Supply		
Bus	P_k^D	Q_k^D	Unit #	P_u°	Q_u°
Abel	108	22	1,2	10	0
			3,4	76	14.1
Adams	97	20	1,2	10	0
			3,4	76	7
Adler	180	37			
Agricola	74	15			
Aiken	71	14			
Alber	136	28			
Alder	125	25	1–3	80	17.2
Alger	171	35			
Ali	175	36			
Allen	195	40			
Arne	265	54	1–3	95.1	40.7
Arnold	194	39	1	0	13.7
Arthur	317	64	1–5	12	0
			6	155	0.05
Asser	100	20	1	155	25.22
Astor	333	68	1	400	137.4
Attar	181	37			
Attila	128	26			
Attlee			1	400	108.2
Aubrey			1–6	50	-4.96
Austen			1,2	155	31.79
Austen			3	350	71.78

Table 2.5: Specified terminal conditions for IEEE RTS '96 loadflow problem

Bus	$\|V\|$	θ	P	Q
Abel	1.035		64	
Adams	1.025		75	
Adler			-180	-37
Agricola			-74	-15
Aiken			-71	-14
Alber			-136	-28
Alder	1.025		115	
Alger			-171	-35
Ali			-175	-36
Allen			-195	-40
Anna			0	0
Archer			0	0
Arne	1.020		20.3	
Arnold	0.980		-194	
Arthur	1.014		-102	
Asser	1.017		55	
Aston			0	0
Astor	1.050		67	
Attar			-181	-37
Attila			-128	-26
Attlee	1.050	0		
Aubrey	1.050		300	
Austen	1.050		660	
Avery			0	0

Table 2.6: Transmission line parameters in IEEE RTS '96

Transmission line		R	X	B^C
Name	Number	pu	pu	pu
Abel–Adams	1–2	0.003	0.014	0.461
Abel–Adler	1–3	0.055	0.211	0.057
Abel–Aiken	1–5	0.022	0.085	0.023
Adams–Agricola	2–4	0.033	0.127	0.034
Adams–Alber	2–6	0.050	0.192	0.052
Adler–Ali	3–9	0.031	0.119	0.032
Adler–Avery	3–24	0.002	0.084	0.000
Agricola–Ali	4–9	0.027	0.104	0.028
Aiken–Allen	5–10	0.023	0.088	0.024
Alber–Allen	6–10	0.014	0.061	2.459
Alder–Alger	7–8	0.016	0.061	0.017
Alger–Ali	8–9	0.043	0.165	0.045
Alger–Allen	8–10	0.043	0.165	0.045
Ali–Anna	9–11	0.002	0.084	0.000
Ali–Archer	9–12	0.002	0.084	0.000
Allen–Anna	10–11	0.002	0.084	0.000
Allen–Archer	10–12	0.002	0.084	0.000
Anna–Arne	11–13	0.006	0.048	0.100
Anna–Arnold	11–14	0.005	0.042	0.088
Archer–Arne	12–13	0.006	0.048	0.100
Archer–Austen	12–23	0.012	0.097	0.203
Arne–Austen	13–23	0.011	0.087	0.182
Arnold–Asser	14–16	0.005	0.059	0.082
Arthur–Asser	15–16	0.002	0.017	0.036
Arthur–Attlee (1,2)	15–21	0.006	0.049	0.103
Arthur–Avery	15–24	0.007	0.052	0.109
Asser–Aston	16–17	0.003	0.026	0.055
Asser–Attar	16–19	0.003	0.023	0.049
Aston–Astor	17–18	0.002	0.014	0.030
Aston–Aubrey	17–22	0.014	0.105	0.221
Astor–Attlee (1,2)	18–21	0.003	0.026	0.055
Attar–Attila (1,2)	19–20	0.005	0.040	0.083
Attila–Austen (1,2)	20–23	0.003	0.022	0.046
Attlee–Aubrey	21–22	0.009	0.068	0.142

The initial calculation of self- and mutual-admittances is carried out as in Section 2.2.1 and, like there, adjustments are made for transformers with off-nominal transformer ratios — these lines and their transformer ratios are reproduced in Table 2.7.

Table 2.7: Branches with off-nominal transformer ratios in IEEE RTS '96

Branch		n_{km}
Adler–Avery	3–24	1.015
Ali–Anna	9–11	1.030
Ali–Archer	9–12	1.030
Allen–Anna	10–11	1.015
Allen–Archer	10–12	1.015

Unlike the electricity system presented by Ward and Hale, for the IEEE RTS '96, line-charging susceptance of each transmission line is provided. This is used to update the self-admittances calculated thus far by adding half of the line-charging susceptance of each transmission line terminating at a given bus to the self-admittance of that bus. That is:

$$Y^{Im\prime}{}_{kk} = \left(Y^{Im}_{kk}\right) + \sum_{m \in j_k} \frac{B^C_{mk}}{2}$$

This is in keeping with [50, p 399] in which line-charging capacitance () is lumped on buses at line terminals.[3]

The other type of "transmission line" is the 100 MVAr rector at the Alber bus (#6). It is modelled as a transmission line connecting Alber to "neutral" (or "ground", if you prefer) with conductance, susceptance, and line-charging all equal to zero.

Initialization of IEEE RTS '96 loadflow problem

By default, GAMS initializes variables to zero and, from this starting point, a feasible solution is not found to the loadflow problem for the IEEE RTS '96. An alternate problem initialization is used:

1. Set $V^{Re}_k = 1.0$ and $V^{Im}_k = 0.0 \; \forall \, k \neq \mathit{slack}$ (recall that the imaginary component of the slack bus voltage has already been set to zero). Note that voltage magnitudes are controlled to be at or near unity, on a per-unit basis, in real electricity systems.

2. Solve the loadflow problem using an admittance matrix in which the line-charging susceptances of transmission lines are ignored.

[3] It is common practice to ignore line-charging susceptance for transmission lines less than 80 km in length and, in keeping with this convention, line-charging susceptances for 90% of the lines in the system would be ignored. However, given that the data is available and has negligible impact on computational speed, line-charging susceptance is considered for all transmission lines.

With this advanced initialization, a feasible solution to the final problem is obtained. The GAMS implementation of the loadflow problem is given in Appendix E.3. The terminal conditions for the IEEE RTS '96 are shown in Table 2.8; results from the solution of the GAMS implementation of the loadflow problem are in italics. There are a couple things worth noting:

Table 2.8: Results of GAMS implementation of loadflow problem for IEEE RTS '96

Bus	$\lvert V \rvert$	θ	P	Q
Abel	1.035	*-23*	64	*-12*
Adams	1.035	*-22*	75	*-66*
Adler	*0.964*	*-21*	-180	-37
Agricola	*0.984*	*-25*	-74	-15
Aiken	*1.038*	*-26*	-71	-14
Alber	*1.152*	*-29*	-136	*105*
Alder	1.025	*-23*	115	*22*
Alger	*0.996*	*-26*	-171	-35
Ali	*0.976*	*-23*	-175	-36
Allen	*1.067*	*-25*	-195	-40
Anna	*1.009*	*-18*	0	0
Archer	*1.025*	*-17*	0	0
Arne	1.020	*-15*	20.3	*-21*
Arnold	0.980	*-15*	-194	*-97*
Arthur	1.014	*-5*	-102	*-92*
Asser	1.017	*-5*	55	*-2*
Aston	*1.023*	*-2*	0	0
Astor	1.050	*-1*	67	*68*
Attar	*1.023*	*-7*	-181	-37
Attila	*1.038*	*-6*	-128	-26
Attlee	1.050	0	*302*	*119*
Aubrey	1.050	*6*	300	*-31*
Austen	1.050	*-5*	660	*109*
Avery	*0.985*	*-11*	0	0

- A common assumption is that, in a well-controlled electricity system, voltage magnitudes are maintained within the interval $[0.95, 1.05]$. In the base loadflow, the buses Alber and Allen exceed the upper bound of this interval.
- In the development of models to analyze the economics of electricity systems, it is common for the power flow equations to be simplified by:

1. The Maclaurin series expansion of sine and cosine functions are given below.[4]

$$\sin\theta = \theta - \frac{1}{6}\theta^3 \cdots \tag{2.21}$$

$$\cos\theta = 1 - \frac{1}{2}\theta^2 + \cdots \tag{2.22}$$

2. The phase angle difference between adjacent buses is assumed to be small and the second- or first-order approximations (2.21) and (2.22) are used.

Table 2.9 shows the difference in phase angle between adjacent buses for the base loadflow problem for the IEEE RTS '96. In many cases, the difference between phase angles at adjacent buses is non-negligible and the second assumption is certainly not valid.

Out of curiosity, the results obtained in the base loadflow are compared with a case where the line charging susceptance is ignored. At a high level, the results differ significantly especially with respect to the net reactive power at each bus and the reactive power flows along the transmission lines.

For completeness and because there is no apparent incremental computational effort required to do so, line charging susceptances are included in the model moving forward.

Validating IEEE RTS '96 loadflow problem with PSAT

The loadflow problem for the IEEE RTS '96 is implemented in PSAT (see Appendix E.4). The results are identical to those provided in the literature and calculated using GAMS.

2.3 Solving the economic dispatch problem

The objective of this section is to:

- Present the formulation of the economic dispatch problem used in this work.
- Show that the formulation is successful (*e.g.*, dispatch does not respect merit order).
- Discuss the importance of providing a good starting point for the MINLP solvers.

For the loadflow problem described in Table 2.5, the net power injected at each bus reflects the electricity demand for a single moment in time and a particular response of the generating units in the system to that demand. Of course, there exist other unit dispatches that would also satisfy the electricity demand in that time period though in different ways. Solving the economic dispatch problem means identifying the optimum output levels for the

[4] A power flow model using trigonometric functions is shown in (2.46).

Table 2.9: Difference in phase angle between adjacent buses in IEEE RTS '96

Bus k	Bus m	θ_{km} / °
Abel	Adams	0.1
Abel	Adler	-1.6
Abel	Aiken	2.7
Adams	Agricola	2.3
Adams	Alber	6.1
Adler	Ali	1.7
Adler	Avery	-10.3
Agricola	Ali	-2.4
Aiken	Allen	-0.4
Alber	Allen	-3.9
Alder	Alger	3.7
Alger	Ali	-3.7
Alger	Allen	-6.0
Ali	Anna	-4.5
Ali	Archer	-6.0
Allen	Anna	-6.7
Allen	Archer	-8.2
Anna	Arne	-3.8
Anna	Arnold	-2.8
Archer	Arne	-2.3
Archer	Austen	-12.1
Arne	Austen	-9.8
Arnold	Asser	-10.2
Arthur	Asser	0.7
Arthur	Attlee	-4.8
Arthur	Avery	6.1
Asser	Aston	-3.9
Asser	Attar	1.3
Aston	Astor	-1.0
Aston	Aubrey	-7.5
Astor	Attlee	-0.6
Attar	Attila	-0.8
Attila	Austen	-1.2
Attlee	Aubrey	-5.9

generators that satisfies the demand for electricity while also satisfying any and all technical and operational requirements. In this work, the economic dispatch problem is formulated as an MINLP. Section 2.3.1 discusses the objective function, Section 2.3.2 discusses the constraints, and Section 2.3.3 discusses the implementation in GAMS and indications that the formulation is successful.

2.3.1 Formulating the objective function

The surplus (or net energy benefit) for the n^{th} unit can be expressed as:

$$z_n = \int_0^{P_n^S} \left[\rho - \left(\frac{dC_n^{OM}}{dP_n^S}\right)\right] dP_n^S \tag{2.23}$$

The producer's surplus is obtained by summing the surplus over all units:

$$z = \sum_{n \in NG} \int_0^{P_n^S} \left[\rho - \left(\frac{dC_n^{OM}}{dP_n^S}\right)\right] dP_n^S \tag{2.24}$$

Social welfare is the total benefit realized by producers and consumers. Assuming that the consumers are *price insensitive*, the social welfare is equal to the producer's surplus just described. The dispatch objective is to maximize the social welfare of the electricity system and that can be expressed mathematically as:

$$\max z = \int_0^{P_S} \left[\rho - \left(\frac{dC_n^{OM}}{dP_n^S}\right)\right] dP_n^S \tag{2.25}$$

In the above formulation, the price depends only on electricity demand which is, as per the price-insensitive assumption, inelastic. Therefore, maximizing the social welfare of the system, is equivalent to

$$\min z = \int_0^{P_S} \left(\frac{dC_n^{OM}}{dP_n^S}\right) dP_n^S \tag{2.26}$$

Operating and maintenance costs can be subdivided into two categories: fixed and variable:

$$C_n^{OM} = C_n^{FOM} + C_n^{VOM} \tag{2.27}$$

As the name implies, fixed operating and maintenance costs do no vary with the power output of the unit. As (2.26) is concerned with the change in operating and maintenance costs, this term can be ignored. The objective function can now be written in terms of C_n^{VOM} alone:

$$\min z = \int_0^{P_S} \left(\frac{dC_n^{VOM}}{dP_n^S}\right) dP_n^S \tag{2.28}$$

The most important contribution to the variable operating and maintenance costs is fuel, C_n^{fuel}, and substituting the above expression for C_n^{VOM} into (2.28) gives:

$$\min z = \int_0^{P_S} \left(\frac{dC_n^{fuel}}{dP_n^S} \right) dP_n^S \tag{2.29}$$

Fuel costs

The fuel costs can expressed in terms of the heat input to the boiler as follows:

$$C_n^{fuel} = \dot{q}_n FC_n L \tag{2.30}$$

In many cases, it is more convenient to express the cost of fuel as a function of the unit's incremental heat rate. The marginal cost of generation is obtained by taking the first derivative of (2.30) with respect to P_n^S:

$$\frac{dC_n^{fuel}}{dP_n^S} = FC_n L \frac{d\dot{q}_n}{dP_n^S}$$

Now, integrating both sides gives

$$\begin{aligned} \int_0^{P_{nt}^S} \frac{dC_n^{fuel}}{dP_n^S} &= FC_n L \int_0^{P_n^S} \frac{d\dot{q}_n}{dP_n^S} \\ &\approx FC_n L \sum_{b=1}^{N_b} y_{bn} IHR_{bn} \end{aligned} \tag{2.31}$$

Summary of objective function

So, using the above expressions for start-up and fuel costs in (2.58), one can write expression for the objective function:

$$\begin{aligned} z = &\sum_{n \in NG_D} \sum_{b=1}^{N_b} y_{bn} IHR_{bn} FC_n L \frac{1}{10^3} \\ &+ \sum_{r \in RM} C^{import} \cdot RM_r^{slack} \end{aligned} \tag{2.32}$$

The last term in the objective function represents the cost needed to provision reserve power from outside of the electricity system. It is not unheard of for imported electricity to be orders of magnitude greater than the typical HEP (Hourly Electricity Price) which has provoked electricity systems to set price caps (*e.g.*, $10,000 per megawatt hour in Ontario's electricity system). In the electricity system simulator, C^{import} is set at a ten percent premium to the most expensive bid of any generator in the system.

2.3.2 Specifying constraints

With respect to constraints, the focus is on those governing the performance of the generating units and those which guarantee that a reasonable quantity of reserve power is maintained. The power flow model is the other set of important constraints governing the operation of the system and, as they have already been described in detail in Section 2.2, they will be mentioned only in passing.

Generating Unit Constraints

Capacity utilization A unit's *availability* is the quantity of power that it is able to produce in a given time period. This is nominally different from the unit's *capacity* — the nominal quantity of power that the unit is designed to output — but, for the purposes of this work, the two terms are used interchangeably.

Each unit is obliged to offer its full capacity in every time period. It is assumed that the offer price of each supply 'bid' is equal to the the marginal cost of generating that power. This constraint specifies that the capacity utilization of each unit in each time period is equal to the sum of the portion of each of its bids that was accepted in the time period.

$$P_n = \sum_{b=1}^{N_b} y_{bn} \tag{2.33}$$

As $P_{b,n}^{bid} > P_{b-1,n}^{bid}$ is true in all cases, in an optimal solution it must also be the case that $y_{b-1,n} = y_{b-1,n}^{max}$ for $y_{bn} > 0$ to be true.

In any given time period, there are a number of separate 'markets' into which units are bidding. In this study, in addition to the power market, a number of different markets for reserve power are considered. A description of the constraints specifying the requirements for each of these markets follows in Sections 2.3.2 and 2.3.2. The following constraint specifies that the capacity utilization of each unit in each time period must equal the sum of the unit's contribution to the energy and reserve markets in that time period.

$$P_n = P_n^S + \sum_{r \in RM} P_{nr}^R \tag{2.34}$$

Minimum and maximum power output In general, there is some minimum output $P^{min} > 0$ below which a unit cannot operate. And, there is of course an upper bound to the power that a unit can produce. These constraints fix units availability at zero when units are 'off' and specify the lower and upper bounds of units capacity when units are 'on'.

$$(1 - \omega_n)\, P_n^{\min} \leq P_n^S \leq (1 - \omega_n)\, P_n^{max} \tag{2.35}$$

$$(1 - \omega_n)\, Q_n^{\min} \leq Q_n^S \leq (1 - \omega_n)\, Q_n^{max} \tag{2.36}$$

ω_n is a binary variable used to represent the state of unit n in time period t; it should have a value of one if the unit is off and zero otherwise. This leads to two cases in (2.36):

1. When $\omega_n = 0$, the allowable range of values for P_n^S and Q_n^S is:

$$\begin{array}{ccccc} P_n^{min} & \leq & P_n^S & \leq & P_n^{max} \\ Q_n^{min} & \leq & Q_n^S & \leq & Q_n^{max} \end{array}$$

2. When $\omega_n = 1$, the allowable range of values for P_n^S and Q_n^S collapses such that $P_n^S = 0$ and $Q_n^S = 0$. The unit cannot output power hence the interpretation that $\omega_n = 1$ indicates the unit is off.

Within [20], hydroelectric units have assumed to have negligible start-up costs, negligible marginal operating costs, and able to output power over the interval $[0, P^{max}]$. As such, when $P^S = 0$, the value of ω is indeterminate; it is possible that $\omega_n = 0$ even though the plant is *off*. With $\omega_n = 0$, as per (2.36), a hydroelectric unit would be able to have non-zero reactive power output while having zero real power output.

Steps taken to mitigate the effect of this during electricity system simulation are discussed in Section 2.4.

Power flow constraints The net real power injected at each bus is the difference between the total output from generating units generators and the local demand. The same is true for reactive power except at buses with a shunt admittance to ground; these have extra reactive power. The coefficient '100' converts the admittance of the bus from a *per-unit* basis to a *MVAr* basis.

$$P_k = \sum_{n \in NG_k} \left(P_n^S\right) - P_k^D \tag{2.37}$$

$$Q_{kt} = \begin{cases} \displaystyle\sum_{n \in N_k} Q_n^S - Q_k^D \; k \notin N^{shunt} \\ \displaystyle\sum_{n \in N_k} Q_n^S - Q_k^D + 100\,|V_k|^2 \; k \in N^{shunt} \end{cases} \tag{2.38}$$

Combining the polar representation for complex voltage, $V = |V| e^{\hat{\jmath}\theta}$ with Euler's formula, $e^{\pm\hat{\jmath}\theta} = \cos\theta \pm \hat{\jmath}\sin\theta$ yields the following expression of complex voltage at node k using trigonometric functions.

$$V_k = |V_k| \left(\cos\theta_k + \hat{\jmath}\sin\theta_k\right) \tag{2.39}$$

Substituting this expression in (2.2) gives the following expression for the current at node k:

$$I_k = \sum_{m\in N_k} Y_{km} |V_m| \left(\cos\theta_m + \hat{\jmath}\sin\theta_m\right) \tag{2.40}$$

1. Expanding the RHS (2.40) and collecting the real and imaginary parts yields the following expression for the current at bus k:

$$I_k^{Re} = \sum_{m\in N_k} \left(Y_m^{Re} |V_m| \cos\theta_m - Y_{km}^{Im} |V_m| \sin\theta_m\right) \tag{2.41}$$

$$I_k^{Im} = \sum_{m\in N_k} \left(Y_m^{Re} |V_m| \sin\theta_m + Y_{km}^{Im} |V_m| \cos\theta_m\right) \tag{2.42}$$

2. Using the expression for voltage from (2.40), one obtains expressions for real and reactive power flow at node k in terms of voltage magnitude, phase angle, and current

$$P_k^S + \hat{\jmath}Q_k^S = |V_k| \left(\cos\theta_k + \hat{\jmath}\sin\theta_k\right)\left(I_k^{Re} - \hat{\jmath}I_k^{Im}\right) \tag{2.43}$$

   Again, expanding the RHS of (2.43) and collecting the real and imaginary parts yields the following expressions for the power flow at bus k.

$$P_k^S = I_k^{Re} |V_k| \cos\theta_k + I_k^{Im} |V_k| \sin\theta_k \tag{2.44}$$

$$Q_k^S = I_k^{Re} |V_k| \sin\theta_k - I_k^{Im} |V_k| \cos\theta_k \tag{2.45}$$

Using (2.41), (2.42), (2.44), and (2.45) yields a power flow model equivalent to (2.12) using trigonometric functions:

$$\begin{aligned}
I_k^{Re} &= \sum_{m\in N_k} \left(Y_m^{Re} |V_m| \cos\theta_m - Y_{km}^{Im} |V_m| \sin\theta_m\right) && \forall\, k \in N \\
I_k^{Im} &= \sum_{m\in N_k} \left(Y_m^{Re} |V_m| \sin\theta_m + Y_{km}^{Im} |V_m| \cos\theta_m\right) && \forall\, k \in N \\
P_k^S/100 &= I_k^{Re} |V_k| \cos\theta_k + I_k^{Im} |V_k| \sin\theta_k && \forall\, k \in N \\
Q_k^S/100 &= I_k^{Re} |V_k| \sin\theta_k - I_k^{Im} |V_k| \cos\theta_k && \forall\, k \in N
\end{aligned} \tag{2.46}$$

Reserve power constraints

In modern electricity systems, reliability is important. Therefore, from the pool of available capacity, a portion is selected for a back-up role. This provides the system operator with flexibility in meeting demand should, for example, a dispatched unit unexpectedly go off-line or demand significantly exceed that which was anticipated.

A *contingency* is an unforeseen event that causes a shortfall between the current supply and the current demand. Examples of contingencies are the tripping of a unit, an unanticipated load, and the grounding of a transmission line. Having reserve power available increases the likelihood that the system operator can successfully deal with these and other contingencies.

Different electricity systems have different standards for reserve power. Reserves are typically classified with respect to time and synchronicity:

Time: This indicates the allotted time within which the generator must deliver the requested quantity of reserve power.

Synchronicity: This indicates whether or not the unit providing the reserve power is synchronized to the grid.

The reserve requirements used in this study are based upon those used in Ontario which, in turn, adhere to NERC (North American Electric Reliability Corporation). It is assumed that the ten-minute reserve requirement is equal to the largest contingency and the 30-minute reserve is greater by half the second-largest contingency. The two 400 MW_e nuclear units operate as 'base' load units. Therefore, the ten-minute reserve is set at 400 MW_e — half of which must be spinning — and the 30-minute reserve is set at 600 MW_e.

Reserve power requirements P^R_{nr} represents the capacity of unit n that is committed to reserve market r. In the study, three reserve markets are considered and the total power committed to each is expressed as follows:

- Ten-minute spinning reserve.

$$RM^S_{10^{sp}} = \sum_{n \in NG} P^R_{n,10^{sp}} \left(1 - \omega_n\right) \tag{2.47}$$

- Ten-minute non-spinning reserves.

$$RM^S_{10^{ns}} = RM^S_{10^{sp}} + \sum_{n \in NG, \tau^{up}_n = 0} \omega_n P^R_{n,10^{ns}} \tag{2.48}$$

- 30-minute non-spinning reserve.

$$RM_{30}^{S} = RM_{10^{ns}}^{S} + \sum_{n \in NG} P_{n,30}^{R} \left(1 - \omega_n\right) + \sum_{n \in NG, \tau_n^{up}=0} \omega_n P_{n,30}^{R} \tag{2.49}$$

The amount of power that a unit can provide to each class of reserve is limited by its ramp rate. Unit ramp rates for the IEEE RTS '96 [20] are shown in Table C.6.

$$P_{nr}^{R} \leq \left(\Delta P\right)_n \tau_r^{R} \tag{2.50}$$

Maximum reserve power contribution There must be sufficient ten-minute reserves to cover the largest contingency and at least half of the ten-minute reserves must be spinning. In addition, there should be sufficient additional 30-minute reserves to cover half of the second-largest contingency. The supply/demand balance for each reserve market is:

$$RM_r^S \geq RM_r^D \tag{2.51}$$

In practice, there may not be sufficient availability within the system to meet the obligations for reserve power. Either, then, the system operates with less than the desired quantity of reserve power or other provisions are made. In this study, $\left(P_r^R\right)^{slack}$ represents the shortfall between the reserve power required and the reserve power that the system can provide.

$$RM_r^S + RM_r^{slack} \geq RM_r^D \tag{2.52}$$

2.3.3 Economic dispatch model validation

The economic dispatch problem is summarized below.

$$\begin{array}{ll}
\underset{\substack{\omega_n, y_{bn} \\ P_n, P_n^S, P_{nr}^R \\ Q_n^S, P_k, Q_k \\ I_k^{Re}, I_k^{Im}, \theta_k, |V_k| \\ RM_r^S, RM_r^{slack}}}{\text{minimize}} & z = \displaystyle\sum_{n \in NG_D} \sum_{b=1}^{N_b} y_{bn} IHR_{bn} FC_n \frac{1}{10^3} \\
& \quad + \displaystyle\sum_{r \in RM} C^{import} \cdot RM_r^{slack}
\end{array}$$

subject to:

Capacity utilization

$$P_n = \sum_{b=1}^{N_b} y_{bn} \qquad \forall\, n \in NG$$

Power disaggregation between real and reserve markets

$$P_n = P_n^S + \sum_{r \in RM} P_{nr}^R \qquad \forall\, n \in NG$$

Minimum and maximum real and reactive power output

$$\begin{aligned}
(1-\omega_n)\, P_n^{\min} \leq P_n^S \leq (1-\omega_n)\, P_n^{max} &\qquad \forall\, n \in NG \\
(1-\omega_n)\, Q_n^{\min} \leq Q_n^S \leq (1-\omega_n)\, Q_n^{max} &\qquad \forall\, n \in NG
\end{aligned}$$

Net power available at each bus

$$P_k = \sum_{n \in NG_k} \left(P_n^S\right) - P_k^D \qquad \forall\, k \in N$$

$$Q_k = \begin{cases} \displaystyle\sum_{n \in N_k} Q_n^S - Q_k^D & \forall\, k \notin N^{shunt} \\ \displaystyle\sum_{n \in N_k} Q_n^S - Q_k^D + 100\,|V_k|^2 & \forall\, k \in N^{shunt} \end{cases}$$

Full power flow model

$$\begin{aligned}
I_k^{Re} &= \sum_{m \in N_k} \left(Y_m^{Re}\,|V_m| \cos\theta_m - Y_{km}^{Im}\,|V_m| \sin\theta_{mt}\right) &\qquad \forall\, k \in N \\
I_k^{Im} &= \sum_{m \in N_k} \left(Y_m^{Re}\,|V_m| \sin\theta_m + Y_{km}^{Im}\,|V_m| \cos\theta_m\right) &\qquad \forall\, k \in N \\
P_k^S/100 &= I_k^{Re}\,|V_k| \cos\theta_k + I_k^{Im}\,|V_k| \sin\theta_k &\qquad \forall\, k \in N \\
Q_k^S/100 &= I_k^{Re}\,|V_k| \sin\theta_k - I_k^{Im}\,|V_k| \cos\theta_k &\qquad \forall\, k \in N
\end{aligned}$$

Reserve power

$$
\begin{aligned}
RM^S_{10^{sp}} &= \sum_{n \in NG} P^R_{n,10^{sp}} \left(1 - \omega_n\right) \\
RM^S_{10^{ns}} &= RM^S_{10^{sp}} + \sum_{n \in NG, \tau^{up}_n = 0} \omega_n P^R_{n,10^{ns}} \\
RM^S_{30} &= RM^S_{10^{ns}} + \sum_{n \in NG} P^R_{n,30} \left(1 - \omega_n\right) \\
&\quad + \sum_{n \in NG, \tau^{up}_n = 0} \omega_n P^R_{n,30}
\end{aligned}
$$

Maximum reserve power contribution

$$
\begin{aligned}
P^R_{nr} &\leq (\Delta P)_n \, \tau^R_r && \forall\, k \in N, r \in RM \\
RM^S_r + RM^{slack}_r &\geq RM^D_r && \forall\, r \in RM
\end{aligned}
$$

Variable bounds

$$
\begin{array}{rcccl}
0 & \leq & y_{bn} & \leq & P^{bid}_{bn} \\
0 & \leq & P_n & \leq & P^{max}_n \\
0 & \leq & P^S_n & \leq & P^{max}_n \\
0 & \leq & P^R_n & \leq & P^{max}_n \\
Q^{min}_n & \leq & Q^S_n & \leq & Q^{max}_n \\
-\infty & \leq & P_k & \leq & +\infty \\
-\infty & \leq & Q_k & \leq & +\infty \\
-\infty & \leq & I^{Re}_k & \leq & +\infty \\
-\infty & \leq & I^{Im}_k & \leq & +\infty \\
-\infty & \leq & \theta_k & \leq & +\infty \\
0 & \leq & |V_k| & \leq & +\infty \\
0 & \leq & RM^S_r & \leq & +\infty \\
-\infty & \leq & RM^{slack}_r & \leq & +\infty
\end{array}
$$

A program to solve this problem is implemented in GAMS. The program is solved using the DICOPT (DIscrete and Continuous OPTimizer) MINLP solver with CONOPT specified [15] to solve the relaxed MINLP problem and the NLP sub-problems and CPLEX specified for the MIP (Mixed-Interger Programming) master problems.[5] The GAMS program executes successfully in 0.05 seconds on an Intel Core i7 Commodity personal computer.

[4] The Power Flow Study design exercise [9, p 370] offers guidelines on reasonable bounds for the voltage magnitudes. Bounding the voltage at each non-supply bus to ±0.05 pu is a good start.

[5] The NLP solver MINOS worked equally as well as an NLP solver.

Parameter values and initial values for the decision variables are the same as specified for the loadflow problem in Section 2.2.3. For the record, Table 2.10 summarizes the state of each bus in the solution of the economic dispatch problem.

Table 2.10: Results of GAMS implementation of economic dispatch problem for IEEE RTS '96: real power market

Bus	$\|V\|$	θ	P	Q	P^R
Abel	1.035	-27	12	6	72
Adams	1.035	-27	1	-48	94
Adler	0.961	-22	-180	-37	
Agricola	0.981	-27	-74	-15	
Aiken	1.036	-27	-71	-14	
Alber	1.149	-30	-136	104	
Alder	1.025	-28	52	39	123
Alger	0.993	-30	-171	-35	
Ali	0.973	-22	-175	-36	
Allen	1.063	-25	-195	-40	
Anna	1.004	-16	0	0	
Archer	1.018	-14	0	0	
Arne	1.020	-9	326	-26	
Arnold	0.980	-14	-194	-89	
Arthur	1.014	-5	-102	-88	
Asser	1.017	-5	55	-14	
Aston	1.039	-2	0	0	
Astor	1.050	-1	67	62	
Attar	1.023	-6	-181	-37	
Attila	1.038	-5	-128	-26	
Attlee	1.050	0	400	97	
Aubrey	1.050	2	134	-24	166
Austen	1.050	-3	611	111	49
Avery	0.983	-11	0	0	

It is worth noting that R_{30}^{slack} is non-zero in the optimal solution; there is insufficient capacity within the electricity system to meet all the requirements for reserve power.

To put the results in Table 2.10 in perspective, two additional scenarios are considered:

No reserve is the economic dispatch problem with the reserve power constraints removed.

Loadflow is an economic dispatch problem where, in addition to the reserve power constraints having been removed, the real and reactive power injected at each bus is fixed at the values in the solution of the loadflow problem.

Table 2.11: Power injected at each node for loadflow and economic dispatch problems

Bus	Net real power			Net reactive power		
	Loadflow	No reserves	Dispatch	Loadflow	No reserves	Dispatch
Abel	64	44	12	-12	-5	6
Adams	75	55	1	-66	-61	-48
Alber	-136	-136	-136	105	104	104
Alder	115	54	52	22	37	39
Arne	20	90	326	-21	-15	-26
Arnold	-194	-194	-194	-96	-88	-89
Arthur	-102	-162	-102	-92	-71	-88
Asser	55	55	55	-2	4	-14
Astor	67	67	67	68	70	67
Attlee	302	400	400	119	113	97
Aubrey	300	300	134	-31	-31	-24
Austen	660	660	611	110	114	111

In the solution to the loadflow problem, the net reactive power at the bus Arnold is -97 MVAr. The synchronous condenser at Arnold would need to output -57 MVAr to satisfy the supply-demand balance at this bus but this exceeds its lower bound of -50 MVAr.

Table 2.11 contrasts the real and reactive power injected at the buses with load regulation for the three different scenarios. Note that the power flows in each case are quite different.

Table 2.12 compares the difference in operating cost between the solutions to the three scenarios. The results are as expected:

Table 2.12: Difference in operating cost between loadflow and economic dispatch problems.

Scenario	z^*
Loadflow	31557
No reserves	29106
Dispatch	45601

- The operating cost in the *loadflow* scenario is \$31,557. This includes a charge equivalent to 0.1% of the VOM (Variable Operating and Maintenance) for the shortfall in reserve power at Arnold.
- One would expect the operating cost in the *no reserves* scenario to be better, or at least no worse, than that in the *loadflow* scenario and that is indeed the case. By:

– increasing output from the nuclear-powered generating unit at Attlee and the oil-fired units at Arne and

– decreasing output at oil-fired generating units at Arthur and Alder and output from the combustion turbines at Adams,

an alternative dispatch is found that satisfies the power demand at a cost that is 8% lower: Figure 2.3 shows the output of generating units grouped by location and type of power for all three scenarios.

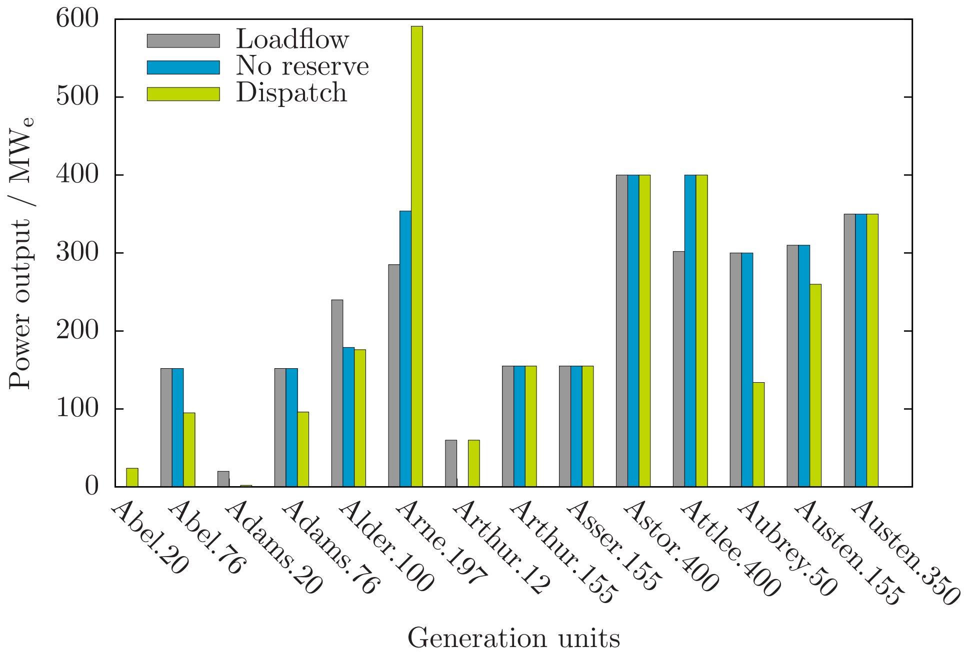

Figure 2.3: Comparison of generator output for cases with and without reserve power constraints

- One would expect the operating cost in the *dispatch* scenario to be greater than that in the *no reserves* as, in the former, there is an additional 600 MW_e of capacity that is required. The quantity of power that each generating unit has committed to the reserve market is shown in Table 2.10. There are a couple of additional comments of note regarding the *dispatch* scenario:

  – For the given demand, there is insufficent capacity in the system to provide the 600 MW_e of 30-minute, non-spinning reserve that is required. The cost incurred by the system for procurring the 96 MW_e of reserve capacity is 10% of the total operating cost.

– Figure 2.3 shows the power injected to the grid for each type of unit in the system. Note that the dispatch varies greatly between the *no reserves* and *dispatch* scenarios. Maintaining a reasonable quantity of reserve power is essential for reliable operation of electricity systems and taking this account leads to a significantly different generating unit dispatch than had this consideration not been included.

2.4 Simulating the electricity system

The electricty system simulator is modelled after the operation of the electrity system in Ontario [22]. Deregulated electricity systems in other jurisdictions (*e.g.*, NEM (National Electricity Market) in Australia) operate analagously.

As stated in the introduction, there are three phases to the simulation of the electricity system — pre-dispatch, real-time operation, and market settlement — and each phase involves solving an optimization problem (*i.e.*, maximizing the economic benefit to producers and consumers subject to a set of constraints). The general procedure for the electricity simulation is shown in Figure 2.4.

What follows is, for each phase, the requisite optimization problem and a discussion of the results.

2.4.1 Phase 1: Pre-dispatch

Optimizing the utilization of the capacity in the system requires that the system operator undertake preliminary scheduling of units well in advance. Generators need pre-notification of the electricty their units will need to produce and, for units that are energy constrainted, a decision needs to be taken *a priori* regarding how the available energy should be distributed in time. The *pre-dispatch* is a dynamic problem; conceptually, it consists of a series of economic dispatch problems where the solution in one period depends upon the solution of its predecessors. The formulation of the *pre-dispatch* problem as the economic dispatch problem extended by:

1. Adding a time index to the variables.
2. Adding dynamic constraints.

The *pre-dispatch* MINLP problem is considerably larger (*i.e.*, as measured, for example, by the number of equations and variables) than the preceding economic dispatch problem; its size changes proportionately with the number of time periods. Especially problematic is growth in the number of integer variables as upon which computational effort could depend exponentially. The problem of exponential growth in computation time is tackled within the scope of problem formulation in the following three ways:

1. Simiplification of the power-flow model.

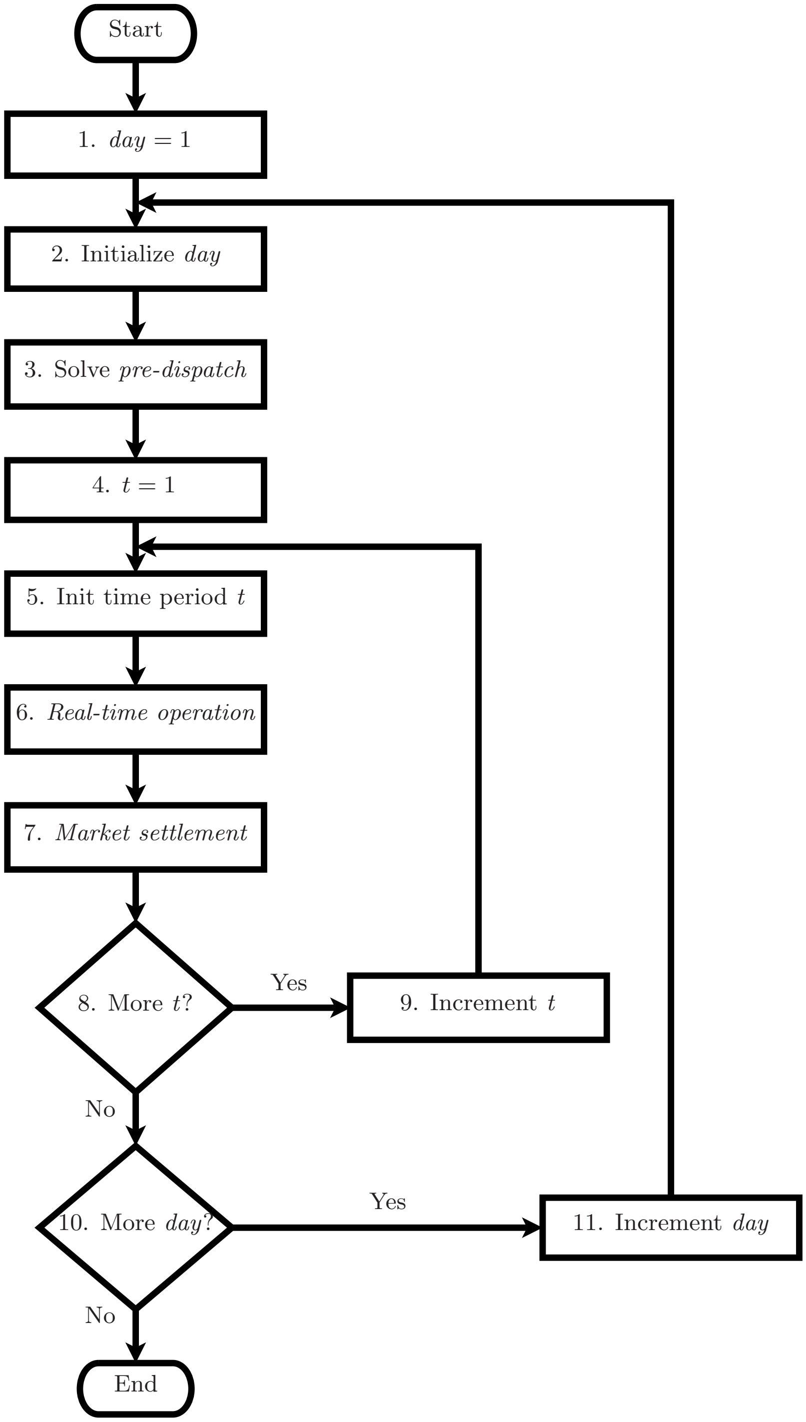

Figure 2.4: General procedure for electricity system simulation

2. Exact linearization of non-linear terms.

3. Enabling parallelism in the solution of the MIP master problems.

Adding time index

To all variables is added the index t delineating that variable values, in general, change from one time period to the next. The length of each time period is captured within the variable L_t; in this work, L_t is equal to one hour.

Adding dynamic constraints

Dynamic constraints contain variables with different values of the index t. A simple example of a dynamic constraint is:

$$V_t = V_{t-1} + \dot{m}_t^{in} - \dot{m}_t^{out} \tag{2.53}$$

where V_t, the volume in time t is equal to V_{t-1}, the volume at the end the previous period, and the difference between the additions, $\dot{m}_t^{in}$, and the withdrawals, $\dot{m}_t^{out}$ in the current time period.

Some care is required to ensure the *pre-dispatch* problem is reasonably specified at the first time periods of the electricity system simulation. When GAMS converts program statements specifying dynamic constraints into model equations it omits any terms containing variables with indices outside the domain of the controlling set. GAMS will ignore the term $V_{t=0}$ when processing the contraint represented by (2.53) which implicitly sets $V_{t=0} = 0$, which may not be a reasonable initial state. Therefore, for each of the dynamic constraints presented below, both the general form of the constraint and the form that applies to the initial time periods are presented.

In the present work, it is critical that 'special' dynamic equations are provided (or, alternatively, not specifying a reasonalbe initial state). Otherwise, the implicit assumption is that the electricity system is undergoing a 'black-start' (*i.e.*, recovering from a state in which all the generation is shut-down) and, given the dynamic constraints soon to be discussed, a feasible solution to the *pre-dispatch* will not exist.

Unit start-up The following constraint is added; it introduces the variable u which has a value of one if the unit started-up in the time period and zero otherwise.

$$u_{nt} \geq \omega_{n,t-1} - \omega_{nt} \tag{2.54}$$

Thermal units that are off require a relative large input of energy before they can begin generating electric power and this outlay could be significant. Noting this, the expression for a unit's variable operating and maintenance cost is updated such that:

$$C_{nt}^{VOM} = C_{nt}^{\textit{start-up}} + C_{nt}^{\textit{fuel}} \tag{2.55}$$

which leads to an additional term in the objective function:

$$\min z_{nt} = \int_0^{P^S} \left(\frac{dC_{nt}^{\textit{start-up}}}{dP_{nt}^S} \right) dP_{nt}^S = C_{nt}^{\textit{start-up}} \tag{2.56}$$

To a first approximation, the start-up cost is equal to the cost in terms of fuel to supply the input energy for start-up:

$$C_{nt}^{\textit{start-up}} = u_{nt} HI_n FC_n \tag{2.57}$$

Substituting (2.31) the above expression for C_n^{VOM} into (2.58) gives the new objective function:

$$\begin{aligned} z = & \sum_{t=1}^{T} \sum_{n \in NG} u_{nt} HI_n FC_n \\ & + \sum_{t=1}^{T} \sum_{n \in NG_D} \sum_{b=1}^{N_b} y_{bnt} IHR_{bnt} FC_n L_t \frac{1}{10^3} \\ & + \sum_{t=1}^{T} \sum_{r \in RM} C^{import} \cdot RM_{rt}^{slack} \end{aligned} \tag{2.58}$$

Black-start considerations: In the first time period, (2.54) reduces to

$$u_{nt} \geq -\omega_{nt}$$

For units with non-zero start-up costs, u_{nt} will be zero in the optimal solution and indeterminate for units whose start-up costs are zero. Given this, a 'special' version of (2.54) is not required.

Minimum uptimes and downtimes Once a decision has been made to turn a thermal power plant on or off, it must remain in that state for a minimum amount of time. $x_{nt}^{\textit{off}}$ and x_{nt}^{on} are introduced, representing the number of time periods for which the generator has been either on or off, respectively. These are defined as follows:

$$x_{nt}^{on} = \left(x_{n,t-1}^{on} + 1 \right) (1 - \omega_{nt}) \tag{2.59}$$

$$x_{nt}^{\textit{off}} = \left(x_{n,t-1}^{\textit{off}} + 1 \right) \omega_{nt} \tag{2.60}$$

The constraint on minimum uptime and downtime are expressed in terms of x_{nt}^{off} and x_{nt}^{on} as follows:

$$\left(x_{n,t-1}^{on} - \tau_n^{on}\right)\left(\omega_{nt} - \omega_{n,t-1}\right) \geq 0 \tag{2.61}$$

$$\left(x_{n,t-1}^{off} - \tau_n^{off}\right)\left(\omega_{n,t-1} - \omega_{nt}\right) \geq 0 \tag{2.62}$$

Black-start considerations: In the first time period, (2.59) and (2.60) reduce to:

$$\begin{aligned} x_{nt}^{on} &= 1 - \omega_{nt} \\ x_{nt}^{off} &= \omega_{nt} \end{aligned}$$

So, implicitly, it is indeterminate whether unit n was on or off at $t = 0$ nor is it known how long unit n has been in that (unknown) state. Coupled with the minimum uptime and downtime constraint — (2.61) and (2.62) — the consequece is a *pre-dispatch* problem for which no feasible solution exists:

- If the generating unit is 'on' in the initial time period (*i.e.*, $\omega_{nt} = 0$), then the unit must reamin 'on' for τ_n^{on} time periods.
- Conversely, if the generating unit is 'off' in the initial time period (*i.e.*, $\omega_{nt} = 1$), then the unit must reamin 'off' for τ_n^{off} time periods.
- There is a substantial difference between the peak and off-peak electricity demand. Suppose the first period is midnight, where demand is close to the daily minimum. Many of the generating units will necessarily be off in this first period and, due to the minimum downtime constraint, will not be available for the spike in demand that occurs in the morning. The *pre-dispatch* problem, as formulated, is infeasible.
- Similarly, the opposite situation would arise were to simulation to begin at a time near the daily maximum. Nearly all of the generating units would be dispatched in this first period and, due to the minimum uptime constraint, unable to shutdown when demand dropped off.

There is an implied operating history at the beginning of the electricity system simulation and this is incorporated by gradually imposing the minimum uptime and downtime constraints upon each generator until τ^{on} and τ^{off} time periods, respectively, have elapsed.

Constraints (2.61) and (2.62) then become:

$$\begin{aligned}
\left[x^{on}_{n,t-1} - (t-1)\right](\omega_{nt} - \omega_{n,t-1}) &\geq 0 & \qquad 2 \leq t \leq \tau^{on}_n \\
\left(x^{on}_{n,t-1} - \tau^{on}_n\right)(\omega_{nt} - \omega_{n,t-1}) &\geq 0 & t > \tau^{on}_n
\end{aligned}$$

$$\begin{aligned}
\left[x^{\mathit{off}}_{n,t-1} - (t-1)\right](\omega_{n,t-1} - \omega_{nt}) &\geq 0 & \qquad 2 \leq t \leq \tau^{\mathit{off}}_n \\
\left(x^{\mathit{off}}_{n,t-1} - \tau^{\mathit{off}}_n\right)(\omega_{n,t-1} - \omega_{nt}) &\geq 0 & t > \tau^{\mathit{off}}_n
\end{aligned}$$

As an example, consider a 76 MW_e coal-fired power plant. From Table C.7, we see that $\tau^{on} = 8$ and $\tau^{\mathit{off}} = 4$. Unlike constraints (2.61) and (2.62), the ones shown above would allow this generator to be active or idle for the first three periods (*i.e.*, $t = 1, 2, 3$) and then switch state. Implied, then, is that the generator had been either on for $t = -4, -3, \ldots, 0$ or off for $t = 0$.[6]

Unit ramp rates Thermal generating units are limited with respect to how quickly they can change their power output. This limit is known as a unit's ramp rate, ΔP^S. These constraints restrict a unit's power output in time period t based upon its output in time period *t-1* and its ramp rate.

$$\begin{aligned}
P^S_{nt} &\geq P^S_{n,t-1} - \left(\Delta P^S\right)_n L_t \\
P^S_{nt} &\leq P^S_{n,t-1} + \left(\Delta P^S\right)_n L_t
\end{aligned} \tag{2.63}$$

Black-start considerations: In the first time period, constraint (2.63) reduces to:

$$-\left(\Delta P^S\right)_n L_t \leq P^S_{t=1} \leq \left(\Delta P^S\right)_n L_t$$

Giving the ramp rates for the units in the IEEE RTS '96 (see Table C.6), the 197 MW_e oil-fired generators (at Arne) and the 350 MW_e coal-fired generator (at Austen) would be precluded from operating at maximum output during the first time period, as if they had both been off prior. The solution to this is to impose the ramp rate constraints starting with the second time period (*i.e.*, $t = 2$).

Unit energy constraints There exist generating units within electricity systems that are constrained not only in terms of power output but also in terms of *energy* output.

[6]This implementation would not work if τ^{on} and τ^{off} differed by more than a factor of two. Thankfully, this is not the case for the IEEE RTS-96!

For example, a hydroelectric generating unit — not run-of-the-river — could not produce energy in excess than that represented by the volume of water in its reservoir.

$$E_{kt} = E_{k,t-1} + \left(\dot{E}^{H}_{kt} - \sum_{n \in NG_k} P^{S}_{knt} \right) L_t \tag{2.64}$$

$$P_{kt} L_t \leq E_{kt} \tag{2.65}$$

Equation 2.64 defines the available energy in each time period t as the energy in time period *t-1* plus the net additions during the t time period. The limit on the output of these energy-constrained units is achieved via (2.65).

Black-start considerations: As the constraints currently stand, the reservoir is implicitly empty at the beginning of the simulation. During normal operation, one would expect the quantity of stored energy to fluctuate about some average: perhaps never full and also never empty. It is not obvious, though, what an reasonable starting value should be.

The solution is to begin the electricity system simulation a day in advance of the actual intitial period of interest. The energy reservoir is assumed to be half-full (or half-empty depending upon one's perspective) at the beginning of the preceeding day. The value of E_{kt} — and, for that matter, the other dynamic variables — at the end of the preceeding day is used to initialize the corresponding variables in the first time period of interest.

Simplification of the power flow model

Next to reducing the number of integer variables, reducing the complexity of the power model is the change that will have the greatest moderating effect on computational effort required to solve the pre-dispatch problem. This is done by substituting first-order MacLaurin series approximations of $\sin\theta$ and $\cos\theta$:

$$\sin\theta \approx \theta \tag{2.66}$$

$$\cos\theta \approx 1 \tag{2.67}$$

for $\sin\theta$ and $\cos\theta$ in (2.46). The resulting first-order power flow model is then:

$$I_{kt}^{Re} = \sum_{m=1}^{N_k} \left(Y_m^{Re} |V_{mt}| - Y_{km}^{Im} |V_{mt}| \theta_{mt} \right) \qquad \forall\, k \in N \tag{2.68}$$

$$I_{kt}^{Im} = \sum_{m=1}^{N_k} \left(Y_m^{Re} |V_{mt}| \theta_{mt} + Y_{km}^{Im} |V_{mt}| \right) \qquad \forall\, k \in N \tag{2.69}$$

$$P_{kt} = I_{kt}^{Re} |V_{kt}| + I_{kt}^{Im} |V_{kt}| \theta_{kt} \qquad \forall\, k \in N \tag{2.70}$$

$$Q_{kt} = I_{kt}^{Re} |V_{kt}| \theta_{kt} - I_{kt}^{Im} |V_{kt}| \qquad \forall\, k \in N \tag{2.71}$$

By employing an approximate power flow model, the *pre-dispatch* problem emulates the approach used in managing real power systems.[22] Note that, unlike the other strategies here employed to reduce the computational effort required to solve the *pre-dispatch* problem, simplifying the power flow model materially affects the results. That is, the dispatch obtained is different than would have been obtained had the full power flow model been used.

Due to the approximate nature of the power flow model, it is not certain that the calculated dispatch would be feasible in practice. To make sure, one would need to verify or redo the dispatch in each time period using an exact power flow model. This is precisely what is undertaken in the *real-time operation* phase of the electricity system simulation.

Exact linearization of non-linear terms

The constraints shown in (2.59)–(2.62) and (2.47)–(2.49) are non-linear; when expanded, each contains the product of a continuous variable and a binary variable. There are in total five such terms:

1. $x_{n,t-1}^{on} \omega_{nt}$
2. $x_{n,t-1}^{on} \omega_{n,t-1}$
3. $x_{n,t-1}^{off} \omega_{nt}$
4. $x_{n,t-1}^{off} \omega_{n,t-1}$
5. $P_{nrt}^{R} \omega_{nt}$

These terms are exactly linearizable. Reducing the number of non-linearities is expected to reduce the computational effort required to solve the *pre-dispatch* MINLP formulation: simpler NLP sub-problems and fewer linear approximations in the MIP master problems.

The linearization procedure, outlined in Appendix D, requires, for each non-linear term substituting a continous variable for the non-linear term, defining a new parameter, and adding a set of three constraints. Table 2.13 lists the terms, the continuous variables used to replace then, and the model constraints that are implicated and the new constraints are given below.

Table 2.13: Exactly linearizable terms in initial *pre-dispatch* phase economic dispatch problem

Term	Var	Constraint in which term is found				
		Minimum uptime defintion	Minimum downtime defintion	Minimum uptime constraint	Minimum downtime constraint	Reserve power supply
$x^{on}_{n,t-1}\omega_{nt}$	$\chi^{on}_{n,t-1}$	✓				
$x^{on}_{n,t-1}\omega_{n,t-1}$	$\psi^{on}_{n,t-1}$			✓		
$x^{off}_{n,t-1}\omega_{nt}$	$\chi^{off}_{n,t-1}$	✓	✓			
$x^{off}_{n,t-1}\omega_{n,t-1}$	$\psi^{off}_{n,t-1}$			✓	✓	
$P^{R}_{nrt}\omega_{nt}$	ρ_{nrt}					✓

Linearized minimum generator uptime constraints:

$$\chi^{on}_{n,t-1} - \psi^{on}_{n,t-1} - \tau^{on}\left(\omega_{nt} - \omega_{n,t-1}\right) \geq 0 \qquad \forall\, n \in NG, t = 1, 2, \ldots, T$$

$$x^{on}_{nt} = x^{on}_{n,t-1} - \chi^{on}_{n,t-1} + 1 - \omega_{nt} \qquad \forall\, n \in NG, t = 1, 2, \ldots, T$$

$$\chi^{on}_{nt} \leq x^{on}_{nt} \qquad \forall\, n \in NG, t = 1, 2, \ldots, T-1$$

$$\chi^{on}_{n,t-1} \geq x^{on}_{n,t-1} - M^{\chi}\left(1 - \omega_{nt}\right) \qquad \forall\, n \in NG, t = 1, 2, \ldots, T$$

$$\chi^{on}_{n,t-1} \leq M^{\chi}\omega_{nt} \qquad \forall\, n \in NG, t = 1, 2, \ldots, T$$

$$\psi^{on}_{nt} \leq x^{on}_{nt} \qquad \forall\, n \in NG, t = 1, 2, \ldots, T-1$$

$$\psi^{on}_{nt} \geq x^{on}_{nt} - M^{\psi}\left(1 - \omega_{nt}\right) \qquad \forall\, n \in NG, t = 1, 2, \ldots, T-1$$

$$\psi^{on}_{nt} \leq M^{\psi}\omega_{nt} \qquad \forall\, n \in NG, t = 1, 2, \ldots, T-1$$

Linearized minimum generator downtime constraints:

$$
\begin{aligned}
\psi^{\mathit{off}}_{n,t-1} - \chi^{\mathit{off}}_{n,t-1}\omega_{nt} - \tau^{\mathit{off}}\left(\omega_{n,t-1} - \omega_{nt}\right) &\geq 0 && \forall\, n \in NG, t = 1, 2, \ldots, T \\
x^{\mathit{off}} &= \chi^{\mathit{off}}_{n,t-1} + \omega_{nt} && \forall\, n \in NG, t = 1, 2, \ldots, T \\
\chi^{\mathit{off}}_{nt} &\leq x^{\mathit{off}}_{nt} && \forall\, n \in NG, t = 1, 2, \ldots, T-1 \\
\chi^{\mathit{off}}_{n,t-1} &\geq x^{\mathit{off}}_{n,t-1} - M^{\chi}\left(1 - \omega_{nt}\right) && \forall\, n \in NG, t = 1, 2, \ldots, T \\
\chi^{\mathit{off}}_{n,t-1} &\leq M^{\chi}\omega_{nt} && \forall\, n \in NG, t = 1, 2, \ldots, T \\
\psi^{\mathit{off}}_{nt} &\leq x^{\mathit{off}}_{nt} && \forall\, n \in NG, t = 1, 2, \ldots, T-1 \\
\psi^{\mathit{off}}_{nt} &\geq x^{\mathit{off}}_{nt} - M^{\psi}\left(1 - \omega_{nt}\right) && \forall\, n \in NG, t = 1, 2, \ldots, T-1 \\
\psi^{\mathit{off}}_{nt} &\leq M^{\psi}\omega_{nt} && \forall\, n \in NG, t = 1, 2, \ldots, T-1
\end{aligned}
$$

Linearized reserve power constraints:

$$
\begin{aligned}
P^{R}_{10^{sp},t} &= \sum_{n \in NG}\left(P^{R}_{n,10^{sp},t} - \rho_{n,10^{sp},t}\right) && \forall\, t \in T \\
P^{R}_{10^{ns},t} &= P^{S}_{10^{sp},t} + \sum_{n \in NG}\rho_{n,10^{ns},t}\ \forall \tau^{up}_{n} = 0 && \forall\, t \in T \\
P^{R}_{30,t} &= P^{R}_{10^{ns},t} + \sum_{n \in NG}\left(P^{R}_{n,30,t} - \rho_{n,30,t}\right) + \sum_{n \in NG}\rho_{n,30,t} && \forall\, t \in T \\
\rho_{nrt} &\leq P^{R}_{nrt}\ \forall r \in RM && \forall\, t \in T \\
\rho_{nrt} &\geq P^{R}_{nrt} - M^{\rho}_{n}\left(1 - \omega_{nt}\right) && \forall\, t \in T \\
\rho_{nrt} &\leq M^{\rho}_{n}\omega_{nt} && \forall\, t \in T
\end{aligned}
$$

Enabling parallelism in the solution of the MIP master problems

A branch-and-bound strategy is used to solve the MIP master problems. In non-trivial search trees, there are several candidate nodes to be evaluated each of which requires solving a related but distinct LP (Linear Programming) problem. With n processing cores available, it is possible for n nodes to be considered simultaneously with no impact on the solution time of any individual node. As the overall time required to perform an electricity system simulation is dominated by time spent solving MIP master problems, the overall simulation time sees an almost linear improvement with increased number of cores used.

Pre-dispatch problem formulation, implementation, and execution

The complete formulation of the *pre-dispatch* problem is as follows. The problem is implemented in GAMS.

$$
\begin{array}{cl}
\underset{\substack{u_{nt},y_{bnt} \\ P_{nt},P_{nt}^{S},P_{nrt}^{R} \\ Q_{nt}^{S},P_{kt},Q_{kt} \\ I_{kt}^{Re},I_{kt}^{Im},\theta_{kt},|V_{kt}| \\ x_{nt}^{on},x_{nt}^{off},\omega_{nt} \\ \chi_{n,t}^{on},\psi_{n,t}^{on},\chi_{n,t}^{off},\psi_{n,t1}^{off} \\ P_{rt}^{R},\rho_{nrt},E_{kt} \\ RM_{rt}^{S},RM_{rt}^{slack}}}{\text{minimize}} & z = \sum_{t=1}^{T}\sum_{n\in NG} u_{nt}HI_{n}FC_{n} \\
& \quad + \sum_{t=1}^{T}\sum_{n\in NG_{D}}\sum_{b=1}^{N_b} y_{bnt}IHR_{bnt}FC_{n}L_{t}\frac{1}{10^{3}} \\
& \quad + \sum_{t=1}^{T}\sum_{r\in RM} C^{import}\cdot RM_{rt}^{slack}
\end{array}
$$

subject to:

Capacity utilization

$$P_{nt} = \sum_{b=1}^{N_b} y_{bnt} \qquad \forall\, n\in NG, t\in T$$

Power disaggregation between real and reserve markets

$$P_{nt} = P_{nt}^{S} + \sum_{r\in RM} P_{nrt}^{R} \qquad \forall\, n\in NG, t\in T$$

Minimum and maximum real and reactive power output

$$
\begin{aligned}
(1-\omega_{nt})\,P_{n}^{\min} \le P_{nt}^{S} \le (1-\omega_{nt})\,P_{n}^{max} \qquad & \forall\, n\in NG, t\in T \\
(1-\omega_{nt})\,Q_{n}^{\min} \le Q_{nt}^{S} \le (1-\omega_{nt})\,Q_{n}^{max} \qquad & \forall\, n\in NG, t\in T
\end{aligned}
$$

Unit ramp rates

$$
\begin{aligned}
P_{nt}^{S} \ge P_{n,t-1}^{S} - \left(\Delta P^{S}\right)_{n} L_{t} \qquad & \forall\, n\in NG, t=2,3,\ldots,T \\
P_{nt}^{S} \le P_{n,t-1}^{S} + \left(\Delta P^{S}\right)_{n} L_{t} \qquad & \forall\, n\in NG, t=2,3,\ldots,T
\end{aligned}
$$

Unit start-up definition

$$u_{nt} \ge \omega_{n,t-1} - \omega_{nt} \qquad \forall\, n\in NG, t\in T$$

Minimum unit uptime (linearized)

$$\begin{aligned}
\chi^{on}_{n,t-1} - \psi^{on}_{n,t-1} - \tau^{on}\left(\omega_{nt} - \omega_{n,t-1}\right) &\geq 0 && \forall\, n \in NG, t = 1, 2, \ldots, T \\
x^{on}_{nt} &= x^{on}_{n,t-1} - \chi^{on}_{n,t-1} + 1 - \omega_{nt} && \forall\, n \in NG, t = 1, 2, \ldots, T \\
\chi^{on}_{nt} &\leq x^{on}_{nt} && \forall\, n \in NG, t = 1, 2, \ldots, T-1 \\
\chi^{on}_{n,t-1} &\geq x^{on}_{n,t-1} - M^{\chi}\left(1 - \omega_{nt}\right) && \forall\, n \in NG, t = 1, 2, \ldots, T \\
\chi^{on}_{n,t-1} &\leq M^{\chi}\omega_{nt} && \forall\, n \in NG, t = 1, 2, \ldots, T \\
\psi^{on}_{nt} &\leq x^{on}_{nt} && \forall\, n \in NG, t = 1, 2, \ldots, T-1 \\
\psi^{on}_{nt} &\geq x^{on}_{nt} - M^{\psi}\left(1 - \omega_{nt}\right) && \forall\, n \in NG, t = 1, 2, \ldots, T-1 \\
\psi^{on}_{nt} &\leq M^{\psi}\omega_{nt} && \forall\, n \in NG, t = 1, 2, \ldots, T-1
\end{aligned}$$

Minimum unit downtime (linearized)

$$\begin{aligned}
\psi^{off}_{n,t-1} - \chi^{off}_{n,t-1}\omega_{nt} - \tau^{off}\left(\omega_{n,t-1} - \omega_{nt}\right) &\geq 0 && \forall\, n \in NG, t = 1, 2, \ldots, T \\
x^{off} &= \chi^{off}_{n,t-1} + \omega_{nt} && \forall\, n \in NG, t = 1, 2, \ldots, T \\
\chi^{off}_{nt} &\leq x^{off}_{nt} && \forall\, n \in NG, t = 1, 2, \ldots, T-1 \\
\chi^{off}_{n,t-1} &\geq x^{off}_{n,t-1} - M^{\chi}\left(1 - \omega_{nt}\right) && \forall\, n \in NG, t = 1, 2, \ldots, T \\
\chi^{off}_{n,t-1} &\leq M^{\chi}\omega_{nt} && \forall\, n \in NG, t = 1, 2, \ldots, T \\
\psi^{off}_{nt} &\leq x^{off}_{nt} && \forall\, n \in NG, t = 1, 2, \ldots, T-1 \\
\psi^{off}_{nt} &\geq x^{off}_{nt} - M^{\psi}\left(1 - \omega_{nt}\right) && \forall\, n \in NG, t = 1, 2, \ldots, T-1 \\
\psi^{off}_{nt} &\leq M^{\psi}\omega_{nt} && \forall\, n \in NG, t = 1, 2, \ldots, T-1
\end{aligned}$$

Energy-constrained units

$$\begin{aligned}
E_{kt} &= E_{k,t-1} + \left(\dot{E}_{kt} - \sum_{n \in NG_k} P^S_{knt}\right) L_t && \forall\, k \in N^{ST}, t \in T \\
P_{kt}L_t &\leq E_{kt} && \forall\, k \in N^{ST}, t \in T
\end{aligned}$$

Net power available at each bus

$$\begin{aligned}
P_{kt} &= \sum_{n \in NG_k} \left(P^S_{nt}\right) - P^D_{kt} && \forall\, k \in N, t \in T \\
Q_{kt} &= \begin{cases} \sum_{n \in N_k} Q^S_{nt} - Q^D_{kt} & \forall\, k \notin N^{shunt} \\ \sum_{n \in N_k} Q^S_{nt} - Q^D_{kt} + 100\left|V_{kt}\right|^2 & \forall\, k \in N^{shunt} \end{cases} && \forall\, t \in T
\end{aligned}$$

Approximate power flow model

$$
\begin{aligned}
I_{kt}^{Re} &= \sum_{m=1}^{N_k} \left(Y_m^{Re} \left| V_{mt} \right| - Y_{km}^{Im} \left| V_{mt} \right| \theta_{mt} \right) && \forall\, k \in N, t \in T \\
I_{kt}^{Im} &= \sum_{m=1}^{N_k} \left(Y_m^{Re} \left| V_{mt} \right| \theta_{mt} + Y_{km}^{Im} \left| V_{mt} \right| \right) && \forall\, k \in N, t \in T \\
P_{kt} &= I_{kt}^{Re} \left| V_{kt} \right| + I_{kt}^{Im} \left| V_{kt} \right| \theta_{kt} && \forall\, k \in N, t \in T \\
Q_{kt} &= I_{kt}^{Re} \left| V_{kt} \right| \theta_{kt} - I_{kt}^{Im} \left| V_{kt} \right| && \forall\, k \in N, t \in T
\end{aligned}
$$

Reserve power (linearized)

$$
\begin{aligned}
P_{10^{sp},t}^{R} &= \sum_{n \in NG} \left(P_{n,10^{sp},t}^{R} - \rho_{n,10^{sp},t} \right) && \forall\, t \in T \\
P_{10^{ns},t}^{R} &= P_{10^{sp},t}^{S} + \sum_{n \in NG} \rho_{n,10^{ns},t} && \forall\, \tau_n^{up} = 0, t \in T \\
P_{30,t}^{R} &= P_{10^{ns},t}^{R} + \sum_{n \in NG} \left(P_{n,30,t}^{R} - \rho_{n,30,t} \right) && \\
&\quad + \sum_{n \in NG} \rho_{n,30,t} && \forall\, t \in T \\
\rho_{nrt} &\leq P_{nrt}^{R} \ \forall r \in RM && \forall\, t \in T \\
\rho_{nrt} &\geq P_{nrt}^{R} - M_n^{\rho} \left(1 - \omega_{nt} \right) && \forall\, t \in T \\
\rho_{nrt} &\leq M_n^{\rho} \omega_{nt} && \forall\, t \in T
\end{aligned}
$$

Maximum reserve power contribution

$$
\begin{aligned}
P_{nrt}^{R} &\leq \left(\Delta P \right)_{nt} \tau_r^{R} && \forall\, k \in N, r \in RM, t \in T \\
RM_{rt}^{S} + RM_{rt}^{slack} &\geq RM_r^{D} && \forall\, r \in RM, t \in T
\end{aligned}
$$

Variable bounds

$$
\begin{array}{rclcl}
0 & \leq & y_{bnt} & \leq & P_{bn}^{bid} \\
0 & \leq & P_{nt} & \leq & P_{n}^{max} \\
0 & \leq & P_{nt}^{S} & \leq & P_{n}^{max} \\
0 & \leq & P_{nrt}^{R} & \leq & P_{n}^{max} \\
Q_{n}^{min} & \leq & Q_{nt}^{S} & \leq & Q_{n}^{max} \\
0 & \leq & \omega_{nt} & \leq & 1 \\
0 & \leq & u_{nt} & \leq & 1 \\
0 & \leq & x_{nt}^{on} & \leq & +\infty \\
0 & \leq & \chi_{nt}^{on} & \leq & +\infty \\
0 & \leq & \psi_{nt}^{on} & \leq & +\infty \\
0 & \leq & x_{nt}^{off} & \leq & +\infty \\
0 & \leq & \chi_{nt}^{off} & \leq & +\infty \\
0 & \leq & \psi_{nt}^{off} & \leq & +\infty \\
0 & \leq & E_{kt} & \leq & E^{max} \\
-\infty & \leq & P_{kt} & \leq & +\infty \\
-\infty & \leq & Q_{kt} & \leq & +\infty \\
-\infty & \leq & I_{kt}^{Re} & \leq & +\infty \\
-\infty & \leq & I_{kt}^{Im} & \leq & +\infty \\
0.95 & \leq & |V_{kt}| & \leq & 1.05^{7} \\
-\infty & \leq & \theta_{kt} & \leq & +\infty \\
0 & \leq & \rho_{nrt} & \leq & P_{n}^{max} \\
0 & \leq & RM_{rt}^{S} & \leq & +\infty \\
-\infty & \leq & RM_{rt}^{slack} & \leq & +\infty
\end{array}
$$

The load duration curve for the system is shown in Figure 2.5. Peak demand is 3135 $\mathrm{MW_e}$ and off-peak demand is 1062 $\mathrm{MW_e}$. Also shown in the Figure is the system capacity of 3405 $\mathrm{MW_e}$. Given that the 30-minute non-spining reserve requirement is 600 $\mathrm{MW_e}$ and the surplus generating capacity is 270 $\mathrm{MW_e}$, the system will not be able to internally meet the reliability standards at or near peak loads.

In this study, each simulation begins on the first day of the year which is arbitrarily chose to be a Monday. *Pre-dispatch* spans a time horizon of one day subdivided into one-hour time periods. Figure 2.6 shows the aggregate electricity demand in the IEEE RTS '96 for the week of interest plus the single day that immediately preceeds it.[8] There is a cyclical trend to the demand over the course of each — peak during the evening and off-peak late at night/early in the morning — with demand on the weekends being markedly lower than during the week.

To avoid anomalies in the results during the period of interest, the initial *pre-dispatch*

[7]The Power Flow Study design exercise [9, p 370] offers guidelines on reasonable bounds for the voltage magnitudes. Voltages at buses with voltage regulation is fixed; voltages at buses without voltage regulation (*i.e.*, non-supply buses) is bounded to ±0.05 pu.

[8]Appendix B explains the methodology used to calculate the demand in each time period.

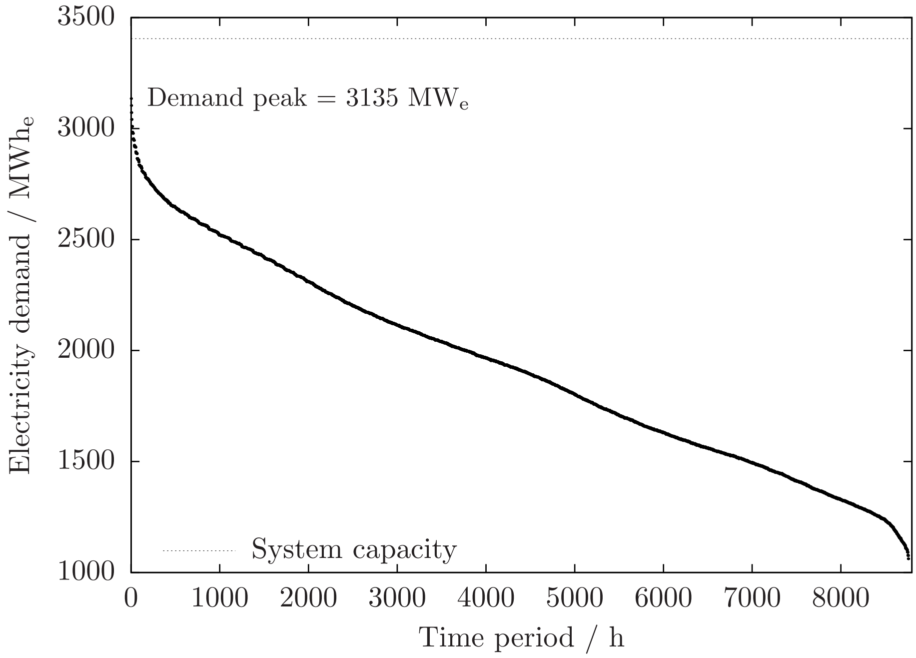

Figure 2.5: Load duration curve for IEEE RTS '96

period occurs over a 48-hour period.[9] The division between the 'black-start' period and the period of interest is highlighted in Figure 2.6.

Pre-dispatch results

There are three ways in which the results of the *pre-dispatch* phase inform the remainder of the electricity system simulation: establishing the utilization of energy-constrained generating units and providing a good initialization for the *real-time operation* problem.

Output of energy-constrained units The IEEE RTS '96 contains six hydroelectric generating units located at bus Aubrey, each with a capacity of 50 MW$_e$ during the first half of the year, reduced by 10% during the second half of the year. These units are assumed to draw a supply of water from a common reservoir. The inflow of water varies by season with an hourly average of 192 MWh$_{e,eq}$ in the first half of the year, a low of 55 MWh$_{e,eq}$ during the third quarter, and a mid-level of 110 MWh$_{e,eq}$ from October through December. The reservoir capacity is assumed to be 5385 MWh$_{e,eq}$: one week's worth of storage during peak-flow periods.

[9] In practice, this achieved by solving two *pre-dispatch* of 24-hour horizons in sequence starting with the beginning of the day immediately preceding the period of interest.

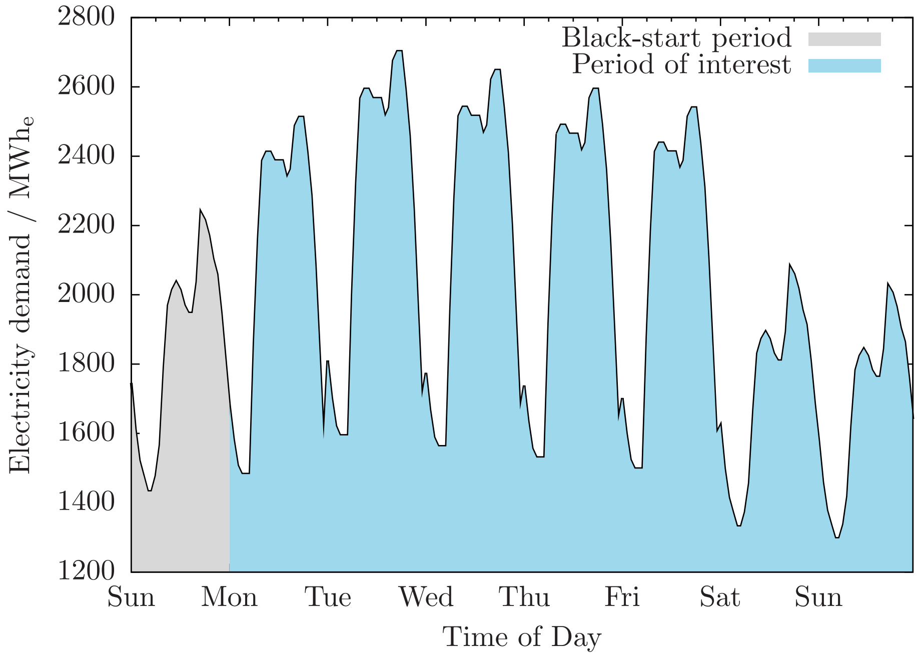

Figure 2.6: Aggregate electricity demand in IEEE RTS '96 for week of interest

Given that the inflow is less than the total capacity of the hydroelectric units, some rationing of the available water is necessary. It would seem reasonable to use less of the available energy when demand is low such that the full capacity of the units can be harnessed when demand is greatest. Figure 2.7 illustrates the outcome of the *pre-dispatch* as relates specifically to the hydroelectric units at the beginning of the electricity system simultation.

The electrical output from the hydroelectric generating units during the first 24-hours is zero. During this time, the output of these units is fully committed to the reserve market and the reservoir volume increase from an initial 2962 $\mathrm{MWh}_{e,eq}$ to 5330 $\mathrm{MWh}_{e,eq}$ at the end of the day.

Given the rate of water influx and reservoir capacity limit, some discharge of water is necessary starting in the second day — the first of the actual simulation period. On average, the generating unit output matches the rate of water inflow; that is, there is no net change in the quantity of energy stored. The remaining hydroelectric capacity is fully dispatched to the reserve market.

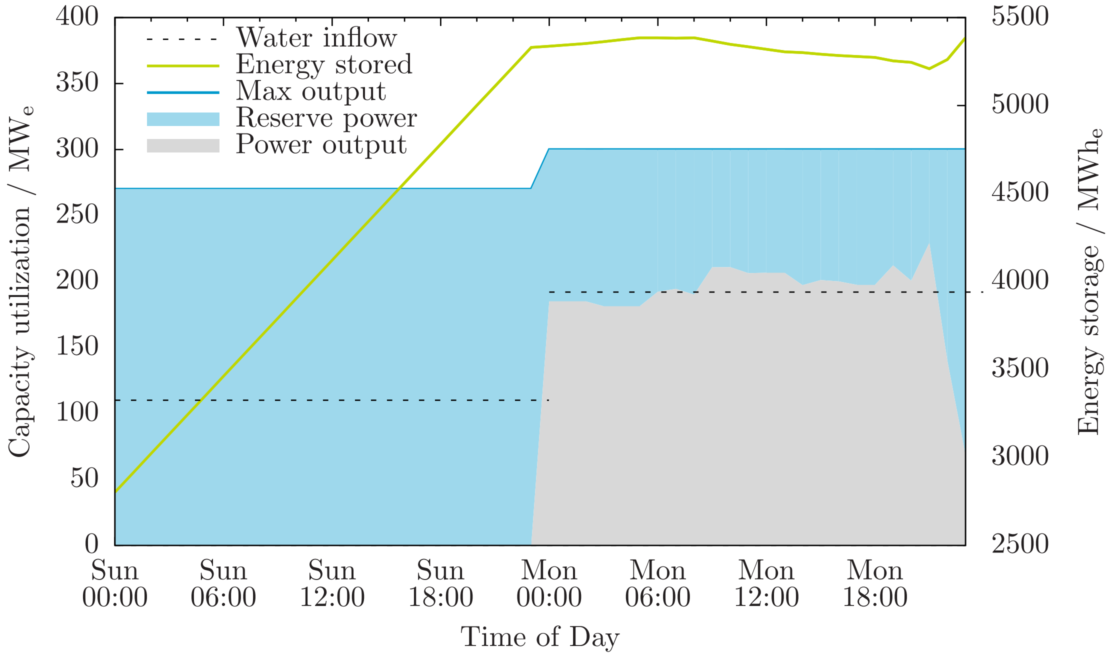

Figure 2.7: Energy scheduling results of pre-dispatch phase

2.4.2 Phase 2: Real-time operation

The demand for electricity changes continuosuly and frequent changes to the output of generating untis is required to regulate voltage and respond to contingencies and to do so in an economically optimal way. Up until perhaps as little as five minutes before any given time, the system operator is updating its forecast of demand, recalculating the optimal utilization of the generating units, and resending dispatch instructions to generators. There is normally some (small) difference between the actual demand, generator outputs, and power flows and the that predicted by the solution of the final economic dispatch problem. In the electricity system simulation, the difference is assumed to be negligible and the solution of this problem to be indicative of the actual system performance.

The *real-time operation* MINLP problem can be thought of as a simplified *pre-dispatch* phase problem. Important areas of deviation include:

1. The model is no longer dynamic though time dependancy is preserved.
2. Real power flow model is reinstituted.
3. Output of some generating units, notably the hydroelectric units, is constrained.

Time dependency

The MINLP problem in the *real-time operation* phase considers economic dispatch for a single time period. The state of time-dependent variables is specified using parameters whose values are obtained from the solution of the MINLP problem for the previous time period. For example, the minimum uptime constraint in the *real-time operation* phase MINLP is written as:

$$x_n^{on} = \left[(x_n^{on})^\circ + 1 \right] (1 - \omega_n) \tag{2.72}$$

where $(x_n^{on})^\circ$ is a parameter specifying the number of time periods generating unit n has been on prior.

Exact linearization not necessary In the development of the *pre-dispatch* MINLP problem, five exactly linearizable non-linear terms are identified (see Table 2.13) and this is exploited to render the *pre-dispatch* problem more readily soluble. In the *real-time operation*, the fact that the minimum uptime and downtime constraints are no longer dynamic means that the first four non-linear terms in Table 2.13 do not exist in this phases MINLP problem.

Moreso, the fact that there is a single time period, in and of itself, reduces the problem complexity and there is no longer an impetus to linearize the reserve power constraint. Indeed, the economic dispatch problem from Section 2.3 is of similar size to the *real-time operation* MINLP problem and solves routinely without the need for any such transformation.

Power flow modelling

The premise of the *real-time operation* phase is that the acutal performance of the electricity system is being described. This requires that the full power flow be used.

Especially with the use of the full power flow model, a poor choice of initialization values for the variables results in either the RMINLP (Relaxed Mixed-Interger Non-Linear Programming) problem or the NLP subproblems being found to be infeasible. In the former case, DICOPT will terminate unsuccessfully and, in the latter, DICOPT may undergo an excessive number of iterations making little if any progress. It has been found in practice that a good initialization can be obtained from the solution of the *pre-dispatch* phase MINLP.

Generating unit output

Generating unit availability The *real-time operation* phase's perspective of the optimal operation of the system is myopic relative to that within the *pre-dispatch* phase. The diffeence in perspective can lead to conflicting signals regarding the optimal dispatch of units.

The *pre-dispatch* solution may suggest that an expensive oil-fired unit remain on through periods of low demand so that it is available for high-demand periods later on. To shut the unit down immediately would, due to the minimum downtime constraint, preclude it from being available. The *real-time operation* problem would suggest the more locally-optimal solution that shuts the oil-fired unit down. The implication for the high-demand period is potentially shortfall in available power.

The solution is to enforce the unit commitment of *pre-dispatch* within the *real-time operation* phase. This is achieved in the model by fixing $\omega_n = 0$ for all units that were 'on' in the solution to the *pre-dispatch* problem. So, units committed cannot shutdown but, if need be, units that were shutdown are able to start-up.

Units that are energy constrained As mentioned at the beginning of Section 2.4.1, one of the purposes of the *pre-dispatch* phase is to determine a plan for using energy-constrained units (*i.e.*, the hydroelectric generating units in the IEEE RTS '96). The value of $P^S_{kn}\ \forall\, n \in NG^H$, already initialized using the results from the *pre-dispatch* phase, are fixed at those values.

Unlike the other generating units in the IEEE RTS '96, the hydroelectric units have a minimum real power output of zero. Thus, in the model, it is possible for the hydroelectric units to have zero real power output and non-zero reactive power output. This is tolerated in the *pre-dispatch* phase. In the *real-time operation* phase, Q^S_n is fixed at zero for any hydroelectric unit where $P^S_n = 0$.

Real-time operation problem formulation, implementation, and execution

The complete formulation of the *real-time operation* problem is as follows.

$$
\begin{aligned}
\underset{\substack{u_n,\, y_{bn} \\ P_n,\, P^S_n,\, P^R_{nr} \\ Q^S_n,\, P_k,\, Q_k \\ I^{Re}_k,\, I^{Im}_k,\, \theta_k,\, |V_k| \\ x^{on}_n,\, x^{off}_n,\, \omega_n \\ RM^R_r,\, RM^{slack}_r}}{\text{minimize}} \quad z = & \sum_{n\in NG} u_n HI_n FC_n \\
& + \sum_{n\in NG_D} \sum_{b=1}^{N_b} y_{bn} IHR_{bn} FC_n L_t \frac{1}{10^3} \\
& + \sum_{r\in RM} C^{import} \cdot RM^{slack}_r
\end{aligned}
$$

subject to:

Capacity utilization

$$
P_n = \sum_{b=1}^{N_b} y_{bn} \qquad \forall\, n \in NG
$$

Power disaggregation between real and reserve markets

$$P_n = P_n^S + \sum_{r \in RM} P_{nr}^R \qquad \forall\, n \in NG$$

Minimum and maximum real and reactive power output

$$(1-\omega_n)\, P_n^{\min} \le P_n^S \le (1-\omega_n)\, P_n^{max} \qquad \forall\, n \in NG$$
$$(1-\omega_n)\, Q_n^{\min} \le Q_n^S \le (1-\omega_n)\, Q_n^{max} \qquad \forall\, n \in NG$$

Unit ramp rates

$$P_n^S \ge \left(P_n^S\right)^\circ - \left(\Delta P^S\right)_n L_t \qquad \forall\, n \in NG$$
$$P_{nt}^S \le \left(P_n^S\right)^\circ + \left(\Delta P^S\right)_n L_t \qquad \forall\, n \in NG$$

Unit start-up definition

$$u_n \ge \omega_n^\circ - \omega_n \qquad \forall\, n \in NG$$

Minimum unit uptime

$$x_n^{on} = \left[\left(x_n^{on}\right)^\circ + 1\right](1-\omega_n) \qquad \forall\, n \in NG$$
$$\left[\left(x_n^{on}\right)^\circ - \tau_n^{on}\right](\omega_n^\circ - \omega_n) \ge 0 \qquad \forall\, n \in NG$$

Minimum unit downtime

$$x_n^{off} = \left[\left(x_n^{off}\right)^\circ + 1\right]\omega_n \qquad \forall\, n \in NG$$
$$\left[\left(x_n^{off}\right)^\circ - \tau_n^{off}\right](\omega_n^\circ - \omega_n) \ge 0 \qquad \forall\, n \in NG$$

Net power available at each bus

$$P_k = \sum_{n \in NG_k} \left(P_n^S\right) - P_k^D \qquad \forall\, k \in N$$
$$Q_{kt} = \begin{cases} \displaystyle\sum_{n \in N_k} Q_n^S - Q_k^D & \forall\, k \notin N^{shunt} \\ \displaystyle\sum_{n \in N_k} Q_n^S - Q_k^D + 100\left|V_{kt}\right|^2 & \forall\, k \in N^{shunt} \end{cases}$$

Full power flow model

$$
\begin{aligned}
I_k^{Re} &= \sum_{m \in N_k} \left(Y_m^{Re} \left| V_m \right| \cos \theta_m - Y_{km}^{Im} \left| V_m \right| \sin \theta_{mt} \right) && \forall\, k \in N \\
I_k^{Im} &= \sum_{m \in N_k} \left(Y_m^{Re} \left| V_m \right| \sin \theta_m + Y_{km}^{Im} \left| V_m \right| \cos \theta_m \right) && \forall\, k \in N \\
P_k^S / 100 &= I_k^{Re} \left| V_k \right| \cos \theta_k + I_k^{Im} \left| V_k \right| \sin \theta_k && \forall\, k \in N \\
Q_k^S / 100 &= I_k^{Re} \left| V_k \right| \sin \theta_k - I_k^{Im} \left| V_k \right| \cos \theta_k && \forall\, k \in N
\end{aligned}
$$

Reserve power

$$
\begin{aligned}
RM_{10^{sp}}^S &= \sum_{n \in NG} P_{n,10^{sp}}^R \left(1 - \omega_n\right) \\
RM_{10^{ns}}^S &= RM_{10^{sp}}^S + \sum_{n \in NG, \tau_n^{up} = 0} \omega_n P_{n,10^{ns}}^R \\
RM_{30}^S &= RM_{10^{ns}}^S + \sum_{n \in NG} P_{n,30}^R \left(1 - \omega_n\right) \\
&\quad + \sum_{n \in NG, \tau_n^{up} = 0} \omega_n P_{n,30}^R
\end{aligned}
$$

Maximum reserve power contribution

$$
\begin{aligned}
P_{nr}^R &\leq \left(\Delta P\right)_n \tau_r^R && \forall\, k \in N, r \in RM \\
RM_r^S + RM_r^{slack} &\geq RM_r^D && \forall\, r \in RM
\end{aligned}
$$

Variable bounds

$$
\begin{array}{rcccl}
0 & \leq & y_{bn} & \leq & P_{bn}^{bid} & \\
 & & P_n & = & P_n^* & n \in NG^H \\
0 & \leq & P_n & \leq & P_n^{max} & n \notin NG^H \\
 & & P_n^S & = & {P^S}^*_n & n \in NG^H \\
0 & \leq & P_n^S & \leq & P_n^{max} & n \notin NG^H \\
0 & \leq & P_n^R & \leq & P_n^{max} & \\
 & & Q_n^S & = & {Q^S}^*_n & n \in NG^H \\
Q_n^{min} & \leq & Q_n^S & \leq & Q_n^{max} & n \notin NG^H \\
0 & \leq & \omega_n & \leq & 1 & \\
0 & \leq & u_n & \leq & 1 & \\
0 & \leq & x_n^{on} & \leq & {x^{on}}^*_n + 1 & \\
0 & \leq & x_n^{off} & \leq & {x^{off}}^*_n + 1 & \\
-\infty & \leq & P_k & \leq & +\infty & \\
-\infty & \leq & Q_k & \leq & +\infty & \\
-\infty & \leq & I_k^{Re} & \leq & +\infty & \\
-\infty & \leq & I_k^{Im} & \leq & +\infty & \\
0.95 & \leq & |V_k| & \leq & 1.05^{10} & \\
 & & \theta_k & = & 0 & k \in N_{VR} \\
-\infty & \leq & \theta_k & \leq & +\infty & k \notin N_{VR} \\
0 & \leq & RM_r^S & \leq & +\infty & \\
-\infty & \leq & RM_r^{slack} & \leq & +\infty &
\end{array}
$$

Problem execution In the *real-time operation* phase, the 'actual' generator outputs and power flows are determined for every time period in the day of interest. In this study, like in the *pre-dispatch* phase, each day consists of 24 time periods each of one-hour in length. DICOPT is the MINLP solver with CONOPT or MINOS used to solve the relaxed MINLP problem, CONOPT used for the NLP sub-problems, and CPLEX specified for the MIP master problems. Each GAMS program requires less than one second of computing time on an Intel Core i7 Commodity PC and less than a minute is required for the *real-time operation* phase.

The initial state for the electricity system simulation (*i.e.*, the first time period of the first day) is taken from the last time period of the *pre-dispatch* phase simulation for the day in advance. For subsequent time periods, the initial state is taken from the solution of the *real-time operation* MINLP for the previous time period.

Real-time operation results

Capacity utilization Figure 2.8 shows the bids that are selected during the off-peak time period of the first day in the simulation. Bids are not selected in strict order of increasing marginal bid price. The recognition of minimum uptime and downtime constraints within the economic dispatch problem leads to some bids being passed over for more expensive ones.

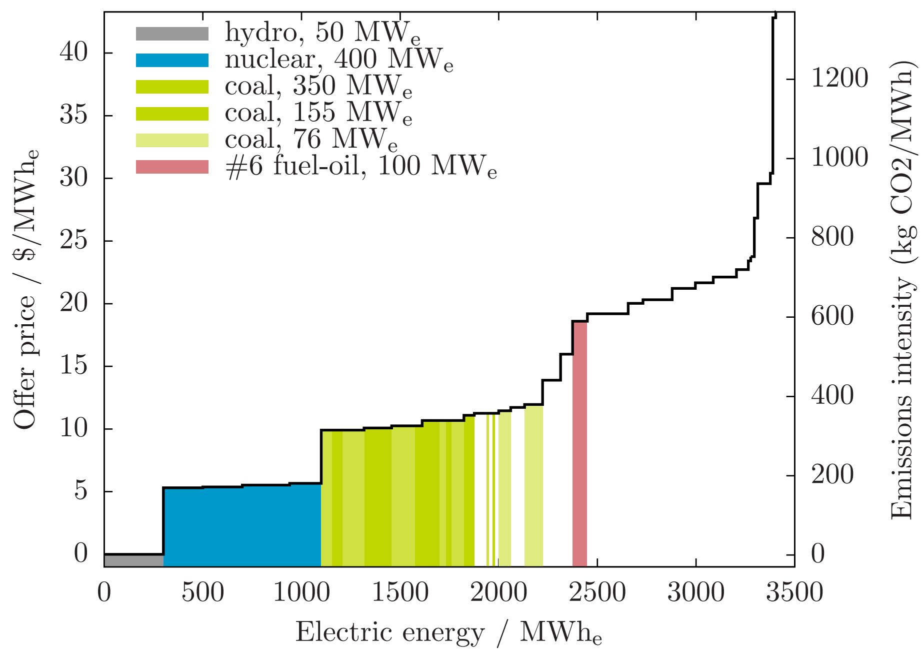

Figure 2.8: Accepted bids for Monday off-peak period

Figure 2.9 indicates, for each type of generating unit and in each time period, how much real power is output. Some comments:

- The nuclear units, at Astor and Attlee, operate continuously at full capacity.
- Aubrey, with its hydroelectric units, maintains fairly constant output except for occasional, sharp declines some nights.
- More power is produced at Austen than at any other bus.
- Arne is basically a 'peaking' plant. It goes from maximum load to shutdown in a few hours. On days with low demand (*e.g.*, weekends), it may go undispatched completely.
- The output from the other generator buses tracks demand, approaching peak output at peak demand and minimum output at the daily off-peak.

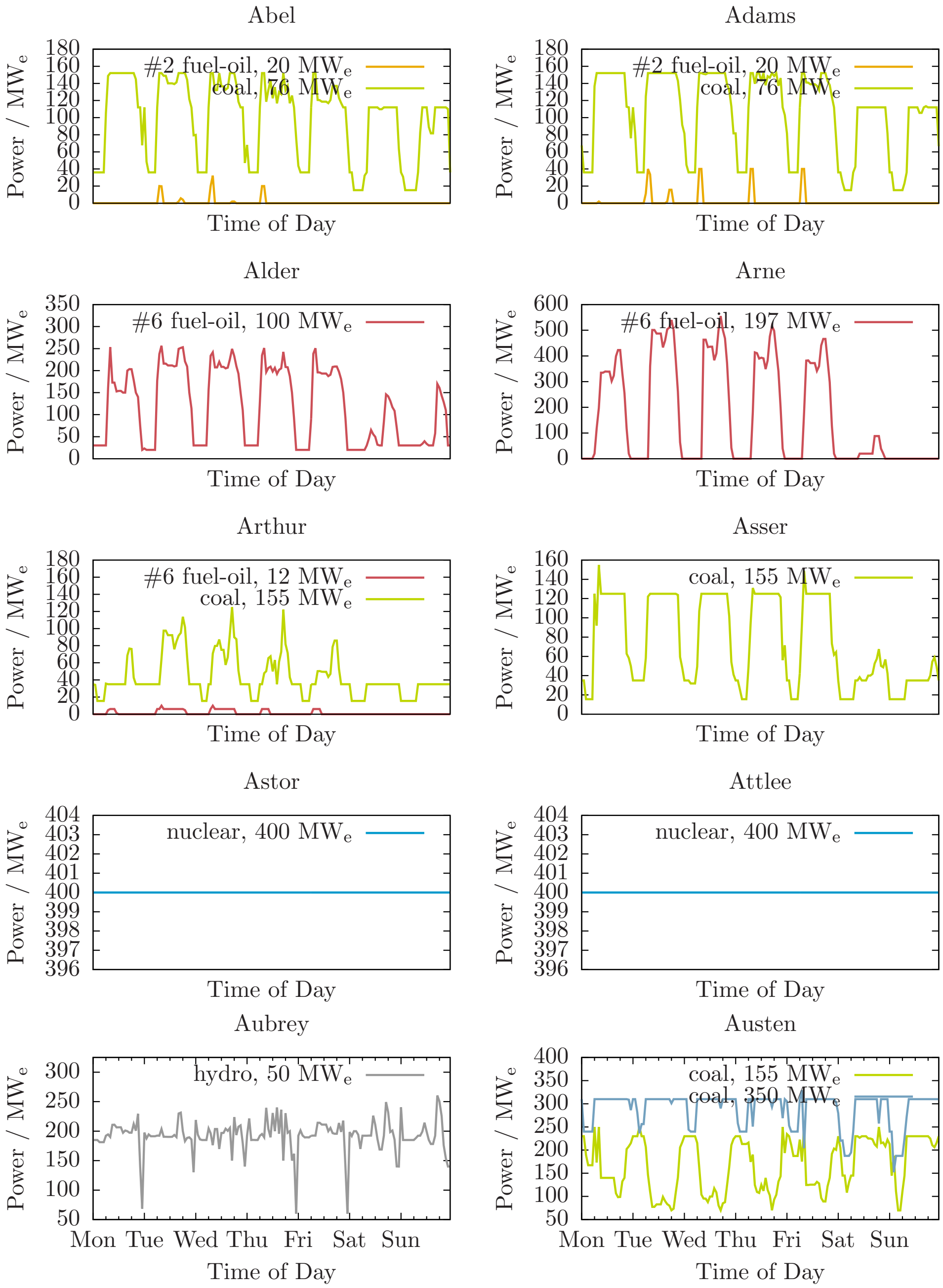

Figure 2.9: Real power output of each type of generating unit in each time period

Summary statistics for the utilization of the different types of generating capacity is presented in Table 2.14. Two heat rates are reported for each thermal generating unit: one time-weighted average and the other the energy-weighted average. This is done to highlight the significant difference that exists between these two approaches for calculating the 'average'. Also note there is not an insignificant number of unit starts — and, by implication unit shutdowns — that occur and that these are confined to the fuel oil-fired thermal and combustion generating units.

Table 2.14: Summary of generating unit power output

	Unit type			CF	$\bar{HR}_n$		$N^{start\text{-}up}$
Bus	Fuel	Capacity	Number		Time	Energy	
		MW_e			Btu/kWh		
Abel	#2 Fuel Oil	20	2	0.02	14821	14607	7
Abel	Coal	76	2	0.65	12475	12080	0
Adams	#2 Fuel Oil	20	2	0.05	14673	14592	10
Adams	Coal	76	2	0.70	12408	12064	0
Alder	#6 Fuel Oil	100	3	0.39	11465	10535	3
Arne	#6 Fuel Oil	197	3	0.28	9816	9696	16
Arthur	#6 Fuel Oil	12	5	0.02	16017	16017	25
Arthur	Coal	155	1	0.28	10951	10680	0
Asser	Coal	155	1	0.48	10428	9965	0
Astor	Nuclear	400	1	1.00	10000	10000	0
Attlee	Nuclear	400	1	1.00	10000	10000	0
Aubrey	Hydro	50	6	0.64	N/A	N/A	N/A
Austen	Coal	155	2	0.53	10197	9931	0
Austen	Coal	350	1	0.83	9508	9505	0

Capacity factor is defined as the ratio of energy output to the maximum theoretical energy output given the unit's availability. Table 2.14 might give the impression that the generating units, except for the nuclear ones, are significantly under utilized. Figure 2.10 shows, for each type of generating unit, the capacity utilization in each time period; capacity utilization includes the power output of each type of generating unit and the capacity that is on reserve. For the hydroelectric and coal-fired units, it is readily apparent that while these units are typically outputting at less than full load, their capacity is mostly spoken for. Figure 5.7 shows the split of each type of generating unit capacity between power injected into the grid and capacity successfully bid into the reserve market.

Congestion There are physical limits to the quantity of electric power that a transmission line can support. On this basis, transmission lines are rated; that is, the maximum quantity of power the line should carry is specified.

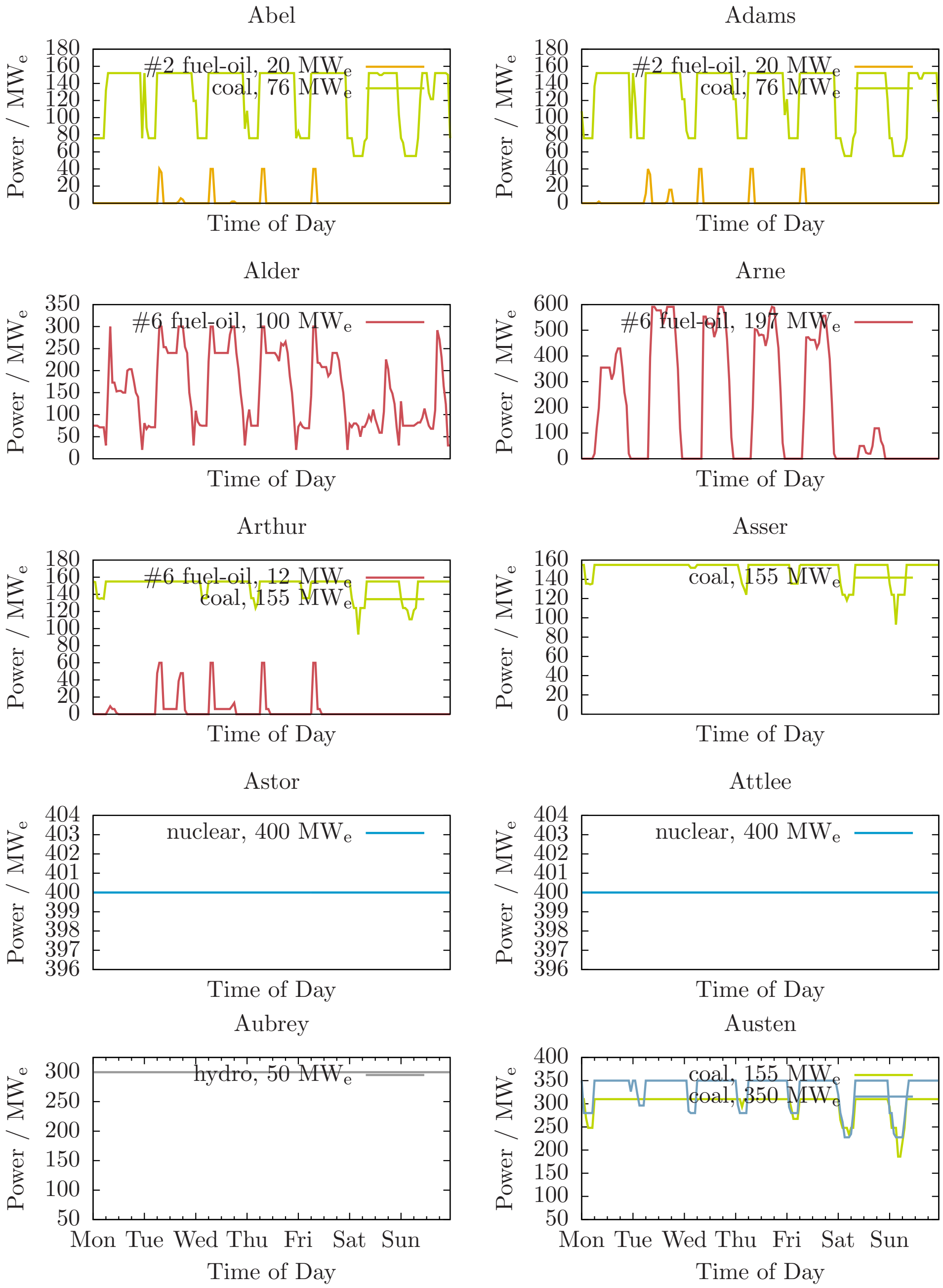

Figure 2.10: Capacity utilization of each type of generating unit in each time period

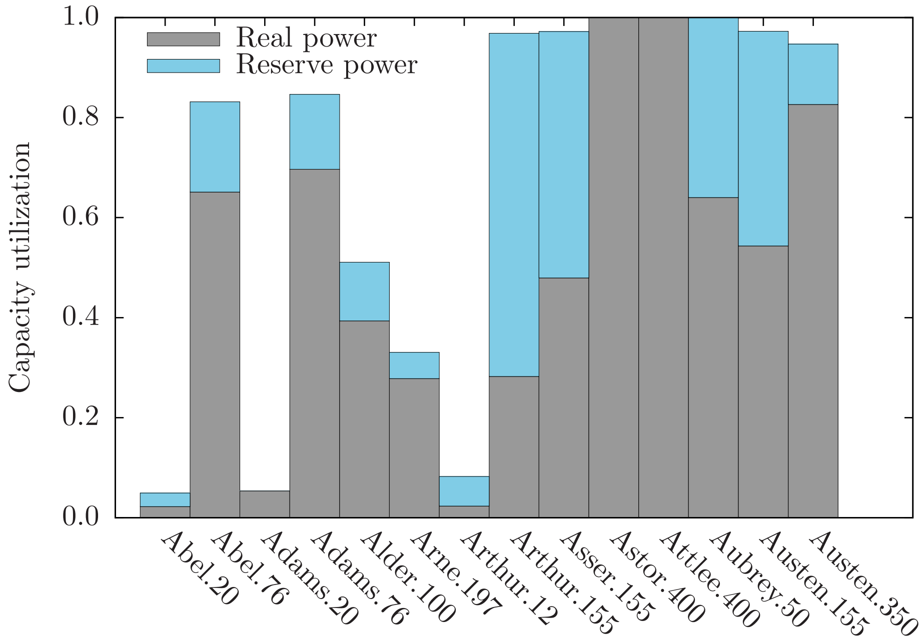

Figure 2.11: Average capacity utilization of units in IEEE RTS '96

It may happen that a set of dispatch instructions would result in power flows that cause one or more transmission lines to exceed its specified continuous rating. To avoid this, the dispatch schedule may need to be reformulated. In such an situation, *congestion* is said to exist.

Identifying congestion in the IEEE RTS '96 is done by examining the unused capacity of its transmission lines; *unused capacity* is the difference between its continuous rating and the apparent power flow along that line. There are 38 transmission lines in the IEEE RTS '96 and Figure 2.12 summarizes the unused line capacity of each one during the week of interest. The height of the bars gives the mean quantity of unused capacity for the week and the error bars indicate the minimum and maximum unused capacity observed.

For all the transmission lines, the power flow is always less than the continuous rating. The power flow along the Alder–Alger transmission line comes closest to the limit being within some 20 MVA from the maximum continuous rating during three time periods during the week of interest.

Transmission losses Figure 2.13 indicates the losses of electricity that occur as a result of transmission within the IEEE RTS '96. The graph on the left specifies the aggregate electricity losses that occur throughout the system in absolute terms. At any given time, between 30 MW_e and 50 MW_e of the electricity being generated is wasted. In general, the

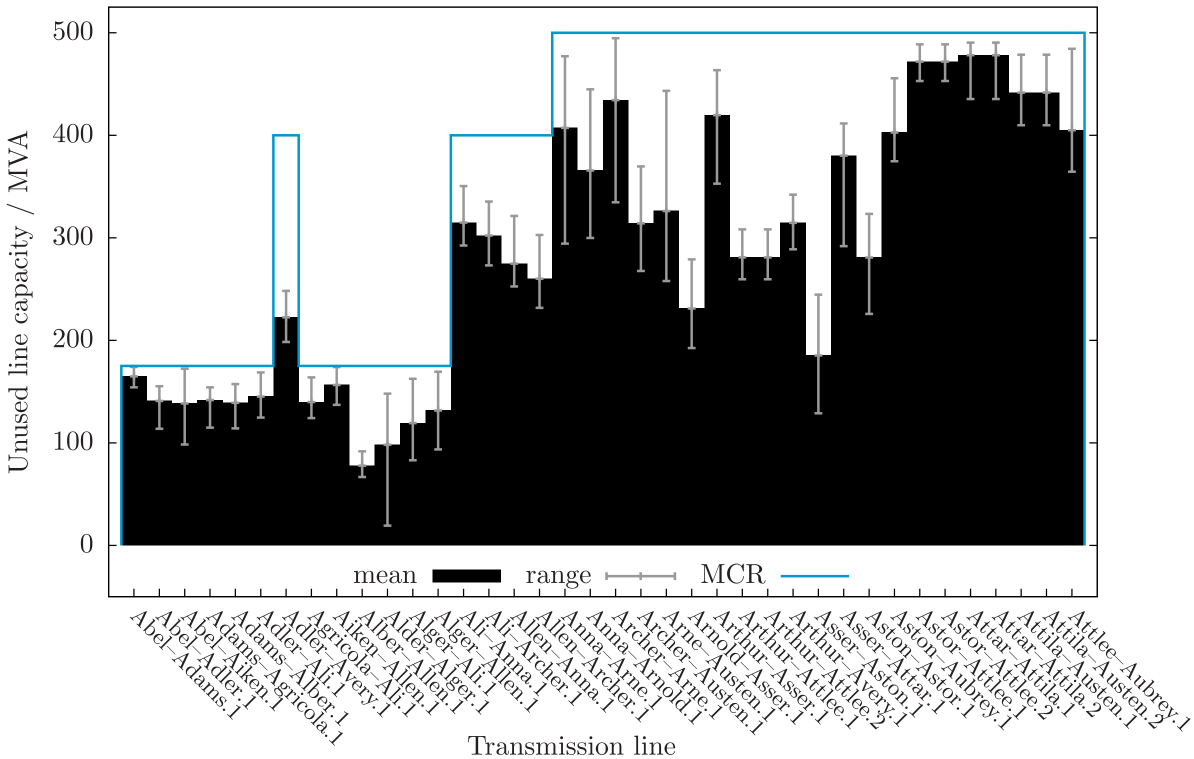

Figure 2.12: Unused line capacity in IEEE RTS ’96

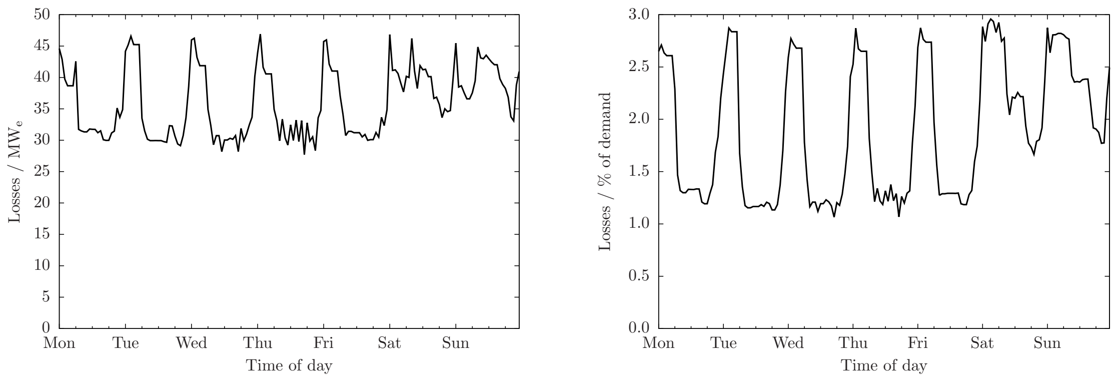

(a) Absolute terms (b) Relative terms

Figure 2.13: Transmission losses in IEEE RTS '96

magnitude of the losses changes monotonically with electricity demand. However, losses on the weekend are significantly *greater* than during weekdays even though demand on the weekend is about 20% lower (see Table B.1).

The weekend uptick in transmission losses is caused by the significant differences in dispatch schedule during the weekend versus weekdays. The lower electricity demand on the weekend leads to a quite different outcome with respect to capacity utilization.

Consider Figure 2.9. The generation profiles of some units — coal-fired at Abel, Adams, and Austen, nuclear at Astor and Attlee, and hydroelectric at Aubrey — change little from day to day whereas the output from the other units drops substantially on the weekend. As it happens, buses that are co-located with loads, Arne and Alder in particular, see their production drop off; buses with no local demand (*e.g.*, Attlee, Aubrey, and Austen) see their share of production increase. Thus, while overall demand is lower, the electricity that is required is travelling greater distances. The increased transmission is, of course, accompanied by increased transmission losses.

Greenhouse gas emissions Last but not least, Figure 2.14 shows the aggregate GHG emissions for the system as a function of time. Note that the change in emissions maintains the same rhythm as the change in electricity demand shown in Figure 2.6. The formula used to calculate GHG emissions in each time period is given in (2.73).

$$\dot{m}^{CO_2} = \sum_{n \in NG} P_n^S \cdot HR_n \cdot EI_n^{CO_2} \cdot L_t \cdot \frac{1}{2.205 \times 10^6} \tag{2.73}$$

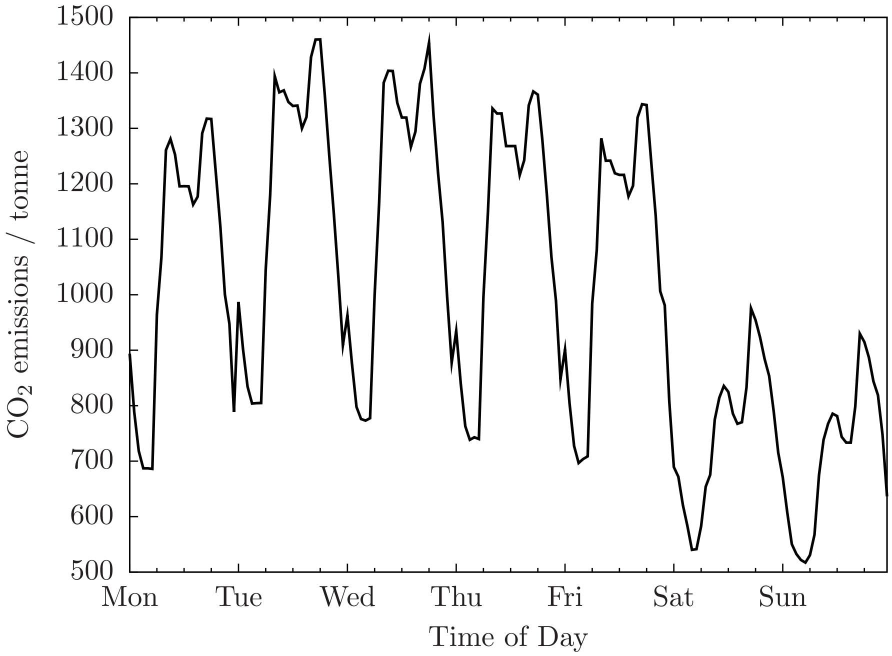

Figure 2.14: Aggregate CO_2 emissions

2.4.3 Phase 3: Market settlement

In a deregulated electricity system, the electricity price in each time period is determined *ex post* based upon the actual demand for electricity and the supply bids of the generating units that were 'active' in the market at that time. An 'active' generating unit is one that either output power or was on-standy in case of a contingency. The supply bids of the 'active' units are sorted in order of increasing price and the price of the *marginal* bid sets the electricity price for the time period.

Determining the HEP in the *market settlement* phase of the electricity system simulation is achieved by solving a simplified version of the MINLP problem used during the *real-time operation* phase. In general, the changes are as follows and described below.

- Power flow in the electricity system is ignored which effectively treats the generating units and loads as being connected to the same bus.
- Offers to produce electricity that were not accepted in the *real-time operation* phase are not considered during *market settlement*.

Power flow is ignored. In the *market settlement* phase, power flow in the IEEE RTS '96 is ignored which is akin to assuming that the generating units and loads are connected to same bus.

- The references (*i.e.*, variables and constraints) related to power flow are removed. Gone are the variables $I_k^{Re}, I_k^{Im}, \theta_k,$ and $|V_k|$ and the power flow model.

- All references (*i.e.*, variables and constraitns) to reactive power are removed. Gone are the variables Q_n^SandQ_k and the MINIMUM AND MAXIMUM REACTIVE POWER OUTPUT constraints.

- With all generating units and loads connected to a single bus, the NET POWER AVAILABLE AT EACH BUS constraints morph into the supply/demand balance for the system; there's (2.74) for real power and an additional constraint (2.75) to ensure that, of the units that are selected, there is sufficient reactive power capacity available.

$$\sum_{n \in NG} P_n^S \geq \sum_{k \in N} P_k^D \tag{2.74}$$

$$\sum_{n \in NG} Q_n^{max} (1 - \omega_n) \geq \sum_{k \in N} Q_k^D \tag{2.75}$$

As a result of the above, the variable P_k no longer appears in the MINLP problem.

Rejected supply bids are ignored. Recall that ω_n has a value of one if the unit is off and zero otherwise. The *market settlement* phase problem is initialized using values of the variables from the *real-time operation* results and the value of ω_n is fixed. This has the effect of discarding from consideration in the market settlement the bids from units that did not participate in the time period.

$$\omega_n = \omega_n^*$$

This also effectively fixes the value of $u_n, x_n^{on},$ and x_n^{off} in the MINLP problem.

$$\begin{aligned} u_n &= \omega_n^\circ - \omega_n^* \\ x_n^{on} &= \left[(x_n^{on})^\circ + 1 \right] (1 - \omega_n^*) \\ x_n^{off} &= \left[\left(x_n^{off} \right)^\circ + 1 \right] \omega_n^* \end{aligned}$$

The UNIT START-UP DEFINITION, MINIMUM UNIT UPTIME, and MINIMUM UNIT DOWN-TIME constraints are no longer present.

Real-time operation problem formulation, implementation, and execution

The corresponding MINLP problem is given below.

$$\begin{aligned}
\underset{\substack{u_n, y_{bn} \\ P_n, P_n^S, P_{nr}^R \\ x_n^{on}, x_n^{off} \\ RM_r^R, RM_r^{slack}}}{\text{minimize}} \quad z = & \sum_{n \in NG} u_n HI_n FC_n \\
& + \sum_{n \in NG_D} \sum_{b=1}^{N_b} y_{bn} IHR_{bn} FC_n L_t \frac{1}{10^3} \\
& + \sum_{r \in RM} C^{import} \cdot RM_r^{slack}
\end{aligned}$$

subject to:

Capacity utilization

$$P_n = \sum_{b=1}^{N_b} y_{bn} \qquad \forall n \in NG$$

Power disaggregation between real and reserve markets

$$P_n = P_n^S + \sum_{r \in RM} P_{nr}^R \qquad \forall n \in NG$$

Minimum and maximum real power output

$$(1 - \omega_n^*) P_n^{\min} \leq P_n^S \leq (1 - \omega_n^*) P_n^{max} \qquad \forall n \in NG$$

Unit ramp rates

$$P_n^S \geq \left(P_n^S\right)^\circ - \left(\Delta P^S\right)_n L_t \qquad \forall n \in NG$$

$$P_{nt}^S \leq \left(P_n^S\right)^\circ + \left(\Delta P^S\right)_n L_t \qquad \forall n \in NG$$

Real and reactive power supply/demand balance

$$\sum_{n \in NG} P_n^S \geq \sum_{k \in N} P_k^D$$

$$\sum_{n \in NG} Q_n^{max} (1 - \omega_n^*) \geq \sum_{k \in N} Q_k^D$$

Reserve power

$$RM^S_{10^{sp}} = \sum_{n\in NG} P^R_{n,10^{sp}}\left(1-\omega^*_n\right)$$

$$RM^S_{10^{ns}} = RM^S_{10^{sp}} + \sum_{n\in NG,\tau^{up}_n=0} \omega^*_n P^R_{n,10^{ns}}$$

$$RM^S_{30} = RM^S_{10^{ns}} + \sum_{n\in NG} P^R_{n,30}\left(1-\omega^*_n\right) + \sum_{n\in NG,\tau^{up}_n=0} \omega^*_n P^R_{n,30}$$

Maximum reserve power contribution

$$P^R_{nr} \le \left(\Delta P\right)_n \tau^R_r \qquad \forall\, k\in N, r\in RM$$

$$RM^S_r + RM^{slack}_r \ge RM^D_r \qquad \forall\, r\in RM$$

Variable bounds

$$\begin{array}{rcccll}
0 & \le & y_{bn} & \le & P^{bid}_{bn} & \\
 & & P_n & = & P^*_n & n\in NG^H \\
0 & \le & P_n & \le & P^{max}_n & n\notin NG^H \\
 & & P^S_n & = & P^{S*}_n & n\in NG^H \\
0 & \le & P^S_n & \le & P^{max}_n & n\notin NG^H \\
0 & \le & P^R_n & \le & P^{max}_n & \\
 & & \omega_n & = & \omega^*_n & \\
 & & u_n & = & \omega^\circ_n - \omega^*_n & \\
 & & x^{on}_n & = & \left(x^{on\,\circ}_n + 1\right)\left(1-\omega^*_n\right) & \\
 & & x^{off}_n & = & \left(x^{off\,\circ}_n + 1\right)\omega^*_n & \\
-\infty & \le & P_k & \le & +\infty & \\
0 & \le & RM^S_r & \le & +\infty & \\
-\infty & \le & RM^{slack}_r & \le & +\infty &
\end{array}$$

Problem execution DICOPT is the MINLP solver with CONOPT used to solve the relaxed MINLP problem and the NLP sub-problems and CPLEX specified for the MIP master problems. Each GAMS program requires less than one second of computing time on an Intel Core i7 Commodity PC and less than a minute is required for the *market settlement* phase.

The initial state for the electricity system simulation (*i.e.*, the first time period of the first day) is taken from the last time period of the *pre-dispatch* phase simulation for the day in advance. For subsequent time periods, the initial state is taken from the solution of the *real-time operation* MINLP for the previous time period. The problem variables are initialized using the results from the solution of the *real-time operation* MINLP problem for the same time period.

Market settlement results

Electricity prices Figure 2.15 shows the electricity prices over the week of interest. Each time period is identified by the bus containing the unit(s) that are price setting. Also shown in the figure is the average cost of generating electricity in each time period.

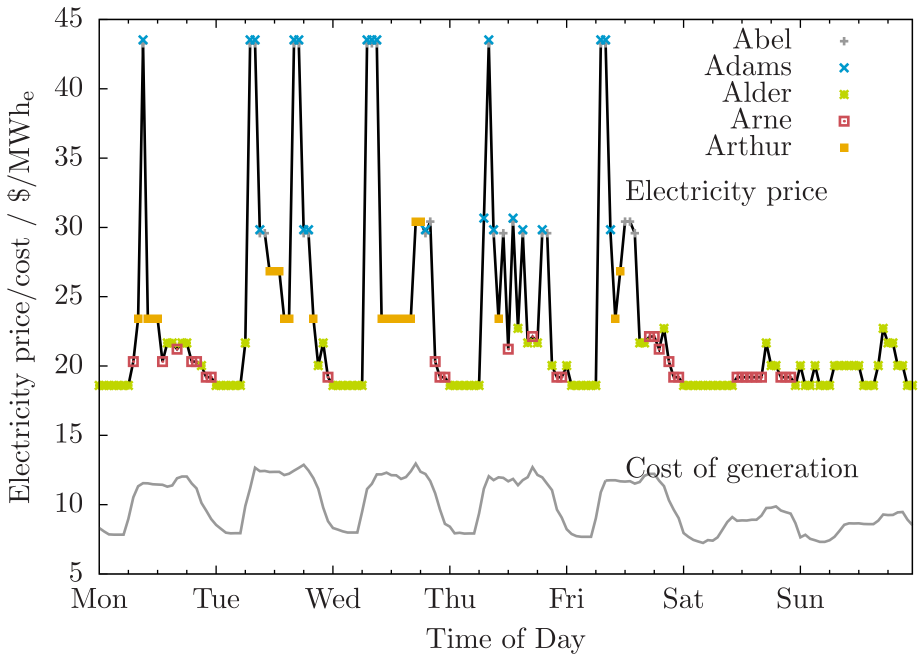

Figure 2.15: Electricity price and location of price-setting units in IEEE RTS '96

The electricity price varies from \$18.60/MWh$_e$ to \$43.28/MWh$_e$. The price setting units are those that use #2 or #6 fuel oil as an energy source. Prices tend to be greatest when demand is greatest and *vice versa*. It is also interesting to note that, compared to the electricity price, the *CoE* is relatively stable and not obviously a strong indicator of electricity price.

Energy benefit *Energy benefit* is the revenue a unit receives from selling its capacity into the market. Figure 2.16 shows the energy benefit, on aggregate, generated during the period of interest. It also illustrates the aggregate *net energy benefit*: the difference between the energy benefit and the costs to produce electricity — in this case fuel both for start-up and power generation.

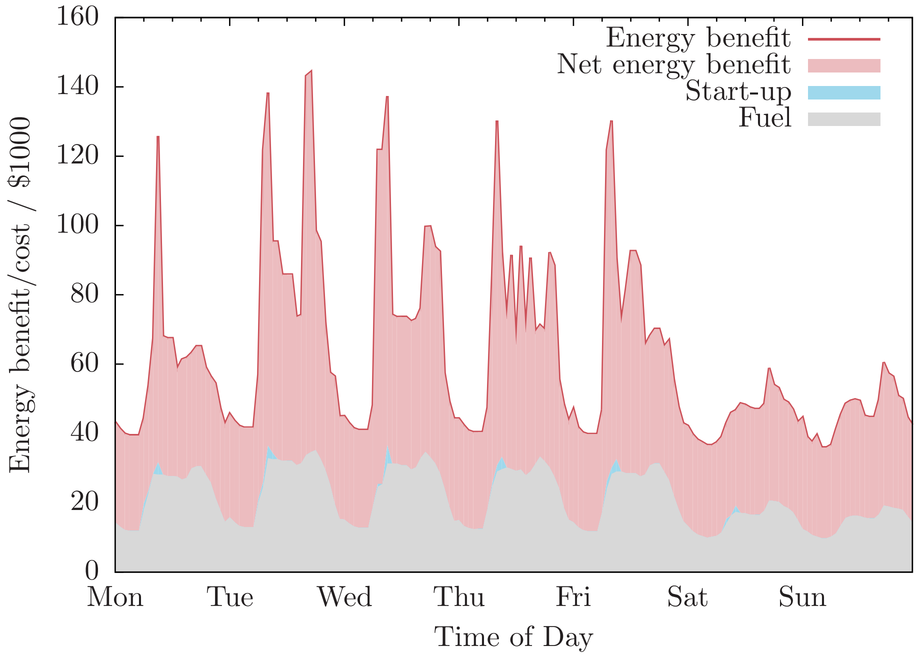

Figure 2.16: Aggregate energy benefit and fuel costs in IEEE RTS '96

Averaged over time, the net energy benefit is $41,000 which is about twice the average fuel cost of $21,000. The net energy benefit ranges from a low of $25,000 to a high of $110,000, or five times the average generation cost. Overall, the start-up costs represent 1% of the total cost of generation though, in some time-periods, 15% of the generation cost is attributed to starting-up genrating untis. Figures 2.17 and 2.18 illustrate how this energy benefit is distributed amongst the different types of generating units.

Figure 2.17 shows the energy benefit for each type of unit in the IEEE RTS '96. Not all time periods are equally profitable and this is best illustrated for the units at Astor, Attlee, and Aubrey. As seen in Figure 2.10, the capacity of these units is fully committed in all time periods so the variation in net energy benefit is entirely due to fluctuations in electricty price. Figure 2.18 summarizes the net energy benefit for each type of unit.

Transmission losses Figure 2.19 attempts to put the magnitude of the transmission losses in context by presenting them as a percentage of the aggregate electricity demand and on a value basis. In the latter case, the market value of electricity is calculated as shown in (2.76).

$$\begin{matrix} \textit{value} \\ \textit{of} \\ \textit{losses} \end{matrix} = P^D \times \rho \tag{2.76}$$

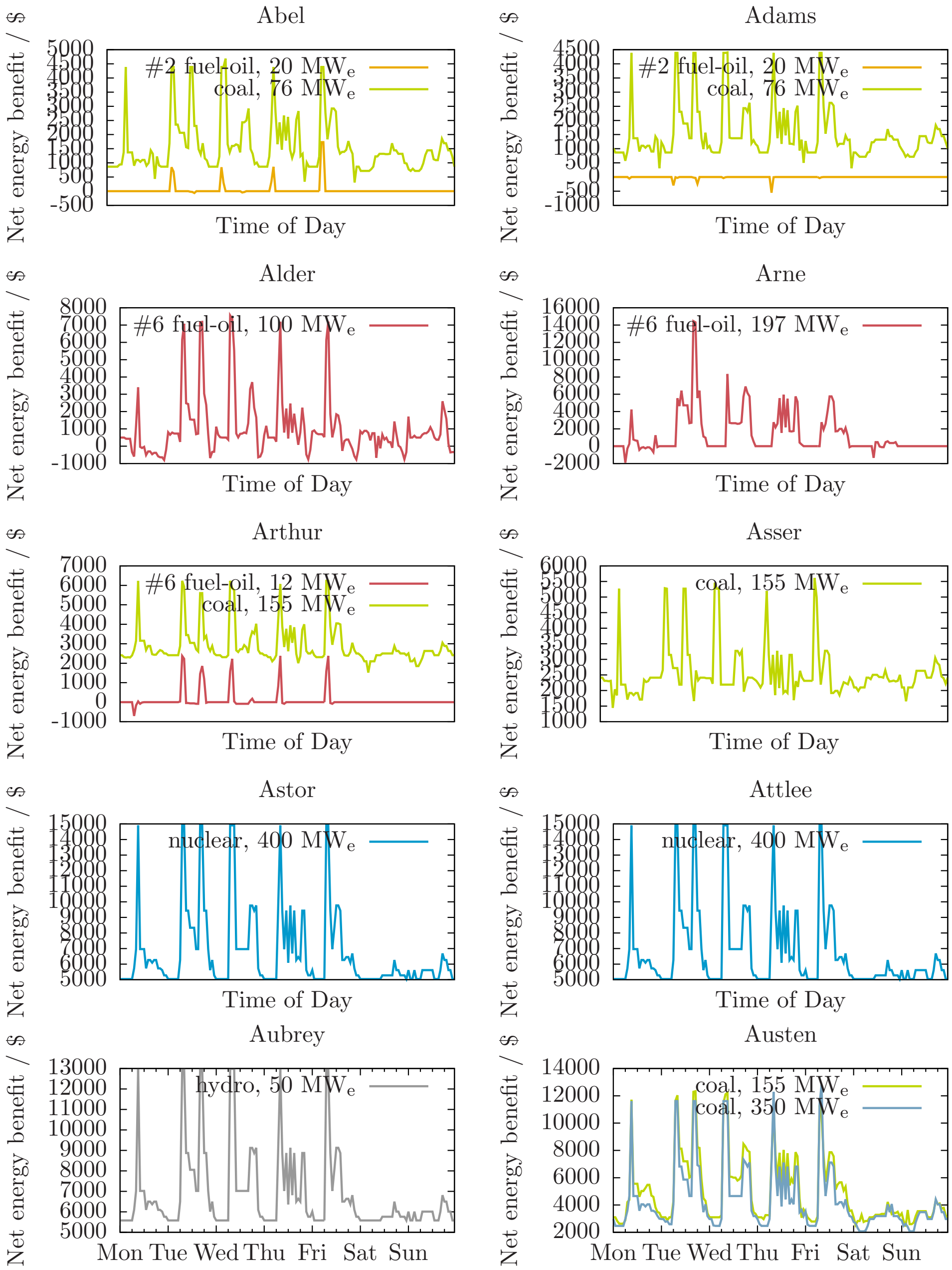

Figure 2.17: Net energy benefit of units in IEEE RTS '96

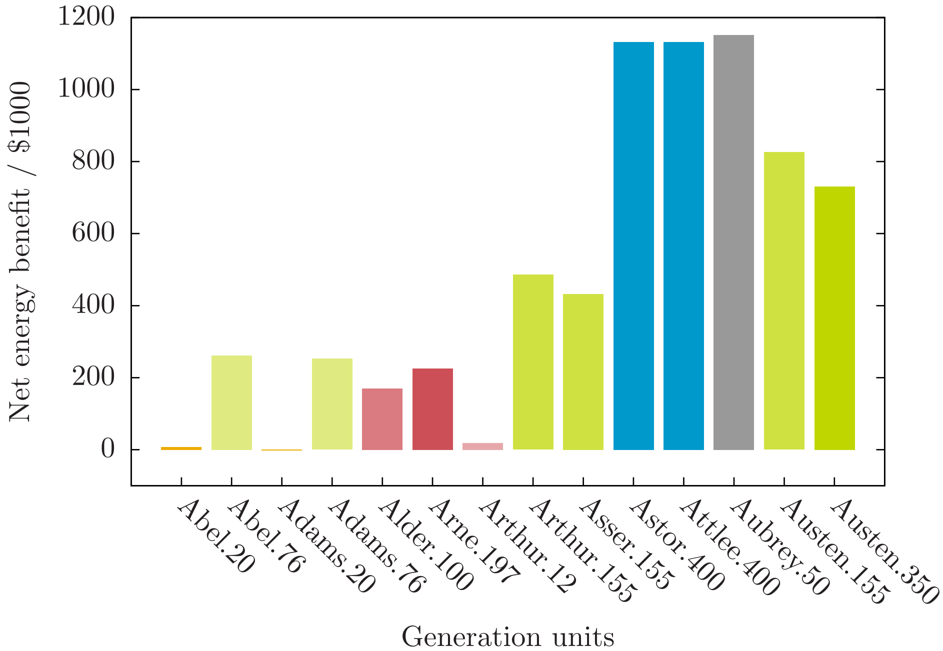

Figure 2.18: Net energy benefit of units in IEEE RTS '96 for one week of operation

Electricity losses are slightly higher during the weekend than during the week. However, since electricity prices are lower on the weekend (see Figure 2.15), the market value of the losses is greater on weekdays.

2.5 Discussion of approach used for electricity system simulator

2.5.1 Merit order for short-term generation scheduling

An alternative approach to determining economic dispatch and electricity price is described by Chalmers *et al.* [12] where it is assumed that units are dispatched strictly according to merit. For a given time period, all the bids to the left of demand are assumed to be accepted and the system electricity price is the bid price at this level of output. The approach is conceptually simple and the solution for any time period can be determined by inspection of the appropriate composite supply curve.

Figure 2.8 shows the selected bids for the off-peak period on Monday and Figure 2.20 shows the selected bids for the same time period using a strict merit-order approach. Compared to the electricity system simulation, the merit-order approach over estimates the utilization of the 155 and 350 MW_e coal-fired units and underestimates the utilization

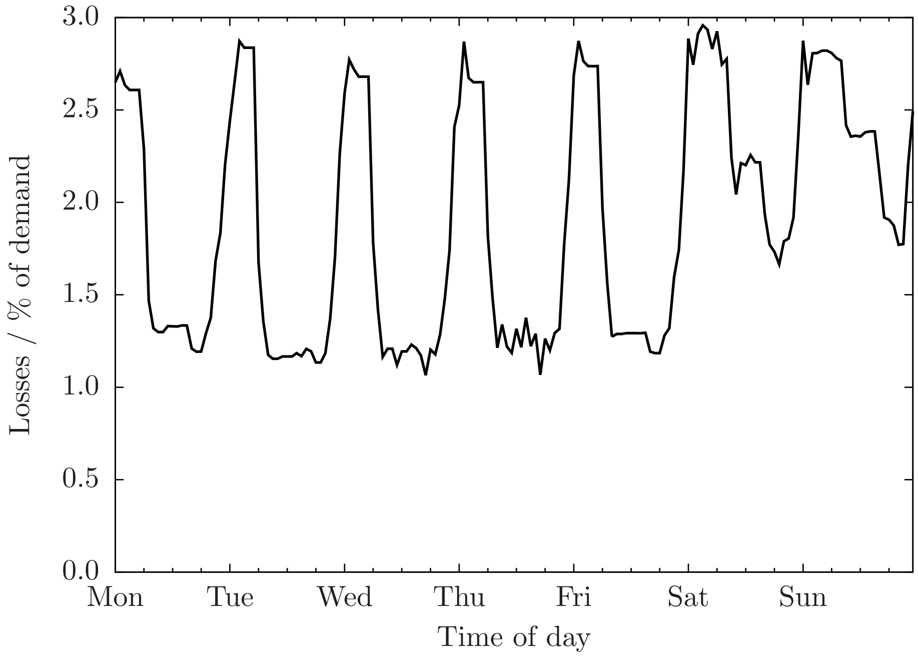

Figure 2.19: Market value of transmissions losses in IEEE RTS '96

of the 76 MW_e coal-fired units and the 100 MW_e units at Alder.

With respect to price, the electricity system simulator calculates an electricity price of \$18.60/MWh_e during this time period versus the \$11.72/MWh_e determined using the merit-order approach. These observations suggest that one should be careful about drawing conclusions about system performance using a strict merit-order unit dispatch.

2.5.2 Robustness of unit commitment schedules to OPF and environmental constraints

In a series of publications, Shahidehpour with lead authors Wang [49], Abdul-Rahman [1], and Ma [34] discuss the benefits of increasing the degree to which OPF (Optimal Power Flow) requirements and environmental constraints are incorporated in the unit commitment component of short-term generation scheduling. The general observation is that the greater the extent to which these constraints are incorporated into the unit commitment problem, the better the solution of the economic dispatch. In the limit, the unit commitment and economic dispatch problem would be solved simultaneously.

The approach taken here is to approach the limit of simultaneous unit commitment and economic dispatch while avoiding mathematical difficulties that would preclude the use of GAMS and commercially-available, off-the-shelf solvers (*e.g.*, DICOPT, CPLEX,

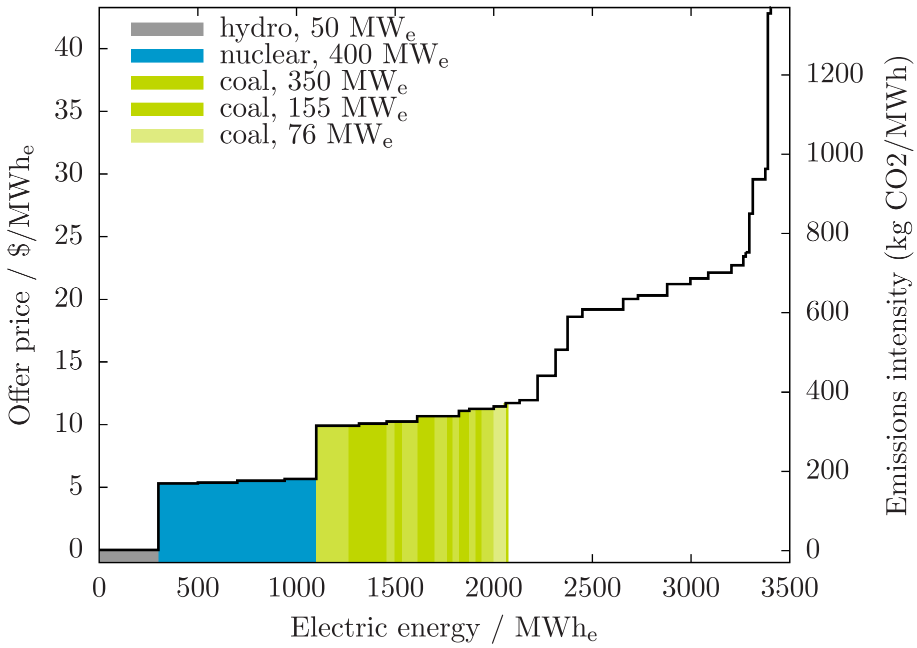

Figure 2.20: Accepted bids for Monday off-peak period using merit-order approach

MINOS/CONOPT). In the end, the model describe in Section 2.4.1 is comparable to the work of Shahidehpour referenced above.

- In [49, 1, 34], the cost to start-up a generating unit increases exponentially with the number of time periods that the unit has been shut-down:

$$C_{nt}^{start-up} = u_{nt}\left\{\alpha_n + \beta_n\left[1 - \exp\left(\frac{-x_{nt}^{off}}{\tau_n^{off}}\right)\right]\right\}$$

  In this work, the start-up cost is assumed not to vary with the length of time the unit has been off (see (2.57)).

- In [49, 1], transmission line capacity constraints are incorporated into the short-term generation scheduling and they are not included in this work.[11]

- That being said, in this work, apparent power flows are represented in the unit commitment problem using a first-order, linear approximation of an AC (Alternating Current) power flow model. An important result is that power losses associated with

[11] The electricity system simulator does verify that computed power flows are within the transmission line capacity limits and, to-date, no violations have been detected.

electricity transmission are accounted for. In [49, 1, 34], power flows are estimated using a DC (Direct Current) power flow model and transmission losses are apparently ignored.

- In [49, 1], reactive power is not considered; there is no reactive power supply or demand and the transmission line capacity limits are in terms of real power and not apparent power. In this work, reactive power demand balance constraint is included, transmission is calculated in terms of apparent power, and phase angles and voltage magnitudes of the buses are decision variables.

2.6 Summary

In this Chapter, the development of an electricity system simulator is described. Key aspects of the electricity system simulator have been validated using commerical software and results from literature and there is confidence that no material errors exist in the formulation or implementation.

The results of the electricity system simulator speak to the engineering (*i.e.*, technical), economic, and enviornmental performance of the electricity system. It provides information that is of interest to a cross-section of stakeholders: generators, consumers, and policy makers. As such, it is a suitable platform for assessing the performance of GHG mitigation options in the electricity system, the principal focus of the Chapters to follow. At the same time, it is important to acknowledge the potential shortcomings of the electricity system simulator.

It is assumed that generators bid their power at their units SRMC (Short-Run Marginal Cost). While this is sensible in theory, it does occur in existing deregulated electricity systems that generators bid their power either above or significantly below the SRMC, for example, to avoid a unit from being outbid and forced to shutdown. The assumption that generators bid their power at the SRMC is lilkely appropriate for simulating the operation of the IEEE RTS '96 but, for simulating the operation of existing electricity system, it may make the most sense to replicate the bidding strategy employed within that context.

Fundamental to the electricity system simulator is the solving economic dispatch problems each formulated as MINLP. Being non-convex, it is not guaranteed that the optimal solution returned by DICOPT will be the global optimal solution. Three comments with respect to this fact:

1. Global MINLP solvers have emerged relatively recently and an unsuccessful attempt was made to use one such solver — BARON (Brand And Reduce Optimization Navigator) for solving the economic dispatch problem in Section 2.3. As these solvers mature, it may be possible to substitute BARON for DICOPT within the electricity system simulator and still run it on commodity computer hardware.

2. An assessment was done on the sensitivity of the solution to the economic dispatch problem in Section 2.3 to the problem initialization. All of the feasible starting points returned the same optimal solution.

3. The electricity system simulator is informed by the approach taken to manage real electricity systems. In particular, operators of real electricity systems solve economic dispatch problems analagous to those proposed in this work and in the same way. Presumably, then, the fact that the solutions to the economic dispatch problems are not guaranteed to represent the global optimums is not a limitation.

Chapter 3

Reducing GHG emissions through load balancing

3.1 Introduction

Typically, in any given power system, there is more than one set of dispatch instructions that will satisfy a given demand. The convention is to use the dispatch that maximizes the economic benefit of the market participants subject to the technical constraints of the generators and the transmission system. Figure 3.1 again shows the composite supply curve for the system and, highlighted, the quantity of each bid that has been selected in the off-peak period of Monday.

New to Figure 3.1 is the addition of the emissions intensity of each bid. This to show that the drive to select the cheapest bids first has resulted in the dispatch of some of the highest emitting units in the system while lower-emitting units sit idle. Had lower intensity — but albeit more expensive — bids been used instead, it would have been possible to satisfy the same electricity demand with significantly fewer CO_2 emissions. This is the underlying principle of load balancing.

In the extreme case, the dispatch of units would be determined based solely upon the relative emissions intensity of the generating units. Figure 3.2 shows the CO_2 emissions-based merit curve for the IEEE RTS '96; this curve differs from the composite supply curve in Figure 3.3 in that units are ranked in increasing order of emissions intensity rather than in increasing order of bid price. Whereas before, coal units would come on before oil-fired ones, the opposite is true when the an emissions-intensity centric dispatch order is preferred.

So, *load balancing* is used to describe the approach of preferentially dispatching generating units power by lower-carbon intensity fuels. The load balancing approach is interesting as it requires no new capital investment; implementation of this mitigation strategy could be achieved immediately with a correspondingly immediate benefit with respect to GHG

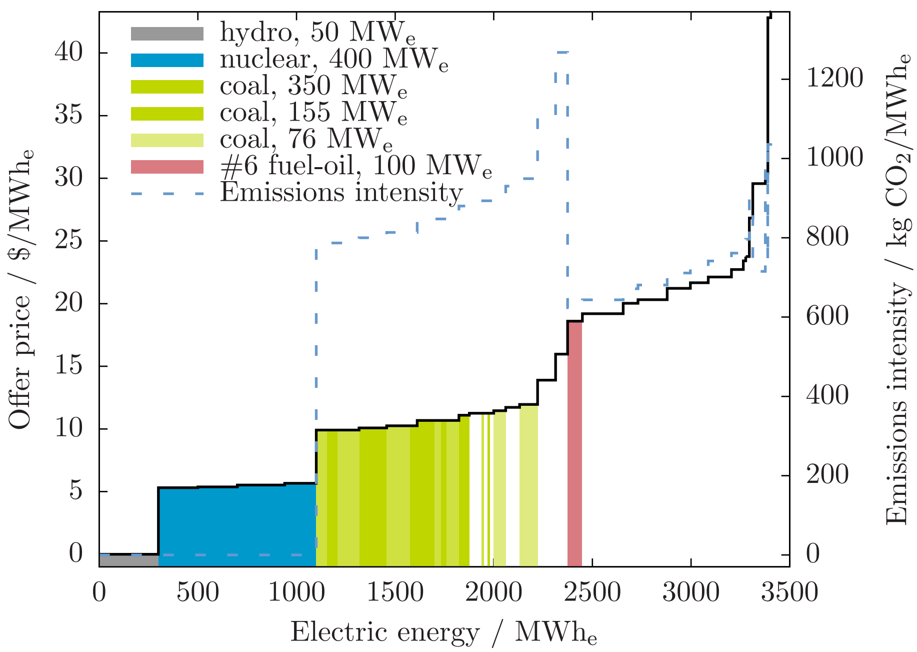

Figure 3.1: Price and emissions intensity of offers selected in first hour of IEEE RTS '96 simulation

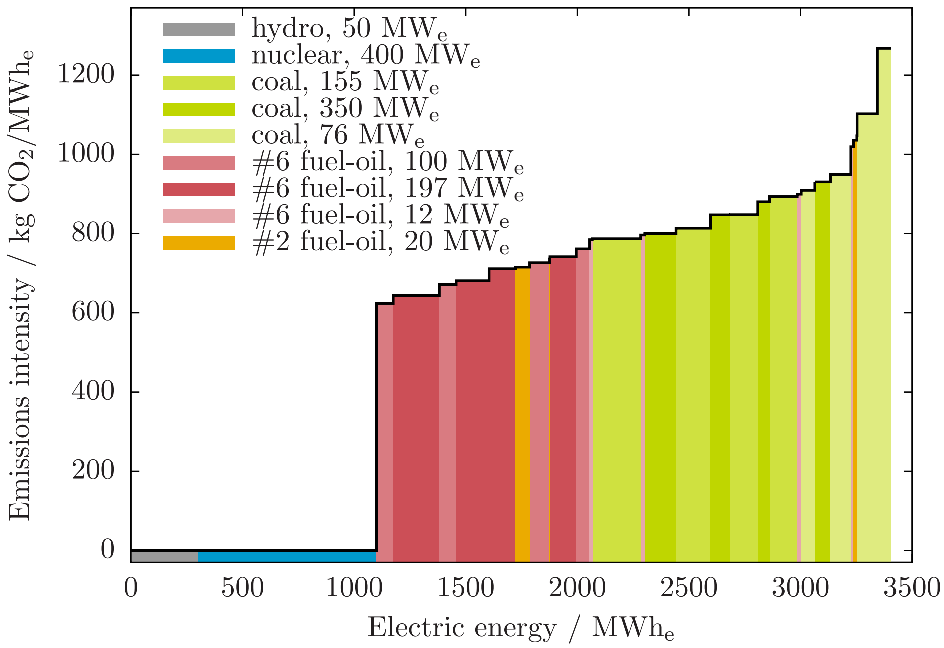

Figure 3.2: Pseudo-composite supply curve with ranking based on emissions intensity

emissions. In this chapter, the electricity system simulator is used to assess the effectiveness of load balancing for reducing GHG emissions. This chapter is divided as follows:

- To better understand the utility of the electricity system simulator in characterizing *load balancing* within the IEEE RTS '96, Section 3.2 assesses the benefits of load balancing using a top-down approach.
- Section 3.3 describes the extension of the electricity system simulator in order to enable load balancing.
- Section 3.4 presents the results of the load balancing analysis.
- The chapter ends with some concluding remarks in Section 3.5.

3.2 Using 'top-down' approach to assess the effect of load balancing

Contrasting Figures 3.2 and 3.3 suggests an opportunity within the IEEE RTS '96 to reduce GHG emissions by preferentially using oil-fired generating units over coal-fired ones. This is supported by Table 2.14 that indicates, for example, the 350 MW_e coal-fired unit at

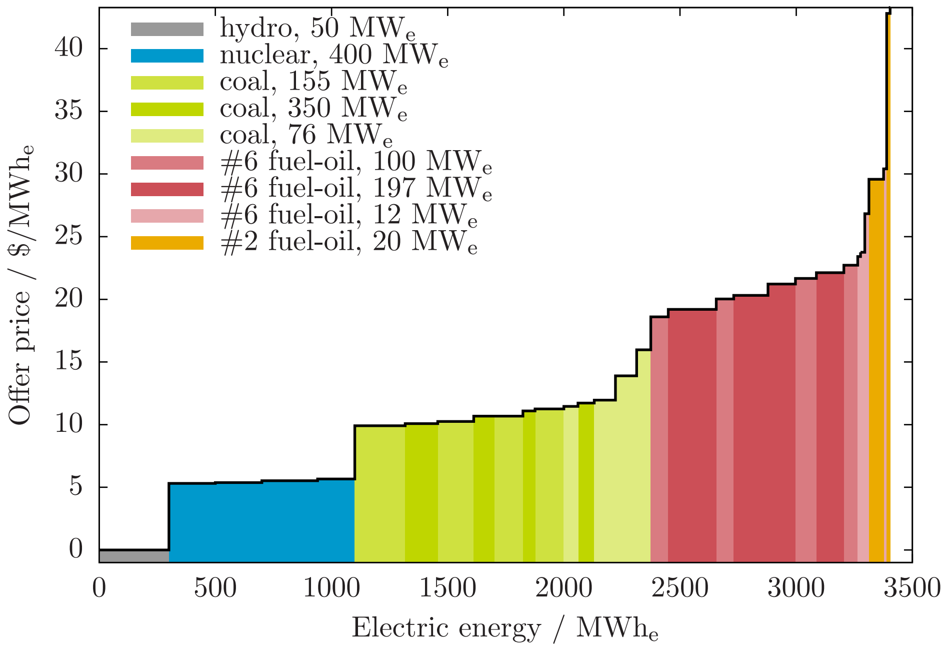

Figure 3.3: Composite supply curve with ranking based on bid price

Austen having a high (*i.e.*, 83%) capacity factor and one more than twice that of the oil-fired units at Arne (28%) or Alder (39%). What would the benefit be, then, of turning down the 350 MW$_e$ coal-fired unit at Austen with the shortfall being made-up by the units at Alder and at Arne? It is a response to this question that is the focus of this section; two scenarios are considered:

Scenario #1: Arne Capacity utilization of 350 MW$_e$ unit at Austen decreases and the three 197 MW$_e$ units at Arne pick up the slack.

Scenario #2: Alder Capacity utilization of the 350 MW$_e$ unit at Austen again decreases and it is the three 100 MW$_e$ units at Alder make up the shortfall.

3.2.1 Estimating the Cost of CO_2 Avoided

In spite of their flaws [45], abatement curves, in which GHG mitigation options are ranked on the basis of *CCA*, are quite common. Thus, *CCA* is used here to quantify the effectiveness of the load balancing scenarios under consideration. An expression for *CCA* is given in (3.1).

$$CCA = \frac{(CoE) - (CoE)_{ref}}{(CEI)_{ref} - (CEI)} \tag{3.1}$$

CCA is the ratio of the incremental cost of the GHG mitigation action to the incremental change in GHG emissions. The derivation of generic expressions for CoE and CEI are given in Chapter 1. For the scenarios being considered, the following assumptions and/or considerations are made:

- The units at Austen, Alder, and Arne have had their capital fully amortized (*i.e.*, $CAPEX_n = 0$.
- Unit heat rates at the nameplate rating are used and any dependency with respect to capacity factor is ignored.
- The contribution to CoE from unit start-up are negligible.
- The other variable operating and maintenance costs are unaffected by load balancing.

Given the above, the following expressions for CoE and CEI are obtained:

$$CoE = \frac{\sum_{n \in NG} \dot{C}_n^{FOM} P_n^{max}}{HPY \sum_{n \in NG} CF_n P_n^{max}} + \frac{\sum_{n \in NG} FC_n HR_n CF_n P_n^{max} L}{\sum_{n \in NG} CF_n P_n^{max}} \tag{3.2}$$

$$CEI = \frac{\sum_{n \in NG} HR_n EI_n^{CO_2} CF_n P_n^{max} L}{\sum_{n \in NG} CF_n P_n^{max}} \tag{3.3}$$

Table 3.1 shows the parameter values used in the analysis: CF is taken from the base-case simulation of the IEEE RTS '96 (see Section 2.4.2), $\dot{C}_n^{FOM}$ is taken from literature , and the rest are taken from [20] (reproduced for convenience in Appendix C). The final consideration consideration is that the extent to which load can be shifted from the 350 MW_e unit at Austen to units at Arne and Alder:

Table 3.1: Parameters of units at Austen, Arne, and Alder in reference case

Parameter	Units	Reference-case values		
		Austen	Arne	Alder
CF		0.826	0.278	0.393
HR	Btu/kWh	9500	9600	10000
$\dot{C}^{FOM}$	\$/MW/year	25000	7500	7500
P^{max}	MW_e	350	591	300
EI^{CO_2}	lb CO_2/MMBtu	210	170	170
FC	\$/MMBtu	1.20	2.30	2.30

- In **Scenario #1: Arne**, load balancing is limited by the capacity of the 350 MW_e unit at Austen. In this scenario, at maximum load balancing, $CF_{Austen} = 0$ and $CF_{Arne} = 0.767$.

- In **Scenario #2: Alder**, load balancing is limited by the capacity of the 100 MW_e units at Alder. In this scenario, at maximum load balancing, $CF_{Austen} = 0.306$ and $CF_{Alder} = 1.0$.

3.2.2 Results

Table 3.2 shows the estimated *CoE*, *CEI*, and *CCA* for the two scenarios of interest and Figure 3.4 shows how the extent of load balancing affects the reduction in CO_2 emissions that are realized.

Table 3.2: Cost of CO_2 Avoided for load balancing scenarios

Parameter	Units	Scenario #1		Scenario #2	
		Initial	Final	Initial	Final
CoE	\$/MWh_e	18.59	25.40	17.85	23.04
CEI	t CO_2/MWh_e	0.845	0.740	0.866	0.806
CCA	\$/t CO_2	65		87	
$(\Delta CO_2)^{max}$	t CO_2/h	48		24	

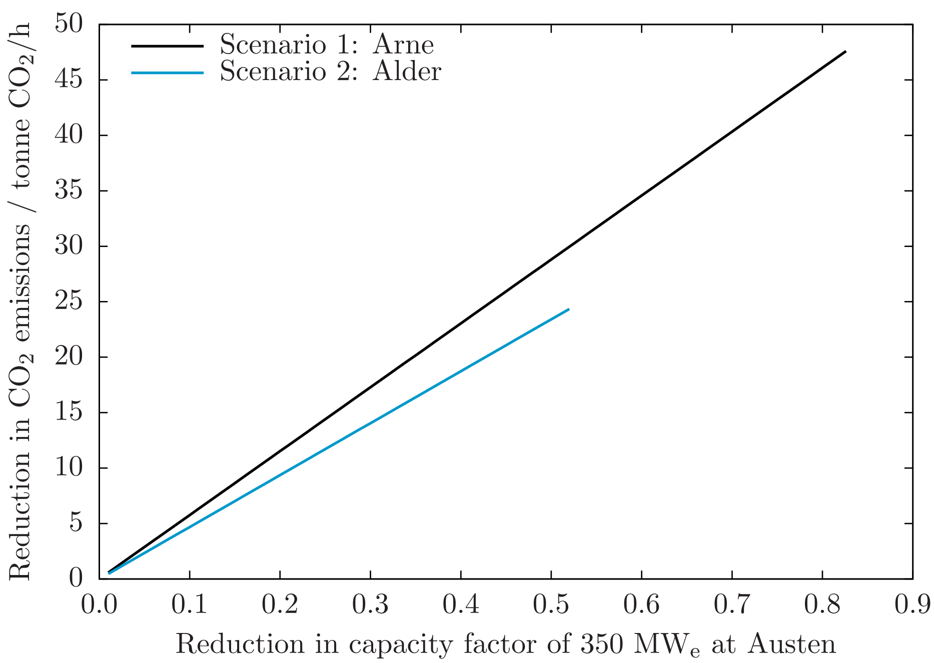

Figure 3.4: Effect of load balancing on CO2 emission reductions

CCA can be understood as the carbon price at which the mitigation action 'breaks even' with the reference case. So, with a carbon price exceeding \$65/tonne CO_2, it would be economical to transfer load from Austen to Arne: doing so would reduce *CoE* and achieve reductions of up to 48 tonne CO_2/h. For load balancing between Austen and Alder to make sense, a carbon price exceeding \$87/tonne CO_2 would be needed and CO_2 could be reduced up to 24 tonne CO_2/h vis-à-vis the reference case. Note that the overall rate of CO_2 emissions from the system is approximately 1000 tonne CO_2/h.

3.2.3 Discussion

The results indicate that load balancing could immediately trigger a reduction in emissions. The basis used for the analysis is representative of the bases used in many published studies (Hashim *et al.*, Chalmers *et al.*) and it is worth considering its validity. For example, the basis includes *HR* (Heat Rate) values corresponding to those of the generating units at base load. Had other values for *HR* been used — the *HR* values observed in the simulation of the IEEE RTS '96, for example (see Table 2.10) — *CCA* for Scenarios #1 and #2 would be \$65 and \$138/tonne CO_2, respectively. And, the maximum achievable CO_2 reductions would be reduced to 46 and 17 tonne CO_2/h. There are still other reasonable values of *HR* that could be selected that would lead to values for *CCA* and $(\Delta CO_2)^{max}$ still further removed than what is shown in Table 3.2.

Implicit in the above analysis is that the location of the units vis--vis the other generating units and the loads in the system is unimportant: a unit of power injected at Alder or Arne is undifferentiated from a unit of power injected at Austen. In reality, Austen and Alder are several nodes apart (see Figure 3.5) and it may not be valid to assume that units from Alder can makeup for lost power at Austen in a simple one-to-one ratio. This is further reinforced by the observation that there is limited unused capacity along the transmission line that connects Alder to the rest of the system (see Figure 2.12). So, the transmission system likely has implications on the effectiveness of load balancing that the above analysis fails to capture.

Assuming that the basis is valid, the analysis indicates the conditions (*i.e.*, carbon pricing) under which the particular load balancing scenarios are economical and the extent to which the particular load balancing scenarios can reduce GHG emissions. But, it does not address the existence of other load balancing scenarios, the carbon prices needed to drive those — could be higher or lower — or the overall reduction in GHG emissions could achieve. Other factors that call the validity of the basis include:

- The 350 MW_e unit at Austen and, to a lesser extent, the units at Alder and Arne have an important role satisfying the requirement for *reserve power* in the IEEE RTS '96 (see Figure 2.11). This likely limits the extent to which the load can shifted from the 350 MW_e unit at Austen to the units at Alder or Arne. As is typically the case in these kinds of studies, reserve power is not considered in the analysis in this section.

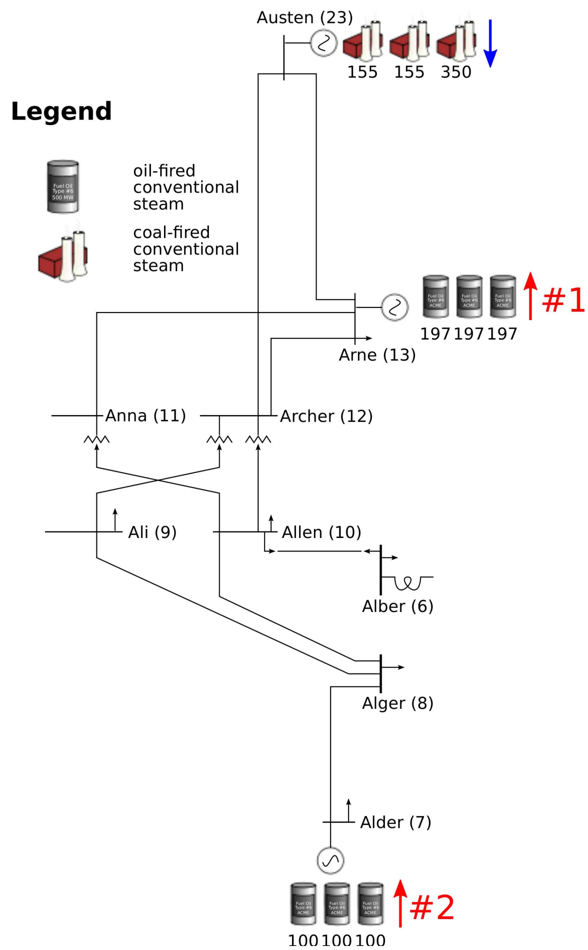

Figure 3.5: IEEE RTS '96 Alder-Arne-Austen sub-network

3.2.4 Conclusion

The above analysis is inconclusive with respect to the merits of load balancing. There are circumstances in which load balancing would economically reduce CO_2 emissions yet the analysis is not able to indicate if one can expect these circumstances to actually materialize. And, though the analysis can ascertain whether or not a particular scenario is favourable, better scenarios might exist and this approach would not lead us to them.

3.3 Adding GHG regulation to electricity system simulator

The results indicate that load balancing could immediately trigger a reduction in emissions by making it economical to preferentially dispatch lower CO_2 emission-intensity units. For the examples considered, a carbon prices of \$65 and \$87/tonne CO_2 are found to be necessary.

Economic dispatch seeks to make the 'best' use of the available generating capacity such demand is satisfied. Regulating GHG emissions increases the cost of generating electricity from GHG-emitting sources: the higher the emissions intensity of the unit, the greater it is affected by said regulation. As the stringency of the regulation increases, the 'best' generation capacity becomes that with a lower carbon intensity. If the regulation is significant, one would expect to see a change with respect to the utilization of these generation units and *load balancing* should occur. There are several different forms that regulation of CO_2 emissions could take including:

1. Cap on aggregate CO_2 emissions of the electricity system
2. Cap on CO_2 emissions of each facility
3. Cap on CO_2 emissions intensity of each facility
4. Charge for every unit of CO_2 emissions

In this study, generators are required to pay for every unit of CO_2 that is emitted to the atmosphere. Thus, with respect to each unit's variable operating and maintenance costs, there is now a contribution based upon the quantity of CO_2 that the unit emits: $C_{nt}^{CO_2}$. A unit's variable operating and maintenance costs in time period t can be expressed as:

$$C_{nt}^{VOM} = C_{nt}^{start-up} + C_{nt}^{fuel} + C_{nt}^{CO_2} \tag{3.4}$$

Figure 3.6 shows the composite supply curve for the IEEE RTS '96 with increasingly higher carbon prices. The offer price of each bid approximates the marginal cost of producing that block of power. As the carbon price goes up, the marginal cost of each bid also goes up proportionally to the carbon price and unit's incremental heat rate. The impact on the composite supply curve is that bids from coal units tend to move toward the higher end of the curve and *vice versa* for bids from oil-fired units. At a sufficiently high enough carbon price — something greater than the maximum of \$100/tonne CO_2 presented here — the relative position of the units would match that based purely on CO_2 emissions intensity shown in Figure 3.2.

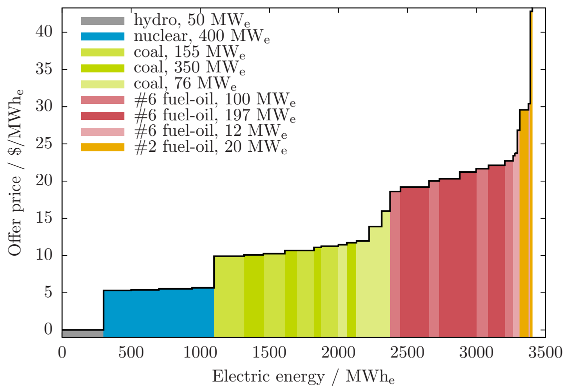

(a) Base IEEE RTS '96

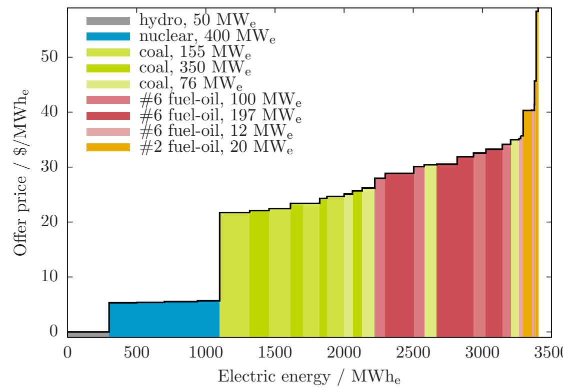

(b) CO_2 price: \$15/tonne CO_2

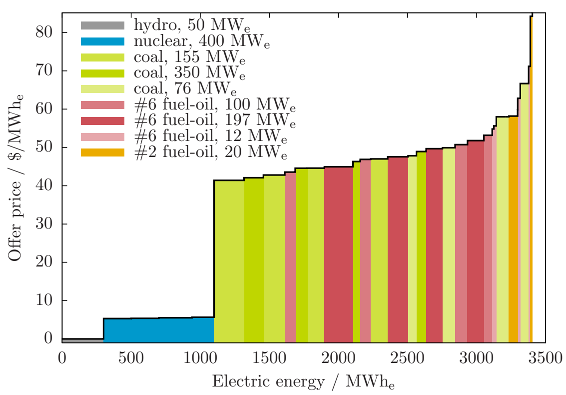

(c) CO_2 price: \$40/tonne CO_2

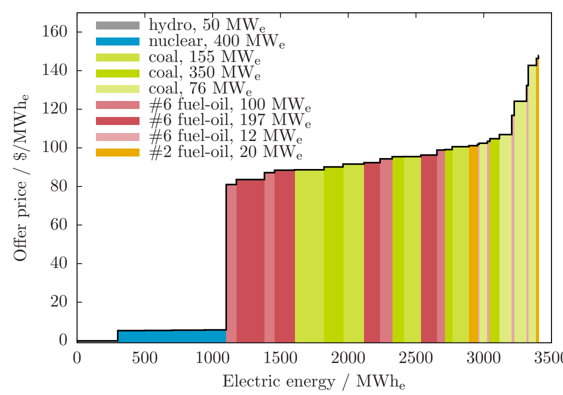

(d) CO_2 price: \$100/tonne CO_2

Figure 3.6: Composite supply curves for IEEE RTS '96 for different levels of carbon pricing

As was done in Sections 2.3.1 and 2.4.1 for fuel and start-up costs, one needs to derive expressions for CO_2 permit costs. The emissions cost can be expressed in terms of heat input to the boiler as follows:

$$C_{nt}^{CO_2} = u_{nt} HI_n EI_n^{CO_2} TAX^{CO_2} + \dot{q}_{nt} EI_n^{CO_2} TAX^{CO_2} L_t \tag{3.5}$$

The first term in (3.5) accounts for fuel consumed during start-up and the second term accounts for fuel use during normal operation. Again, it is convenient to express the permit cost in terms of incremental heat rate. The marginal emissions cost is obtained by taking the first derivative of the first term of (3.5) with respect to P^S_{nt}:

$$\begin{aligned}
C_{nt}^{CO_2,fuel} &= \dot{q}_{nt} EI_n^{CO_2} TAX^{CO_2} L_t && (3.6)\\
\frac{dC_{nt}^{CO_2}}{dP_{nt}^S} &= EI_n^{CO_2} TAX^{CO_2} L_t \frac{d\dot{q}_n}{dP_n^S} \\
\int_0^{P_{nt}^S} \frac{dC_{nt}^{CO_2}}{dP_{nt}^S} &= EI_n^{CO_2} TAX^{CO_2} L_t \int_0^{P_{nt}^S} \frac{d\dot{q}_n}{dP_n^S} \\
&\approx EI_n^{CO_2} TAX^{CO_2} L_t \sum_{b=1}^{N_b} y_{bnt} IHR_{bnt} && (3.7)
\end{aligned}$$

For each unit, the contribution to the objective function is:

$$z_{nt} = \overbrace{u_{nt} HI_n FC_n}^{\text{start-up}} + \overbrace{FC_{nt} L_t \sum_{b=1}^{N_b} y_{bnt} IHR_{bnt}}^{\text{fuel}} + \overbrace{EI_{nt}^{CO_2} TAX^{CO_2} \left(u_{nt} HI_n + \sum_{b=1}^{N_b} y_{bnt} IHR_{bnt} L_t \right)}^{CO_2 \text{ permits}}$$

For load balancing, the objective function used in each of the *pre-dispatch*, *real-time operation*, and *market settlement* phases is given in Equation (3.8).

$$\begin{aligned}
z =& \sum_{t=1}^{T} \sum_{n \in NG} u_{nt} HI_n FC_n \\
&+ \sum_{t=1}^{T} \sum_{n \in NG} \sum_{b=1}^{N_b} y_{bnt} IHR_{bnt} FC_n L_t \frac{1}{10^3} \\
&+ \sum_{t=1}^{T} \sum_{n \in NG} \sum_{k=1}^{N_b} y_{knt} IHR_{knt} EI_n^{CO_2} TAX^{CO_2} L_t \frac{1}{2.205 \cdot 10^6} && (3.8)\\
&+ \sum_{t=1}^{T} \sum_{n \in NG} u_{nt} HI_n EI_n^{CO_2} TAX^{CO_2} \frac{1}{2.205 \cdot 10^3} \\
&+ \sum_{t=1}^{T} \sum_{r \in RM} C^{import} \cdot RM_{rt}^{slack}
\end{aligned}$$

The model constraints and the bounds on the variables are unchanged.

3.4 Results of electricity system simulator

The IEEE RTS '96 is simulated for one full week under the three different carbon prices previously discussed: \$15/tonne CO_2, \$40/tonne CO_2, and \$100/tonne CO_2.

- \$15/tonne CO_2 is a permit price that had been proposed by the Canadian federal government circa 2005. It also serves as the rate at which LFEs need to contribute to the Climate Change and Emissions Management Fund under the Alberta government's SGER (Specified Gas Emitters Regulation). It is perceived as being sufficient to simulate CCS where CO_2 is an input to the production of a saleable commodity. Examples of large-scale projects that fit into this category are EOR and ECBM (Enhanced Coal-Bed Methane).

- \$40/tonne CO_2 is about equivalent to the most optimistic costs of CO_2 avoided reported for CCS. According to these reports, then, a \$40/tonne CO_2 permit price would be sufficient to make CCS economic in some sectors.

- \$100/tonne CO_2 is about the permit price that is now being touted as being necessary for widespread adoption of CCS. [23]

These three permit prices run the gamut of what one would expect to see if serious regulation of GHG emissions were to occur.

3.4.1 General results from electricity system simulation

Capacity utilization

Figure 3.7 shows the change in capacity factor for each type of unit under the three different stringencies of GHG regulation. Another indication of the response of generating unit utilization to GHG regulation is provided via Figure 3.8 which shows the change in the average power output of the various types of units. The results are consistent with the expected behaviour:

- Coal-fired units (*e.g.*, 76 MW_e units at Abel and Adams, the 155 MW_e units at Arthur, and the units at Asser and Austen) see a reduction in their capacity factors and lower emissions-intensity units — notably those at Arne — see increased utilization.

- As the stringency of GHG regulation increases, the effect on a unit's utilization — for better or worse — also increases: higher CO_2 permit price increases results in more shifting of supply from high- to low- emissions intensity units.

- The utilization of the nuclear units (at Astor and Attlee) and the hydroelectric units (at Aubrey) is unaffected by GHG regulation. These units are non-emitting and have marginal operating costs that are lower than the fossil fuel-fired generating units. Thus, they were pretty much fully utilized in the base case and remain so after carbon prices are imposed.

Table 3.3 shows the number of starts for each scenario. Overall, there are less units being started-up (and, hence, being shut-down) in the scenarios with GHG emission regulation.

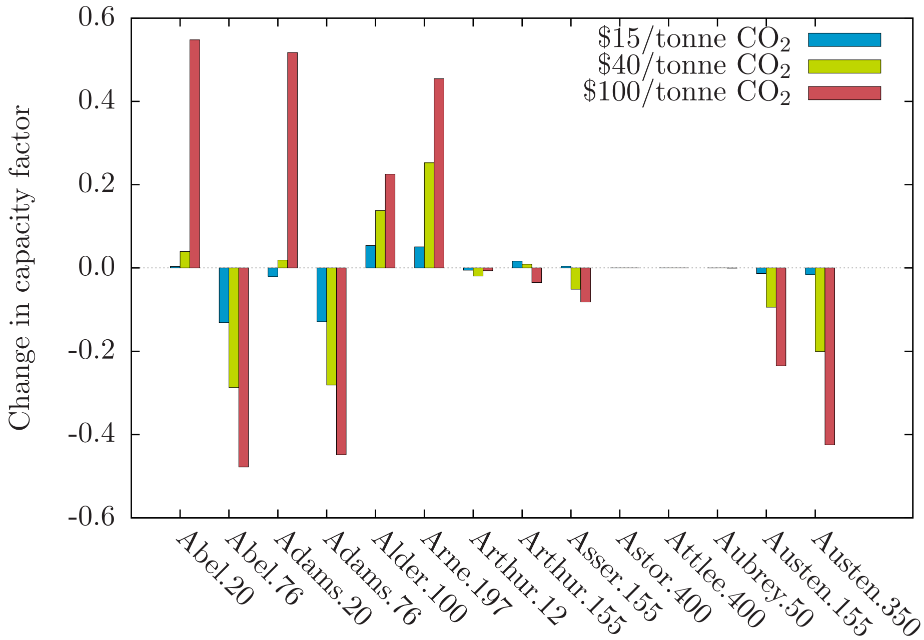

Figure 3.7: Change in capacity factor under different CO_2 permit prices

Table 3.3: Summary of unit utilization

	Unit type			$N^{start\text{-}up}$			
Bus	Fuel	Capacity MW_e	Number	Base	\$15	\$40	\$100
Abel	#2 Fuel Oil	20	2	7	8	10	1
Abel	Coal	76	2	0	0	0	6
Adams	#2 Fuel Oil	20	2	10	8	10	4
Adams	Coal	76	2	0	0	0	4
Alder	#6 Fuel Oil	100	3	3	0	0	0
Arne	#6 Fuel Oil	197	3	16	12	0	0
Arthur	#6 Fuel Oil	12	5	25	20	6	19
Arthur	Coal	155	1	0	0	0	0
Asser	Coal	155	1	0	0	0	0
Astor	Nuclear	400	1	0	0	0	0
Attlee	Nuclear	400	1	0	0	0	0
Aubrey	Hydro	50	6	N/A	N/A	N/A	N/A
Austen	Coal	155	2	0	0	0	0
Austen	Coal	350	1	0	0	0	0

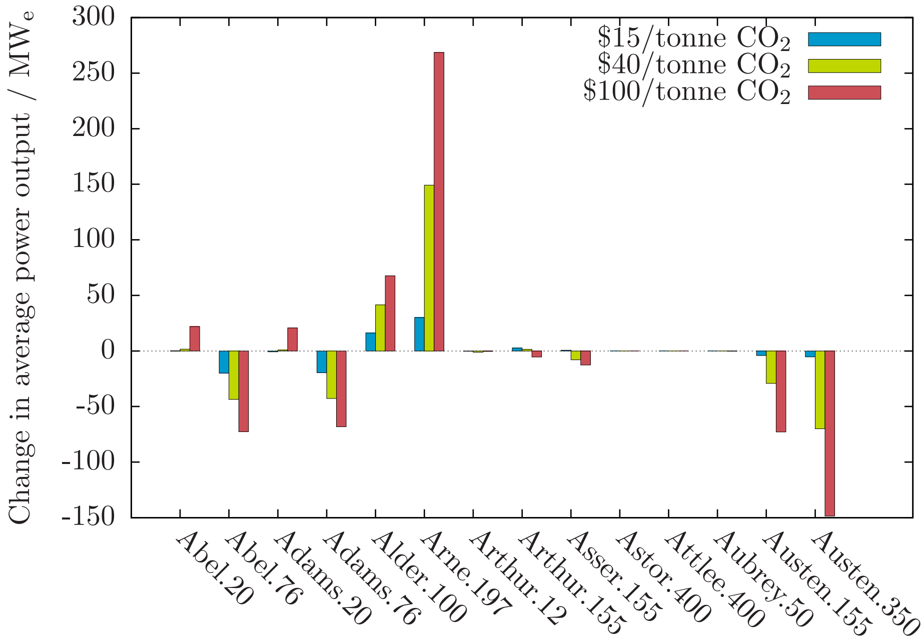

Figure 3.8: Change in average power output under different CO_2 permit prices

GHG emissions

Figure 3.9 shows the aggregate CO_2 emissions during the period of interest. CO_2 emissions are lower when a price on carbon exists than in the base case and the greater the carbon price, the lower the emissions.

Figure 3.10 shows the difference in CO_2 emissions relative to the base case. In any scenario, the reduction in CO_2 emissions relative to the base case can vary considerably from hour to hour.

Table 3.4 summarizes the results in terms of CO_2 emissions for the base case and different stringencies of GHG regulation. To assist in understanding the relationship between TAX^{CO_2} and CO_2 emissions, linear regression is used to fit the data to a second-order polynomial model yielding (3.9).

$$\dot{m}^{CO_2} = 995 - 1.00\,TAX^{CO_2} + 0.0025\left(TAX^{CO_2}\right)^2 \tag{3.9}$$

At low values of TAX^{CO_2}, there is 1 tonne CO_2/h reduction for every \$1/tonne CO_2 increase in CO_2 permit price. As the CO_2 permit price increases, though, there is a diminishing return from further increases in permit price in terms of the CO_2 reductions that load balancing delivers.

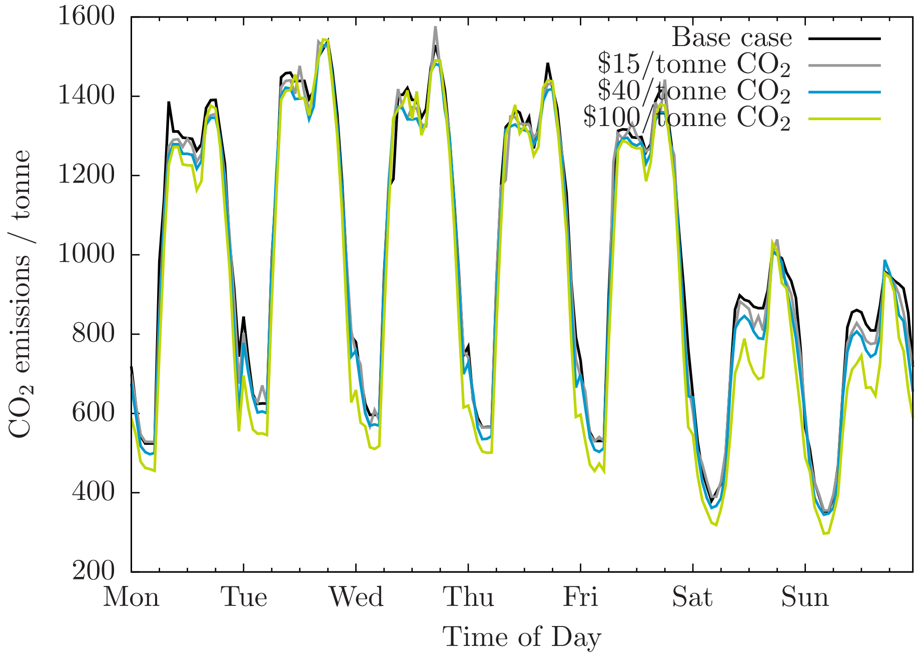

Figure 3.9: Aggregate CO_2 emissions

Table 3.4: Summary of CO_2 emissions and reductions

Scenario	$\dot{m}^{CO_2}$	Δ CO_2		*CEI*
	t CO_2/h	t CO_2/h	%	t CO_2/MWh$_e$
Base case	995			0.483
$15/tonne CO_2	980	14.9	1.5	0.476
$40/tonne CO_2	959	36.5	3.7	0.466
$100/tonne CO_2	920	75.0	7.5	0.447

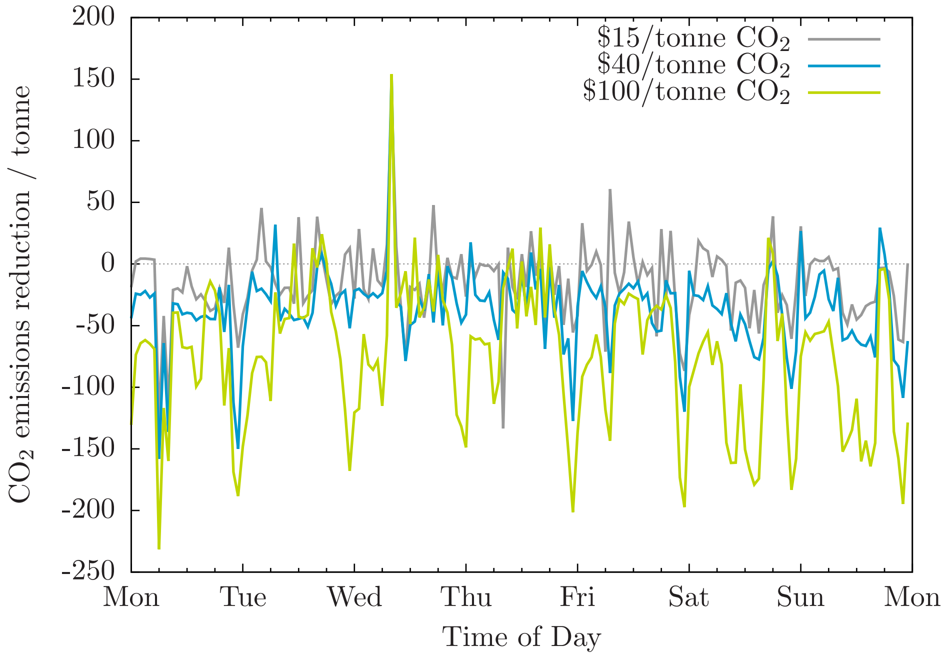

Figure 3.10: Change in CO_2 emissions

Cost of electricity

A key question is "At what cost are the above CO_2 emissions reductions achieved?" There are three components to the electricity cost: cost to start up units, cost of fuel to generate electricity, and the cost of acquiring CO_2 permits. On an aggregate basis, start-up costs are small relative to the other two. Figures 3.11 and 3.12 show the cost of fuel to generate electricity and the cost of acquiring permits, respectively, in each time period for the week of interest.

Both the fuel and CO_2 permit components of CoE increase with increasing permit price. Fuel costs increases as, on the whole, a lower carbon intensive but more expensive fuel (*i.e.*, fuel oil) is being used preferentially over coal for generating electricity. The amount paid to acquire CO_2 permits goes up as the difference in the per-unit permit price greatly exceeds the reduction in CEI that is realized.

Note in Figure 3.11 that the change in $C^{VOM,fuel}$ is significantly different during the week than on the weekend. There is a step-change decrease in electricity demand in going from weekday to weekend and the take-away is that the change in fuel costs is dependent not only on permit price but also on the electricity demand in he given time period.

The generation cost results are summarized is Table 3.5. Though the increase in fuel costs is significant, the cost of acquiring CO_2 permits is the cause for most of the increase

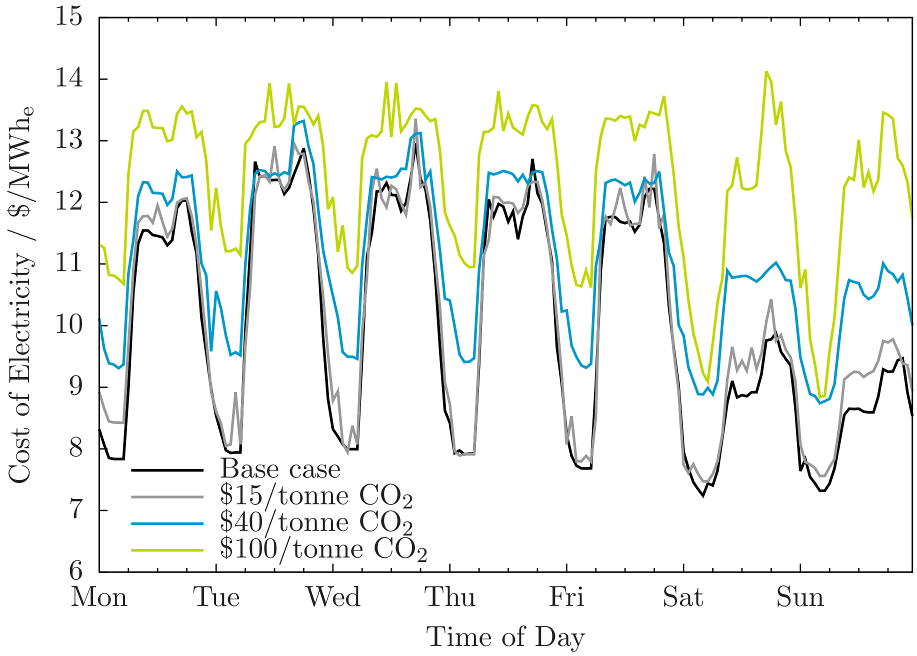

Figure 3.11: Cost of fuel over time for different permit prices

in the cost of generation.

Table 3.5: Summary of change in cost of electricity generation

Scenario	$C^{VOM,fuel}$	$\Delta C^{VOM,fuel}$		C^{VOM,CO_2}	C^{VOM}
	$/MWh$_e$	$/MWh$_e$	%	$/MWh$_e$	$/MWh$_e$
Base case	10.31				10.31
$15/tonne CO_2	10.51	-0.20	-2	7.14	17.65
$40/tonne CO_2	11.34	-1.03	-10	18.63	29.97
$100/tonne CO_2	12.60	-2.29	-22	44.74	57.34

Cost of CO_2 avoided

CCA is a measure of the effectiveness of a GHG mitigation action and an expression for *CCA* is given in (3.1). Using the emissions and *CoE* data from Tables 3.9 and 3.5, the *CCA* for each scenario are calculated and shown in Table 3.6.

The first column is the result of the *CCA* calculation using values of *CoE* that do *not* include the cost of acquiring CO_2 emission permits whereas the values in the second row do include the cost of CO_2 emission permits.

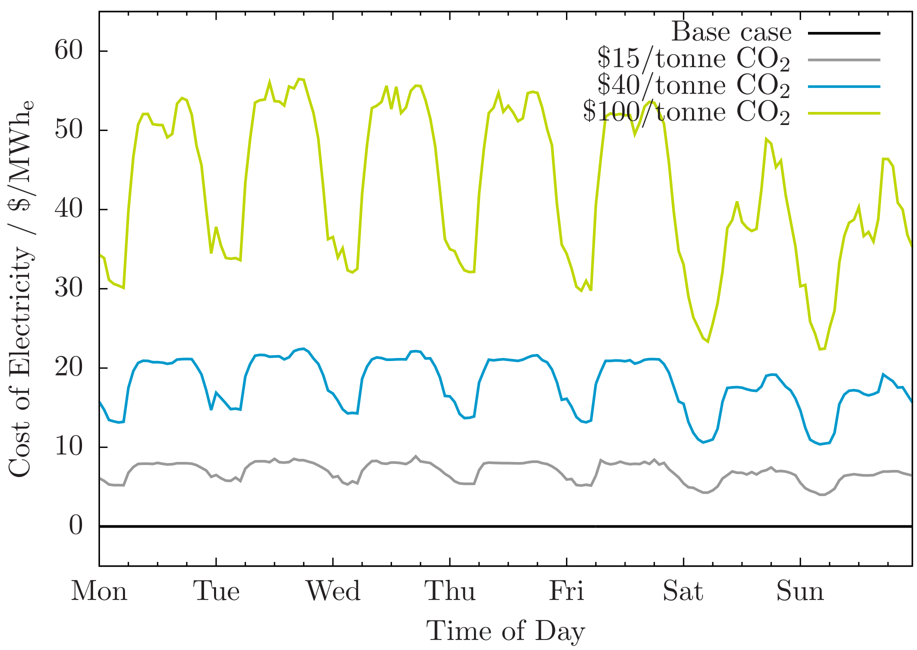

Figure 3.12: Cost of CO_2 permits over time for different permit prices

Table 3.6: Cost of CO_2 Avoided for load balancing scenarios

Scenario	*CCA*, w/o permits $/tonne CO_2	*CCA*, w/ permits $/tonne CO_2
$15/tonne CO_2	29	1049
$40/tonne CO_2	61	1156
$100/tonne CO_2	64	1306

Other economic impacts

CoE and *CCA* are important metrics of the economic impact of achieving reductions in GHG emissions. Some other observations of relevance are provided below.

Electricity price Figures 3.13 and 3.14 show the electricity price and the difference from the base case as a function of time, respectively, for each carbon price scenario. In general, the greater the permit price, the greater the electricity price. A summary of the HEP for the period of interest is given in Table 3.7.

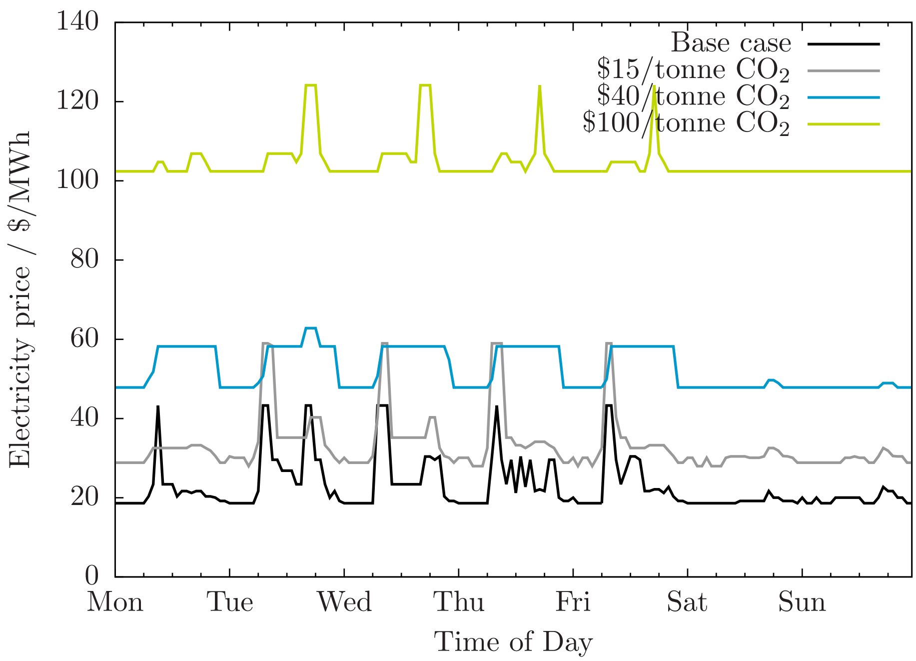

Figure 3.13: Electricity price

Table 3.7: Summary of electricity price for load balancing scenario

Scenario	HEP	Δ HEP	
	\$/MWh$_e$	\$/MWh$_e$	%
Base case	23.68		
\$15/tonne CO_2	33.95	10.27	43
\$40/tonne CO_2	53.38	29.70	125
\$100/tonne CO_2	104.88	81.20	343

Figure 3.15 shows the price setting units at each time period for each level of carbon

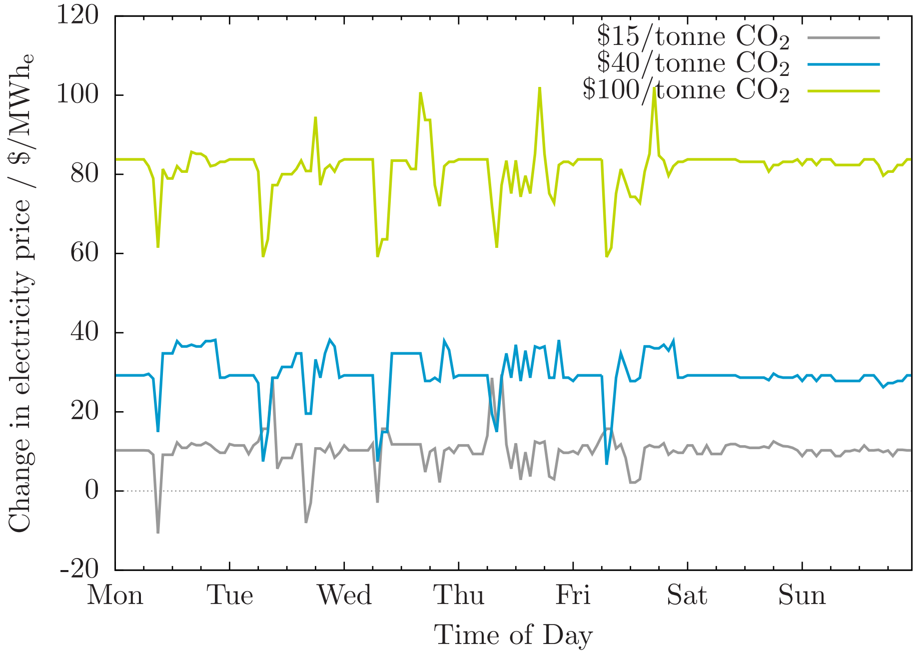

Figure 3.14: Change in electricity price

pricing. In the base case and at \$15/tonne CO_2, it is the oil-fired units that are price-setting. At \$40/tonne CO_2, it is a mix of oil-fired and coal-fired units that are marginal until, finally, at \$100/tonne CO_2, it is bids from coal-fired units that are the most expensive ones selected in every time period.

Table 3.8 compares increases in the average electricity price to increases in the cost of generation. It is interesting to note that increases in electricity price are greater than the increases in the cost of generation.

Table 3.8: Change in electricity price and *CoE* due to GHG regulation

Permit price \$/tonne CO_2	Δ *CoE* \$/MWh$_e$	$\Delta\rho$ \$/MWh$_e$
15	7.34	10.27
40	19.66	29.70
100	47.03	81.20

Energy benefit *Energy benefit* is the revenue earned by a generator from selling power into the electricity market and a generator's *net energy benefit* is the difference between its

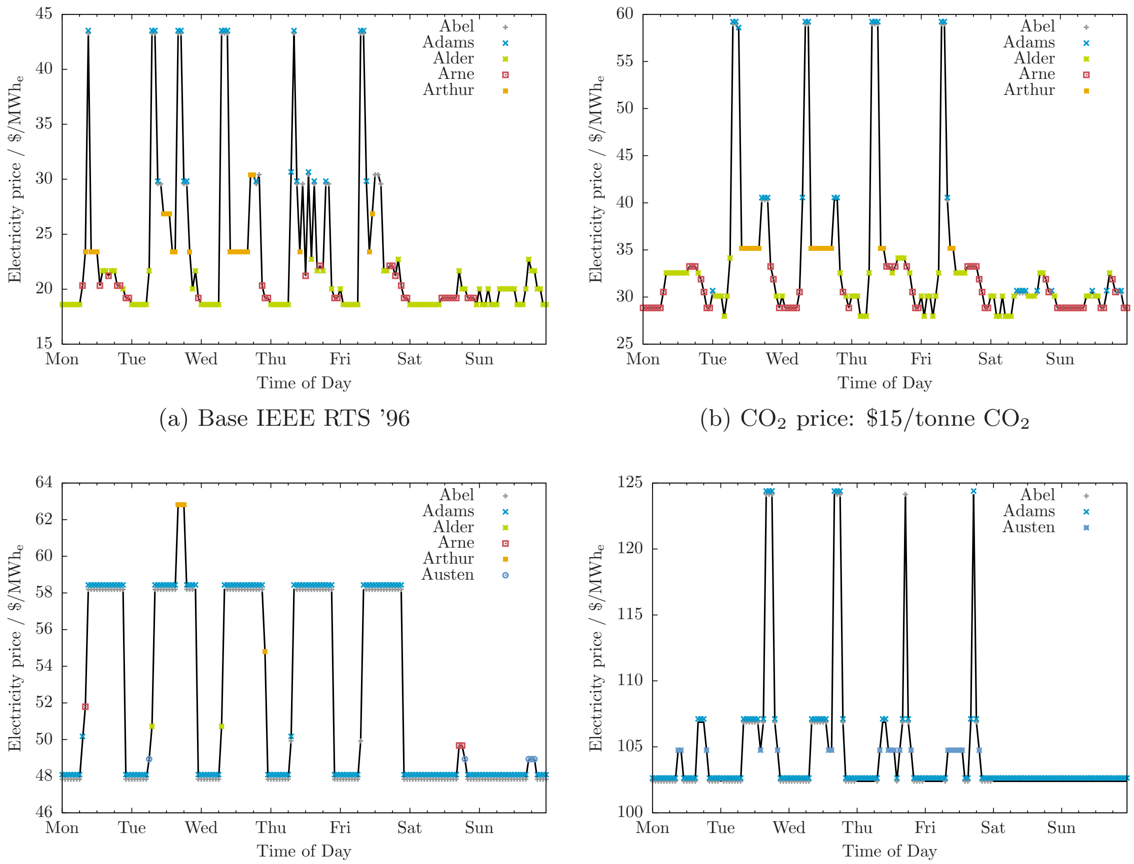

(a) Base IEEE RTS '96

(b) CO_2 price: \$15/tonne CO_2

(c) CO_2 price: \$40/tonne CO_2

(d) CO_2 price: \$100/tonne CO_2

Figure 3.15: Generating units setting market price of electricity

energy benefit and the cost of operating its units. Figure 3.16 shows the change in aggregate net energy benefit realized by generators at the different levels of GHG regulation. Note that the net energy benefit shown in Figure 3.16 is calculated using a *CoE* that includes both fuel and CO_2 permit components. One perhaps surprising observation is that, *en masse*, the generators are more profitable with GHG regulation than without it. The change in net energy benefit is summarized in Table 3.9.

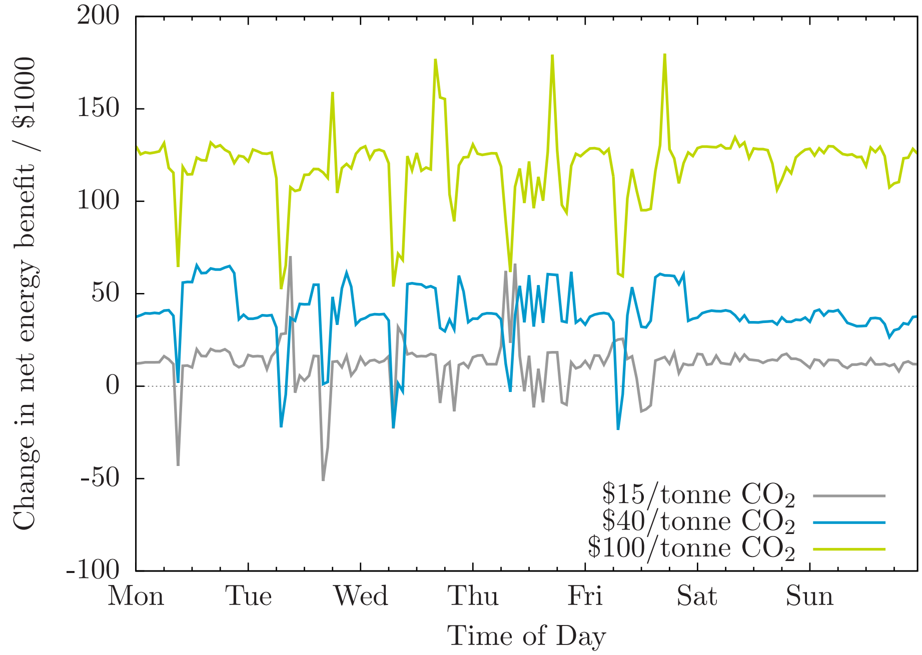

Figure 3.16: Change in net energy benefit relative to base case for different levels of permit pricing

Table 3.9: Change in net energy benefit due to GHG regulation

Scenario	Net energy benefit	Δ net energy benefit	
	$/MWh$_e$	$/MWh$_e$	%
Base case	13.31		
$15/tonne CO_2	16.30	2.99	22
$40/tonne CO_2	23.41	10.10	76
$100/tonne CO_2	47.54	34.23	257

3.4.2 Discussion

The electricity system simulation approach demonstrates that significant reductions in GHG emissions can be achieved by preferentially dispatching fossil fuel generating units with lower CO_2 emissions intensity. In this, the different assessment approaches speak with one voice. In contrasting the results of the two different approaches, some important differences are observed and these are noted and discussed below.

1. The scenario selection for the techno-economic analysis was not the best.

   Within the techno-economic study approach, two scenarios where crafted. Both had the 350 MW_e unit at Austen reducing its output and either units at Arne or Alder making up the shortfall. Examining Figures 3.7 and 3.8, the simulation approach would seem to indicate that:

   - Amongst the coal-fired units, the 76 MW_e units at Abel and Adams are the first ones that should have their output curtailed and not Austen's 350 MW_e unit. At a carbon price of \$15/tonne CO_2, the capacity factor of the 76 MW_e units drops by about 0.15 whereas the capacity factor of the 350 MW_e unit at Austen is essentially unchanged. As the carbon price is increased to \$40 and \$100/tonne CO_2, the 'hit' taken by the smaller coal units is always greater than its larger counterparts.
   - In terms of making up for the reduced output of the coal-fired plants, units at Arne are a much better choice than those at Alder appear not to be. At all the carbon prices examined, units at Arne increase their output to make up for reductions elsewhere much more so than the units at Alder.

2. The techno-economic study approach over-estimated the stringency of regulation required to reduce CO_2 emissions.

   A *CCA* of \$65 and \$87/tonne CO_2/ was calculated for the Arne and Alder scenarios, respectively, using the top-down approach in Section 3.2 (see Table 3.2). This would imply that an emissions permit price of at least \$65/tonne CO_2 is required to incentivize the shift in generator output. The electricity simulation analysis showed significant reductions in CO_2 emissions at substantially lower permit prices of \$15 and \$40/tonne CO_2.

3. The electricity system simulation approach predicts the extent to which load balancing will reduce CO_2 emissions.

   Building upon the above, the techno-economic study approach indicated that a permit price of \$65/tonne CO_2 is required for load balancing between Arne and Austen to make economic sense. However, it does not indicate how much load will be shifted and, hence, the resultant reduction in CO_2 emissions. Only an upper bound on emissions reductions is obtained. The electricity system simulation approach, though, is able to determine how CO_2 emissions will change in response to varying stringency in the constraints on emitting GHG's.

4. The average heat rate of the units changes significantly as a result of GHG regulation.

   Figure 3.17 shows the heat rate of the units at Alder, Arne, and the 350 MW_e unit at Austen in the base case and with CO_2 permit prices of \$15, \$40, and \$100/tonne. There are two points to be taken-away:

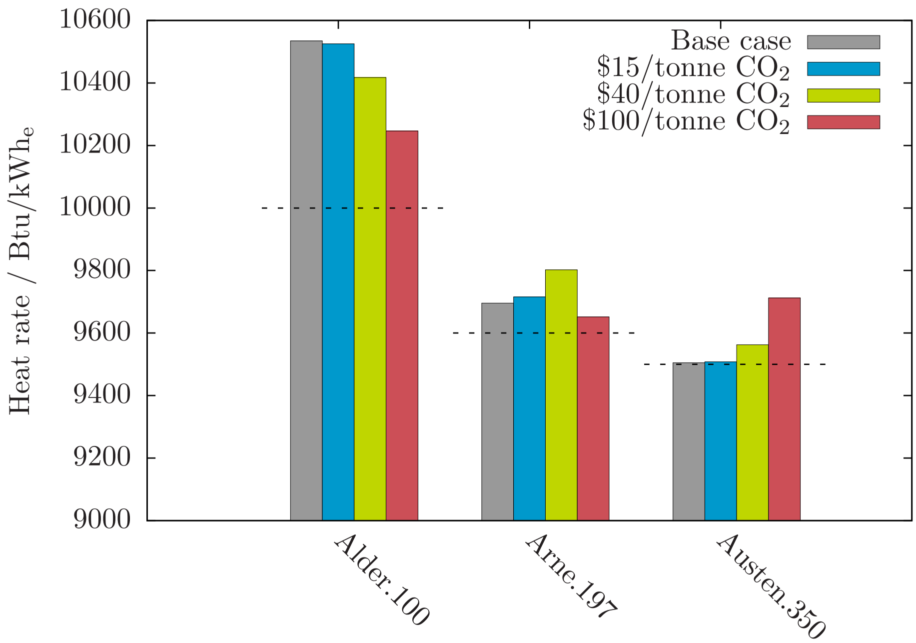

Figure 3.17: Heat rates at Alder, Arne, and Austen under different CO_2 permit prices

- The units' average heat rates can vary significantly from one scenario to the next. Also note that the average heat rate of the units at Arne is greater in the \$40/tonne CO_2 scenario than it is when carbon prices are \$0 and \$15/tonne CO_2 even though the capacity factor is higher. This makes it difficult to know what is the 'correct' heat rate value to use within a top-down analysis.
- The dashed lines on Figure 3.17 indicate the minimum heat rate for each of the units. Typically, within top-down analyses, the minimum heat rate is used for calculating *CCA*. As the figure shows, it is often the case that the heat rates observed in the system are substantially far removed from this optimal level.

5. The electricity market is more profitable with GHG regulation than without it.

   On an aggregate basis, it has already been shown that the net energy benefit of generators *increases* as a result of GHG regulation. Figure 3.18 shows the net energy benefit of each type of unit in the base case and with different emission permit prices and it is clear that some generators make out better than others.

   GHG regulation is a windfall for non-CO_2 emitting sources; these have zero costs for complying with GHG regulation yet receive, for the electricity they produce, the higher prices triggered by regulation. Examples of these are the hydroelectric units at Aubrey and the nuclear units at Astor and Attlee.

   The oil-fired units also come out ahead as they are producing the same or greater power and selling it at a higher price.

   The coal-fired units do not do so poorly considering a drop in their power output. The 155 and 350 MW_e units see net energy benefits that are more or less than what they experienced in the base case. The exception is the 76 MW_e units at Abel and Adams. Net energy benefit of these units declines significantly with increase permit prices and, at a permit price of \$100/tonne CO_2, these units operate at a loss over the time period examined.

3.5 Conclusion

Load balancing is the normal response of the electricity system to a change in the relative SRMC of units. In and of itself, it is not a very effective CO_2 mitigation strategy. However, it was important to consider the effect of load balancing for two reasons:

- The outcomes of other mitigation options will all have a load balancing component. Without first quantifying the effect of load balancing, one would not know how much benefit is truly due to the mitigation option being evaluated.

- The load balancing study gives an indication of the extent to which electricity prices can increase in response to different levels of permit prices. This provides some indication of the CO_2 emissions permit price required to enable the penetration of new, non-emitting, generation technologies. For example, based upon the estimated HEP (see Table 3.13), if a solar thermal generation project is predicted to have an average cost of generation of \$50/MWh_e, then it seems like a CO_2 permit price of \$40/tonne CO_2 is required before that project is economic.

Load balancing is most effective during periods of intermediate demand. During peak demand, all available units are being dispatched and there is insufficient flexibility to be able to preferentially dispatch units based upon their emissions intensity. During off-peak, the low demand coupled with an emissions intensity that is already relatively low (large

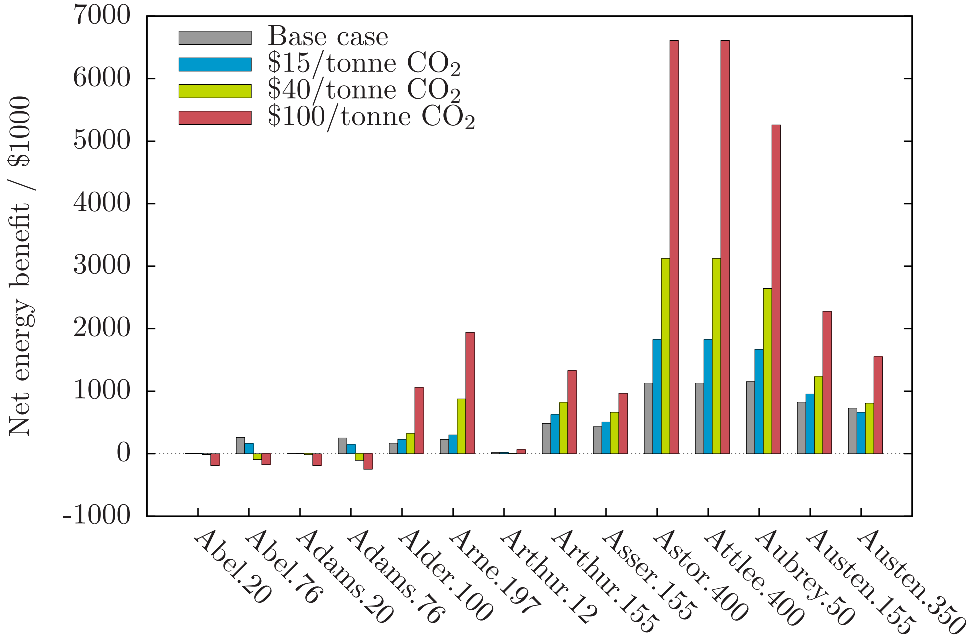

Figure 3.18: Net energy benefit for the different types of units under different CO_2 permit prices

proportion of demand is being satisfied by the non-emitting hydroelectric and nuclear generating units) that the ability to reduce CO_2 emissions is limited.

As a side note, the intermediate shaded region in Figure 3.19 represents the cost borne by the generators in acquiring CO_2 emission permits with permits priced at \$40/tonne CO_2. Note that, even with moderate GHG regulation, this portion of the units' generation cost exceeds by a significant margin the other components of the cost of electricity. And, it would be the regulatory framework that would dictate how this 'cost' is disbursed (*e.g.*, subsidy to generators, rebate to electricity consumers, investment in new technology).

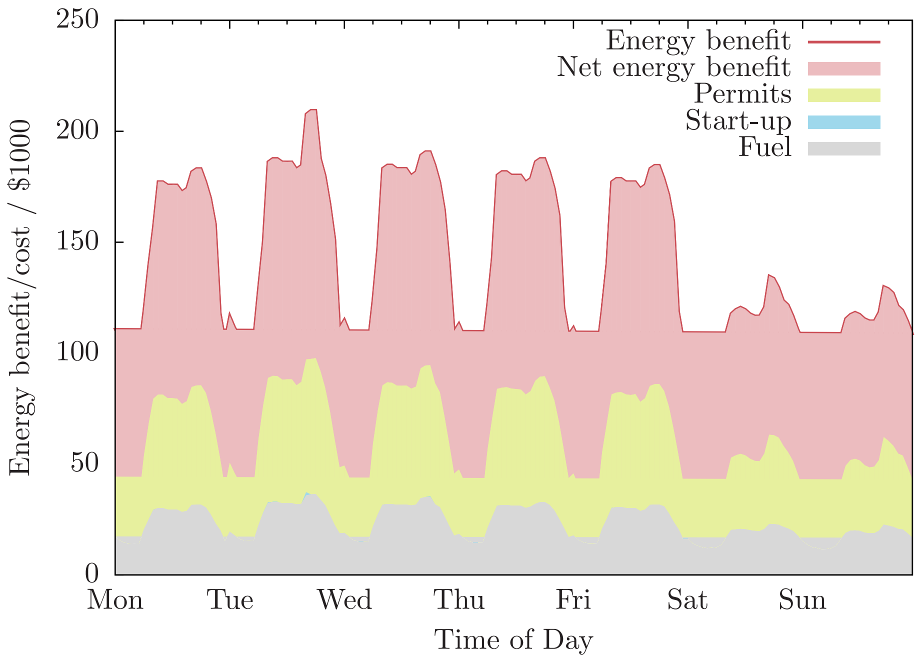

Figure 3.19: Gross and net energy benefit realized by generators: \$40/tonne CO_2

Chapter 4

Development of reduced-order models

4.1 Introduction

It is demonstrated in Chapter 3 that, in the case of load balancing, the assessment of the effectiveness of a mitigation strategy depends upon whether the assessment includes the detailed operation of an electricity system. It is of interest to understand to what extent considering the detailed operation of the electricity system influences the assessment of CCS as a mitigation strategy and this subject is explored in Chapters 5 and 6. To do this, it is necessary to extend the electricity system simulator to include CCS.

In the formulation of the electricity system simulator described in Chapter 2, generating units are represented using reduced-order models: stepwise, linear, univariate functions of power output. This approach is fine for analyses where the output of a generating unit depends upon a single variable (*e.g.*, heat input to a boiler, volumetric flow rate through a turbine). A generating unit with integrated CO_2 capture that is designed for flexible operation, though, would have its maximum power output determined by two variables: the heat input to the boiler and the CO_2 recovery. Therefore, in order to assess the potential advantage(s) conferred by flexible CO_2 capture, a different approach is required.

An alternative to embedding a reduced-order model of a generating unit in the electricity system simulator would be to couple the electricity system simulator to an external generating unit simulator. In this paradigm, the electricity system simulator would create, as required, an instance of, for example, Aspen Plus® to evaluate a model of a generating unit with integrated CO_2 capture. Though feasible, this approach would not work in practice. Underlying the electricity system simulator is an MINLP model for which efficient solution algorithms depend upon the Lagrangian and Hessian of the constraints. Given the complexity of an Aspen Plus® model it is not possible to compute these analytically and numerical estimation of these would render the problem insoluble on commodity computer hardware.

Therefore, the same approach of embedding reduced-order models will be taken for units with flexible CO_2 capture as is taken for the generating units in the stock IEEE RTS '96. This chapter describes the development of two reduced-order models that are required:

1. A reduced-order model of a coal-fired generating unit and
2. A reduced order-model of the same coal-fired generating unit but with integrated CO_2 capture.

4.2 Reduced-order model of coal-fired generating unit

The general procedure for developing the reduced-order model of a coal-fired generating unit is as follows:

- Develop a steady-state process model of the generating unit.
- Simulate the operation of the generating unit over the domain of operating conditions that are of interest.
- Develop a reduced-order process model of the generating unit using linear regression.

4.2.1 Selection of process modelling tool

The selection of a tool for simulating the performance of a power plant was driven by the ultimate desire to have a model of a generating unit with integrated CO_2 capture. A survey of commercially-available process design and simulation tools found some geared toward power systems and others toward separations but no single tool that was proficient at representing both parts of the process.

For example, EBSILON® Professional [18] is targeted toward the design and simulation of power plant systems and is a robust platform for the development of steady-state model of the coal-fired generating unit *without* CO_2 capture. The thermodynamic packages and unit operation models in software in the class of EBSILON® Professional are not sufficiently advanced to accurately predict the performance of MEA-based CO_2 capture processes. Therefore, EBSILON® Professional is inadequate as a standalone tool for developing the rigorous process model of generation with integrated CO_2 capture.

Conversely, with respect to tools adept at modelling separation processes, four platforms are reported in the open literature — Aspen Plus®, UniSim® Design, gPROMS, and ProTreat — as being used for the design and simulation of MEA-based CO_2 capture.[4] Though not their forte, it would be possible to model a generating unit using Aspen Plus®, UniSim® Design, and gPROMS.

An alternative approach to using a single piece of software for the design and simulation of the entire process would have been to develop the models of the generating unit and CO_2

capture process in separate environments that are then linked during model simulation. One piece of software becomes the 'master', calling instances of 'slave' program as required with information passing between the applications via a defined interface. An advantage of this approach is the ability to better match the modelling requirements of the process sub-components with the capabilities of the available software. A disadvantage is the computational overhead introduced by the interprocess communication between the master and the slave and this cost must be weighed against the benefits.

It is anticipated that many evaluations of the master and slave programs will be required for each simulation of the generating unit with integrated CO_2 capture. And, as such, it is assumed that the penalty of using multiple process simulation tools will exceed than the benefits and this coupled approach is not pursued further. Aspen Plus® is selected as the process simulation tool.

4.2.2 Develop process model of the generating unit

The coal-fired generating unit is modelled after the 500 MW_e units at the OPG's Nanticoke Generating Station in Ontario, Canada. These subcritical units are designed to burn subbituminous coal and to generate 1500 tonne per hour of steam at 538°C and 165 bar with a single, 538 °C reheat.

The development of the process model of the power plant is described in [3] and no significant changes are made. An implementation of the generating unit model is given in Appendix F.1 in the form of an Aspen Plus® input file. The simulation of the generating unit proceeds as follows:

1. The target for the steam flow is specified.
2. An initial value for the steam flow is selected.
3. The steam cycle is simulated.
4. The gross and net power output to the turbine is calculated.
5. The heat duty for the *boiler* and *reheater* are calculated.
6. The flow rate of coal required is calculated.
7. If the steam flow is equal to the target, the simulation ends.
8. Otherwise, a new value for the steam flow is selected and the algorithm repeats starting at Step 3.

4.2.3 Simulate operation of the generating unit

The model takes a steam volumetric flow rate as input and returns the corresponding flue gas flow rate, heat input to the boiler, and net power plant output. Nine steam volumetric flow rates ranging from 100% to 25% of the full flow rate were selected and the operation of the generating unit simulated for each one. Table 4.1 summarizes flue gas flow rate, heat input to the boiler, and net power output for each simulation and Figure 4.1 shows a plot of heat input versus net power output. The flue gas composition is the same for each simulation: 14.6 mol% CO_2, 79.0 mol% N_2, and the balance, 6.4%, H_2O.

Table 4.1: Heat input to the boiler and net plant output over generating unit operating range

Unit load	Flue gas flow rate	Heat input	Net power output
%	$10^6 m^3/s$	MW_{th}	MW_e
100	556	1411	497
90	506	1283	448
80	454	1152	399
70	402	1020	349
60	350	887	299
50	296	751	248
40	241	612	197
30	185	470	145
25	157	398	119

4.2.4 Develop reduced-order model of generating unit

Three different forms are proposed for the reduced-order model of the generating unit:

$$P = a_0 + a_1\dot{q} \tag{4.1}$$

$$P = a_0 + a_1\dot{q} + a_2\dot{q}^2 \tag{4.2}$$

$$P = a_0 + a_1\dot{q} + \frac{a_3}{1+\dot{q}} \tag{4.3}$$

(4.1), a first-order polynomial, is proposed based upon visual inspection of Figure 4.1. The idealized representation of the input-output characteristic for a coal-fired generating unit (*i.e.*, heat input to boiler for each unit of net power output) is a smooth, convex curve, often fitted by a second-order polynomial.[51, p 10] (4.2) and (4.3) are obtained by adding to the first-order polynomial the terms $a_2 \cdot \dot{q}^2$ and $a_2 \cdot (1+\dot{q})^{-1}$.

For the dispatch of a generating unit, it is the incremental heat rate characteristic that is important and this is obtained by taking the first derivative of the input-output model

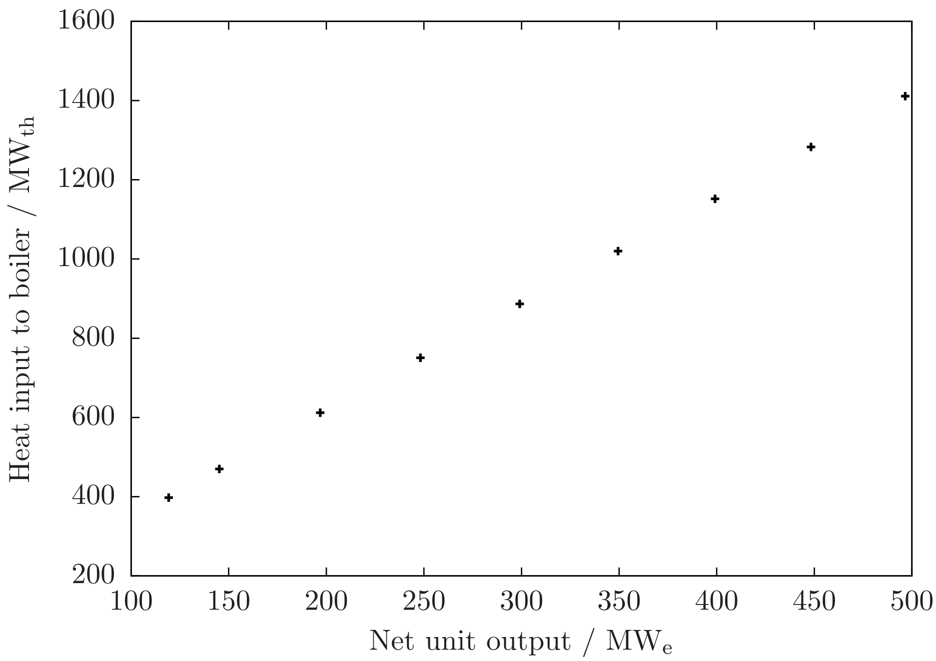

Figure 4.1: Heat input to the boiler versus net plant output over generating unit operating range

with respect to net power output. For the coal-fired generating unit being modelled, the expectation is for the incremental heat rate to increase as a function of net power output. The inclusion of a higher order term in the input-output model of the generating unit is necessary for this behaviour to be captured and, consequently, (4.1) is considered no further.

For each of (4.2) and (4.3), least-squares estimates of the parameters are determined using the GNU R statistical computation software.[48] The results of the regression are shown in Tables 4.2 and 4.3. ANOVA (Analysis of Variance) suggests that both models fit the data; for each case, the high adjusted R-square values indicate that essentially all of the error in the data is explained by the model and the low P-values suggest that all of the parameters are useful.

Table 4.2: Least-square estimates of parameters for reduced-order model of generating unit

Parameter	(4.2)	(4.3)
a_0	-24.90	-42.75
a_1	0.3582	0.3802
a_2	-8.283×10^{-6}	
a_3		4333
adj. R^2	> 0.99	> 0.99

Table 4.3: P-values for regression parameters for reduced-order model of generating unit

Parameter	(4.2)	(4.3)
a_0	5×10^{-7}	2×10^{-9}
a_1	1×10^{-11}	2×10^{-16}
a_2	2×10^{-3}	
a_3		3×10^{-6}

Figure 4.2 shows the models plotted alongside the data from the Aspen Plus® simulations and Figure 4.3 is a plot of the residuals. (4.2) and (4.3) fit the data well with no perceptible difference in terms of goodness of fit. In both cases there is a sinusoidal trend in the residuals. But, given the residuals are small and roughly centered around zero — with the range in variation of (4.3) a bit narrower than (4.2) — the trend is deemed insignificant.

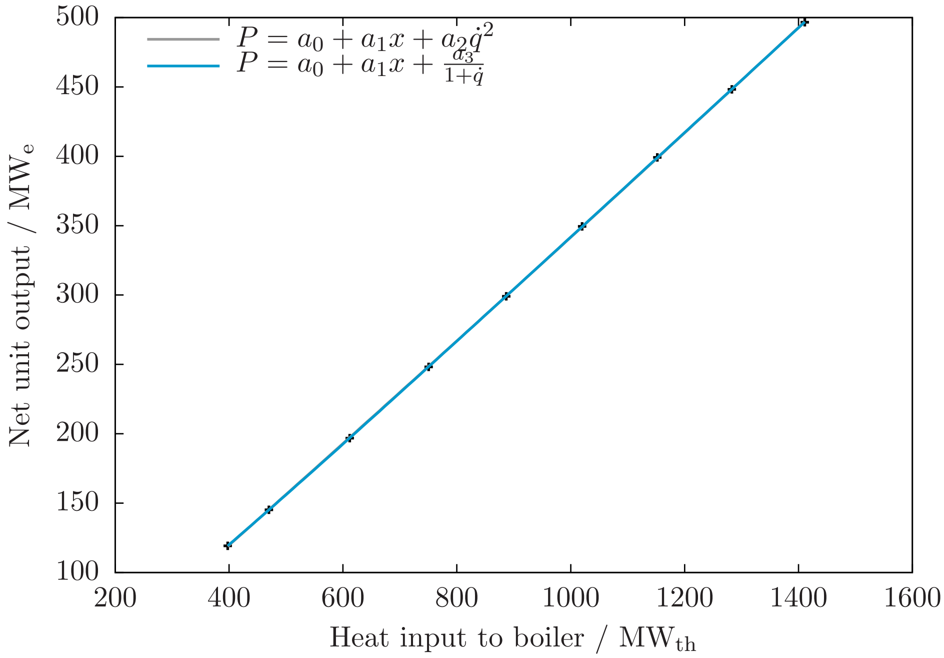

Figure 4.2: Regression models of net power output to heat input to the boiler

4.3 Reduced-order model of coal-fired generating unit with CO_2 capture

Approaches to capturing CO_2 from coal-fired generating units fall into one of three categories:

1. pre-combustion capture
2. oxy-fuel combustion
3. post-combustion capture

PCC (Post-Combustion Capture) of CO_2 using amine solvents is regarded as the best near-term CCS option. It proposes to scale-up well-established technologies that are used to manufacture commercial quantities of CO_2. The benchmark solvent for PCC from the flue gases of coal-fired generating units is MEA, typically in conentrations of 30 wt% in water. It is this technology that is selected for this work.

The development of the reduced-order model of the coal-fired generating unit with MEA-based CO_2 capture follows the same three basics steps used in Section 4.2 for developing the reduced-order model of the generating unit without capture:

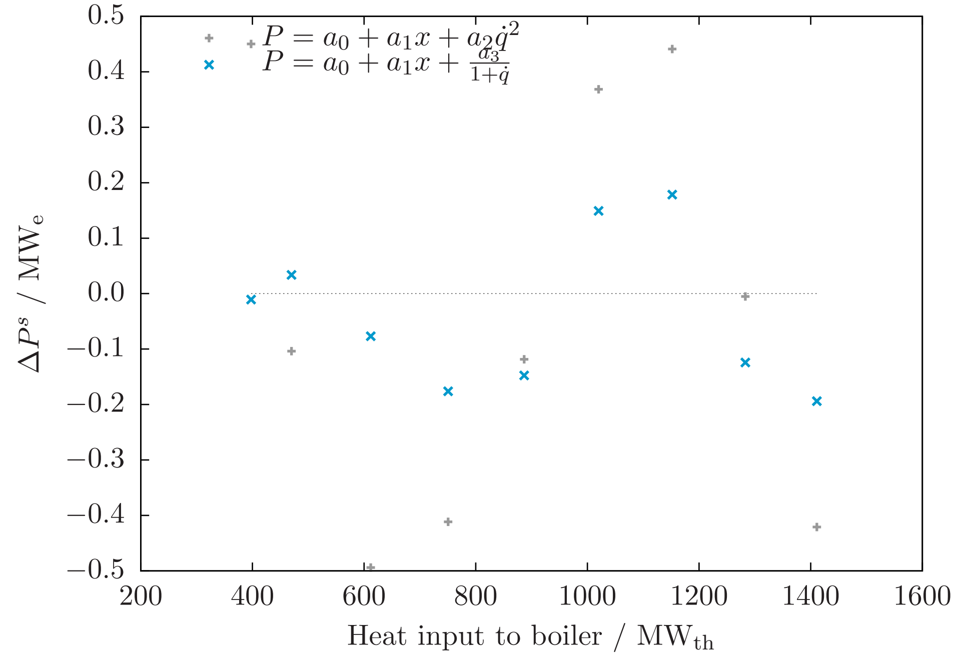

Figure 4.3: Residual plots for regression models of net power output versus heat input to the boiler

1. Develop a steady-state process model of the generating unit with intergrated CO_2 capture.

   A process model of a CO_2 capture process is developed and integrated with the model of the generating unit described in Section 4.2.

2. Simulate the operation of the generating unit over the domain of operating conditions that are of interest.

   The output of a generating unit with integrated CO_2 capture is defined by two inputs: the heat input to the boiler and the quantity of CO_2 captured. In this work, the quantity of CO_2 captured is expressed as a fraction of the generated CO_2 that is recovered.

3. Develop a reduced-order model for the generating unit using linear regression.

   Several forms of a reduced-order model are proposed and least-squares estimates of the parameters in each model are obtained. Ultimately, a single model is selected to represent the coal-fired generating unit with CO_2 capture for incorporation into the electricity system simulator.

4.3.1 Develop process model of the generating unit with CO_2 capture

The design and modelling of MEA-based, post-combustion CO_2 capture processes is reported many times in the literature. The approach used to develop an integrated model of a generating unit with CO_2 capture is based upon that used in [3]. In the following presentation, the emphasis is on areas of the model development which deviate from the basis and the reader is encouraged to review [3, Chapters 4 and 5] for details not presented here. Discussion of model devleopment is presented into five sections:

1. CO_2 capture process flowsheet
2. Physical and chemical properties
3. Specifying streams
4. Specifying UOMs (Unit Operation Model)
5. Integration of generating unit and CO_2 capture processes

Specifying CO_2 capture process flowsheet

A process flow diagram for post-combustion CO_2 capture is shown in Figure 4.4. It differs from the process flowsheet used in [3] in that the rich solvent is flashed upstream of the *Stripper*. The flash vapours are mixed with the *Stripper* overhead vapours and the flash liquid stream is fed to the column. This corresponds to the Kerr-McGee/ABB Lummus

Global's "energy saving design" and should result in a lower *Stripper* reboiler heat duty.[8]

Specifying physical and chemical properties

As in [3], the capture solvent is 30 wt% MEA in water and the physical and chemical property method selection is faciliated using the Aspen Plus® *Electrolyte Wizard*. Aspen Plus® is able to represent the solution chemistry in two ways. With the *true* species approach, the individual components in solution are reported separately. With the *apparent* species approach, only the quantities of the parent compounds are reported. In this work, the true species approach is selected.

Specifying streams

At a minimum, the three input streams to the flowsheet must be specified:

FLUE-SPL The composition and flowrate of the flue gas stream is an output of model of the coal-fired generating unit and was shown in Table 4.1. At full load, the generating unit produces more than 4×10^6 m^3 of flue gas per hour. Given an assumed maximum column diameter of fifteen metres, previous work [3] has shown that a minimum of three trains is required to achieve the recovery target for this volume of flue gas. In this work, it is assumed that the model represents one of these three trains and the inlet flue gas flow rate is scaled down accordingly.

H2O-PUMP Nanticoke Generating Station is located adjacent to Lake Erie and a cooling water temperature of 12°C is assumed. This corresponds to conditions observed during the summer season.

MAKE-UP There are some small yet significant amounts of water and MEA that are lost principally in the treated flue gas. Make-up solvent at 25°C is added to the lean solvent in the *MIXER* downstream of the heat exchanger. The make-up solvent is nominally 30 wt% MEA in water.

Aspen Plus® has two different solution modes — sequential modular and equation-oriented — and it is the former that is used. LEAN-ABS and LEAN-HX are designated as tear streams. Experience has taught that flowsheet convergence can depend upon the initialization of the tear streams and initial values, based upon [3] are shown in Table 4.4 for a target CO_2 loading of 0.25.[1]

[1] Also required to complete the specification of streams H2O-PUMP, MAKE-UP, LEAN-ABS, and LEAN-HX is the stream flow rates. As will be discussed later, the flow rate of each of these streams is determined endogenously during flowsheet convergence so the initial value given is not particularly important.

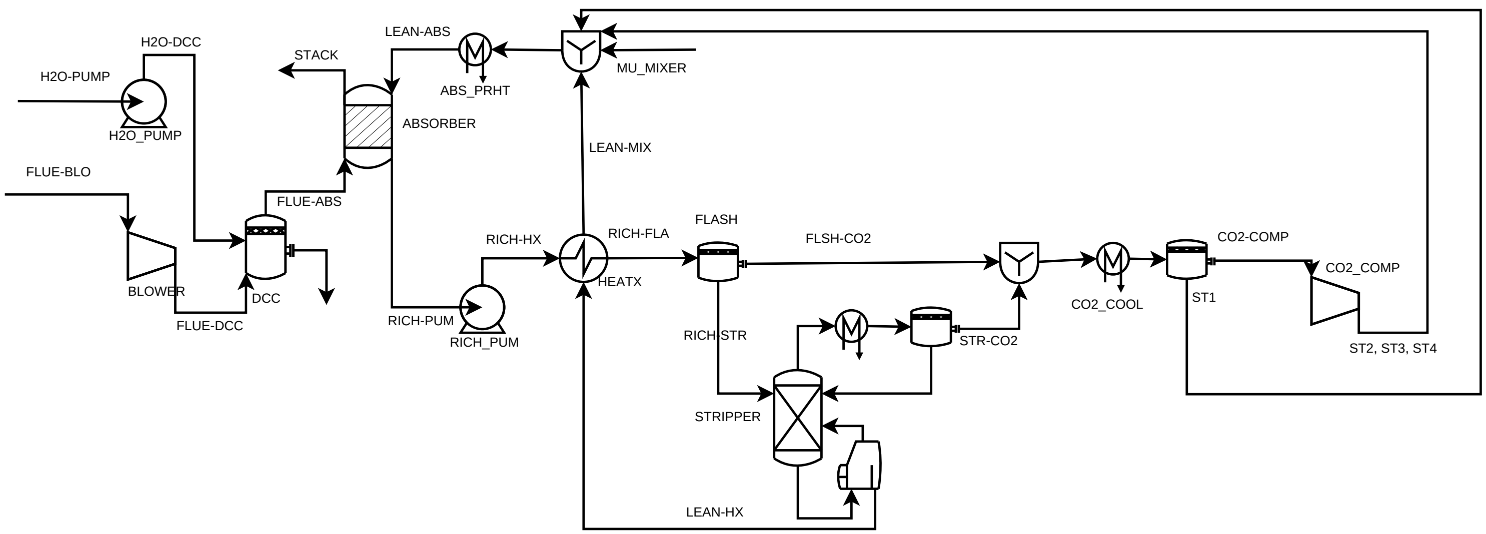

Figure 4.4: MEA-based CO_2 capture process simulation flowsheet

Table 4.4: Sample initial values for Aspen Plus® model of CO_2 capture process

Parameter	Units	LEAN-ABS	LEAN-HX
Temperature	°C	40	
Pressure	kPa	101.3	173
Vapour fraction			0
Mole fraction MEA		0.126	0.126
Mole fraction H_2O		0.874	0.874
Mole fraction CO_2		0.032	0.032

Specifying unit operation models

Table 4.5 summarizes, for each block, the selected Aspen Plus® UOM (Unit Operation Model) and the parameters used in their configuration. With the exception of *Absorber*, *Stripper*, and *FLASH* the blocks shown in Figure 4.4 are specificed identically as in [3]. Implementation of *FLASH* is trivial; it is assumed that the liquid and vapour phases of the rich solvent are separated adiabatically with negligible pressure drop. The implementation of *Absorber* and *Stripper*, though, departs significantly from that undertaken in [3] with respect to the UOM and column internals selected.

Table 4.5: Summary of block definition for Aspen Plus® model of CO_2 capture process

Block name	UOM	Description
H2O_PUMP	PUMP	Water pump; drives cooling water through *DCC* • Outlet pressure (*e.g.*, $101.3\,\text{kPa} + (\Delta P)_{abs}$)
BLOWER	COMPR	Drives flue gas through *DCC* and *Absorber* • isentropic efficiency (*e.g.*, 0.90) • Outlet pressure (*e.g.*, $101.3\,\text{kPa} + (\Delta P)_{abs}$)
DCC	FLASH2	Direct-contact cooler; cools flue gas to 40°C, the desired *Absorber* inlet temperature[2] • Heat duty (*e.g.*, 0) • Pressure drop (*e.g.*, $-10\,\text{kPa}$)
ABSORBER	RADFRAC	Contacts flue gas counter-currently with lean solvent

[2]Previous work has identified 40°C as being the optimal compromise between low temperature, which favours dissolution of CO_2 into solution, and high temperature, which increases the rate of reaction of CO_2 and MEA. As the reaction with CO_2 and MEA is exothermic, the temperature in the middle of the column increases above this optimal temperature. Though not implemented in this work, controlling the *Absorber* temperature via intercooling would improve *Absorber* performance.

Summary of block definition for Aspen Plus® model of CO_2 capture process

Block name	UOM	Description
		• Pressure at top of column (*e.g.*, 101.3 kPa) • Column internals (*e.g.*, random 75 mm metal Raschig rings) • *Column diameter* • *Height of packing* • *Number of column segments* • Pressure calculations (*e.g.*, enabled) • Reactive section (*e.g.*, entire column) • Rate-based mass-transfer calculations (*e.g.*, enabled)
RICH_PUM	PUMP	Drive rich solvent through the *Stripper* • Outlet pressure (*e.g.*, pressure at top of *Stripper*) • Driver efficiency (*e.g.*, 98%)
HEATX	HEATX	Pre-heat rich solvent using lean solvent (*i.e.*, *Stripper* bottoms) • Hot-side temperature approach (*e.g.*, 10°C) • Overall heat transfer coefficient (*e.g.*, 1134 $\mathrm{Wm^{-2}{}^{\circ}C^{-1}}$)[3]
FLASH	FLASH2	Remove vapour component of rich solvent prior to being fed to *Stripper* • Pressure drop (*e.g.*, 0) • Heat duty (*e.g.*, 0)
STRIPPER	RADFRAC	Strip CO_2 from rich solvent

[3] Overall heat transfer coefficient of 1134 $W \cdot m^{-2} \cdot C^{-1}$ is typical of a $H_2O_{(l)}$-$H_2O_{(l)}$ system. [19]

Summary of block definition for Aspen Plus® model of CO_2 capture process

Block name	UOM	Description
		• Condenser type (*e.g.*, partial vapour) • Reboiler type (*e.g.*, kettle) • Feed location (*e.g.*, top of column) • Column internals (*e.g.*, random 75 mm metal Raschig rings) • *Column diameter* • *Height of packing* • *Number of column segments* • *Reflux ratio* • *Bottoms-to-feed ratio* • *Reboiler pressure* • Pressure calculations (*e.g.*, enabled) • Reactive section (*e.g.*, entire column) • Rate-based mass-transfer calculations (*e.g.*, enabled)
CO2_COOL	FLASH2	Knock-out water from CO_2 stream prior to being fed to compressor • Pressure drop (*e.g.*, 0) • Outlet temperature (*e.g.*, 25°C)
CO2_COMP	MCOMPR	Multi-stage compressor with interstage cooling to prepare CO_2 stream for transport[4] • Number of stages (*e.g.*, 4) • Outlet pressure (*e.g.*, 110 kPa) • Isentropic efficiency (*e.g.*, 0.90) • Mechanical efficiency (*e.g.*, 0.99) • Interstage cooling (*e.g.*, 25°C)
MU_MIXER	MIXER	Combines lean solvent with make-up
ABS_PRHT	HEATER	Cools *Absorber* inlet to desired temperature of 40°C • Pressure drop (*e.g.*, 0) • Outlet temperature (*e.g.*, 40°C)

[4]The design basis includes transporting the captured CO_2 for disposal via pipeline as a supercritical fluid. The pressure of the *Stripper* overhead is expected to be 1.5–2.0 bar and a four-stage compressor with intercooling to 25°C is utilized. This corresponds to a pressure ratio of 2.7–2.9 per stage.

Aspen RateSep™ as UOM for *Absorber* and *Stripper* RadFrac™ is the standard unit operation model for separation/distillation columns in Aspen Plus® versions 2004 and later. And, Aspen RateSep™ is an extension to RadFrac™ that calculates mass transfer using a rate-based approach instead of instead of assuming that the vapour and liquid streams are in equilibrium or at a fixed, pre-specified approach to equilibrium. Aspen RateSep™ is used to model the *Absorber* and *Stripper*, replacing the RateFrac™ UOM that is present in earlier versions including that underlying the work in [3]. Aspen RateSep™ is able to incorporate pressure drop calculations with calculation of mass transfer; this was a feature missing in RadFrac™ that was non-trivial to workaround. Thus, from a single pass of the flowsheet is obtained the column performance and the power required to drive the flue gas.

Before settling on using Aspen RateSep™, an attempt was made to find and assess other rate-based column unit operation models that conformed to the CAPE-OPEN standard. ChemSep [30] is such a model and, theoretically, it can act as a drop-in replacement for Aspen RateSep™. In practice, though, using ChemSep in the present circumstances would require that the MEA-related species be added to ChemSep and the way to do this, if possible, is undocumented and unsupported.

***Absorber* and *Stripper* as packed-type columns** The flue gas volumes that must be handled are quite large. In [3], the resistance to flow through an Absorber fitted with *trays* resulted in the best-identified design being one in which the height of the Absorber is minimzed. It is known that packed columns have lower pressure drops than similarly sized trayed columns and, in this study, the *Absorber* and *Stripper* are designed as columns randomly packed with generic, 75 mm metal Raschig rings.

Optimal sizing and process design of CO_2 capture process To complete the specification of the blocks requires specifying values for the parameters in italics in Table 4.5: the height and diamter of the *Absorber* and *Stripper*; the number of segments in each column; the reflux and bottoms-to-feed ratios of the *Stripper*; and the pressure of the *Stripper* reboiler. To that end, the optimization problem shown in (4.4) is formulated that eeks to find the column sizes (i.e., diameter and height) and operating conditions (i.e., reflux ration, bottoms-to-feed ration, reboiler pressure) that minimize the equivalent thermal energy required to capture a minimum of 85% of the CO_2 in the flue gas.

$$
\begin{array}{cccc}
\min & \dot{Q}_{reb} + \frac{P_{pump}+P_{comp}}{\eta} & & \\
d_{abs}, h_{abs} & & & \\
d_{str}, h_{str} & & & \\
B/F, L_1/D, P_{reb} & & & \\
\text{s.t.} & x_{CO_2} & \geq & x^*_{CO_2} \\
 & FA_{abs} & \leq & FA^{max}_{abs} \\
 & FA_{str} & \leq & FA^{max}_{str} \\
 & T_{reb} & \leq & T^*_{reb}
\end{array}
\qquad (4.4)
$$

$$
\begin{array}{ccccc}
1\text{ m} & \leq & d_{abs} & \leq & 15\text{ m} \\
1\text{ m} & \leq & d_{str} & \leq & 15\text{ m} \\
0.97 & \leq & B/F & \leq & 0.97 \\
0.01 & \leq & L_1/D & \leq & 0.50 \\
101.3\text{ kPa} & \leq & P_{reb} & \leq & 303.9\text{ kPa}
\end{array}
$$

The algorithm for solving this problem is given in Figure 4.5 and a sample implementation is given in Appendix F.4.

A solution to (4.4) is not obtained using the above algorithm despite attempts to restructure the convergence loops and to reposition the optimization loop *vis-à-vis* the other convergence loops. One of the *Absorber* or *Stripper* blocks fails to solve successfully, an event from which flowsheet convergence does not recover. Presumably, Aspen RateSep™ is not robust to changes in its inputs from one iteration to the next and it seems that simulatneously manipulating column size and operation renders the convergence algorithm unstable. As in [3], the CO_2 capture process flowsheet is decoupled and parameters for the *Absorber* and *Stripper* are determined independently.

***Absorber* study** The objective is to determine the height and diameter of the *Absorber* for use in the reduced-order model of the generating unit with integrated CO_2 capture. A parametric study of *Absorber* height is undertaken: the optimum diameter is selected for packing heights ranging from one to 22 metres. A column height — and corresponding diameter — is selected where there are diminishing returns from making the column taller.

The flowsheet for the *Absorber* study is given in Figure 4.6. Decoupling of the CO_2 capture process flowsheet requires that LEAN-ABS now be specified the parameter values used are those shown in Table 4.4.

The best choice for column diameter is that value that maximizes the *utility* of the column subject to any design and/or technical constraints. In this case, minimizing the flow rate of lean solvent is taken as a proxy for maximizing the utility of the column. For each column height considered, the column diameter is determined by solving the

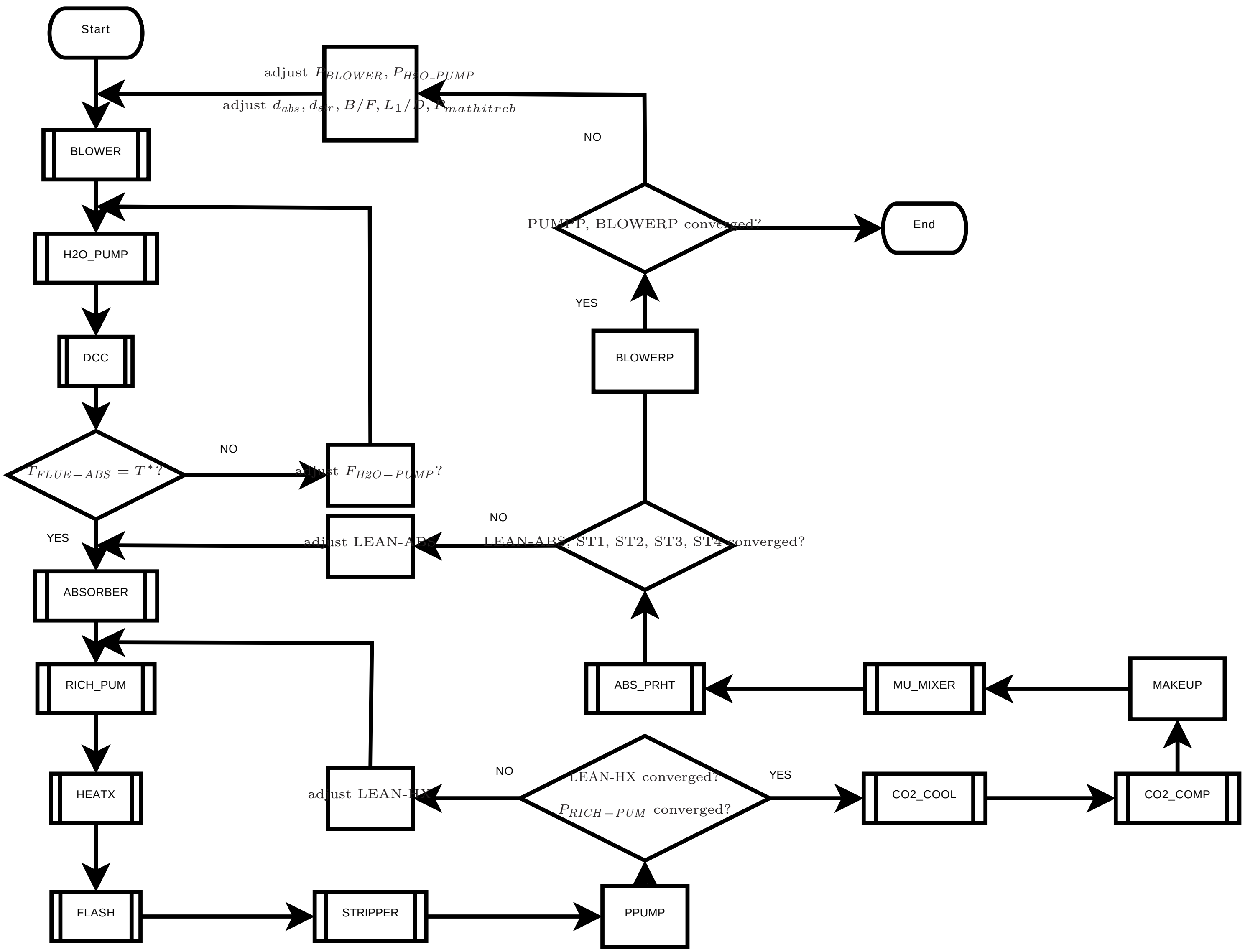

Figure 4.5: Algorithm for simultaneously optimizing design and operation of CO2 capture process

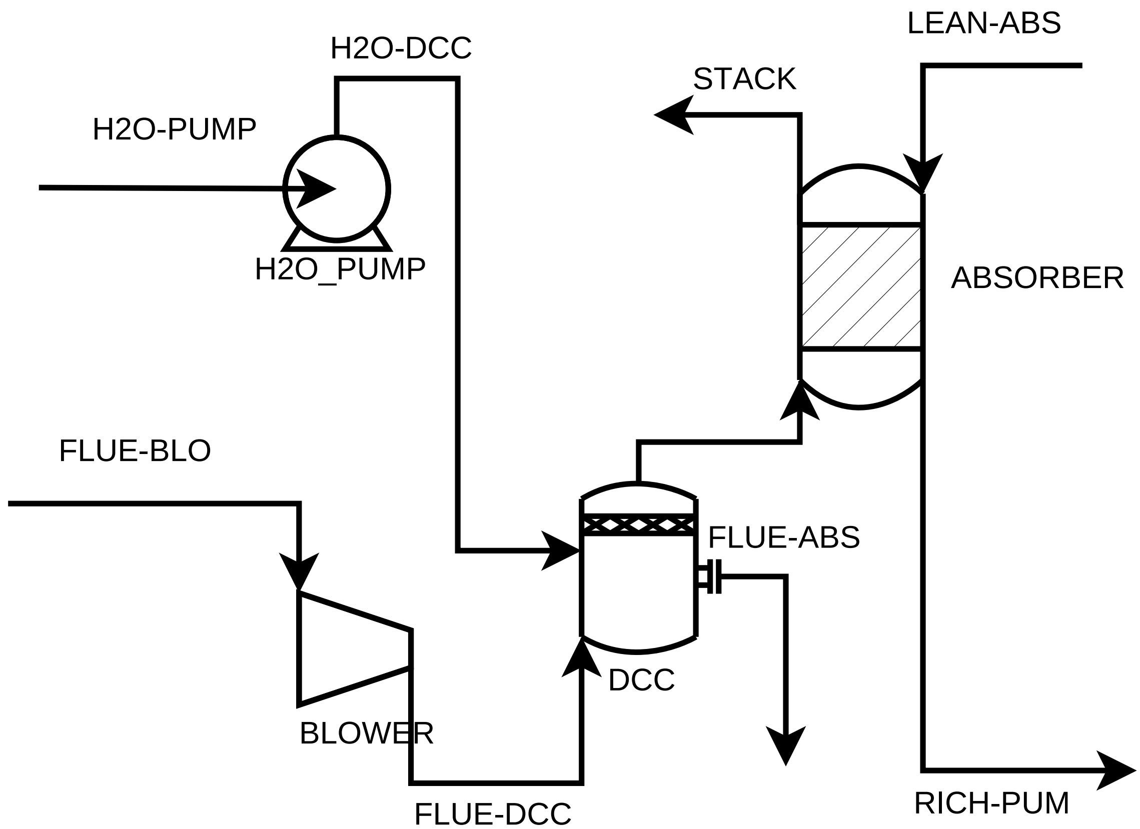

Figure 4.6: Absorber flowsheet

optimization problem shown in (4.5).

$$\begin{array}{ll} \underset{d}{\text{minimize}} & F_{LEAN-ABS} \\ \text{subject to} & \begin{array}{rcl} FA_{vap} & \leq & FA_{vap}^{max} \\ F_{CO_2,out}/F_{CO_2,in} & = & x_{CO_2}^{*} \\ \mathbf{g}(x) & = & 0 \end{array} \end{array} \tag{4.5}$$

$$1 \text{ m} \leq d \leq 15 \text{ m}$$

$\mathbf{g}(x) = 0$ represents the system of equations underlying the Aspen Plus® model of the flowsheet. The algorithm for solving the model is shown in Figure 4.7.

Aspen Plus® has two methods for solving optimization problems: Box's Complex method and SQP (Sequential Quadratic Programming). Some important differences between the methods:[11, 7]

1. Box's Complex follows a feasible path and thus requires a feasible starting point.
2. Box's Complex will not find an unconstrained optimum and will instead return the best constrained solution available.

As a feasible initial point may not always be available, SQP is the optimization method that is employed. An implementation of the *Absorber* flowsheet unit is given in Appendix F.2 in the form of an Aspen Plus® input file.

Number of segments In Aspen RateSep™, the parameter `NSTAGE` specifies the number of segments used in the underlying column model and it is the parameter `PACK-HT` that specifies the height of packing. It is not immediately apparent what the appropriate number segments per unit height of packed column should be specified for the *Absorber*. It is expected that, to a point, increasing the number of segments will improve the accuracy of the simulation. For an *Absorber* with a packed height of three metres, the optimial diameter is determined for a number of segments ranging from two to twenty. The results of this sensitivity analysis are shown in Figure 4.8. It is sobserved that:

- the flow rate of lean solvent decreases asymptotically to 36 kmol/s^{-1} as the number of segments increases,
- the pressure drop across the column increases insignificantly with the number of segments, and
- the number of segments does not signficantly change the *Absorber* diameter.

It is concluded that using five segements per metre height of packing is a ratio at which increasing the number of segements would not noticeably increase the accuracy of the simulation regulsts.

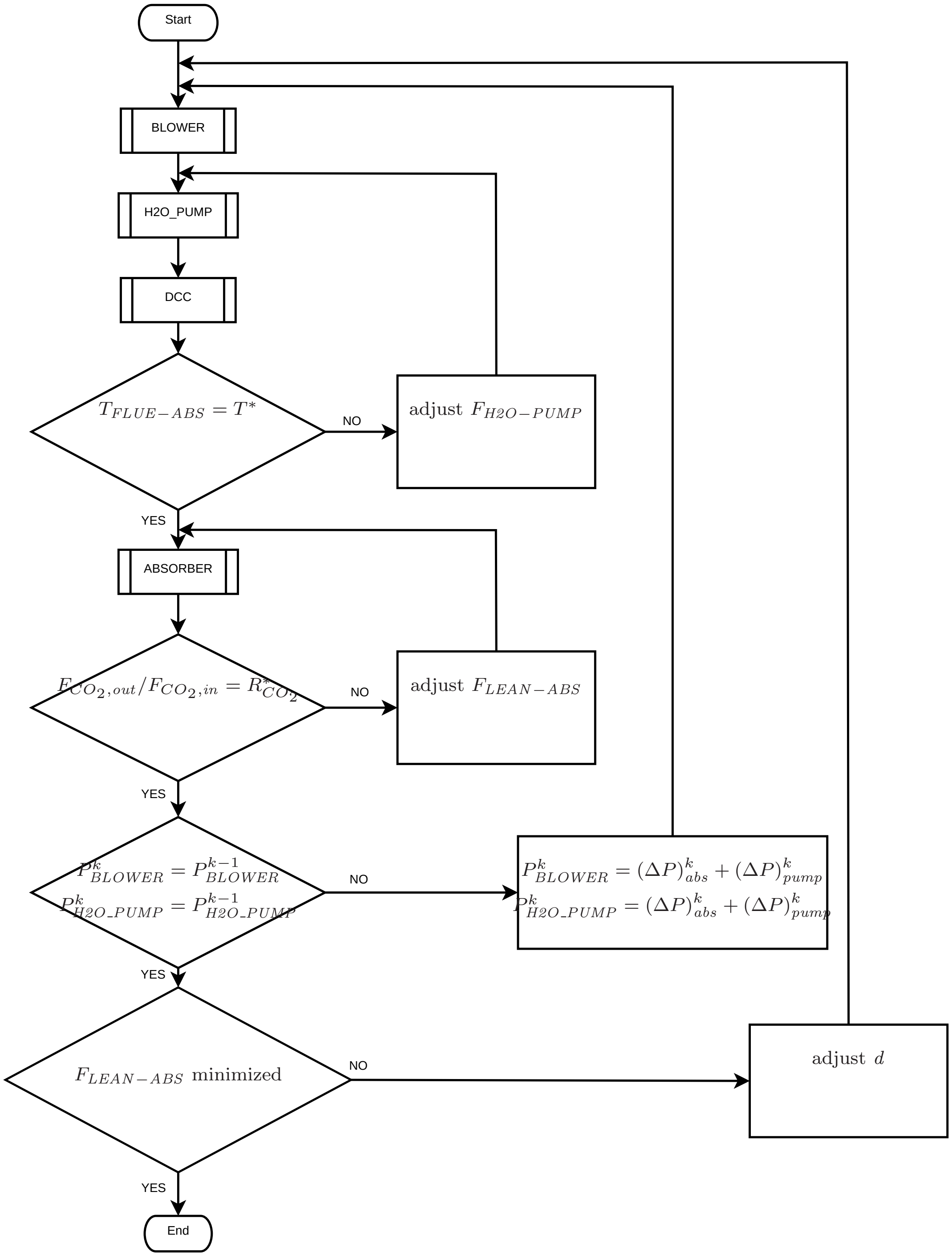

Figure 4.7: Algorithm for solving absorber model

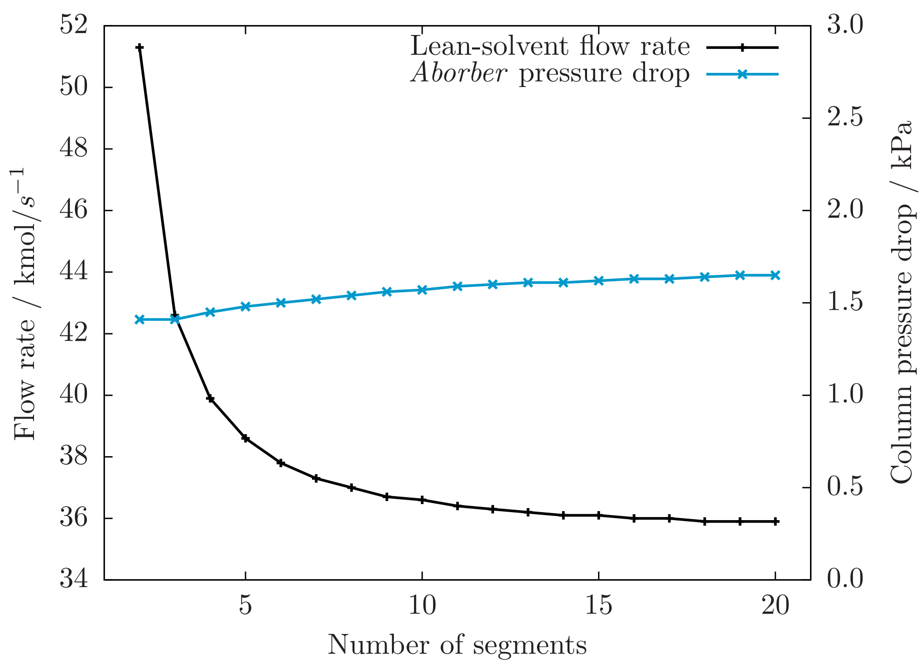

Figure 4.8: Sensitivity of *Absorber* design to number of segments: lean solvent flow rate and column pressure drop

Completing the design of Absorber The *Absorber* model is simulated with packed heights ranging from two to 28 metres in one metre increments and the relationship between column height, pressure drop, and lean solvent flow rate are shown in Figure 4.9. This data, along with the blower duty (NB: the pump duty is negligible, less than 0.03% of the blower duty), is tabulated in Table 4.6. With increasing column height, lean solvent flow rate increases asymptotically and pressure drop (or blower duty, whichever it is) increases linearly at x kPa or MWe per metre height of packing. Based upon inspection, the following parameters are selected for the *Absorber*:

Segments per metre height of packing:	5
Height (metres):	10
Diameter (metres):	10

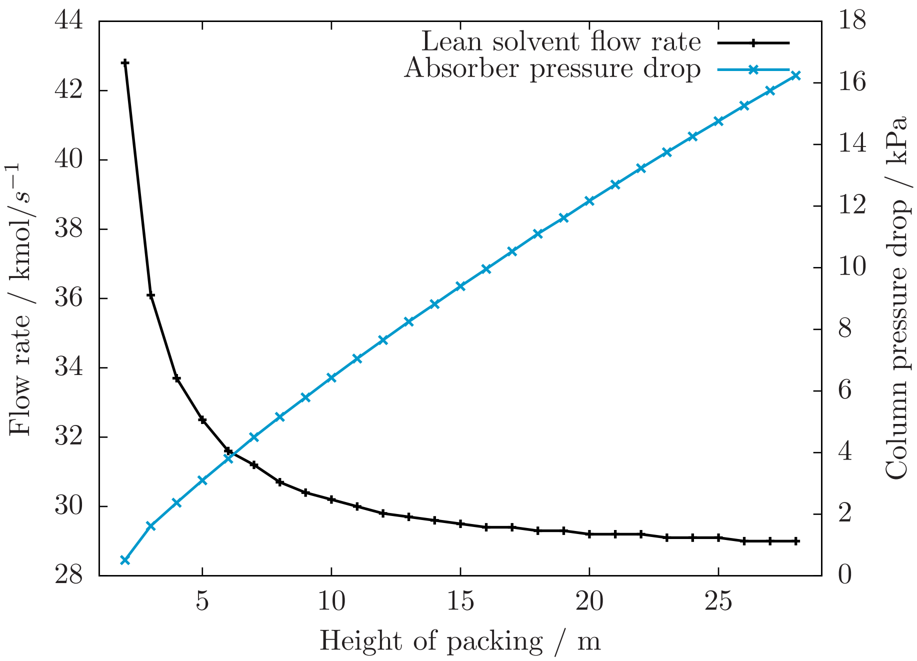

Figure 4.9: Sensitivity of *Absorber* design and performance to height of packing: lean solvent flow rate and column pressure drop

Comparing packed- and tray-type columns for the *Absorber* The use of a packed column design versus one with trays is driven by an assumption that packed columns would perform markedly better than comparable tray-type columns. To check the validity of this assumption, a flowsheet featuring an *Absorber* fitted with trays is developed. The

[5]The column diameter is initialized using a value of 11.2 metres.

Table 4.6: Absorber design and performance.

Height	Diameter[5]	F_{lean}	ΔP	Blower Duty
m	m	kmol/s	kPa	MW_e
2.0	13.8	42.8	0.51	2.1
3.0	12.6	36.1	1.62	2.3
4.0	11.2	33.7	2.37	2.4
5.0	11.2	32.5	3.10	2.5
6.0	11.2	31.6	3.80	2.7
7.0	11.2	31.2	4.50	2.8
8.0	11.2	30.7	5.16	2.9
9.0	11.2	30.4	5.79	3.0
10.0	11.2	30.2	6.43	3.1
11.0	11.2	30.0	7.05	3.3
12.0	11.2	29.8	7.65	3.4
13.0	11.2	29.7	8.25	3.5
14.0	11.2	29.6	8.82	3.6
15.0	11.2	29.5	9.40	3.7
16.0	11.2	29.4	9.96	3.8
17.0	11.2	29.4	10.53	3.9
18.0	11.2	29.3	11.10	4.0
19.0	11.2	29.3	11.62	4.1
20.0	11.2	29.2	12.17	4.2
21.0	11.2	29.2	12.70	4.3
22.0	11.2	29.2	13.23	4.4
23.0	11.2	29.1	13.75	4.5
24.0	11.2	29.1	14.26	4.5
25.0	11.2	29.1	14.76	4.6
26.0	11.2	29.0	15.26	4.7
27.0	11.2	29.0	15.75	4.8
28.0	11.2	29.0	16.24	4.9

optmization problem and solution algorithm are extended by appending tray spacing to the list of decision variables. Figure 4.10 compares the lean solvent flow rate and the blower duty for two different type of *Absorber* internals normalized to the height of the mass transfer zone in each.

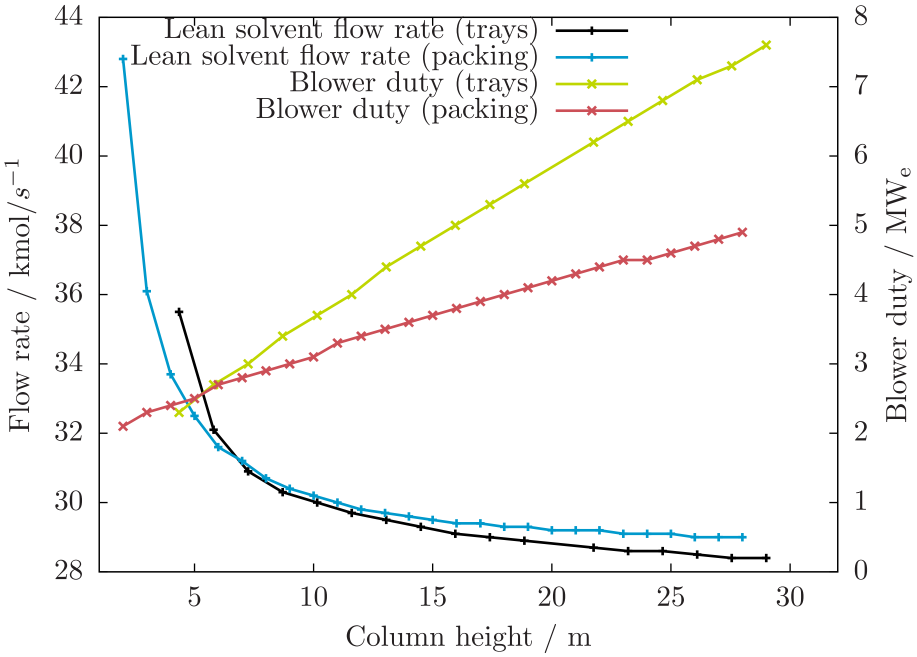

Figure 4.10: Sensitivity of lean solvent flow rate and blower duty to *Absorber* internals

For most of the range of interest (*e.g.*, column heights greater than eight metres), there is little difference in the solvent flow rate between the different types of columns. At the low-end of this range, the *Blower* duty is slightly greater in the case of tray columns and this difference becomes progressively larger as the height of the column increases. Though a packed *Absorber* has a definite advantage in terms of the factors considered here, other factors including cost and operability may, depending upon the application, merit being assessed prior to making a final selection for a real-world deployment.

***Stripper* study** The objective is to determine the height and diameter of the *Stripper* for use in the reduced-order model of the generating unit with integrated CO_2 capture. A parametric study of *Stripper* height is undertaken: the optimum diameter is selected for packing heights ranging from one to 22 metres. A column height — and corresponding diameter — is selected where there are diminishing returns from making the column taller.

The flowsheet for the *Stripper* study is given in Figure 4.11. Decoupling of the CO_2 capture process flowsheet requires that RICH-PUM be specified. The parameter values used are taken from the *Absorber* study simulation with a height of ten metres and are shown in Table 4.7.

Table 4.7: Initial values for LEAN-HX in *Stripper* flowsheet

Property	Packing
State variables	
Temp / °C	50.9669
Pres / kPa	107.6189
Component mole-flows / kmol/s	
H_2O	25.2757
MEA	0.2569
CO_2	7.4843×10^{-3}
N_2	7.9348×10^{-5}
HCO_3^-	0.1264
$MEACOO^-$	1.6962
MEA^+	1.8448
CO_3^{--}	1.1088×10^{-2}
$H3O^+$	3.8657×10^{-9}
OH^-	6.6203×10^{-6}

The best choice for column diameter is that value which maximizes the *utility* of the column subject to any design and/or technical constraints. In this case, minimizing the equivalent thermal energy demand is taken as a proxy for maximizing the utility of the column. For each column height considered, the column diameter is determined by solving the optimization problem shown in (4.6). The algorithm for solving the process model is given in Figure 4.12 and a sample implementation is given in Appendix F.3.

$$
\begin{aligned}
\underset{d,\, B/F,\, \frac{L_1}{D},\, P_{reb}}{\text{minimize}} \quad & \dot{Q}_{reb} + \frac{P_{pump} + P_{comp}}{\eta} \\
\text{subject to} \quad & F_{CO_2,\texttt{STR-CO2}} + F_{CO_2,\texttt{FLSH-CO2}} \geq F_{CO_2,\texttt{FLUE-ABS}} \cdot x_{CO_2} \\
& FA_{vap} \leq FA^*_{vap} \\
& T_{reb} \leq T^*_{reb} \\
& \mathbf{g}(x) = 0 \\
& 1\text{ m} \leq d \leq 15\text{ m} \\
& 0.97 \leq \tfrac{B}{F} \leq 0.99 \\
& 0.01 \leq \tfrac{L_1}{D} \leq 0.50 \\
& 101.3\text{ kPa} \leq P_{reb} \leq 303.9\text{ kPa}
\end{aligned}
\tag{4.6}
$$

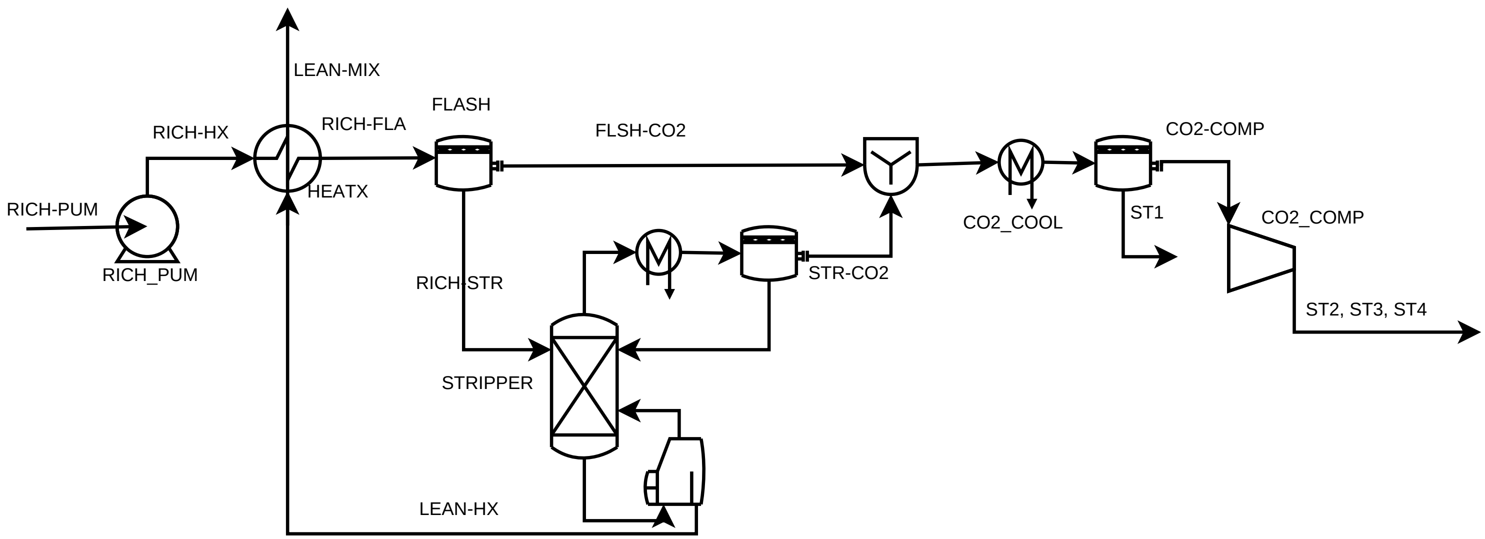

Figure 4.11: Stripper flowsheet

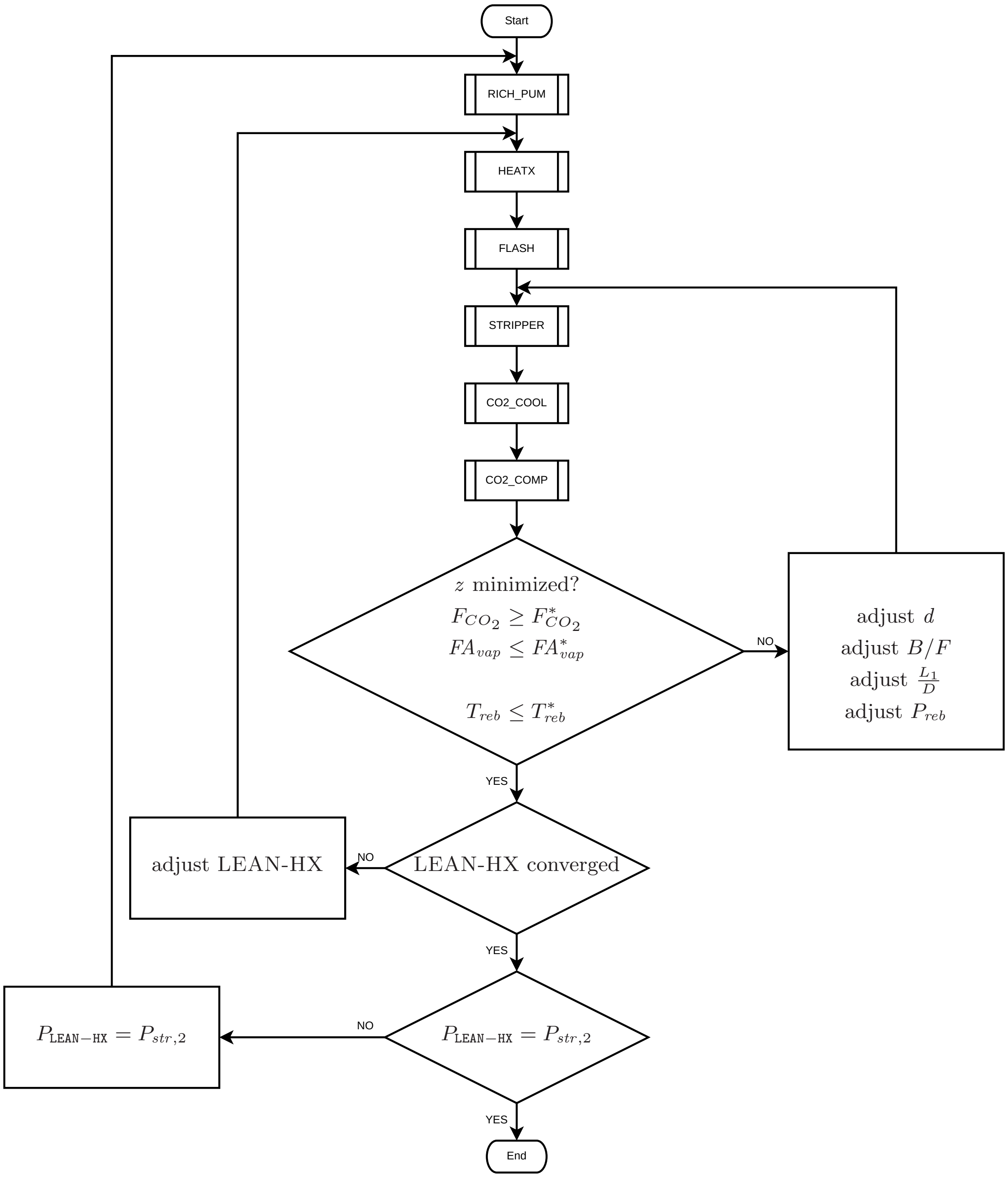

Figure 4.12: Algorithm for stripper model using optimization

With respect to the function, constraints, and variable bounds in (4.6):

Objective function The objective function represents the total power consumption of the process in equivalent thermal energy. η represents the efficiency with which thermal energy is converted to the shaft or electric power required by the pump and compressor.

Constraints Though it is desired that the CO_2 recovery *equal* 0.85, the CO_2 recovery constraint is formulated as an inequality. Doing so provide two benefits:

1. Box's complex method cannot handle optimization problems with equality constraints. Switching to an inequality constraint, both `COMPLEX` and `SQP` methods can be used.
2. With the constraint expressed as an inequality, the feasible solution space is larger which might ease convergence.

And, since capturing more CO_2 requires more energy and the objective is to minimize energy consumption, the CO_2 recovery constraint will be active in the optimum solution. Therefore, the two forms are equivalent.

It is standard practice to design CO_2 capture process using 30 wt% MEA such that the temperature of the solvent does not exceed 122°C. While increasing temperature reduces the specific heat duty of the reboiler, above temperatures of 122°C, the rate of solvent degredation is unacceptable.

Variable bounds A CO_2 recovery of 85% is achieved in the *Absorber* study and, to maintain consistency, the quantity of CO_2 entering the multi-stage compressor must equal the quantity of CO_2 removed from the flue gas: $0.8847\ \text{kmol} \cdot \text{s}^{-1}$. In the *Stripper*, the bottoms-to-feed (B/F) and reflux (L_1/D) ratios are manipulated to control the recovery.

Reasonable initial values for B/F and L_1/D are not known and these are key for achieving convergence of the model. Additionally, it is important to specify reasonable bounds for these variables as the algorithms for converging tear streams, design specifications, *etc.* have difficulty recovering from Aspen RateSep™ calculations that do not terminate successfully becauase of infeasible values for B/F and L_1/D.

Using a *Stripper* with nine trays, a 3.048 metre tray spacing, and diameter of 3.81 metres, the process is simulated for bottoms-to-feed ratios over the interval $[0.90, 0.99]$ and reflux ratios over the interval $[0.01, 1.00]$. The CO_2 recovery for each successul simulation is noted and is shown in Figure 4.13. Key observations from the study:

- CO_2 recovery increases logarithmically with *increasing* reflux ratio.

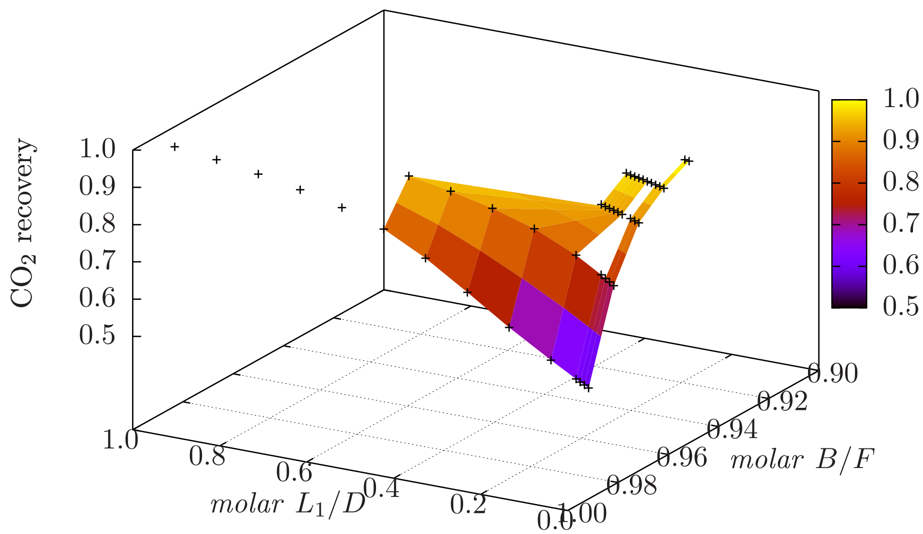

Figure 4.13: Sensitivity of CO_2 recovery to *Stripper* reflux ratio and bottoms-to-feed ratio

- CO_2 recovery increases logarithmically with *decreasing* bottoms-to-feed ratio.
- It is not possible to achieve the target CO_2 recovery with $L_1/D > 0.5$ or $B/F < 0.97$.

The analysis provides a better understanding of the operating envelope of the *Stripper for the present application*. The following constraints are necessary — but not sufficient — for convergence of the *Stripper* flowsheet if 85% capture is to be achieved:

$$0 \leq \frac{L_1}{D} \leq 0.50$$
$$0.97 \leq \frac{B}{F} \leq 0.99$$

Number of segments As in the *Absorber* study, a preliminary step is to determine an appropriate number of segments to use per unit height of packing. For a *Stripper* with a packing height of fifteen metres, the number of segments is varied over the interval $[15, 300]$ in five-segment increments and the results are shown in Figure 4.14. Some observations:

- Simulations had problems converging when the number of segments per unit height of packing exceeded three segments per metre.

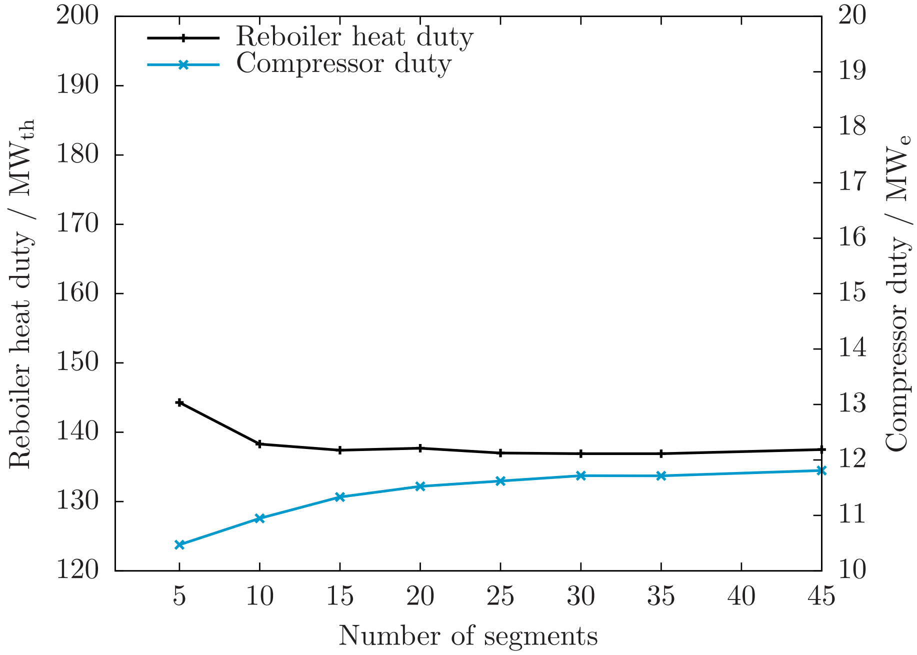

Figure 4.14: Sensitivity of packed *Stripper* power demand to number of segments: reboiler heat duty and compression power

- For the ratios of segments per metre where the simulation did converge, the diameter is at its upper bound of 15 m.
- With less than two segments per metre height of packing, reboiler heat duty and compressor duty are sensitive the the number of segments used. Greater than two segments per metre height of packing and increasing the number of segments does not significantly change the performance of the *Stripper* flowsheet.

Completing the design of *Stripper* The *Stripper* flowsheet with packed heights ranging from one to 28 metres, in one metre increments, is solved and key results of this study are shown in Figure 4.15.

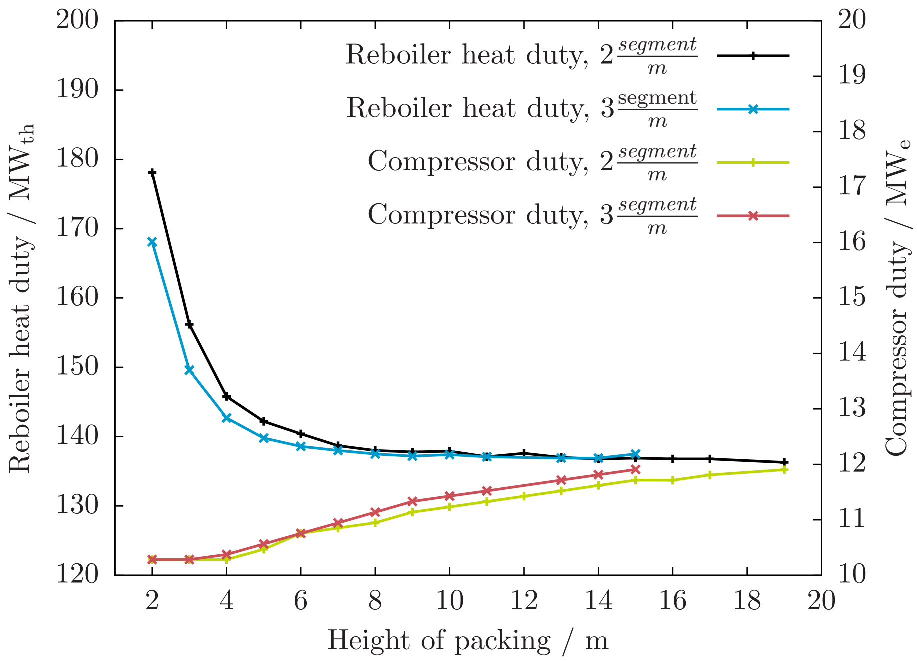

Figure 4.15: Sensitivity of packed *Stripper* power demand to height of packing: reboiler heat duty and compression power

- With two segments per metre height of packing, the *Stripper* flowsheet failed to converge when the *Stripper* height exceeded nineteen metres. With three segments per metre height of packing, it was with *Stripper* heights greater than fifteen metres that the *Stripper* flowsheet failed to converge. It appears that the *de facto* limit on the number of segments that can be used with which the *Stripper* is around 45.

- At low packing heights (*i.e.*, two to six metres), using two segments per metre height of packing results in a higher value of $\dot{Q}_{reb}$. With greater than six metres of packing, there is no significant difference observed in $\dot{Q}_{reb}$ between the two cases.

- At high packing heights (*i.e.*, $\geq$ eight metres), using two segments per metre height of packing results in a slightly lower calculated compressor duty than using three segments per metre. Below eight metres, there is no significant difference between the two cases.

- Focusing on just column performance, reboiler heat duty decreases with increasing column height until about ten metres after which there is little advantage to be gained. The compressor duty, though, continues to increase at a rate of 0.1 MW_e per metre height of packing as the column height is extended to ten metres and beyond.

Based upon inspection, the following parameters are selected for the *Stripper*:

Segments per metre height of packing:	2
Height (metres):	10
Diameter (metres):	7.6
Reflux ratio[6]	0.46
Bottoms-to-feed ratio	0.99
Reboiler pressure (°C)	144.93

Comparing packed- and tray-type columns for the *Stripper* A flowsheet featuring an *Stripper* with trays is developed with the following configuration: sieve trays, 3.6 mm deck thickness, 13 mm hole diameter, 0.15 m weir height, and a hole area fraction of 0.15. This flowsheet is solved repeatedly with the number of trays in the *Stripper* incrementing by one each time; in this way, configurations ranging from two to twenty trays is examined.

Figure 4.16 compares the heat and power demand of the process units for tray-type and packed columns internals normalized to the height of the mass transfer zone in each. At equivalent heights, the reboiler heat duty of the tray-type column is greater though the work duty is smaller.

Figure 4.17 again compares the two different types of columns, this time with respect to equivalent thermal demand (*i.e.*, the value of the objective function in the optimal solution of (4.6) for each simulation). In the range of ten to fifteen metres, both types of columns would derate the power plant to the same degree. Likely it will the relative cost of materials and the value of operability that will dictate the prefered option and further analysis is required.

[6]Values shown for reflux ratio, bottoms-to-feed ratio, and reboiler pressure are used to initialize the CO_2 capture process model. As they are decision variables in the optimization problem used to solve the flowsheet, there final values will be different.

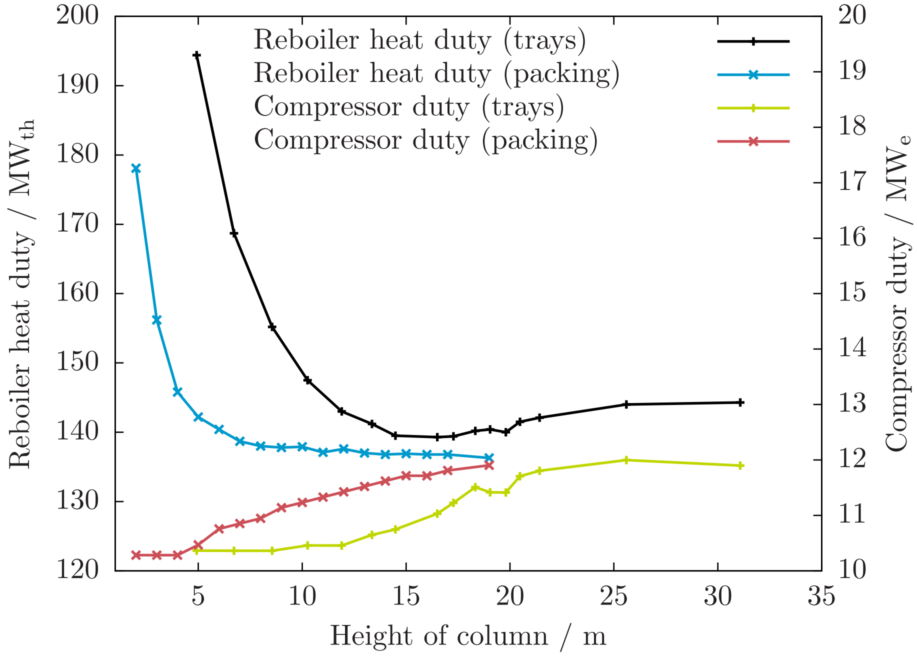

Figure 4.16: Sensitivity of packed *Stripper* power demand to height of packing: reboiler heat duty and compression power

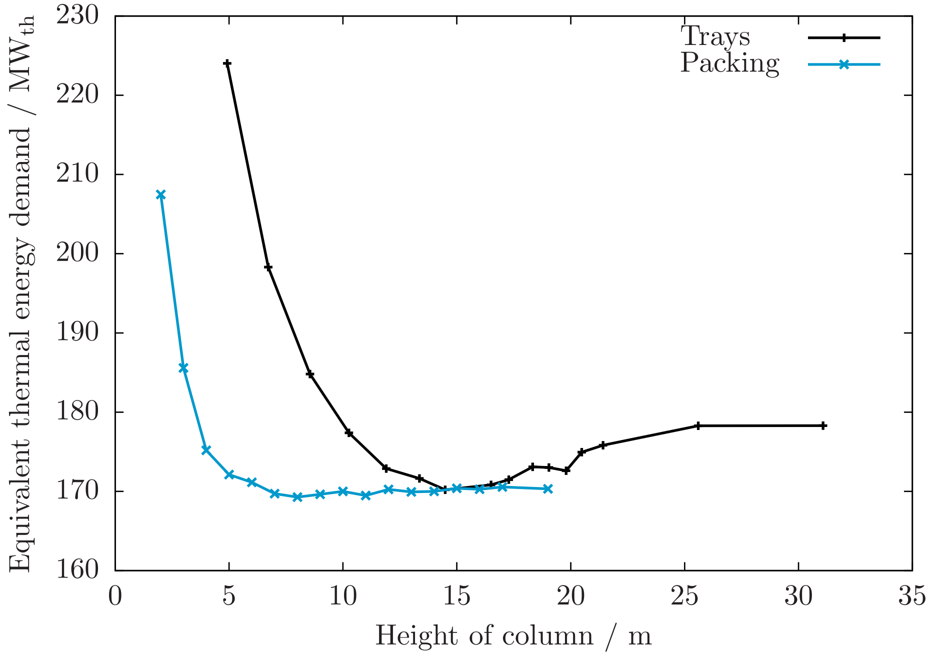

Figure 4.17: Comparison of energy demand for packed and tray-type *Strippers*

Integration of generating unit and CO_2 capture process

The overall flowsheet for the generating unit with integrated CO_2 capture is given in Figure 4.18. Integrating the process models for the generating unit and CO_2 capture comes down to managing the extraction and reinjection of steam and condensate from and to, respectively, the generating unit steam cycle.

Extraction of steam from generating unit The best location for extracting steam is the IP/LP (Intermediate Pressure/Low Pressure) crossover pipe.[3] A flow splitter (*i.e.*, *ST_EXTCT*) is inserted with part of the flow continuing to LP turbine and the rest being diverted to the *Stripper* reboiler. The split fraction is not known *a priori*; it is determined endogenously within the model:

1. The mass flow rate of water to the boiler is specified. From this, the heat input to the boiler is calculated.

2. Coal prepartion and combustion is simulated. The coal flow rate is varied such that the heat generated matches the required heat input from the previous step. The flue gas composition and flowrate is calculated in this step.

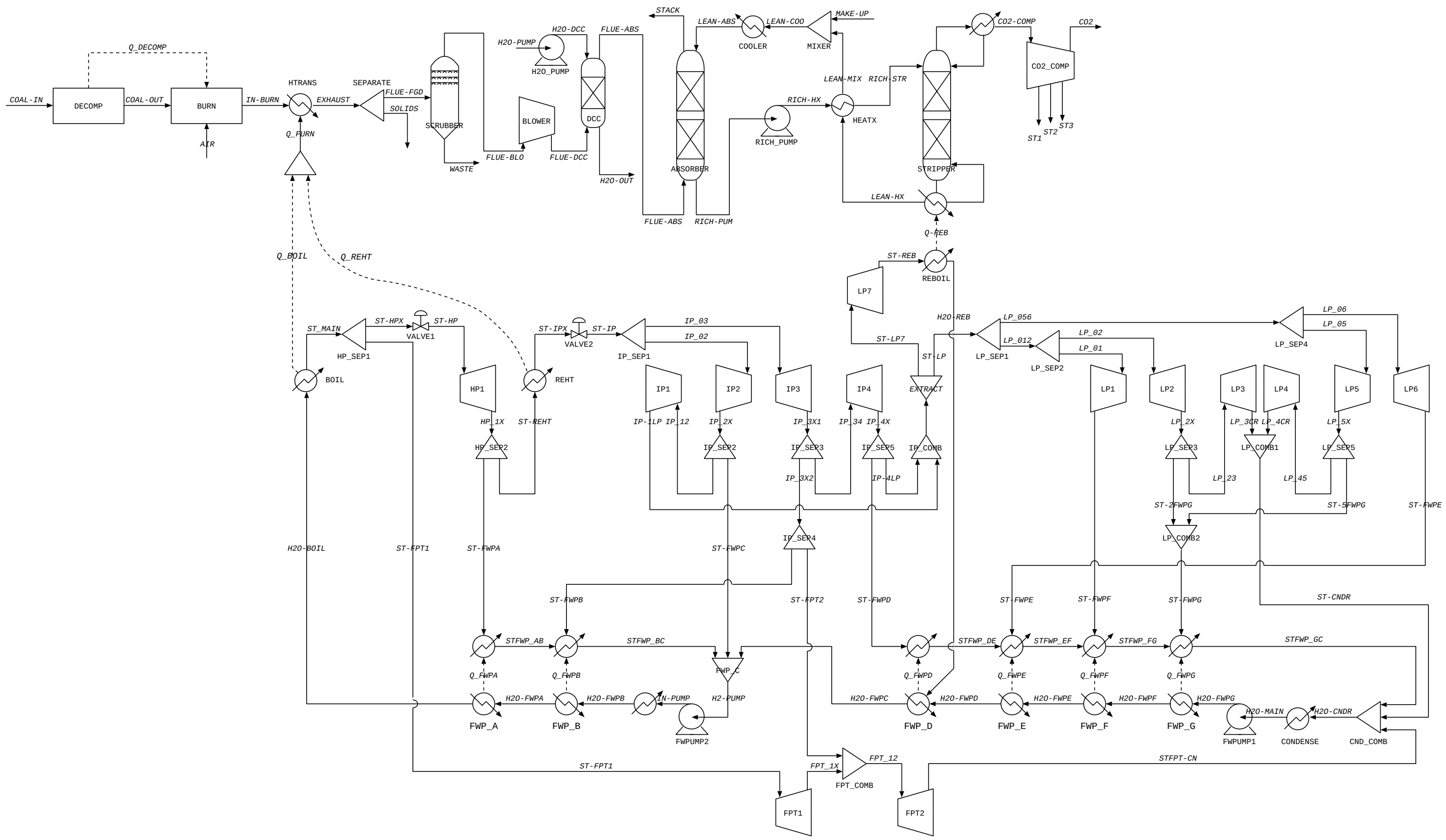

Figure 4.18: Flowsheet of integrated generating unit and CO_2 capture process

3. The flue gas from the furnace is fed to the CO_2 capture process where a specified quantity of the CO_2 is captured. The reboiler temperature, reboiler heat duty, and the work duty of the process is calculated.

4. The split fraction is varied such that the heat released by condensing the steam matches the heat duty of the reboiler.

Extracting steam has an effect on the heat balance in the steam cycle and some iteration through the above steps is needed.

At base-load, to maintain flow at the turbine outlet, no more than 83% of the steam can be extracted from the IP/LP crossover pipe.[3] At base-load, the steam flow rate in the IP/LP crossover pipe is $2.49 \times 10^6 lb/hr$. With 83% of this diverted, there would be $0.42 \times 10^6 lb/hr$ heading into the LP section of the turbine and this is taken as the minimum flow rate required.

Auxiliary power generation and steam desuperheating The extracted steam is at a greater quality than necessary [3], and, in this work, the extracted steam is expanded through an auxiliary turbine (*i.e.*, AUX_TURB) prior to being fed to the *Stripper* reboiler. An isentropic efficiency of 90% is assumed.

The compression ratio (*i.e.*, ratio of outlet pressure to inlet pressure) of AUX_TURB is set such that the steam will have a saturation temperature equal to $T_{reb} + \Delta T_{approach}$. An approach temperature of 10°C is specified.

DSUPRHTR removes superheat from the outlet of auxilary turbine; the outlet conditions are the saturated vapour at inlet pressure. In practice, it is likely necessary that some superheat be maintained to prevent the steam from condensing prior to reaching the *Stripper* reboiler but this is ignored here.

Reboiler, return pump, and reinjection into steam cycle The saturated vapour is condensed to a saturated liquid in the new block *REBOILER*. The pressure of the condensate is increased to match that of the fourth feedwater preheater (*i.e.*, 128 psi) and then is mixed with the rest of the feedwater at the inlet of this unit.

Integrated model formulation The simulation of the integrated process is formulated as the optimization problem show in (4.7). Conceptually, it is a combination of the optimization problems used to solve the *Absorber* and *Stripper* flowsheets (*i.e.*, (4.5) and (4.6), respectively) with some minor changes:

- The objective function was alternatively to minimize the lean solvent flow rate and to minimize the equivalent thermal energy of the power plant consumed by the *Stripper* flowsheet. Here, it is simply to maximize the net power output of the generating unit. P_{MEA} represents the sum of the work duties associated with the CO_2 capture plant: blower duty, water pump duty, rich solvent pump duty, and compressor duty.

- The set of deicision variables is the same excpet for the lean solvent flow rate replacing the bottoms-to-feed ratio.

- The ratio of outlet pressure to inlet pressure for the auxiliary turbine (*i.e.*, $(P_{out}/P_{in})_{aux}$) is a decision variable.

  The specific heat required to stripping CO_2 from the rich solvent decreases with increasing temperature and it is common for the temperature of the *Stripper* reboiler to be set at 122°C, the temperature above which the rate of solvent degradation becomes unacceptable. However, the greater the temperature of the reboiler, the greater quality of utility steam that is needed, and the less power that can be produced in the auxiliary turbine. Adding $(P_{out}/P_{in})_{aux}$ to the decision variables allows this tradeoff to be considered.

$$
\begin{array}{cl}
\underset{\substack{x_{steam},\, P_{out}/P_{in} \\ P_{reb},\, F_{lean},\, L_1/D}}{\text{minimize}} & P_{generator} - \dfrac{P_{MEA}}{\eta_e} + \eta_e P_{aux} \\
\text{subject to} & \begin{array}{rl}
T_{steam} & \geq T_{reb} + 10^{\circ}\mathrm{C} \\
q_{steam} & \geq q_{reb} \\
FA_{abs} & \leq FA_{abs}^{max} \\
FA_{str} & \leq FA_{str}^{max} \\
x_{CO_2} & \geq x_{CO_2}^{*} \\
\mathbf{g}(x) & = 0
\end{array}
\end{array}
\tag{4.7}
$$

$$
\begin{array}{ccccc}
0.00 & \leq & \leq x_{steam} & \leq & \leq 0.83 \\
0.10 & \leq & \leq P_{out}/P_{in} & \leq & \leq 1.00 \\
1\ \mathrm{m} & \leq & d & \leq & 15\ \mathrm{m} \\
0.97 & \leq & \frac{B}{F} & \leq & 0.99 \\
0.01 & \leq & \frac{L_1}{D} & \leq & 0.50 \\
1\mathrm{kmol}\cdot\mathrm{s}^{-1} & \leq & \leq F_{lean} & \leq & \leq 40\mathrm{kmol}\cdot\mathrm{s}^{-1} \\
101.3\ \mathrm{kPa} & \leq & P_{reb} & \leq & 303.9\ \mathrm{kPa}
\end{array}
$$

4.3.2 Simulate the operation of the integrated generating unit and CO_2 capture processes

The operation of the integrated generating unit and power plant model is simulated for steam flow rates ranging from 0.5 to 1.0 of base-load flow and for CO_2 recoveries from 0.05 to 0.95. A summary of the results is given in Table 4.8 and Figure 4.19 shows a plot of net power output versus heat input and CO_2 recovery.

Table 4.8: Heat input to the boiler and net plant output over generating unit and capture process operating range

Unit load %	CO_2 recovery	Heat input MW_{th}	Net power output MW_e
100	0.950	1411	356
100	0.900	1411	367
100	0.849	1411	376
100	0.750	1411	393
100	0.650	1411	409
100	0.549	1411	423
100	0.446	1411	436
100	0.343	1411	449
100	0.250	1411	460
100	0.150	1411	469
100	0.050	1411	481
90	0.950	1283	319
90	0.899	1283	329
90	0.850	1283	337
90	0.749	1283	352
90	0.650	1283	367
90	0.544	1283	380
90	0.445	1283	392
90	0.347	1283	403
90	0.250	1283	414
90	0.149	1283	424
90	0.046	1283	436
80	0.947	1152	281
80	0.899	1152	290
80	0.850	1152	297
80	0.750	1152	311
80	0.649	1152	324
80	0.552	1152	336
80	0.446	1152	347
80	0.345	1152	358
80	0.250	1152	366
80	0.150	1152	374
80	0.050	1152	387
70	0.950	1020	242
70	0.900	1020	250

Unit load %	CO_2 recovery	Heat input MW_{th}	Net power output MW_e
70	0.849	1020	257
70	0.750	1020	269
70	0.650	1020	281
70	0.547	1020	289
70	0.447	1020	302
70	0.349	1020	312
70	0.346	1020	312
70	0.248	1020	321
70	0.150	1020	330
70	0.050	1020	340
60	0.900	886.7	211
60	0.850	886.7	217
60	0.846	886.7	217
60	0.749	886.7	228
60	0.650	886.7	238
60	0.548	886.7	247
60	0.450	886.7	256
60	0.350	886.7	265
60	0.250	886.7	274
60	0.149	886.7	282
60	0.047	886.7	291
50	0.850	750.6	176
50	0.750	750.6	186
50	0.650	750.6	195
50	0.547	750.6	203
50	0.450	750.6	211
50	0.344	750.6	219
50	0.250	750.6	226
50	0.150	750.6	233
50	0.050	750.6	241

The impetus for the simulatons is to obtain the data necessary to develop a reduced-order model of the integrated generating unit and CO_2 capture model. Some interesting ancillary observations are noted:

- 92% of the time, the reboiler temperature is less than 110°C; 86% of the time it is less than 105°C. This is in contrast to 'conventional wisdom' which dictates that the *Stripper* reboiler should be operated as hot as practical. Apparently, there is

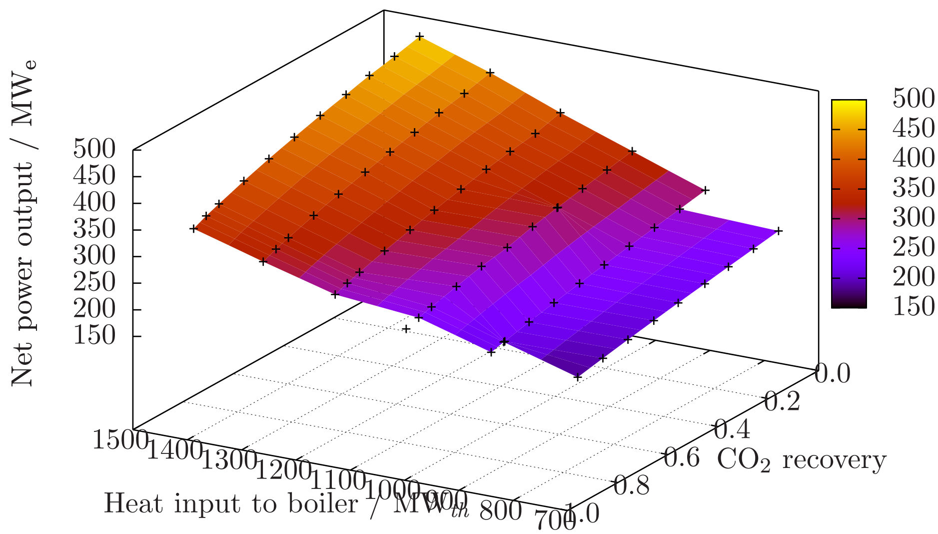

Figure 4.19: Net power output versus heat input to the boiler and fraction of CO_2 recovered

a preference toward maximizing the supplemental power produced in the auxiliary turbine versus lowering the heat duty of the reboiler.

- The loading of the lean solvent ranges from 0.25 to 0.29 with a mean of 0.28 and standard deviation of 0.01.

4.3.3 Develop reduced-order model of generating unit with CO_2 capture

Review of surrogate models

An alternative approach in recent literature is the development of surrogate models. [39] Surrogate models are reduced-order models that attempt to represent the solution space of the the models they are based upon but with fewer variables.

The approach taken here is able to go one step further by recognizing that it is not necessary to represent the entire solution space. Implicit in the electricity system simulation is that the power plants are operated in accordance to their design. That is, in some optimal way. Therefore, according to convention, the reduced-order model only needs to represent the Pareto optimal frontier of the power plant. Given the correct form of the model, it is possible for the reduced-order model to achieve high fidelity with the rigorous process model *for the region of interest* with a minimal number of variables.

Whether the electricity system is regulated or deregulated, the dispatch of generating units seeks to make the best use of the available capacity. For thermal units, the fundamental relationship is that between the heat input to the boiler given a quantity of power injected into the grid.

The value of power changes with time and the dispatch of generating units will change accordingly. In the same way, the value of CO_2, especially relative to that of electric power, is also expected to change with time and generating units with CO_2 capture have incentive to change the amount of CO_2 that is captured in response.

Figure 4.20 shows the input-output characteristic for the generating unit with integrated CO_2 capture for CO_2 recovery at one of thirteen different set points. Three observations to mention:

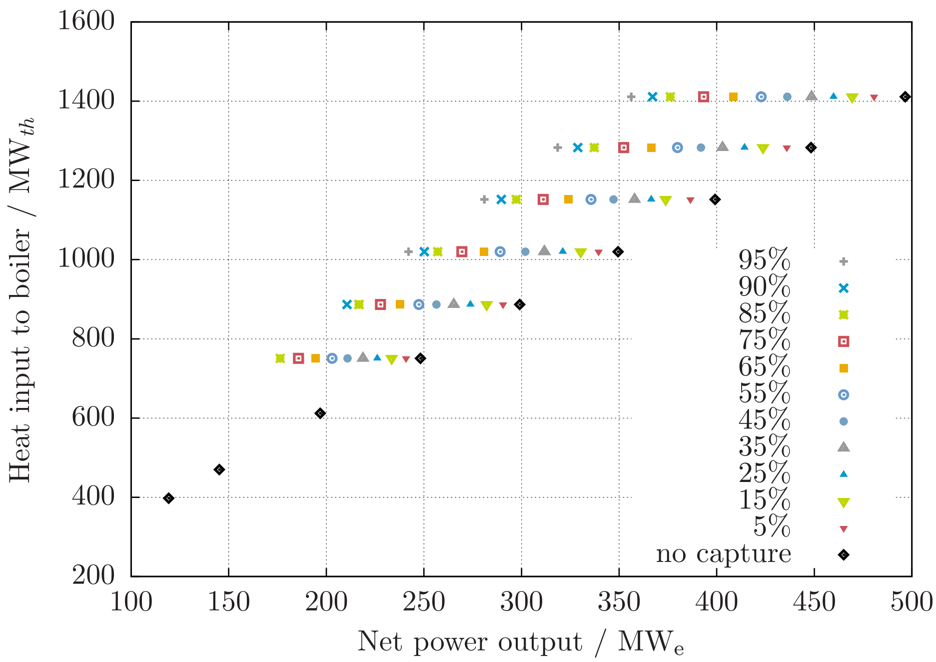

Figure 4.20: Heat input to boiler required to achieve power output and CO_2 recovery set points

1. At any given CO_2 recovery, there appears to be a first-order, linear relationship between net power output and heat input to the boiler.

2. At any given heat input to the boiler, there appears to be a first-order, linear relationship between net power output and CO_2 recovery.

3. There is some interaction between net power output and CO_2 recovery. For example,

at 50% load (*i.e.*, $\dot{q} = 750\,\mathrm{MW_{th}}$), increasing CO_2 recovery from 5% to 85% reduces net power output by 64 $\mathrm{MW_e}$ whereas, at 100% load, increasing CO_2 recovery in this way reduces power output by 104 $\mathrm{MW_e}$.[7]

So, in proposing the form of the reduced-order model for heat input to the boiler in terms of net power output and CO_2 recovery, it is important to have term(s) that account for each of these individually as well as the interaction between them.

Relationship between heat input to boiler and net power output At any given CO_2 recovery, the relationship between heat input to boiler and net power output for the generating unit with integrated CO_2 capture is similar to what was observed for the generating unit without capture. The three terms introduced in Section 4.2 are also considered here:

$$a_1\dot{q} \qquad P \text{ proportional to } \dot{q} \tag{4.8}$$

$$a_2\dot{q}^2 \qquad P \text{ proportional to the square of } \dot{q} \tag{4.9}$$

$$\frac{a_3}{1+\dot{q}} \qquad P \text{ inversely proportional to } \dot{q} \tag{4.10}$$

Relationship between heat input to boiler and net power output Looking at Figure 4.20 and considering the net power output at any particular heat input to boiler, the temptation is to draw a straight line through the points. However, there is the feeling that the incremental heat rate should depend upon CO_2 recovery which means that a higher-order relationship between heat input to the boiler and CO_2 recovery should exist.

Interaction between net power output and CO_2 recovery Two different interaction terms are considered: one of the form $\dot{q}x^{CO_2}$ and the second of the form $x^{CO_2}/\,(1+\dot{q})$.

The process for selecting the model for the generating unit with integrated CO_2 started with determining parameters for the *full* model:

$$P = a_0 + a_1\dot{q} + a_2\dot{q}^2 + \frac{a_3}{1+\dot{q}} + a_4 x^{CO_2} + a_5 {x^{CO_2}}^2 + a_6\dot{q}x^{CO_2} + a_7\frac{x^{CO_2}}{1+\dot{q}} \tag{4.11}$$

Using ANOVA — in particular the t statistic — variations of (4.11) are proposed where each variation has had one or more of the terms in (4.11) eliminated. In general, the following principles are used in selecting a model:

- Model with fewer terms is preferred.
- Model must reasonably fit data.

[7] $2\times$ as much CO_2 is being recovered at 100% load than is being recovered at 50% load yet the derate is $1.6\times$. Suggests that it is more energy efficient to capture CO_2 at higher loads than at lower loads.

- Similarity to the generating unit model from Section 4.2 when CO_2 recovery is zero.
- Partial first derivative with respect to net power output should be a function of net power output and CO_2 recovery.

In total, ANOVA is undertaken for the following ten variations of (4.11):

$$P = a_0 + a_1\dot{q} + \frac{a_3}{1+\dot{q}} + a_4 x^{CO_2} + a_5 {x^{CO_2}}^2 \tag{4.12}$$

$$P = a_0 + a_1\dot{q} + \frac{a_3}{1+\dot{q}} + a_4 x^{CO_2} + a_5 {x^{CO_2}}^2 + a_7 \frac{x^{CO_2}}{1+\dot{q}} \tag{4.13}$$

$$P = a_0 + a_1\dot{q} + \frac{a_3}{1+\dot{q}} + a_4 x^{CO_2} + a_5 {x^{CO_2}}^2 + a_6 \dot{q} x^{CO_2} \tag{4.14}$$

$$P = a_0 + a_1\dot{q} + a_5 {x^{CO_2}}^2 + a_6 \dot{q} x^{CO_2} \tag{4.15}$$

$$P = a_0 + a_1\dot{q} + a_4 x^{CO_2} + a_5 {x^{CO_2}}^2 + a_6 \dot{q} x^{CO_2} \tag{4.16}$$

$$P = a_0 + a_1\dot{q} + \frac{a_3}{1+\dot{q}} + a_5 {x^{CO_2}}^2 + a_6 \dot{q} x^{CO_2} \tag{4.17}$$

$$P = a_0 + a_1\dot{q} + \frac{a_3}{1+\dot{q}} + a_4 x^{CO_2} + a_5 {x^{CO_2}}^2 + a_6 \dot{q} x^{CO_2} + a_7 \frac{x^{CO_2}}{1+\dot{q}} \tag{4.18}$$

$$P = a_0 + a_1\dot{q} + a_4 x^{CO_2} + a_5 {x^{CO_2}}^2 + a_6 \dot{q} x^{CO_2} + a_7 \frac{x^{CO_2}}{1+\dot{q}} \tag{4.19}$$

$$P = a_0 + a_1\dot{q} + a_4 x^{CO_2} + a_5 {x^{CO_2}}^2 + a_6 \dot{q} x^{CO_2} \tag{4.20}$$

$$P = a_0 + a_1\dot{q} + a_2\dot{q}^2 + a_5 {x^{CO_2}}^2 + a_6 \dot{q} x^{CO_2} \tag{4.21}$$

For each of these models least-squares estimates of the parameters are determined using the GNU R statistical computation software [48] for the remainder. The results of the regression are shown in Tables 4.9 and 4.10.

Table 4.9: Least-square estimates of parameters for reduced-order model of generating unit with CO_2 capture

Parameter	(4.12)	(4.13)	(4.14)	(4.15)	(4.16)	(4.17)	(4.18)	(4.19)	(4.20)	(4.21)
a_0	18.68	32.10	-53.14	-34.66	-38.64	-47.30	-53.80	-31.34	-38.64	-27.98
a_1	0.3256	0.3390	0.3793	0.3695	0.3724	0.3755	0.3796	0.3582	0.3724	0.3566
a_2										-5.962×10^{-6}
a_3	-7748	-36671	7301			6433	7641			
a_4	-69.06	-159.9	10.77		10.37		12.12	10.74	10.37	
a_5	-42.77	-32.92	-34.10	-30.47	-34.32	-30.15	-34.11	-34.11	-34.32	-30.16
a_6			-0.07988	-0.07374	-0.07937	-0.07400	-0.08050	-0.07985	-0.07937	-0.07340
a_7		86243					-690.8	6.643×10^{-6}		
adj. R^2	> 0.99	> 0.99	> 0.99	> 0.99	> 0.99	> 0.99	> 0.99	> 0.99	> 0.99	> 0.99

Table 4.10: P-values for regression parameters for reduced-order model of generating unit with CO_2 capture

Parameter	(4.12)	(4.13)	(4.14)	(4.15)	(4.16)	(4.17)	(4.18)	(4.19)	(4.20)	(4.21)
a_0	0.6	4×10^{-3}	1×10^{-7}	2×10^{-16}	2×10^{-16}	3×10^{-6}	3×10^{-3}	4×10^{-9}	2×10^{-16}	1×10^{-7}
a_1	2×10^{-16}	2×10^{-16}	2×10^{-16}	2×10^{-16}	2×10^{-16}	2×10^{-16}	2×10^{-16}	2×10^{-16}	2×10^{-16}	2×10^{-16}
a_2										0.1
a_3	0.7	2×10^{-8}	0.1			0.2	0.4			
a_4	2×10^{-9}	2×10^{-16}	4×10^{-3}		6×10^{-3}		0.7	4×10^{-3}	6×10^{-3}	
a_5	2×10^{-5}	3×10^{-16}	2×10^{-16}	2×10^{-16}	2×10^{-16}	2×10^{-16}	2×10^{-16}	2×10^{-16}	2×10^{-16}	2×10^{-16}
a_6				2×10^{-16}	2×10^{-16}	2×10^{-16}	2×10^{-16}	5×10^{-7}	2×10^{-16}	2×10^{-16}
a_7		2×10^{-16}					1.0	0.1		

- As indicated by the adjusted-R^2 values in Table 4.9, in each case, the regression is able to completely explain the variability in the data. No models are eliminated based upon this criterion.

- Based upon the P-values in Table 4.10, (4.12), (4.14), (4.17), (4.18), (4.19), (4.20), and (4.21) contain terms that may not be necessary to explain the variation in the data. These models are considered no further.

- (4.13) has six terms versus four and five for (4.15) and (4.16), respectively. Given the preference for few terms, (4.13) is also considered no further.

(4.15) and (4.16) differ in that the latter includes a first-order dependency on CO_2 recovery — $a_4 x^{CO_2}$ — in addition to a second-order dependency. Figure 4.21 and Figure 4.22 compares the fit of (4.15) and (4.16), respectively, to the data obtained using Aspen Plus®.

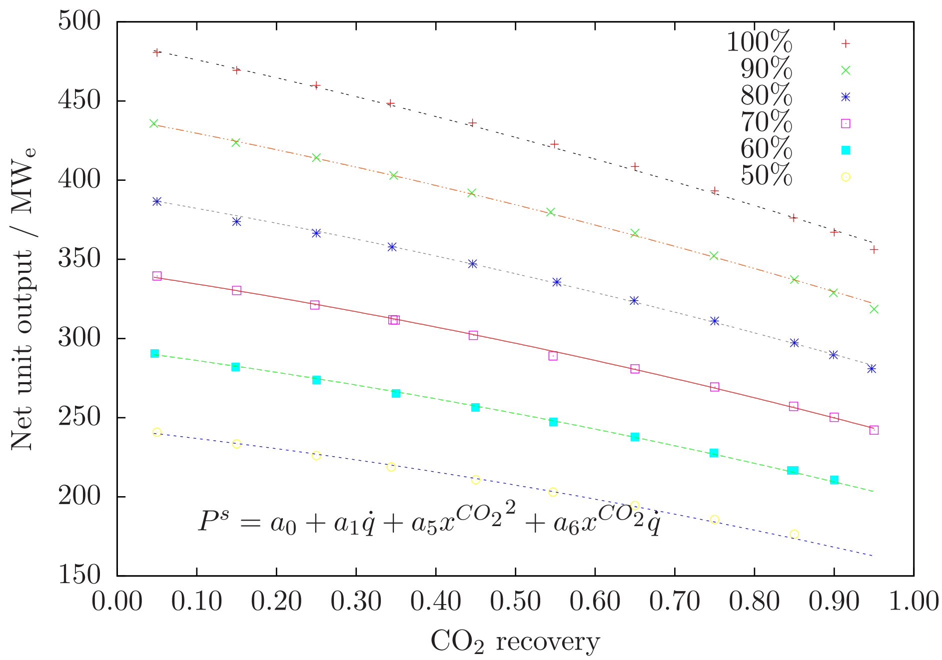

Figure 4.21: Comparison of net power output data from Aspen Plus® and reduced-order regression model (4.15)

Both models achieve good fit with the data for unit loads at or above 50% load (*i.e.*, 750 MW$_{th}$). Figure 4.23 is a plot of the residuals for both candidate models: the magnitude of the residuals is relatively small and there is no significant bias in either model as a function of generating unit load.

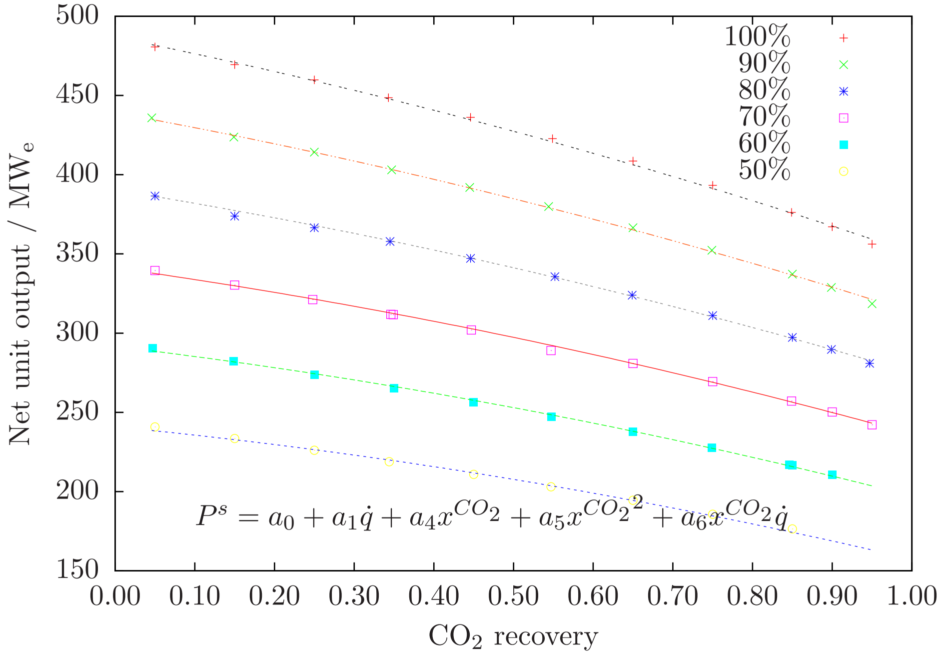

Figure 4.22: Comparison of heat input to boiler data from Aspen Plus® and reduced-order regression model (4.16)

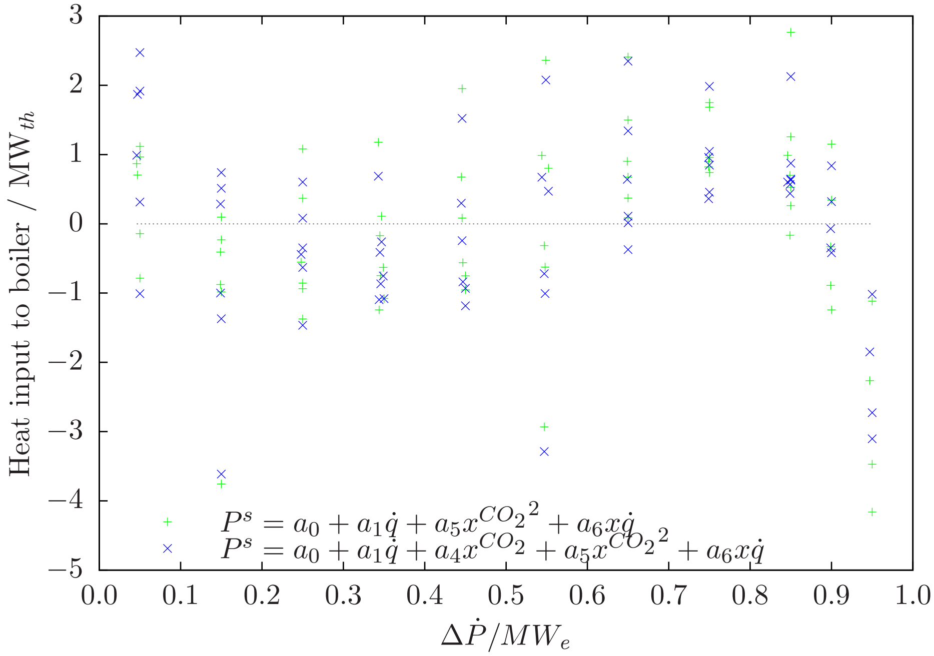

Figure 4.23: Residual plot for net power plant output

4.4 Conclusion

The objective of this section is to develop reduced-order models for a generating unit and a generating unit with CO_2 capture suitable for incorporation into a the electricity system simulator. The following reduced-order models are selected for the generating unit and the generating unit with integrated CO_2 capture.

w/o CO_2 capture	$P = -42.75 + 0.3802\dot{q} + 43331 + \dot{q}$	(4.3)
w/ CO_2 capture	$P = -34.66 + 0.3695\dot{q} - 30.47x^{CO_2}{}^2 - 0.07374\dot{q}x^{CO_2}$	(4.15)

Chapter 5

Reducing GHG emissions using CCS

5.1 Introduction

It is concluded in Chapter 3 that load balancing is effective at reducing GHG emissions from the electricity system. 'Taxing' GHG emissions causes lower-emitting units to be dispatched preferentially which causes GHG emissions to decrease. Table 5.1 summarizes the impact of progressively higher CO_2 prices has on the GHG emissions.

Table 5.1: GHG emissions for different CO_2 prices

CO_2 price	CO_2	Δ CO_2	
\$/tonne CO_2	tonne CO_2	tonne CO_2	%
15	980	30	3
40	953	56	6
100	927	83	8

The primary motivation for load balancing is to reduce GHG emissions yet without expending any capital. Again, it should not be a surprise that this measure also had a limited ability to reduce emissions and, then, with a cost of abatement that is quite high.

In this section, CCS is considered. Conventional wisdom is that CCS is expensive. However, in scenarios where the objective is to avoid the worst impacts of climate change , reductions from CCS are always a significant part of the minimum-cost solution. That is, not capturing and sequestering significant quantities of CO_2 would increase the cost of fulfilling the objective.

The largest coal-fired power plant in the system — the third power plant installed Austen — is retrofitted with PCC based using 30 wt% MEA as a solvent and designed to capture 85% of the CO_2 in the flue gas. The process for the generating unit with integrated unit is modelled in Aspen Plus®[1] and Table 5.2 summarzies the performance of the unit.

Table 5.2: Performance summary for generating unit with 85% CO_2 capture

Parameter	Units	Value
Minimum real power output	MW_e	376
Maximum real power output	MW_e	376
Minimum reactive power output	MW_e	-50
Maximum reactive power output	MW_e	230
Minimum up-time	h	24
Minimum down-time	h	48
Cold start heat input	MMBtu	13407
Cold start heat input	MWh_e	3929
Heat rate	Btu/kWh_e	12797
Incremental heat rate	Btu/kWh_e	11122
Bid price (fuel only)	\$/MWh_e	18.75
Bid price (\$15/tonne CO_2)	\$/MWh_e	21.13
Bid price (\$40/tonne CO_2)	\$/MWh_e	25.10
Bid price (\$100/tonne CO_2)	\$/MWh_e	34.64

Adding CCS to the unit at Austen increases the cost of power from this unit relative to the 350 MW_e unit from the base IEEE RTS '96 and the 500 MW_e generating unit without capture. Figure 5.2 shows the new composite supply curve for the system. The boxes in Figure 5.2 with the dotted outline represent the supply bids for the 350 MW_e unit in the base IEEE RTS '96.

Figures 5.3 through 5.6 contrast composite supply curves at different CO_2 prices for the base IEEE RTS '96 and for the IEEE RTS '96 with the 376 MW_e unit with 85% capture installed at Austen.

- CO_2 capture significantly de-rates the generating unit and also reduces its efficiency. When there is no CO_2 price, the generating unit with CO_2 capture is at a competitive disadvantage compared to other coal-fired units.
- As the CO_2 price increases, the relative position of the bids of the non-nuclear thermal units begins to change as differences in CO_2 emissions intensity comes in to play. The oil-fired units increase in priority and the coal-fired units decrease in priority, with the exception of the 376 MW_e unit with 85% capture installed at Austen. Its emissions intensity is quite low and its marginal cost of generation is relatively insensitive to CO_2 price. Once CO_2 regulation is introduced, it moves from the middle of the non-nuclear thermal units to the front of the line.

[1] Chapter 4.3 contains a detailed description of the development of this process model.

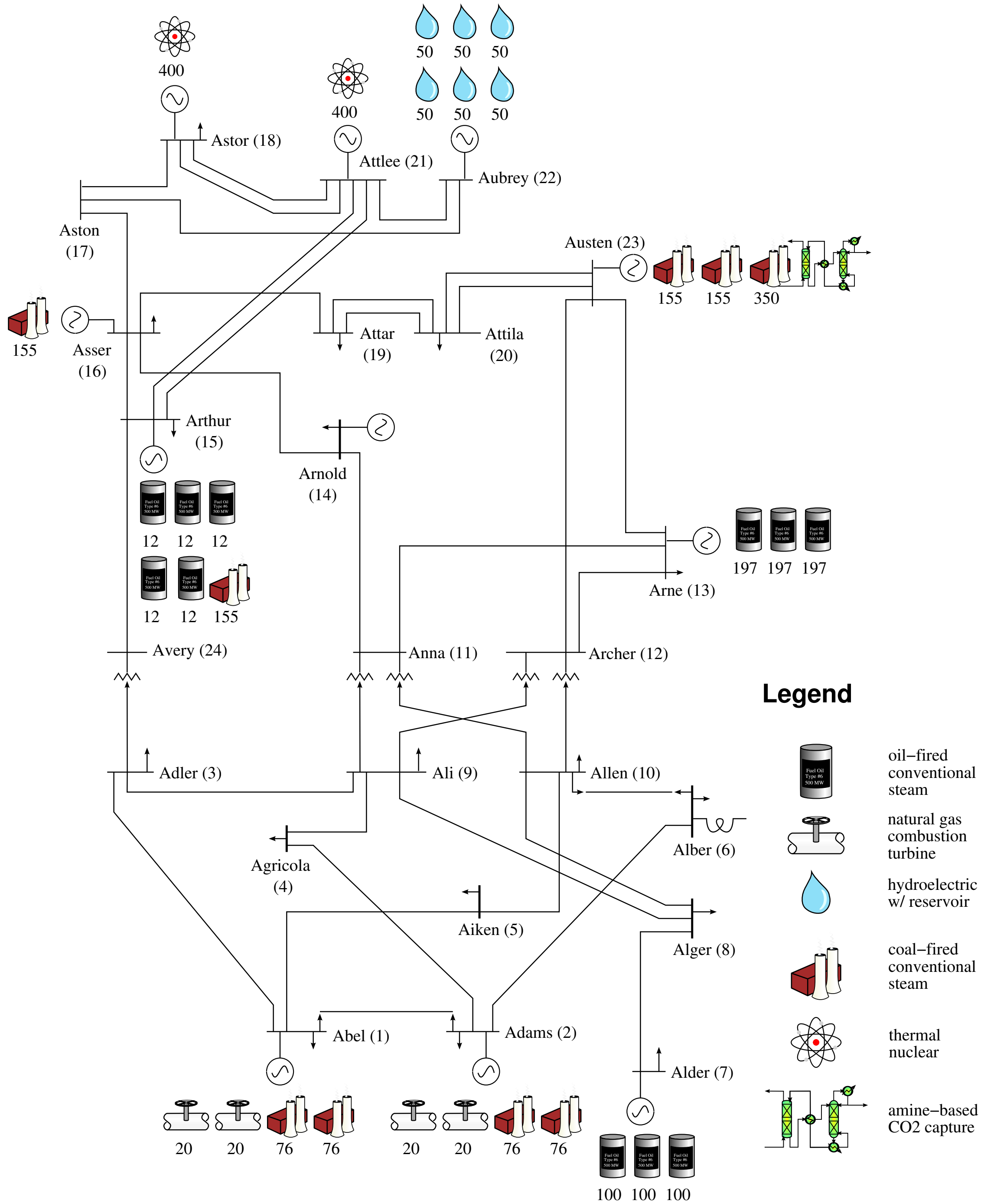

Figure 5.1: One-line diagram of IEEE RTS '96 with CO_2 capture on third unit at Austen

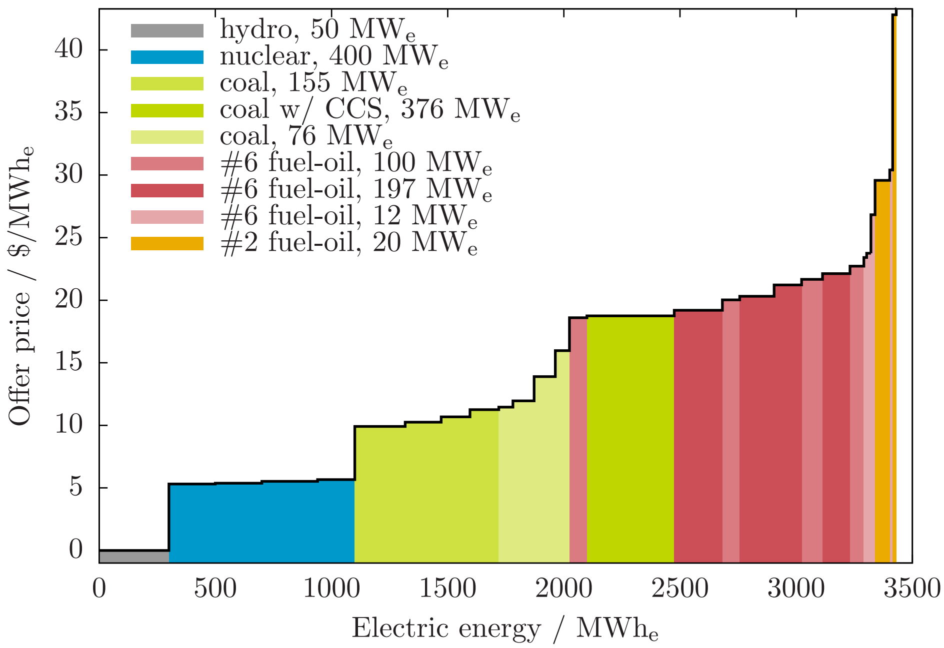

Figure 5.2: Composite supply curve for IEEE RTS '96 with generating unit at Austen with 85% CO_2 capture.

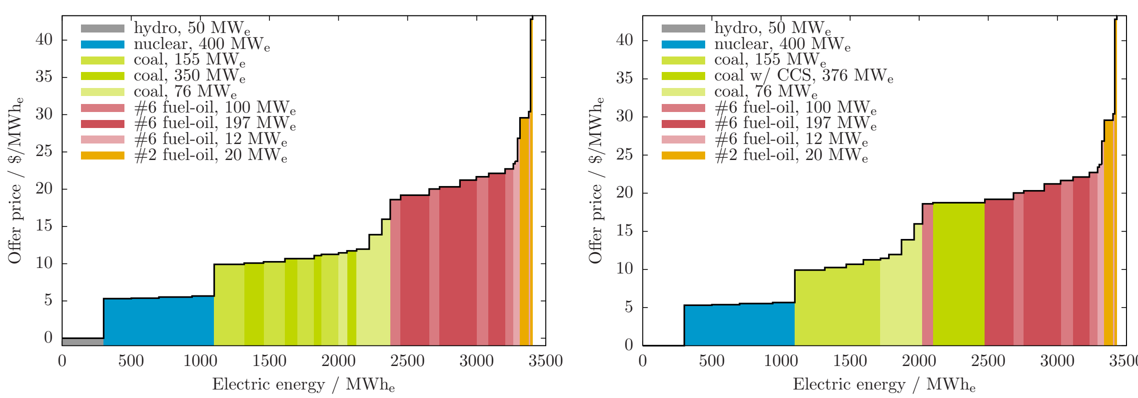

(a) Base IEEE RTS '96

(b) 376 MW_e unit at Austen with 85% CO_2 capture

Figure 5.3: Composite supply curves for IEEE RTS '96 w/ and w/o CCS: \$0/tonne CO_2

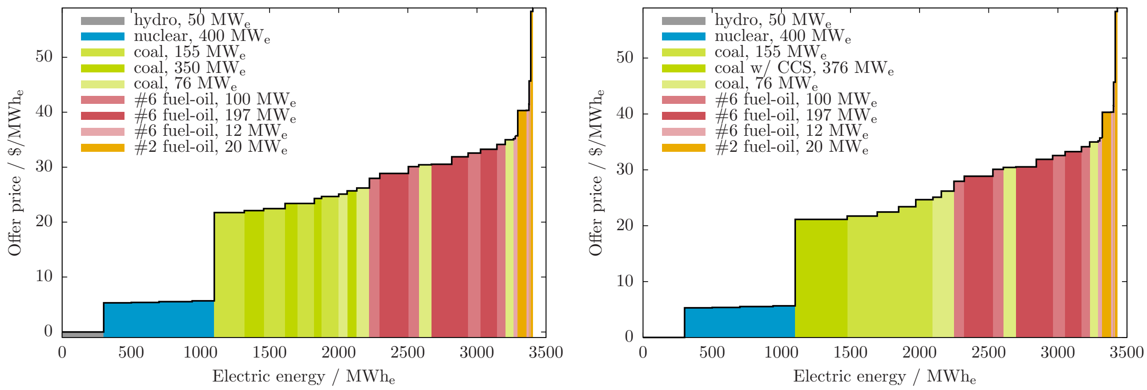

(a) Base IEEE RTS '96 (b) 376 MW$_e$ unit at Austen with 85% CO_2 capture

Figure 5.4: Composite supply curves for IEEE RTS '96 w/ and w/o CCS: \$15/tonne CO_2

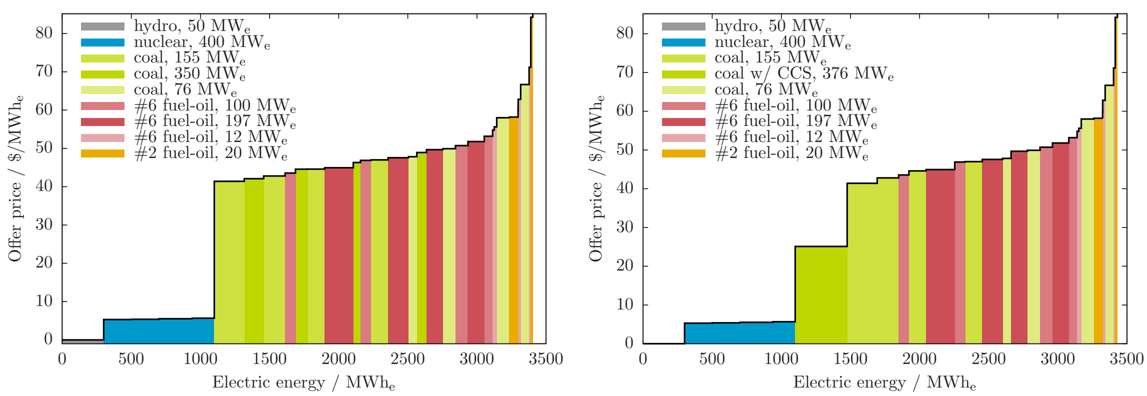

(a) Base IEEE RTS '96 (b) 376 MW$_e$ unit at Austen with 85% CO_2 capture

Figure 5.5: Composite supply curves for IEEE RTS '96 w/ and w/o CCS: \$40/tonne CO_2

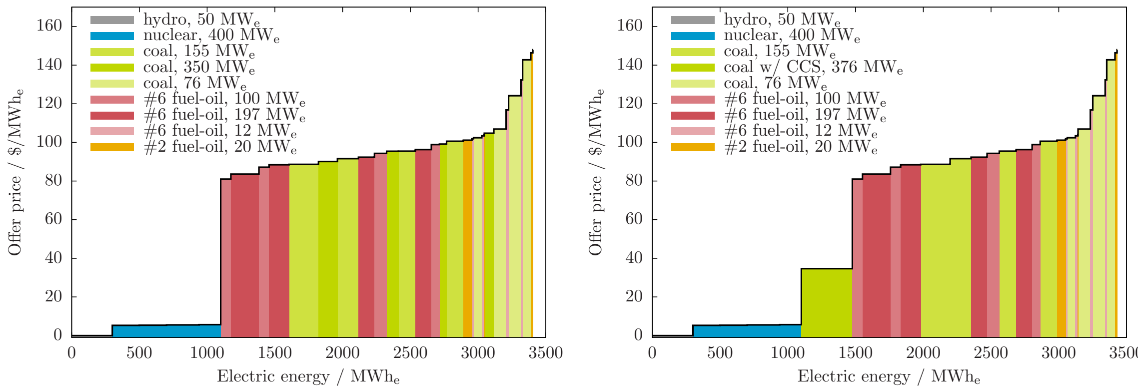

(a) Base IEEE RTS '96 (b) 376 MW_e unit at Austen with 85% CO_2 capture

Figure 5.6: Composite supply curves for IEEE RTS '96 w/ and w/o CCS: $100/tonne CO_2

- It is interesting to note that, even with a relatively small CO_2 price of $15/tonne CO_2, CO_2 capture appears to have given the 376 MW_e unit with 85% capture installed at Austen a competitive advantage that the 350 MW_e unit in the base IEEE RTS '96 did not enjoy.

5.2 Adding fixed CCS to electricity system simulator

The following modifications are made to the GAMS program to add the generating unit with 85% CO_2 capture.

1. The set NG^{CO_2} is defined representing generating units with integrated CO_2 capture. A configuration for such a generating unit is defined using the parameters in Table 5.2.
2. At Austen, 350 MW_e unit is substituted with 376 MW_e unit with respect to the set of available units at this bus.
3. In Chapter 3, the variable part of the generating units' operating and maintenance costs contains up to the following three components:
   (a) cost of fuel for cold start-up,
   (b) cost of fuel during normal operation, and
   (c) cost of acquiring CO_2 permits.

   A generating unit that captures CO_2 does not need to acquire permits for the fraction of CO_2 that is captured assuming that it is all permanently stored. A new cost component is required to represent the rebate generating units receive for the quantity of CO_2 they capture.

At typical operating conditions, an amine-based PCC process requires non-neglible quantities of make-up solvent. It is assumed that the rate of solvent consumption is proportional to the rate of CO_2 that is captured. A new cost component is required expressing the cost of solvent make; a unit cost of one dollar per tonne of CO_2 captured is assumed.

The output of the CO_2 capture process is a transport-ready stream of CO_2 and, hence, the operating cost associated with injecting the CO_2 into the storage reservoir is not yet considered. It is assumed that the (operating) costs for transporting and injecting the CO_2 is proportional to the rate of CO_2 that is captured. A new cost component is required to express these costs; a unit cost of five dollars per tonne of CO_2 captured is assumed.[2]

The variable component of the operating and maintenance cost is given by:

$$C_{nt}^{VOM} = C_{nt}^{start\text{-}up} + C_{nt}^{fuel} + C_{nt}^{CO_2} + C_{nt}^{cap} \tag{5.1}$$

where the impact of CO_2 capture, C_{nt}^{cap}, is itself given by:

$$C_{nt}^{cap} = -x_{nt}^{CO_2} C_{nt}^{CO_2,fuel} + C_{nt}^{MEA} + C_{nt}^{TS} \tag{5.2}$$

Recall from (2.28), that, in general, the objective function is:

$$\min z = \int_0^{P_S} \left(\frac{dC_n^{VOM}}{dP_n^S} \right) dP_n^S$$

An expression for $\int_0^{P_{nt}^S} \frac{dC_{nt}^{CO_2}}{dP_{nt}^S}$ is already available (see (3.7)). What is needed are equivalent expressions for C_{nt}^{MEA} and C_{nt}^{TS}. First, for the cost of acquiring make-up solvent:

$$C_{nt}^{MEA} = \dot{q}_{nt} EI_n^{CO_2} MEA_n L_t \tag{5.3}$$

$$\frac{dC_{nt}^{MEA}}{dP_{nt}^S} = EI_n^{CO_2} MEA_n L_t \frac{d\dot{q}_n}{dP_n^S}$$

$$\int_0^{P_{nt}^S} \frac{dC_{nt}^{MEA}}{dP_{nt}^S} = EI_n^{CO_2} MEA_n L_t \int_0^{P_{nt}^S} \frac{d\dot{q}_n}{dP_n^S}$$

$$\approx EI_n^{CO_2} MEA_n L_t \sum_{b=1}^{N_b} y_{bnt} IHR_{bnt} \tag{5.4}$$

[2]The outlet pressure in the CO_2 capture process is 110 bar which is 36 bar above CO_2's critical pressure of 73.8 bar. In a case where the injection site is relatively close to the generating unit, additional recompression of the CO_2 would not be necessary. This is an implicit assumption in this work which supports the modest unit cost for transportation and storage.

Expressions for the cost of CO_2 transportation and storage are almost identical to those above for solvent costs, with the unit cost of solvent replaced with the unit cost for CO_2 transportation and storage:

$$C_{nt}^{MEA} = \dot{q}_{nt} EI_n^{CO_2} TS_n L_t \tag{5.5}$$

$$\approx EI_n^{CO_2} TS_n L_t \sum_{b=1}^{N_b} y_{bnt} IHR_{bnt} \tag{5.6}$$

In summary, the objective function used in this scenario is given in Equation (5.7).

$$\begin{aligned} z =& \sum_{t=1}^{T} \sum_{n \in NG} u_{nt} HI_n FC_n \\ &+ \sum_{t=1}^{T} \sum_{n \in NG} \sum_{b=1}^{K} y_{bnt} IHR_{bnt} FC_n L_t \frac{1}{10^3} \\ &+ \sum_{t=1}^{T} \sum_{n \in NG} \sum_{k=1}^{K} y_{knt} IHR_{knt} EI_n^{CO_2} TAX^{CO_2} L_t \frac{1}{2.205 \cdot 10^6} \\ &- \sum_{t=1}^{T} \sum_{n \in NG^{CO_2}} y_{nt} IHR_{nt} EI_n^{CO_2} TAX^{CO_2} x^{CO_2}{}_n L_t \frac{1}{2.205 \cdot 10^6} \\ &+ \sum_{t=1}^{T} \sum_{n \in NG^{CO_2}} y_{nt} IHR_{nt} EI_n^{CO_2} MEA_n x^{CO_2}{}_n L_t \frac{1}{2.205 \cdot 10^6} \\ &+ \sum_{t=1}^{T} \sum_{n \in NG^{CO_2}} y_{nt} IHR_{nt} EI_n^{CO_2} TS_n x^{CO_2}{}_n L_t \frac{1}{2.205 \cdot 10^6} \\ &+ \sum_{t=1}^{T} \sum_{n \in NG} u_{nt} HI_n EI_n^{CO_2} TAX^{CO_2} \frac{1}{2.205 \cdot 10^3} \\ &+ \sum_{t=1}^{T} \sum_{r \in RM} C^{import} \cdot RM_{rt}^{slack} \end{aligned} \tag{5.7}$$

Recall that the last term in (5.7) is the value of lost load which represents the 'cost' of gaps between supply and demand.

5.3 Simulation of electricity system with fixed CCS

The first week of operation of the electricity system is simulated four times using CO_2 prices of \$0, \$15, \$40, and \$100/tonne CO_2.

5.4 Results and Discussion

5.4.1 Capacity utilization

Figure 5.7 shows the capacity utilization for the units in the IEEE RTS '96 with the 376 MW_e generating unit with 85% capture installed at Austen with no CO_2 price. The bottom portion of each column represents the average power injected into the grid and the upper portion represents the average capacity bid into the reserve market. The relative utilization of the generating units seen in Chapter 3 — hydroelectric and nuclear, coal-fired, oil-fired steam turbine, and oil-fired combustion turbine — is preserved here with the exception of the coal fired unit with CO_2 capture.

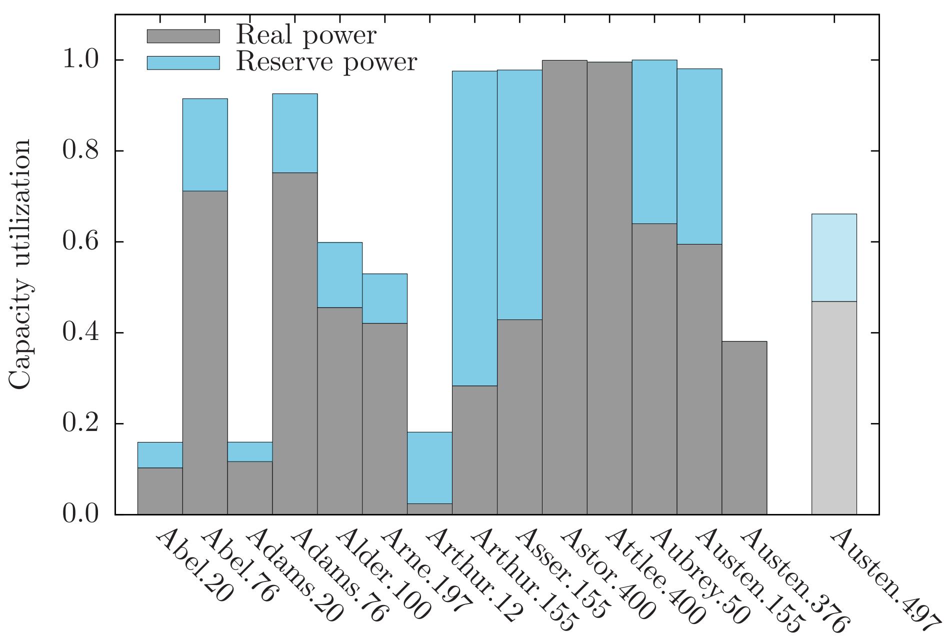

Figure 5.7: Average capacity utilization of units in IEEE RTS '96 with CCS installed at Austen, $0/tonne

The capacity factor for the 376 MW_e generating unit with 85% capture installed at Austen is 0.4, less than the capacity factor of the 500 MW_e unit it replaced. Additionally, this latter unit contributed a significant portion of its capacity to the reserve market. The unit with capture is not able to participate in the reserve market and is again disadvantaged.

The disadvantage disapears once CO_2 prices are introduced. Figure 5.8 compares the capacity utilization of the 376 MW_e generating unit with 85% capture installed at Austen and the 500 MW_e generating unit it replaced at various CO_2 prices. At $15/tonne CO_2, the utilization of the unit without capture is 0.6 *below* that of the unit with capture and the gap increases as the CO_2 price is raised.

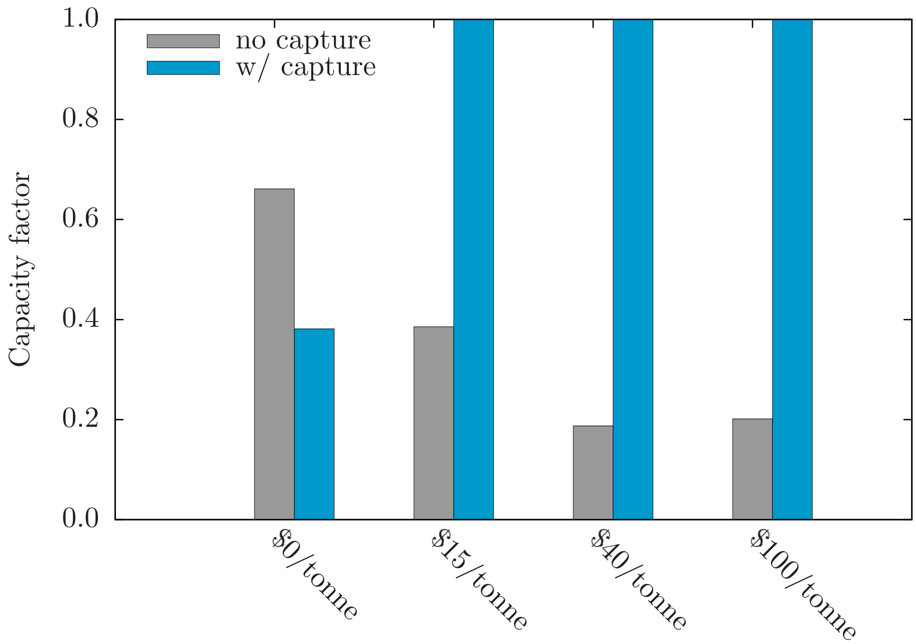

Figure 5.8: Comparison of capacity utilization for units with and without capture at various CO_2 prices

Figure 5.9 indicates how the average capacity utilization of the various types of unit changes as a function of CO_2 price. The utilization of the hydroelectric and nuclear units does not vary with CO_2 price; these units remain fully utilized. The direction of the change in the utilization of the coal- and oil-fired generating units is dependent upon the emissions-intensity of the unit. So, it is observed that, as CO_2 price increases, utilization of the oil-fired units goes up and that of the coal-fired units goes down, with the exception of the 376 MW_e generating unit with 85% capture installed at Austen (more about this in Section 5.4.2).

Figures 5.10 and 5.11 show the accepted bids during the off-peak and peak periods for two consecutive days. In general, lower-priced bids are accepted first. There are exceptions, though, and this has significant consequences:

- The electricity price corresponds with the price of the most expensive bid accepted in that period. Exceptions, then, cause capacity factor, GHG emissions, electricity price, energy benefit, *etc.* to be different — in some cases very different — than predicted if a strict merit-order dispatched is assumed.

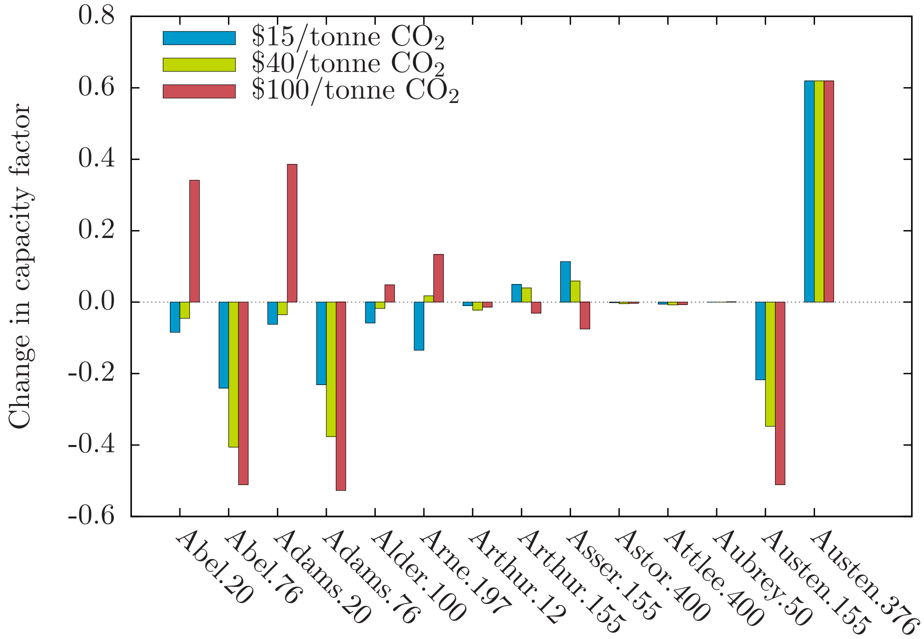

Figure 5.9: Change in capacity factor for different types of generating units at various CO_2 prices

- The difference in peak and off-peak demand between the two days is two percent yet the unit dispatch is quite different.

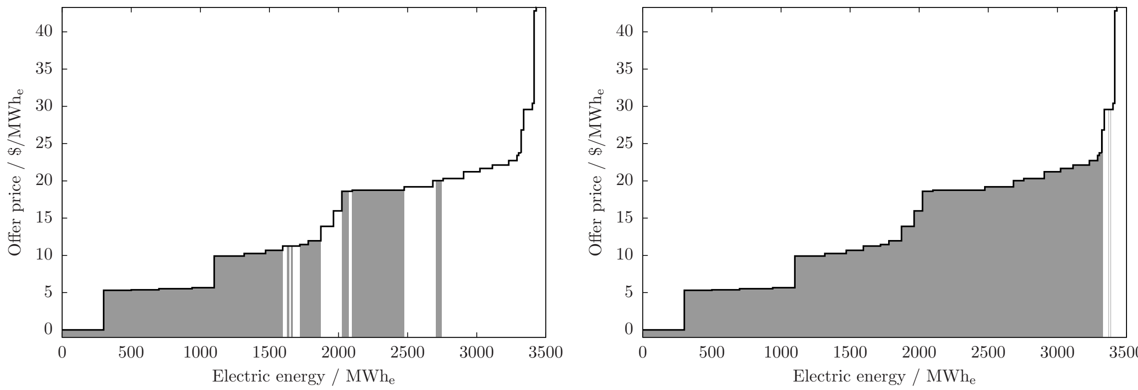

(a) Off-peak — 03:00 (b) Peak — 17:00

Figure 5.10: Accepted bids for Tuesday off-peak and peak periods

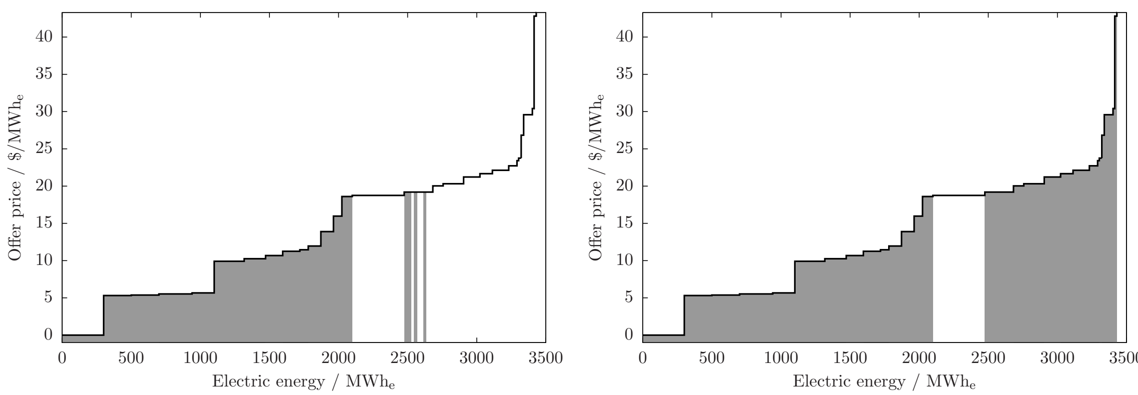

(a) Off-peak — 03:00 (b) Peak — 17:00

Figure 5.11: Accepted bids for Wednesday off-peak and peak periods

5.4.2 GHG emissions

There are a couple of questions that come to mind with respect to GHG emissions::

- What is the impact of increasing CO_2 price on CO_2 emissions?

- What is the impact of adding CCS on the CO_2 emissions?

Figure 5.12 compares the CO_2 emissions for the IEEE RTS '96 with CO_2 capture and Austen and without CO_2 capture and with no price on CO_2. For electricity systems containing units with and without CO_2 capture, GHG emissions are calculated using (5.8). In every time period, CO_2 emissions are lower in the scenario where there is CO_2 capture. In some cases — Monday through Wednesday and Friday to Saturday morning — the difference averages 300 tonne CO_2/hour and, at other times, the emissions are more like 100 tonne CO_2/hour less.

$$\begin{aligned}\dot{m}^{CO_2} = &\sum_{n \in NG^{nocap}} P_n^S \cdot HR_n \cdot EI_n^{CO_2} \cdot L_t \cdot \frac{1}{2.205 \times 10^6} \\ &+ \sum_{n \in NG^{cap}} P_n^S \cdot HR_n \cdot EI_n^{CO_2} \left(1 - x_n^{CO_2}\right) L_t \cdot \frac{1}{2.205 \times 10^6}\end{aligned} \tag{5.8}$$

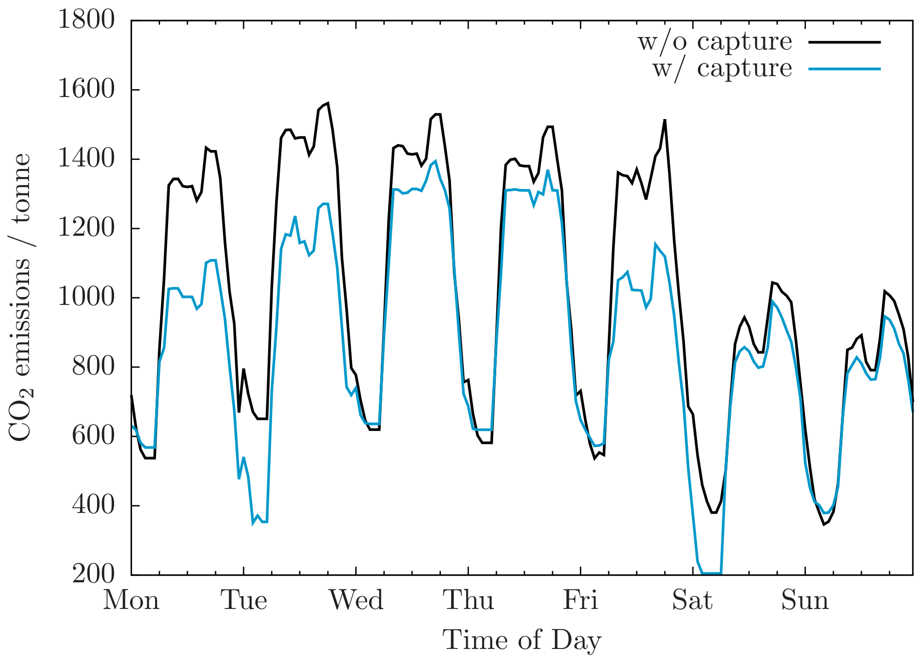

Figure 5.12: Aggregate CO_2 emissions for IEEE RTS '96 during week of interest: with and without CO_2 capture

The magnitude of the difference is related to the power output of the 376 MW_e generating unit with 85% capture installed at Austen. Figure 5.13 shows the output from this unit during the period of interest as compared to a 500 MW_e unit at the same bus. When the unit is on, versus the case without CO_2 capture, it is displacing 376 MW_e of power generated by coal-fired units a much greater CO_2 emissions intensity. Hence, there is 300 tonne CO_2 per hour reduction in emissions. When the unit with capture is off, relative to the case without CO_2 capture, oil-fired capacity makes up the shortfall. The emissions intensity of the oil-fired units is less than that of the coal-fired ones but not as low as for a coal-fired unit equipped with capture. So, the CO_2 emissions for the IEEE RTS '96 are lowered but by a more moderate amount.

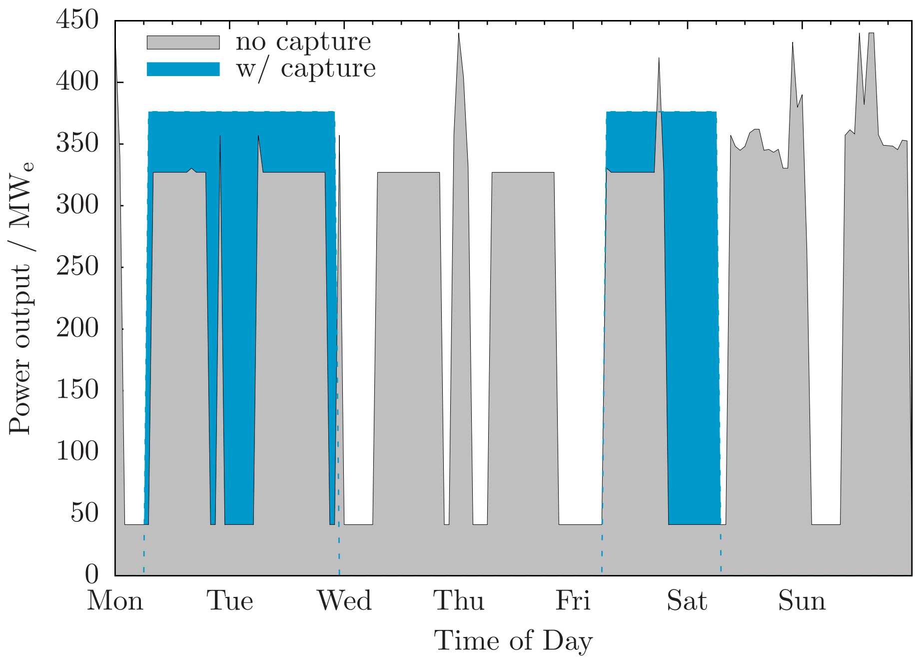

Figure 5.13: Net power output of 500 MW_e unit with and without capture

Already it has been observed that adding CO_2 capture to the system decreases the system's aggregate CO_2 emissions. Figure 5.14 shows the impact of CO_2 price \$15, \$40, and \$100/tonne CO_2 on the aggregate CO_2 emissions for the IEEE RTS '96 with 376 MW_e generating unit with 85% capture installed at Austen at CO_2 prices.

As expected, increasing the CO_2 price increases the reduction in CO_2 emissions. The incremental benefit of going from \$15 to \$40/tonne CO_2 and from \$40 to \$100/tonne CO_2 is minor, as is observed in the case where there is no CO_2 capture in the IEEE RTS '96. However, the decrease between \$0 and \$15/tonne CO_2 is quite large. Figure 5.15 shows the capacity factor grouped by type of unit (*i.e.*, capacity and bus) in the IEEE RTS '96. In the case of the 376 MW_e generating unit with 85% capture installed at Austen, the capacity factor is 0.38 at \$0/tonne CO_2 and jumps to 1.0 at CO_2 prices of \$15/tonne CO_2

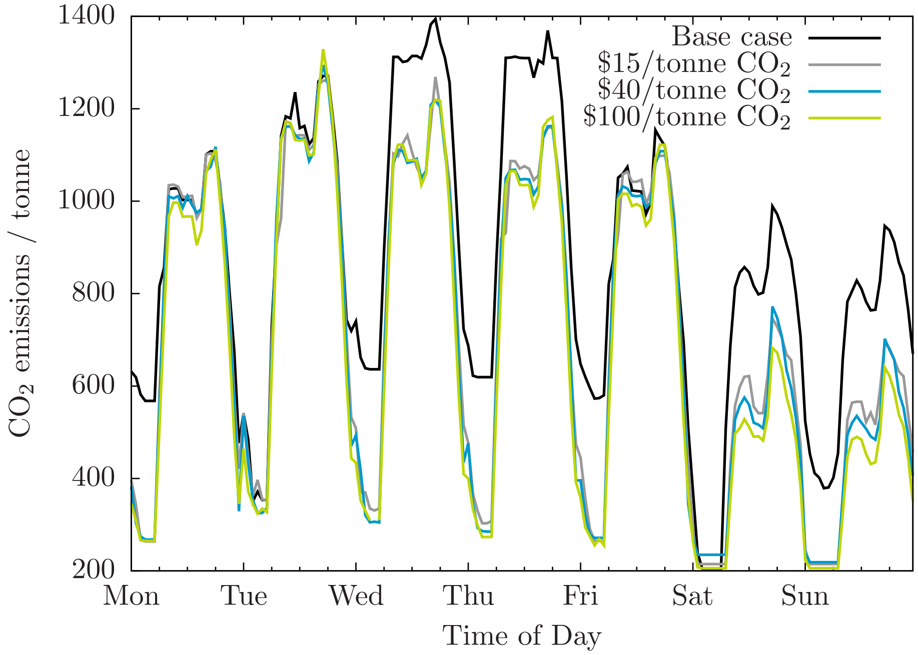

Figure 5.14: Aggregate CO_2 emissions for IEEE RTS '96 with CO_2 capture at various CO_2 prices

and beyond. It is the 150% increase in output from the unit with capture that explains the large decrease in emissions between the \$0 and \$15/tonne CO_2 cases.

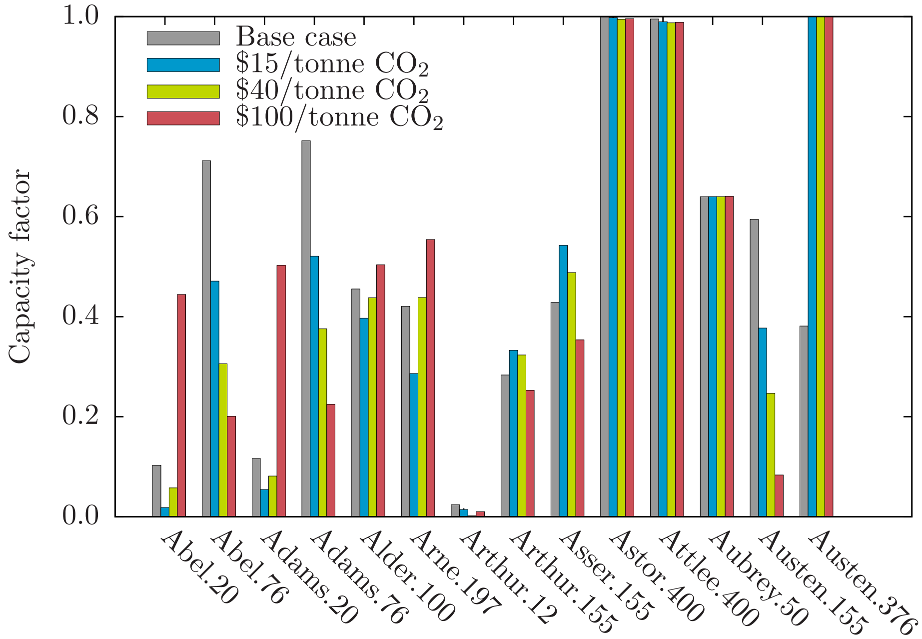

Figure 5.15: Capacity factor for different types of generating units at various CO_2 prices

5.4.3 Cost of electricity

Figures 5.16 through 5.19 shows the composite supply curve for the IEEE RTS '96 with the 376 MW_e generating unit with 85% capture installed at Austen at CO_2 prices of \$0, \$15, \$40, and \$100/tonne CO_2. Also in each Figure is the composite supply curve in corresponding base IEEE RTS '96.

In the case where there is no CO_2 price, between 1250 MW_e to 2400 MW_e, the offer price in the IEEE RTS '96 with capture exceeds that in the base IEEE RTS '96. When the CO_2 price is \$15/tonne CO_2, the composite supply curves are roughly the same. And, for CO_2 prices of \$40 and \$100/tonne CO_2, the supply curve for the capture case is less than that of the base IEEE RTS '96 in the region from 1000 MW_e to 1800 MW_e. Is comparing composite supply curves a good predictor of generation costs?

Firstly, Figure 5.20 shows the average cost of generating electricity in each time period. As CO_2 price increases, the cost of generation increases primarily due to increasing CO_2 expense.

Secondly, Figure 5.21 shows the difference in cost of generation between the IEEE RTS '96

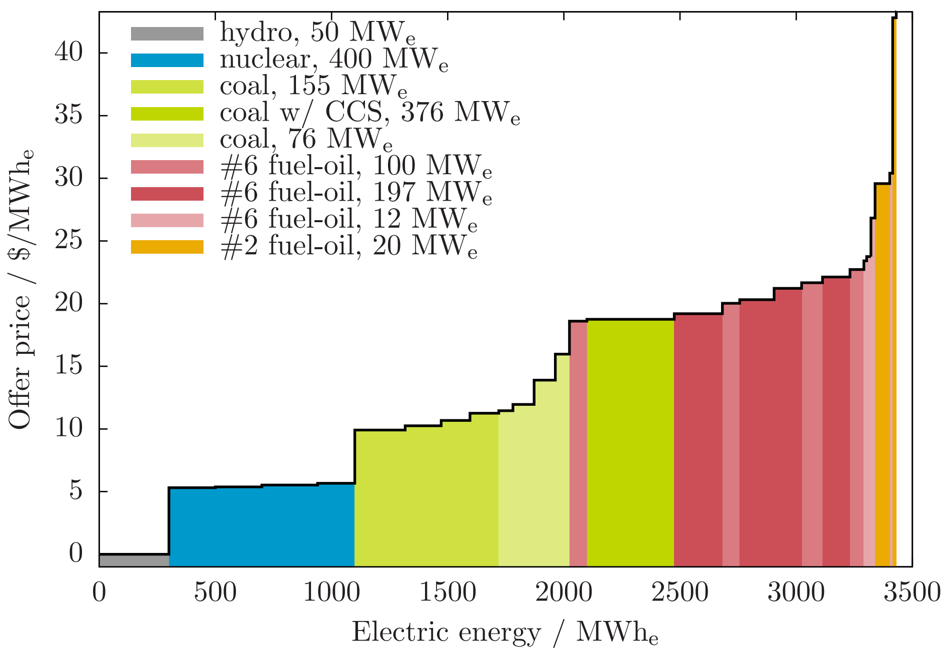

Figure 5.16: Composite supply curve for IEEE RTS '96 with capture and base IEEE RTS '96: \$0/tonne CO_2

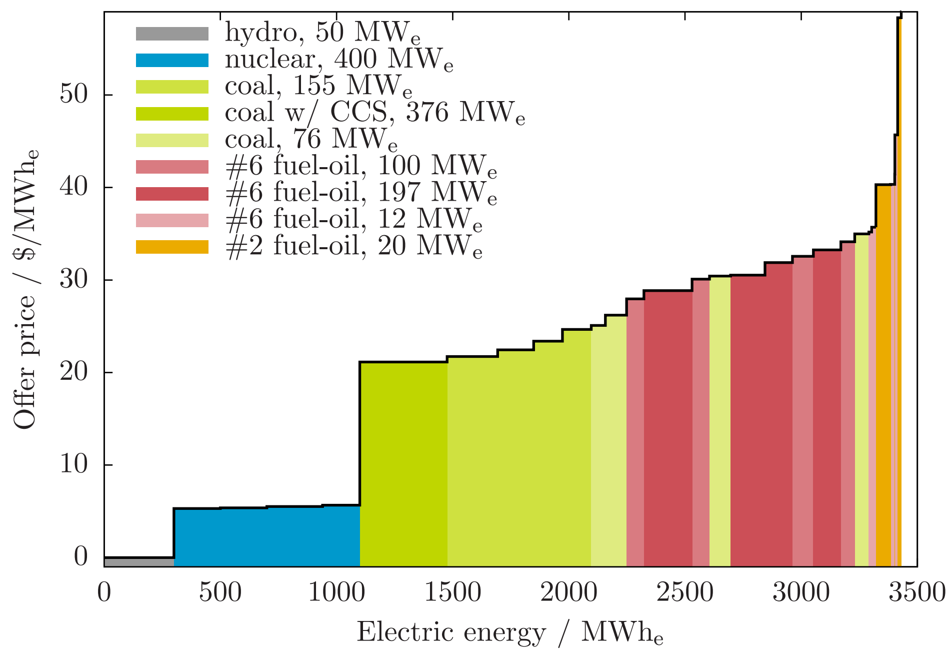

Figure 5.17: Composite supply curve for IEEE RTS '96 with capture and base IEEE RTS '96: \$15/tonne CO_2

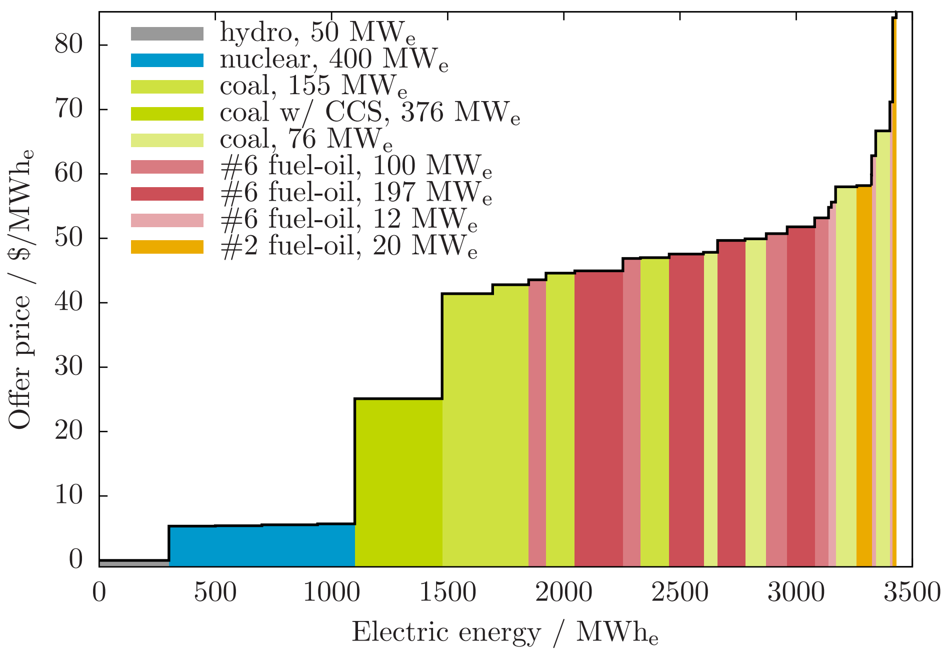

Figure 5.18: Composite supply curve for IEEE RTS '96 with capture and base IEEE RTS '96: \$40/tonne CO_2

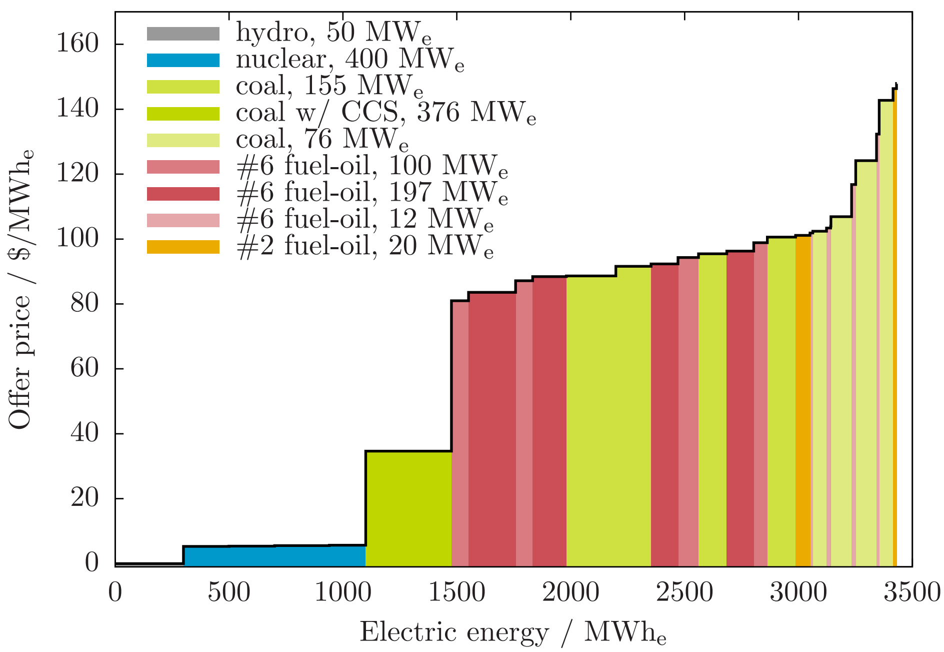

Figure 5.19: Composite supply curve for IEEE RTS '96 with capture and base IEEE RTS '96: \$100/tonne CO_2

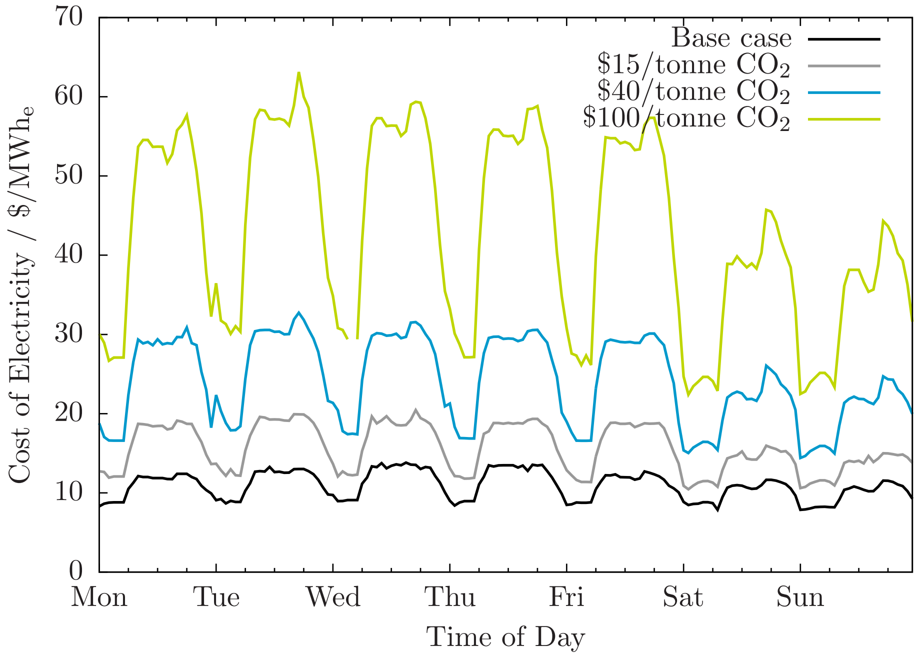

Figure 5.20: Cost of generation during period of interest at different CO_2 prices

case with the 376 MW_e generating unit with 85% capture installed at Austen and that without. At $0/tonne CO_2, somewhat in line with the composite supply curve, the cost of generation is slightly greater with CO_2 capture present in the system. With a non-zero price on CO_2, adding CO_2 capture to the system moderates the increase in the cost of generation. The greater the CO_2 price, the greater in absolute terms that the cost of generation is lower than it otherwise would have been.

5.4.4 Electricity price

In the base IEEE RTS '96 and IEEE RTS '96 without CO_2 capture, electricity price increases with increasing CO_2 price and disproportionately to that of generation cost. Figure 5.22 shows the electricity price in the IEEE RTS '96 with the 376 MW_e generating unit with 85% capture installed at Austen at CO_2 prices of $0, $15, $40, and $100/tonne CO_2. The average electricity price with no CO_2 capture is $23/$MWh_e$ and, the higher the CO_2 price, the higher the electricity price.

Figure 5.23 shows the difference in electricity price between the IEEE RTS '96 with the 376 MW_e generating unit with 85% capture installed at Austen and the IEEE RTS '96 with the 500 MW_e generating unit without capture at Austen.

1. The CO_2 capture scenario enjoys lower electricity prices than the scenario without

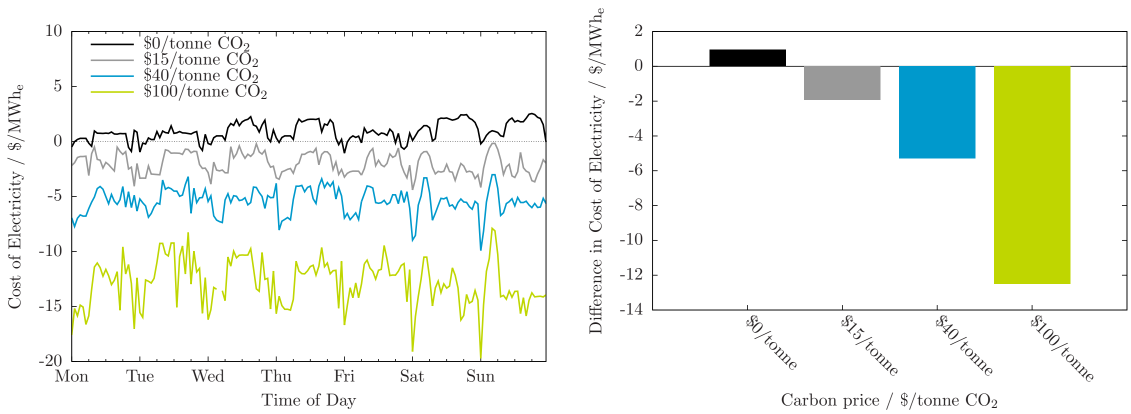

(a) Difference in generation cost in each time period

(b) Average change in generation cost

Figure 5.21: Difference in cost of generation between capture and no capture cases

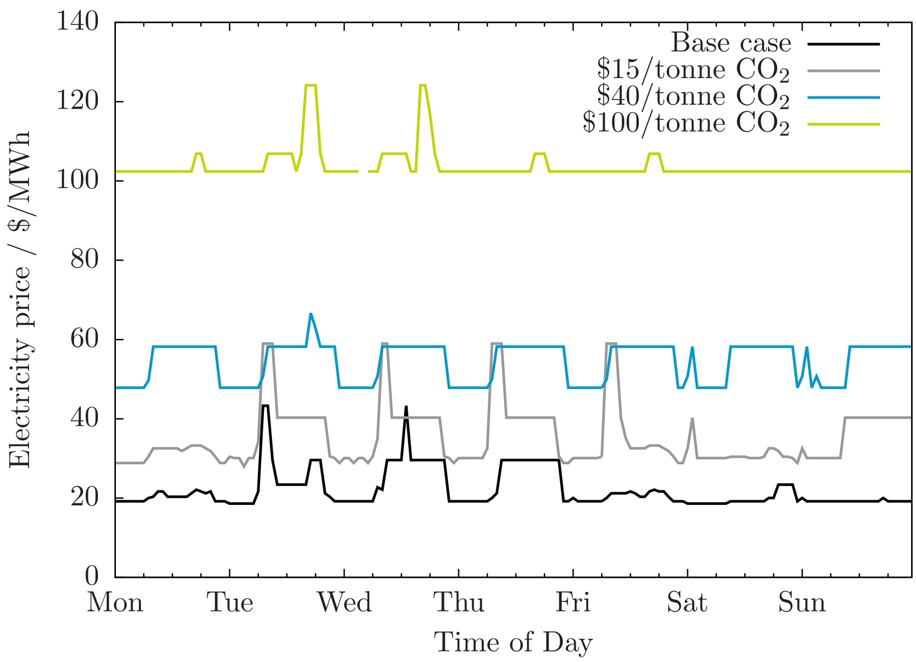

Figure 5.22: Electricity price during period of interest at different CO_2 prices

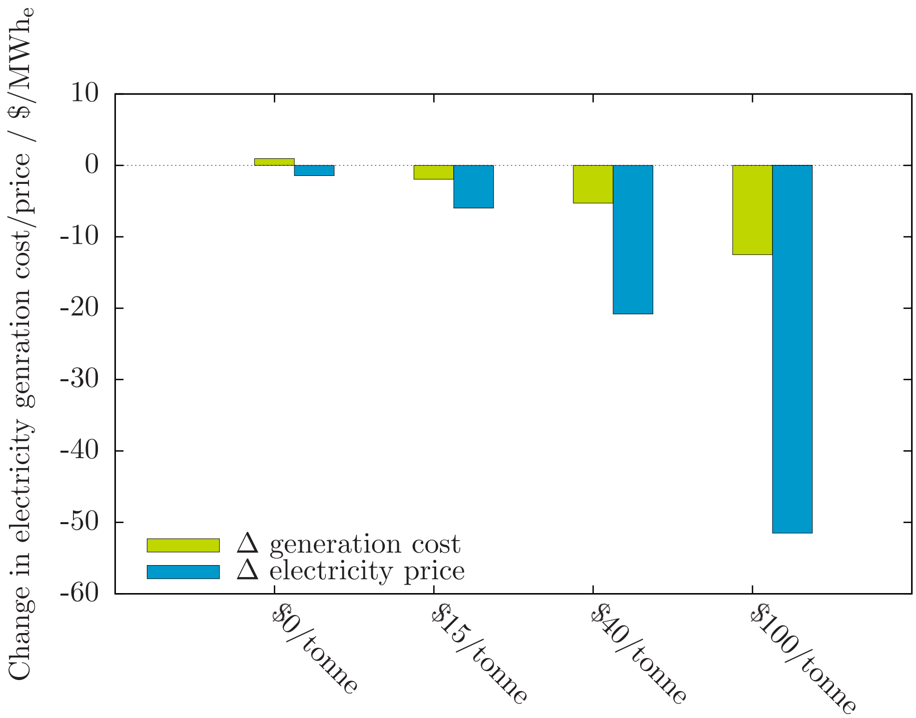

Figure 5.23: Change in electricity price and generation cost at different CO_2 prices

CO_2 capture, even for the case when the CO_2 price is $0/tonne CO_2.

2. The greater the CO_2 price, the greater moderation that having CO_2 capture in the system has on electricity price.

3. The effect of adding CO_2 capture on the generation cost and the electricity price is not always directionally the same. And, the degree to which adding CO_2 capture influences generation cost and electricity price is not the same. This is captured in Table 5.3.

Table 5.3: Effect of adding CO_2 capture on generation cost and electricity price

		$0/tonne	$15/tonne	$40/tonne	$100/tonne
Cost	$\lvert\Delta\rvert$	+0.95	-1.94	-5.29	-12.51
	%Δ	+9	-11	-17	-22
Price	$\lvert\Delta\rvert$	-1.43	-5.97	-20.81	-51.51
	%Δ	-6	-14	-27	-33

5.4.5 Net energy benefit

Both generation cost and electricity price increase with increasing CO_2 price. As Figure 5.24 indicates, the sensitivity of each of these to CO_2 price is not the same; the gap between average electricity price and average generation cost gets larger as the stringency of GHG regulation grows. Overall, the operating margin experienced by generators grows as CO_2 prices increase.

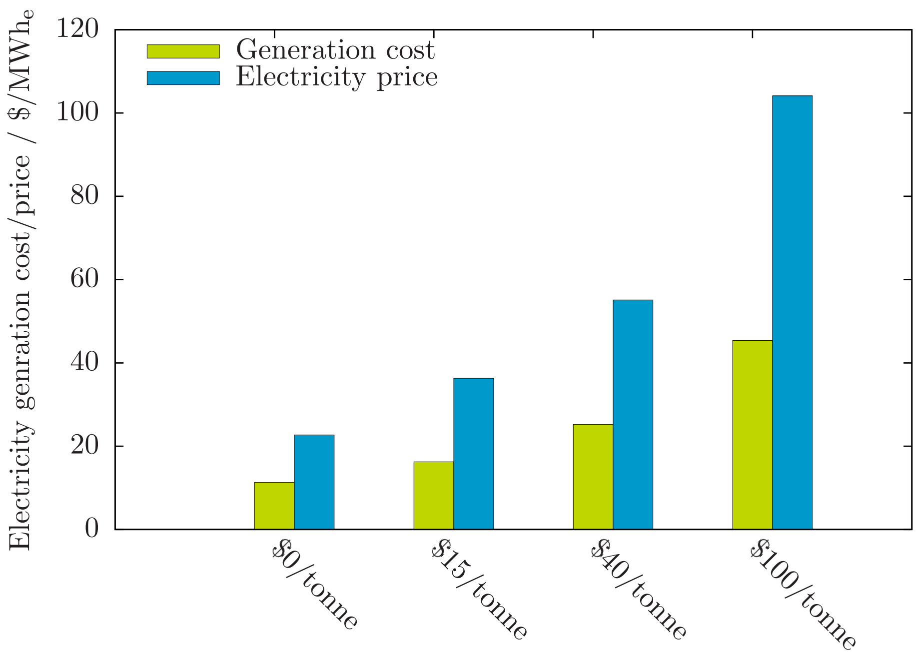

Figure 5.24: Average generation cost and electricity price at different CO_2 prices

This is shown explicitly in Figure 5.25 which shows the difference in net energy benefit for the IEEE RTS '96 with the 376 MW_e generating unit with 85% capture installed at Austen between the case with no GHG regulation and the cases with either \$15, \$40, and \$100/tonne CO_2/ emitted.

Not all units experience a windfall or participate equally. Figure 5.26 shows the net energy benefit of each different type of generating unit in the IEEE RTS '96 with the 376 MW_e generating unit with 85% capture installed at Austen. At \$100/tonne CO_2, the units at Abel and Adams take a loss for the week. Apart from the 12 MW_e units at Arthur, the rest of the units see net energy benefits increase with increasing carbon regulation. The non-emitting nuclear and hydroelectric units are the biggest winners: their generating costs stay the same yet they receive a higher price for the same power.

It is mentioned above that adding CCS to the IEEE RTS '96 has a moderating effect

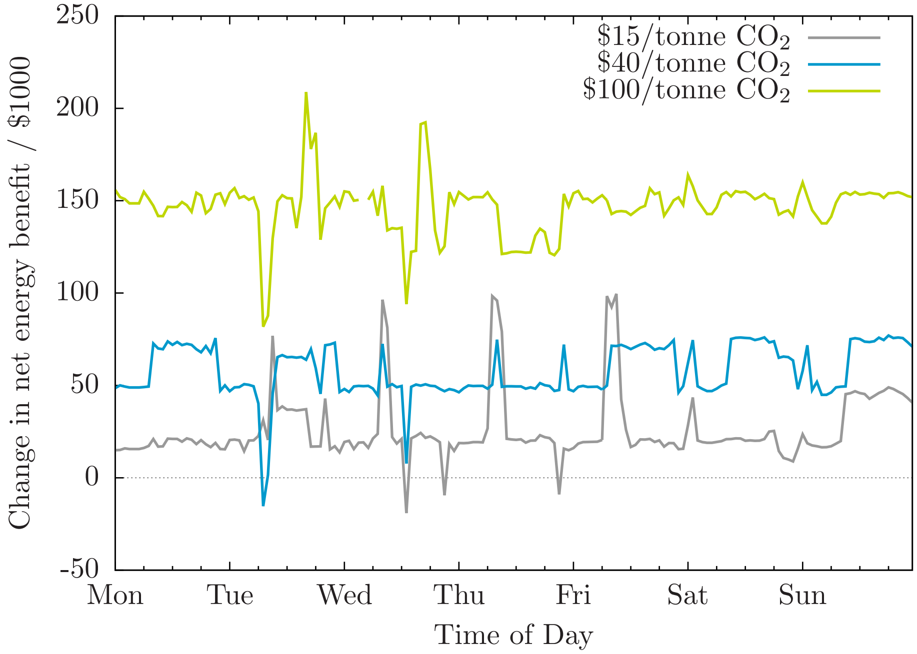

Figure 5.25: Increase in net energy benefit for IEEE RTS '96 with CCS versus CO_2 price

on the average cost of generation and electricity price and that the gap between the two grows as CO_2 price increases. Figure 5.27 contrasts the net energy benefit realized by each type of generator in the IEEE RTS '96 for the case with 376 MW_e generating unit with 85% capture installed at Austen and the case with the 500 MW_e generating unit with no capture.

The reduction in prices has a negative impact on the profitability that the units would otherwise enjoy; a generating unit seems 'lucky' if it's net energy benefit is unaffected by adding capture. The generating unit with capture is a notable exception. With a CO_2 price of \$0/tonne CO_2, the net energy benefit is markedly lower. However, as CO_2 prices increase, the net energy benefit of this unit increases dramatically. For example, at a CO_2 price of \$40/tonne CO_2, the 500 MW_e unit at Austen's energy benefit would be 90% greater — \$3.8 million versus \$2.0 million — if it captured 85% of its CO_2 eventhough doing so would reduce its capacity by 124 MW_e.

5.4.6 Transmission losses

Figure 5.28 summarizes the transmission losses that are observed in the system for the period of interest. In the case where the CO_2 price is \$0/tonne CO_2, the 'high-loss' days correspond to the days in which the 376 MW_e generating unit with 85% capture installed

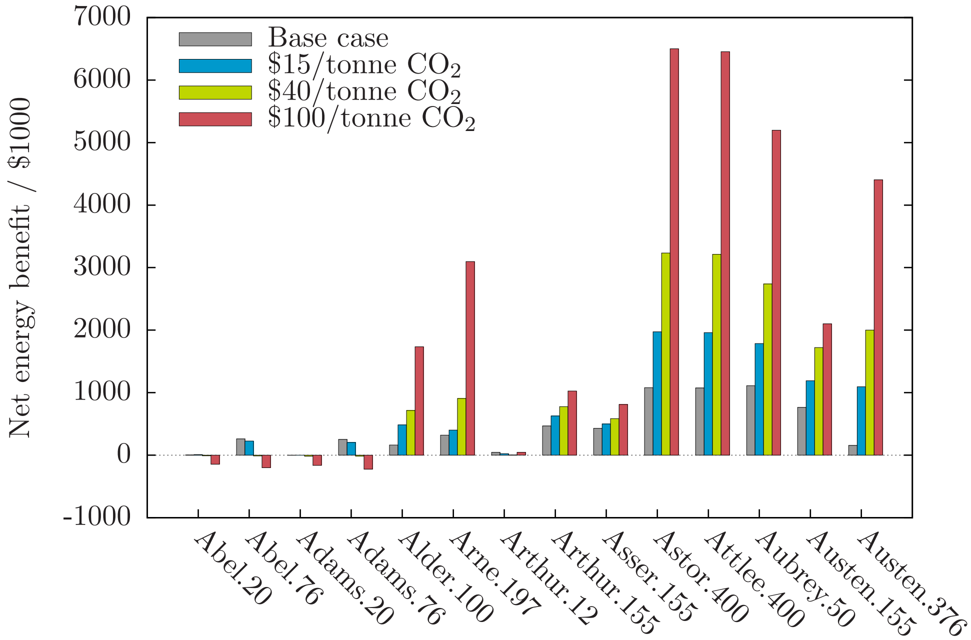

Figure 5.26: Net energy benefit for IEEE RTS '96 with CCS at different CO_2 prices

at Austen is dispatched. Austen is relatively far removed from the demand buses and use of generating units at Austen means that, overall, electricity is travelling greater distances. Hence, the transmission losses are greater.

Where the CO_2 price is non-zero, it is observed that the greater the CO_2 price, the lower the transmission losses. Well, as the CO_2 price goes higher, the electric power becomes more valuable (*i.e.*, , the marginal cost of generation increases) and, in the solution of the optimal power flow problem, transmission losses will tend to be lower.

5.4.7 Congestion

For the period of interest, there is never a time period in which the power flow exceed the maximum continuous rating of a transmission line. For example, Figure 5.29 shows, for each transmission line in the IEEE RTS '96, its MCR and the minimum, mean, and maximum power flow observed for the case with \$15/tonne CO_2. This is the case in which transmission losses were the greatest yet, with the possible exception of the Alder–Alger line, congestion is never an issue.

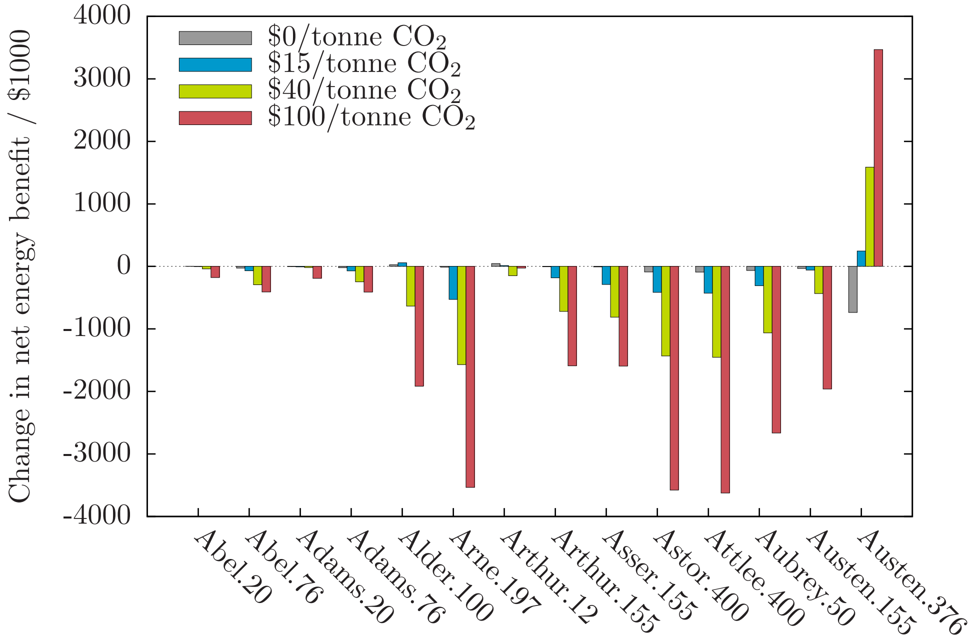

Figure 5.27: Change in net energy benefit between IEEE RTS '96 with and without capture at different CO_2 prices

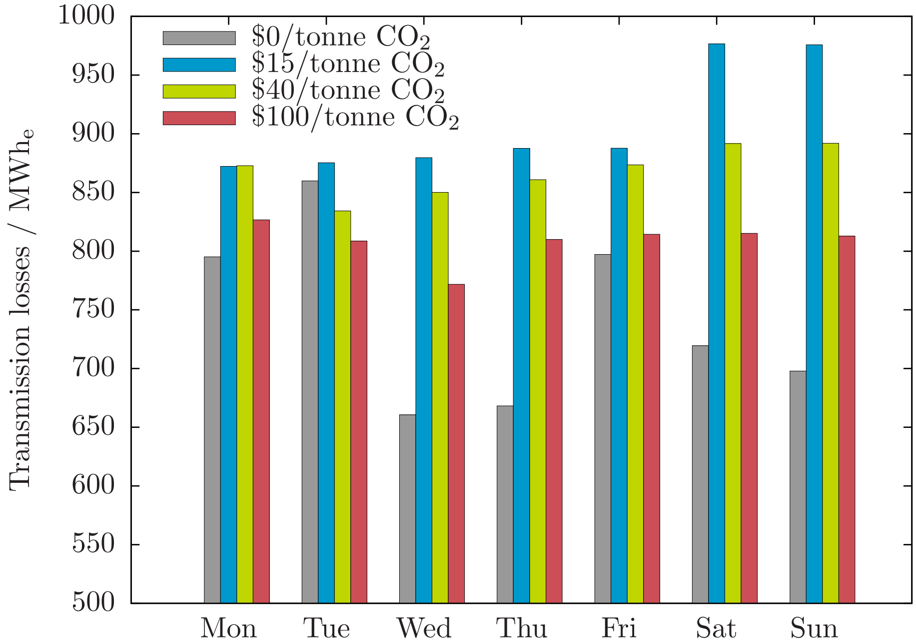

Figure 5.28: Daily aggregate transmission losses for IEEE RTS '96 with capture at various CO_2 prices

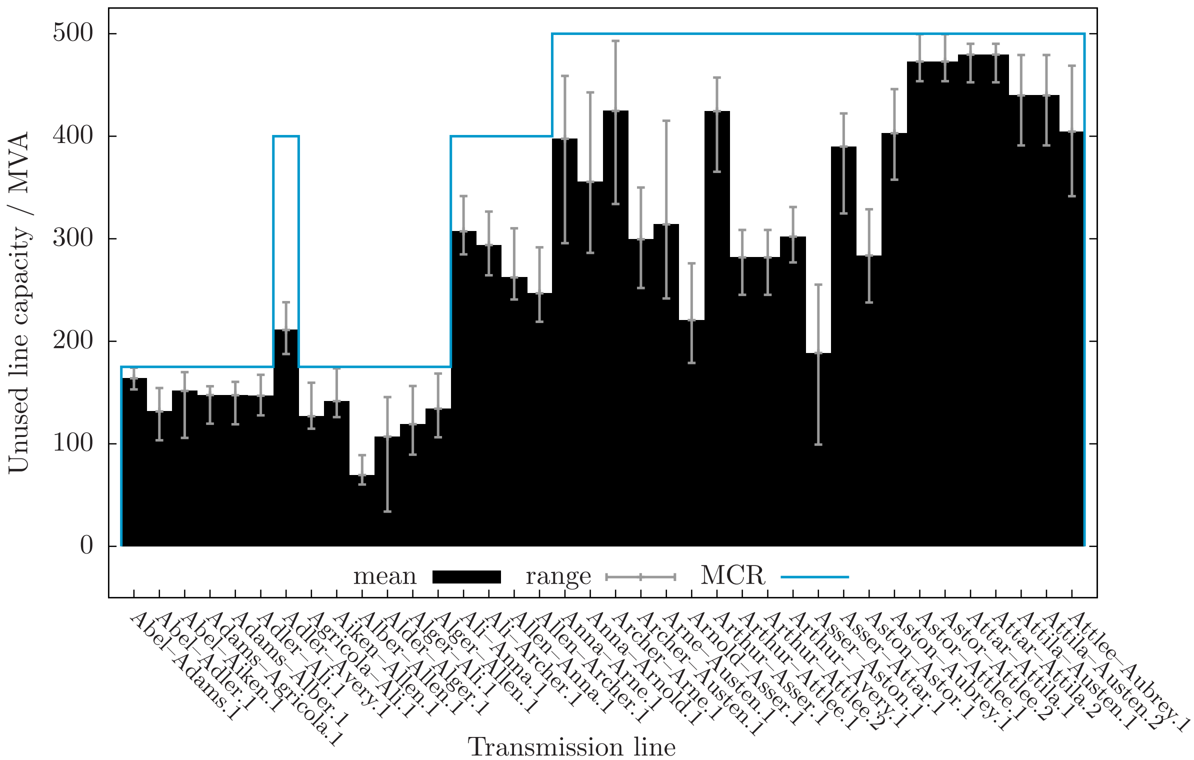

Figure 5.29: Mean, maximum, and minimum power flows along each transmission line for IEEE RTS '96 with capture: \$15/tonne CO_2

5.5 Summary/Conclusion

The difference between the version of the IEEE RTS '96 considered in this Chapter and that in Chapter 3 is essentially the retrofit of the 500 MW_e generating unit Austen with CO_2 capture. This reduces the unit's output by 120 MW_e and it's emissions intensity 80–83%. This one change has a relatively large effect on the performance of the electricity system. With GHG regulation in place, having CO_2 capture in the system:

- reduces GHG emissions by 30%,
- reduces the cost of generation by 11–22%,
- reduces the price of electricity by 14–33%, and
- reduces the net energy benefit of other generating units while increasing its own.

Adding a generating unit with CO_2 capture into the electricity system simulator is simple if one assumes that:

- The generating unit is either operating at full load or is shutdown.
- When operating, the generating unit is capturing CO_2 at a constant rate (*e.g.*, 85%).

Is this reasonable or even desirable? Consider the perspective of a generator. The output profile of the generating unit with capture is in sharp contrast to the other fossil-fuel fired generating units in the system. The power output of the latter tend to follow demand and would not the utility of a generating unit with capture also be increased if it benefited from the same flexibility?

Similarly, would it not be desirable for a generating unit with capture to adjust the fraction of CO_2 being captured? Consider the \$0/tonne CO_2 case. There is no commercial benefit to capturing CO_2 and the generating unit would likely improve its utility by reducing the quantity of CO_2 being captured, perhaps halting CO_2 capture altogether. Also, in the \$100/tonne CO_2 case, there would likely be an incremental commercial benefit to capture beyond the 85% level.

For the system operator, maintaining adequate reserve power is key for maintaining system reliability. The manner in which the generating unit with CO_2 capture is incorporated into the electricity system precludes it from participating in any of the reserve markets.

Chapter 6

Reducing GHG emissions using flexible CCS

6.1 Introduction

In Chapter 5, it was noted that the implementation of CO_2 capture at the largest coal-fired unit in the IEEE RTS '96 had a significant impact on the performance of the system: GHG emissions, generation costs, electricity price were all lower, for example. In the analysis, it was assumed that the power plant was limited to operating at base load and the CO_2 recovery rate was fixed at 85%.

Like in Chapter 5, studies assessing GHG abatement technologies options tend to consider a single mode of operation. For a coal-fired generating unit with CCS, it is the performance at the design heat input to the boiler and CO_2 capture at a fixed and relatively high rate that is the basis. This is an interesting choice of basis as, in practice, coal-fired generating units are often dispatched at less than full-load. It may also be true, then, that optimal dispatch of a coal-fired generating unit with CCS would include time periods when the heat input to the boiler is less than 100%.

The choice to operate the CO_2 capture process at a fixed recovery rate is also interesting. Capturing large amounts of CO_2 significantly reduces the quantity of power that a generating unit can deliver to the grid; for the design of the units at Nanticoke, capturing 85% of the CO_2 imposes a de-rate of 121 MW_e or 24% (see Table 5.2). When electricity is most valuable, like, for example, at or around the daily peak, there would likely be an incentive to produce more power at the expense of emitting more CO_2. One could then seek to recover greater amounts of CO_2 when the value of electricity diminishes.

Figure 6.1 compares the heat rate and CO_2 emissions intensity for three different yet related coal-fired generating units:

1. *Austen, no capture* refers to the nominally 500 MW_e coal-fired unit at Nanticoke upon which the reduced-order model in Section 4.2 is based.

2. *Austen, fixed capture* refers to the nominally 500 MW_e coal-fired unit at Nanticoke retrofitted with CO_2 capture operating at a fixed recovery rate of 85%. The simulation of the IEEE RTS '96 with this unit installed at Austen is the subject of Chapter 5.

3. *Austen, flexible capture* refers to the nominally 500 MW_e coal-fired unit at Nanticoke retrofitted with CO_2 capture upon which the reduced-order model in Section 4.3 is based.

Figure 6.1 illustrates a potential advantage that the generating unit with flexible CO_2 capture enjoys over a unit with fixed capture or no CO_2 capture at all. Figure 6.1a shows that, for most of its output range, a generating unit with flexible capture can operate over a wide range of emissions intensities. Figure 6.1b shows the corresponding envelope of values of unit heat rate. Unit heat rate is a good indicator of the average cost of generation and the indication is that, for most of its output range, the unit with flexible CO_2 can exercise much greater control of its generation costs.

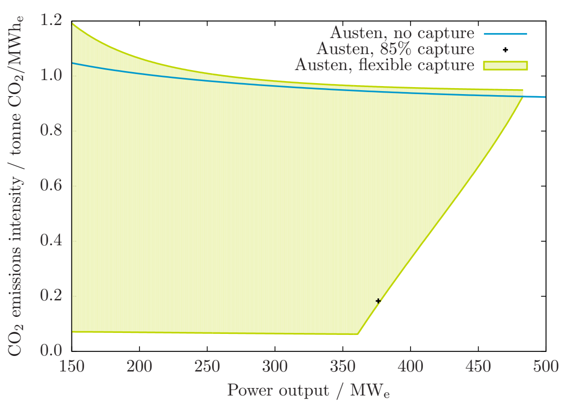

(a) CO_2 emissions intensity

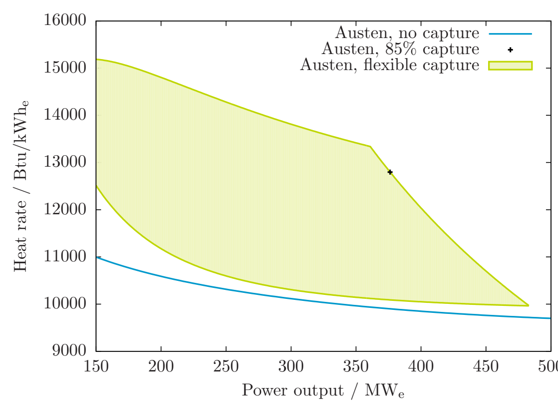

(b) Heat rate

Figure 6.1: Comparison of heat rate and CO_2 emissions intensity for three 500 MW_e generating units: without capture, with 85% capture, and with flexible capture

In this chapter, the operation of the IEEE RTS '96 is simulated again with a coal-fired generating unit with CCS installed at Austen in lieu of the 350 MW_e unit originally present. The difference as compared to Chapter 5 is that the CO_2 capture process can vary the heat input to its boiler and the fraction of CO_2 that is captured. Of interest is observing whether the explicit consideration of the operational flexibility of the CO_2 capture process materially changes the understanding of the impact of CCS.

6.2 Adding flexible CCS to electricity system simulator

In Chapters 2 through 5, stepwise, linear functions are used to describe the relationship between power output and the heat input to the boilers of the generating units. A reduced-order model of a 500 MW_e coal-fired generating unit with flexible CO_2 capture is developed in Chapter 4 and it has the form:

$$P\left(\dot{q}, x^{CO_2}\right) = a_0 + a_1\dot{q} + a_5 {x^{CO_2}}^2 + a_6\dot{q}x^{CO_2} \tag{(4.15)}$$

In the case of a thermal generating unit without CO_2 capture, there is a single value of $\dot{q}$ corresponding to each point P^S on the unit's input-output curve. In the case of the 497 MW_e unit with flexible CO_2 capture, there is typically more than one possible value of $\dot{q}$ at which a given output level P^S_{nt} can be achieved (see Figure 4.19). For example, Table 6.1 lists values of $\dot{q}$ and x^{CO_2} yielding the same net generating unit output of 376 MW_e. The optimum values of $\dot{q}$ and x^{CO_2} will depend on the relative cost of fuel versus the relative cost of acquiring CO_2 permits.

Table 6.1: Operating states corresponding to power output of 376 MW_e for 497 MW_e coal-fired generating unit at Austen with flexible CO_2 capture

$\dot{q}$ MW_{th}	x^{load}	x^{CO_2}
1413	1.00	0.85
1365	0.96	0.75
1320	0.93	0.65
1279	0.91	0.55
1242	0.88	0.45
1209	0.86	0.35
1178	0.83	0.25
1150	0.81	0.15
1126	0.80	0.05
1114	0.79	0.00

In terms of introducing a generating unit with flexible CO_2 capture into the electricity system model, the challenge arises from the fact that, in (4.15), power output depends upon two independent variables (*i.e.*, heat input to the boiler and CO_2 recovery rate) and that these variables are contiuous over their respective domains. The required changes are incremenal to those required in Section 5.2 to accommodate "fixed" CO_2 capture and can be grouped into three categories:

1. Changes to the objective function,

2. Changes to the expressions for real power output of generating units with flexible CO_2 capture, and

3. Changes to the expressions of the contribution to the reserve market from generating units with flexible CO_2 capture.

Each of these categories of changes is discussed in turn starting with the first last.

6.2.1 Reserve power from generating units with flexible CO_2 capture

Participation of generating units without CO_2 capture in the reserve market

A generating unit that, for a given time period, is participating simultaneously in both the real power market and the reserve market can be considered to have specified multiple operating states for this time period. Figure 6.2 shows the capacity utilization of the coal-fired 497 MW_e generating unit at Austen with a carbon price of \$0/tonne CO_2. This unit is active in the real, 10-minute spinning reserve, and 30-minute non-spinning reserve power markets; for example, during Monday's peak, this unit has sold 327 MW_e, 41 MW_e, and 113 MW_e of its capacity into each market, respectively.

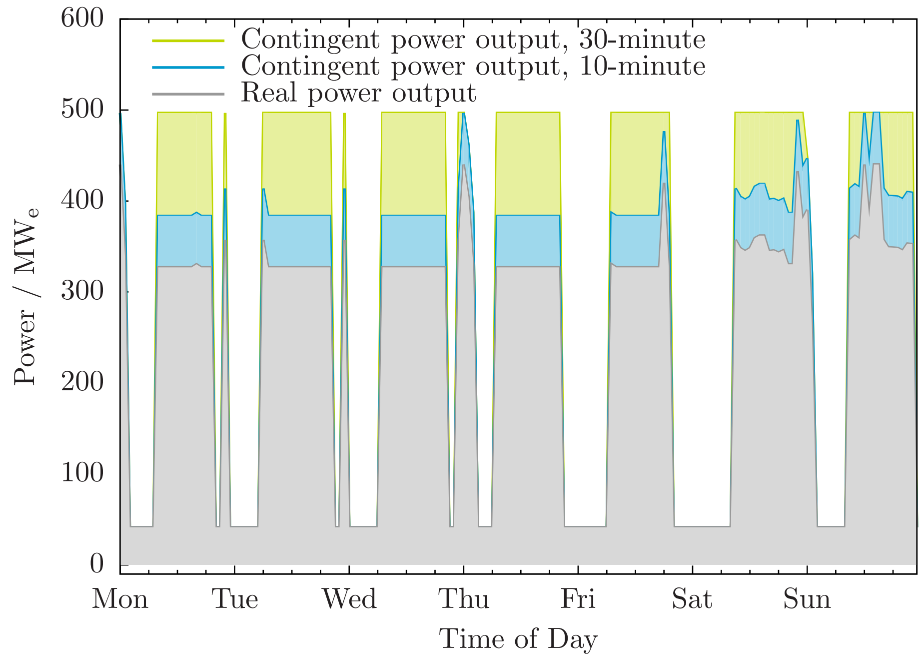

Figure 6.2: Capacity utilization for 497 MW_e coal-fired generating unit at Austen — \$0/tonne CO_2

Put another way, this unit has defined three operating states for the time period and these are shown in Table 6.2. Under normal circumstances, the unit is operating with a heat input to its boiler of 961 MW_{th}. In the case of a contingency, there are two other operating states to which, upon direction from the system operator, the unit is committed to moving:

1. Within ten minutes, the unit is prepared to increase power output to 384.5 MW_e; the corresponding heat input to its boiler would be 1114 MW_{th}.
2. Within 30 minutes, the unit is prepared to increase its power output to 497.7 MW_e; the corresponding heat input to its boiler would be 1413 MW_{th}.

Table 6.2: Operating states for 497 MW_e coal-fired generating unit at Austen during Monday peak period (17:00)

State	P	$\dot{q}$
	MW_e	MW_{th}
P^S	327.1	961
$P^S + P^R_{10^{ns}}$	384.5	1114
$P^S + P^R_{30}$	497.7	1413

Participation of generating units with CO_2 capture in reserve market

The 497 MW_e coal-fired generating unit with fixed CO_2 capture considered in Chapter 5 does not participate in the reserve market (see Figure 5.7). Constrained to a single operating state (*i.e.*, full-load with 85% CO_2 capture) and with relatively long cold-start and minimum down times (*i.e.*, 12 and 48 hours, respectively) , it is not possible for this unit to increase, in a timely manner, its power output in the case of a contingency.

The expectation is that a generating unit with *flexible* CO_2 capture *would* be able to participate in the reserve market. Like the unit that is the subject of Figure 6.2 and Table 6.2, a generating unit with flexible CO_2 capture would be able to increase its power output to produce additional power if and when required and this surplus capacity could be bid into the reserve market.

Further to this is the incremental power that a generating unit with flexible CO_2 capture can generate by reducing the quantity of CO_2 it captures. In the design of the CO_2 capture retrofit of the 500 MW_e generating unit at Nanticoke (see Section 4.3), steam is extracted upstream of the low pressure section of the turbine to satisfy the heat duty of the *Stripper* reboiler. This de-rates the generating unit; the expected reduction in power output is 121 MW_e when the unit is operating at full-load and 85% of the CO_2 is being captured. If the CO_2 capture process were turned down, though, the diversion of steam from the steam cycle would be reduced and additional power would be generated. Assuming that the dynamic performance of the generating unit with integrated CO_2 capture is amenable, a capture process provides an additional degree of freedom to:

- respond to a contingency, from the perspective of the system operator, and

- monetize the flexibility of the generating unit's CO_2 capture process, from the perspective of the generator.

Capacity utilization $\left[(\dot{q}_{nt})', \left(x_{nt}^{CO_2}\right)'\right]$ represents the state of the generating unit with flexible CO_2 capture when it is delivering the maximum power it has committed during the time period, P_{nt}. P_{nt} is the total capacity utilization which, for *continuous* generating units, is given by (6.1). This is analgous to (2.33) which defined the capacity utilization for *discrete* units.

$$P_{nt} = a_0 + a_1 (\dot{q}_{nt})' + \frac{a_2}{1 + (\dot{q}_{nt})'} + a_3 \left(x_{nt}^{CO_2}\right)'^2 + a_4 (\dot{q}_{nt})' \left(x_{nt}^{CO_2}\right)' \tag{6.1}$$

Reserve power requirements For discrete units, the maximum amount of power that a unit can provide to each class of reserve is limited by its ramp rate 2.50. For continuous units, the maximum reserve contribution additionally depends upon CO_2 recovery; the reserve power limits is specified below in (6.2) for 10-minute spinning, 10-minute non-spinning, and 30-minute reserve cases.

$$\begin{aligned} P_{nt}^S + P_{10^{sp},nt}^R &\leq f\left[\dot{q}_{nt} + (\Delta\dot{q})_n \tau_{10^{sp}}^R, \left(x_{nt}^{CO_2}\right)'\right] \\ P_{nt}^S + P_{10^{sp},nt}^R + P_{10^{ns},nt}^R &\leq f\left[\dot{q}_{nt} + (\Delta\dot{q})_n \tau_{10^{ns}}^R, \left(x_{nt}^{CO_2}\right)'\right] \\ P_{nt}^S + P_{10^{sp},nt}^R + P_{10^{ns},nt}^R + P_{30,nt}^R &\leq f\left[\dot{q}_{nt} + (\Delta\dot{q})_n \tau_{30}^R, \left(x_{nt}^{CO_2}\right)'\right] \end{aligned} \tag{6.2}$$

6.2.2 Real power output of generating units with flexible CO_2 capture

Real power output $\left(\dot{q}_{nt}, x_{nt}^{CO_2}\right)$ represents the state of a generating unit with flexible CO_2 capture, dispatched to deliver P_{nt}^S in the given time period and is defined in (6.3).

$$P_{nt}^S = a_0 + a_1 \dot{q}_{nt} + \frac{a_2}{1 + \dot{q}_{nt}} + a_3 x_{nt}^{CO_2 2} + a_4 \dot{q}_{nt} x_{nt}^{CO_2} \tag{6.3}$$

Minimum and maximum heat input to the boiler For discrete units, the minimum and maximum power output from the units is constrained as per (2.36). For continuous units, it is the heat input to the boiler that is kept within set lower and upper limits of 141 MW_{th} (*i.e.*, 10% of heat input to the the boiler at 100% load) and 1411 MW_{th}.

$$\begin{aligned} (1 - \omega_n)\, \dot{q}_n^{\min} \leq \dot{q}_{nt} \leq (1 - \omega_n)\, \dot{q}_n^{max} \\ (1 - \omega_n)\, \dot{q}_n^{\min} \leq (\dot{q}_{nt})' \leq (1 - \omega_n)\, \dot{q}_n^{max} \end{aligned} \tag{6.4}$$

Unit ramp rates The ramp rates of discrete units are specified in terms of power output (2.63). Similarly to the upper and lower limits for the generating units with flexible CO_2 capture, ramp rates are specified in terms of heat input to the boiler.

$$\begin{aligned} \dot{q}_{nt} &\geq \dot{q}_{n,t-1} - (\Delta\dot{q})_n L_t \\ \dot{q}_{nt} &\leq \dot{q}_{n,t-1} + (\Delta\dot{q})_n L_t \end{aligned} \tag{6.5}$$

In the first time period, constraint (6.5) reduces to:

$$-(\Delta\dot{q})_n L_t \leq \dot{q}_{t=1} \leq (\Delta\dot{q})_n L_t$$

6.2.3 Objective function

CO_2 capture is introduced in the electricity system simulator in Chapter 5 and the eight components of the system generating cost were identified:

1. Cost of fuel for cold start-up,
2. Cost of fuel during normal operation,
3. Cost of acquiring permits for CO_2 that is generated during normal operation,
4. Rebate for CO_2 that is generated but not emitted,
5. Cost of acquiring make-up solvent for the CO_2 capture process,
6. Cost of transporting and storing the captured CO_2,
7. Cost of acquiring permits for CO_2 that is generated during start-up, and
8. Value of lost load which represents the 'cost' of gaps between supply and demand.

All the same components are valid for the case where the CO_2 capture process is flexible and what is need is terms specific to generating units with flexible CO_2 capture for components 2 through 6. Recall from (2.28), that, in general, the contribution to the objective function from each unit in each time period is given by:

$$\begin{aligned} z_{nt} &= \int_0^{P_S} \left(\frac{dC_n^{VOM}}{dP_n^S} \right) dP_n^S \\ &= \Delta C_{nt}^{VOM} \\ &= C_{nt}^{VOM} \end{aligned}$$

where, for a unit with a flexible CO_2 capture process, $C_{nt}^{VOM} = f\left(u_{nt}, [\dot{q}_{nt})', \left(x_{nt}^{CO_2}\right)'\right]$. The last step is a consequence of the fact that (by definition) variable operating and maintenance costs are zero when there is zero activity. The additional terms in the objective function for generating units with flexible CO_2 capture is shown in (6.6).

$$
\begin{aligned}
&+\sum_{t=1}^{T}\sum_{n\in NG_C}\left(\dot{q}_{nt}\right)' FC_n L_t \frac{1}{10^3}\\
&+\sum_{t=1}^{T}\sum_{n\in NG_C}\left(\dot{q}_{nt}\right)' EI_n^{CO_2}\, TAX^{CO_2} L_t \frac{1}{2.205\cdot 10^6}\\
&-\sum_{t=1}^{T}\sum_{n\in NG_C^{CO_2}}\left(\dot{q}_{nt}\right)' EI_n^{CO_2}\, TAX^{CO_2}\left(x_{nt}^{CO_2}\right)' L_t \frac{1}{2.205\cdot 10^6}\\
&+\sum_{t=1}^{T}\sum_{n\in NG_C^{CO_2}}\left(\dot{q}_{nt}\right)' EI_n^{CO_2}\, MEA_n\left(x_{nt}^{CO_2}\right)' L_t \frac{1}{2.205\cdot 10^6}\\
&+\sum_{t=1}^{T}\sum_{n\in NG_C^{CO_2}}\left(\dot{q}_{nt}\right)' EI_n^{CO_2}\, TS_n\left(x_{nt}^{CO_2}\right)' L_t \frac{1}{2.205\cdot 10^6}
\end{aligned}
\tag{6.6}
$$

6.2.4 Summary of electricity system simulator modifications

The following modifications are made to the GAMS programs within the electricity system simulator in order to add the generating unit with flexible CO_2 capture. Building upon the electricity system simulator described in Chapter 5:

1. The set $NG_C^{CO_2}$ is defined representing generating *continuous* units with integrated CO_2 capture. A configuration for such a generating unit is defined using the parameters in Table 5.2.

Table 6.3: Performance summary for generating unit with 85% CO_2 capture

Parameter	Units	Value
Minimum heat input to boiler	MW_{th}	141
Maximum heat input to boiler	MW_{th}	1411
Minimum reactive power output	MW_e	-50
Maximum reactive power output	MW_e	230
Minimum up-time	h	24
Minimum down-time	h	48
Cold start heat input	MMBtu	13407
Cold start heat input	MWh_e	3929

2. At Austen, the 376 MW$_e$ generating unit — the one with CO_2 fixed at 85% — is substituted with the 500 MW$_e$ one with flexible CO_2 capture in the set of available units at this bus.

3. In the *market settlement* phase, the marginal cost of generation of generating units with flexible CO_2 capture is computed. For $n \in NG_C^{CO_2}$, the contribution to the objective function is given by:

$$C_{nt}^{VOM} = C_{nt}^{start\text{-}up} + C_{nt}^{fuel} + C_{nt}^{CO_2,start-up} + \left(1 - x_{nt}^{CO_2}\right) C_{nt}^{CO_2,fuel} + C_{nt}^{MEA} + C_{nt}^{TS} \tag{6.7}$$

Taking the partial first-derivative of (6.7) with respect to P_{nt} yields an expression for the marginal generating cost for this unit:

$$\begin{aligned}
\frac{dC_{nt}^{VOM}}{dP_{nt}} &= \frac{dC_{nt}^{fuel}}{dP_{nt}} + \left(1 - x_{nt}^{CO_2}\right) \frac{dC_{nt}^{CO_2,fuel}}{dP_{nt}} + \frac{dC_{nt}^{MEA}}{dP_{nt}} + \frac{dC_{nt}^{TS}}{dP_{nt}} \\
&= FC_n L_t \frac{1}{10^3} \frac{d\dot{q}_{nt}}{dP_{nt}} + \left(1 - x_{nt}^{CO_2}\right) EI_n^{CO_2}\, TAX^{CO_2} L_t \frac{1}{2.205 \cdot 10^6} \frac{d\dot{q}_{nt}}{dP_{nt}} \\
&\quad + EI_n^{CO_2}\, MEA_n x_{nt}^{CO_2} L_t \frac{1}{2.205 \cdot 10^6} \frac{d\dot{q}_{nt}}{dP_{nt}} + EI_n^{CO_2}\, TS_n x_{nt}^{CO_2} L_t \frac{1}{2.205 \cdot 10^6} \frac{d\dot{q}_{nt}}{dP_{nt}} \\
&= \left\{ \frac{FC_n L_t}{10^3} + \left[\left(1 - x_{nt}^{CO_2}\right) TAX^{CO_2} + MEA_n x_{nt}^{CO_2} + TS_n x_{nt}^{CO_2} \right] \frac{EI_n^{CO_2} L_t}{2.205 \cdot 10^6} \right\} \frac{d\dot{q}_{nt}}{dP_{nt}} \\
&= \left\{ \frac{FC_n L_t}{10^3} + \left[TAX^{CO_2} - \left(TAX^{CO_2} - MEA_n - TS_n \right) x_{nt}^{CO_2} \right] \frac{EI_n^{CO_2} L_t}{2.205 \cdot 10^6} \right\} \frac{d\dot{q}_{nt}}{dP_{nt}}
\end{aligned} \tag{6.8}$$

where $\frac{d\dot{q}_{nt}}{dP_{nt}}$ is the Incremental Heat Rate of the generating unit an expression for which is obtained by taking the partial derivative of $dotq$ with respect to P_{nt}.

6.3 Simulation of electricity system with CCS

The first week of operation of the IEEE RTS '96 is simulated. There are two scenarios and, for each scenario, there is one case with CO_2 prices of \$0, \$15, \$40, and \$100/tonne CO_2.

Austen, no capture: The 350 MW$_e$ coal-fired generating unit in the base IEEE RTS '96 is substituted by the nominally 500 MW$_e$ coal-fired unit at Nanticoke upon which the reduced-order model in Section 4.2 is based.

Austen, flexible capture: The 350 MW_e coal-fired generating unit in the base IEEE RTS '96 is substituted by the nominally 500 MW_e coal-fired unit at Nanticoke retrofitted with CO_2 capture upon which the reduced-order model in Section 4.3 is based.

6.4 Results and Discussion

In Chapter 5, the impact of adding CCS to IEEE RTS '96 is presented and discussed. The observations and conclusions noted there with respect to adding a generating unit with *fixed* CO_2 capture to the electricity system also apply for the case where a generating unit with *flexible* CO_2 capture is added to the system. This chapter will focus on differences resulting from fixed versus flexible.

6.4.1 Capacity utilization

Figure 6.3 shows the average total capacity utilization for each type of unit in the IEEE RTS '96 at various carbon prices. The trend observed in the *Austen, flexible capture* scenario is identical to observed in all the others. Briefly, non-emitting sources are fully utilized, coal-fired units see their utilization decrease, and oil-fired units see their utilization increase.

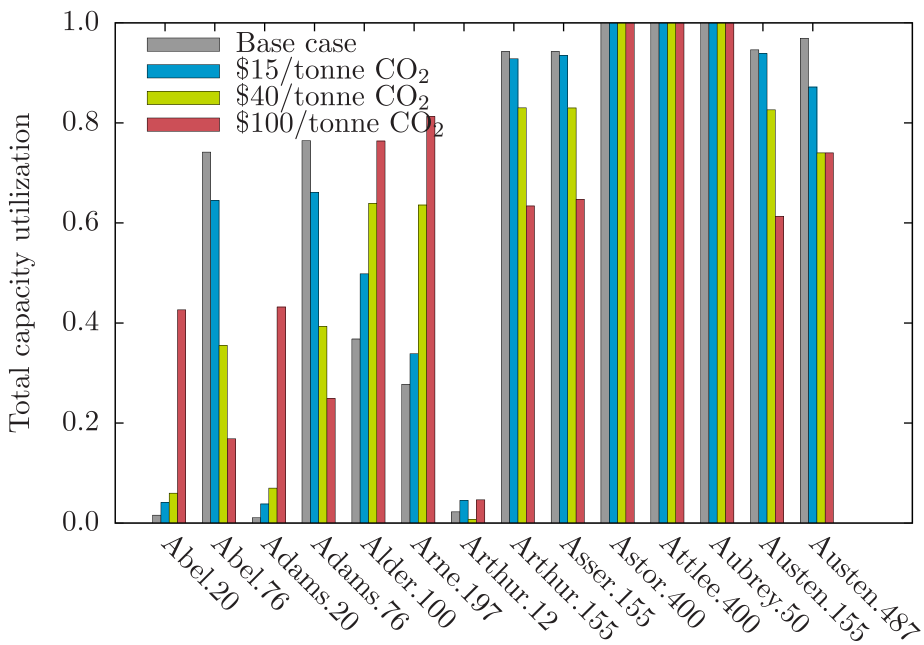

Figure 6.3: Total capacity utilization for different generating units at various CO_2 prices

Figure 6.4 shows the total capacity utilization of the 487 MW_e generating unit with flexible capture over the time period of interest, providing greater detail about how the utilization changes as a function of time. It was already mentioned that the utilization decreases with increasing carbon price and here it is observed that, at \$40 and \$100/tonne CO_2, the capacity utilization has flatligned at 360.4 MW_e.

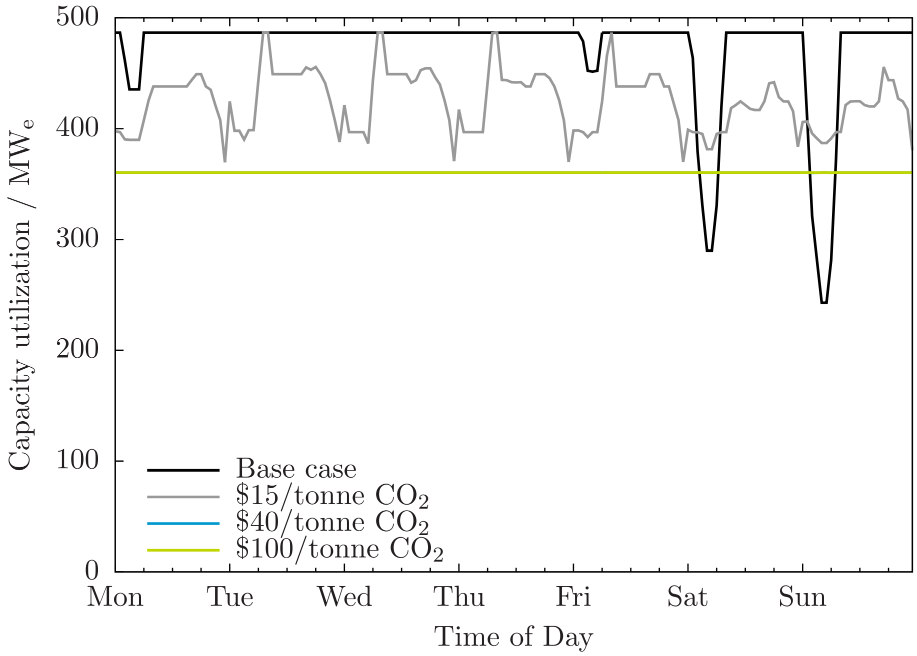

Figure 6.4: Capacity utilization for 487MW_e unit with flexible CO_2 capture at various carbon prices

Figure 6.5 compares the capacity utilization of the nominally 500 MW_e units at Austen from the *no capture*, *85% capture*, and *flexible capture* scenarios. The unit with flexible CO_2 capture has more of its capacity accepted by the system operator than the unit with fixed CO_2 capture. The higher utilization is especially pronounced at lower carbon prices becoming insignificant at \$100/tonne CO_2.

Figure 6.6 compares the quantity of power from each of the nominally 500 MW_e untis at Austen from the *no capture*, *85% capture*, and *flexible capture* scenarios. Not surprising that the flexible unit generates power than the fixed capture unit in the \$0/tonne CO_2 given that, in this case, the unit with fixed capture is off more than it is on. It is interesting that in the \$40/tonne CO_2 case (see Figure 6.6b) and the \$100/tonne CO_2 case, the flexible unit produces significantly less power than the unit with fixed capture. The unit with flexible capture is able to sell comparable amounts of its capacity to that of the unit with fixed capture and accomplishes this while generating substantially less power.

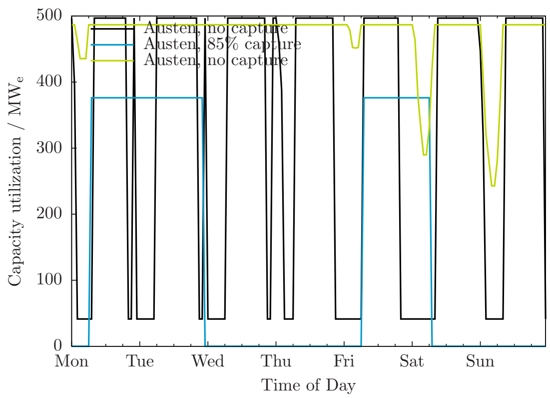

(a) \$0/tonne CO_2

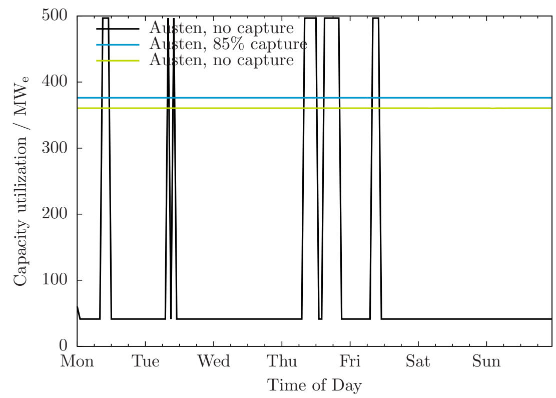

(b) \$40/tonne CO_2

Figure 6.5: Capacity utilization for units at Austen for period of interest

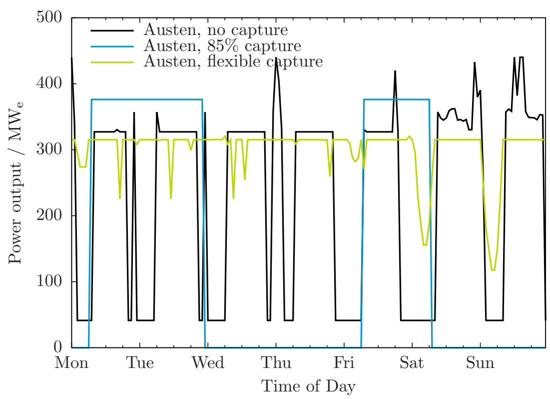

(a) \$0/tonne CO_2

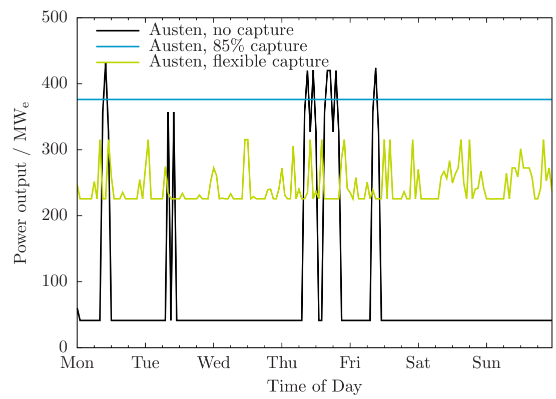

(b) \$40/tonne CO_2

Figure 6.6: Power output for units at Austen for period of interest

The unit wtih flexible CO_2 capture bids an additional $487 - 367 = 120$ MW_e of power into the market so it is perhaps not suprising that it, at times, has a lower capacity utilization than the generating unit with flexible capture on an absolute basis. Figure 6.7 compares the relative capacity utilization of the units in the *flexible capture* scenario to each other and also to the nominally 500 MW_e untis at Austen from the *no capture* and *85% capture* scenarios.

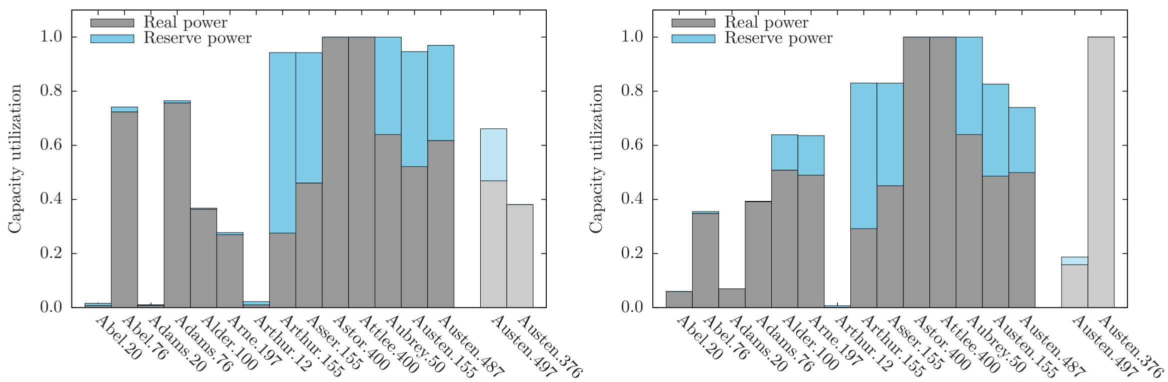

(a) \$0/tonne CO_2 (b) \$40/tonne CO_2

Figure 6.7: Average capacity utilization of units in IEEE RTS '96 with and w/o CCS installed at Austen

6.4.2 GHG emissions

Figure 6.8 shows the difference in the average hourly GHG emssions between the *flexible capture* scenario and each of the *no capture* and *fixed capture* scenarios for the complete set of carbon prices examined. At a CO_2 price of \$0/tonne, emissions are 110 tonne CO_2/h lower in the *flexible capture* scenario than in the *fixed capture* scenario. Recall that the capacity factor of the generating unit with capture was 0.38 in the *fixed capture* scenario versus 0.62 for the unit with capture in the *flexible capture* scenario. The lower emissions in the *flexible capture* scenario is due to the difference in utilization of these very low intensity sources of power.

At CO_2 prices of \$40 and \$100/tonne, CO_2 emissions in the *flexible capture* scenario are 50 tonne/h higher than in the *fixed capture* scenario. The explanation again goes back to differences in capacity factor. At these carbon prices, the capacity factor is unity for the generating unit with CO_2 capture in the *fixed capture* scenario and half that for the unit with capture in the *flexible capture* scenario. Note that, for all the carbon prices considered, the emissions in the *flexible capture* scenario are lower than when no CCS is present.

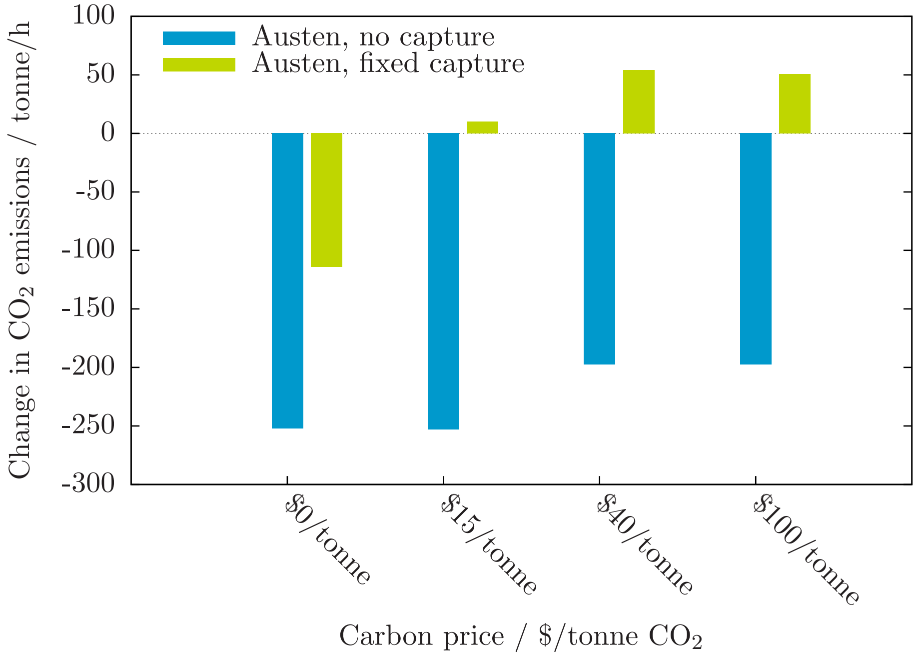

Figure 6.8: Change in CO_2 emissions compared to case with flexible CO_2 capture at various carbon prices

6.4.3 Cost of electricity and electricity price

Figure 6.9 shows the cost of generation and the electricity price for the *flexible capture*, *fixed capture*, and *no capture* scenarios with a carbon price of \$40/tonne CO_2. There is not much difference in the cost of generation or the electricity price between fixed and flexible CO_2 capture. A similar observation is made from Figure 6.10 which shows the difference in the average cost of generation and electricity price between the *flexible capture* scenario and each of the *no capture* and *fixed capture* scenarios.

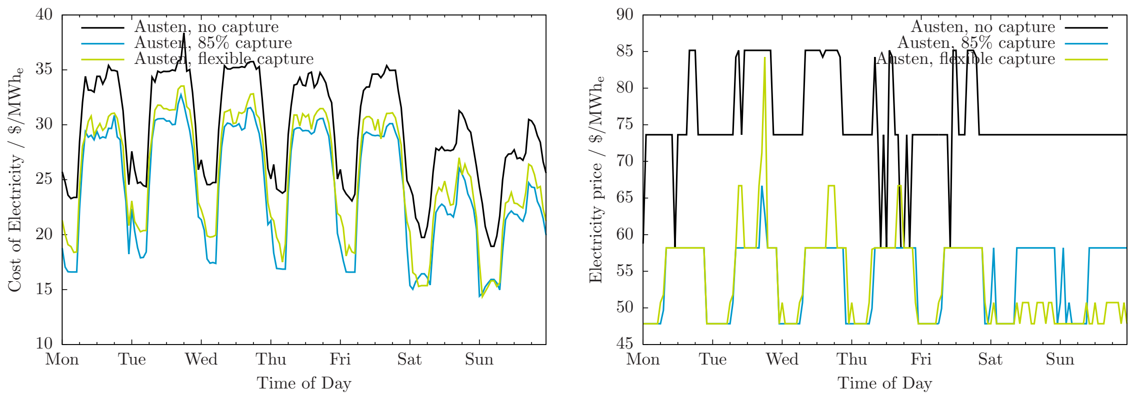

(a) Cost of generation

(b) Electricity price

Figure 6.9: Cost of generation and electricity price for different capture scenarios for period of interest at \$40/tonne CO_2

6.4.4 Net energy benefit

As is observed in all scenarios to-date, the more stringent the GHG regulation, the greater the aggregate energy benefit. This is shown explicitly for the *flexible capture* scenario in Figure 6.11. Also, like in the all scenarios to-date, the net benefits, if any, are not distributed equally amongst the different types of generating units. Figure 6.12 shows how the net energy benefits of the generating units in the *flexible capture* scenario are impacted by GHG regulation. And, like in the *fixed capture*, all of the unit types see a reduction in net energy benefit except for the unit with CCS.

Figure 6.13 compares the net energy benefit for the nominally 500 MW_e units at Austen from the *no capture*, *85% capture*, and *flexible capture* scenarios for carbon prices of \$0, \$15, \$40, and \$100/tonne CO_2. In all cases, the net energy benefit of the generating unit with flexble capture performs better from an economic perspective.

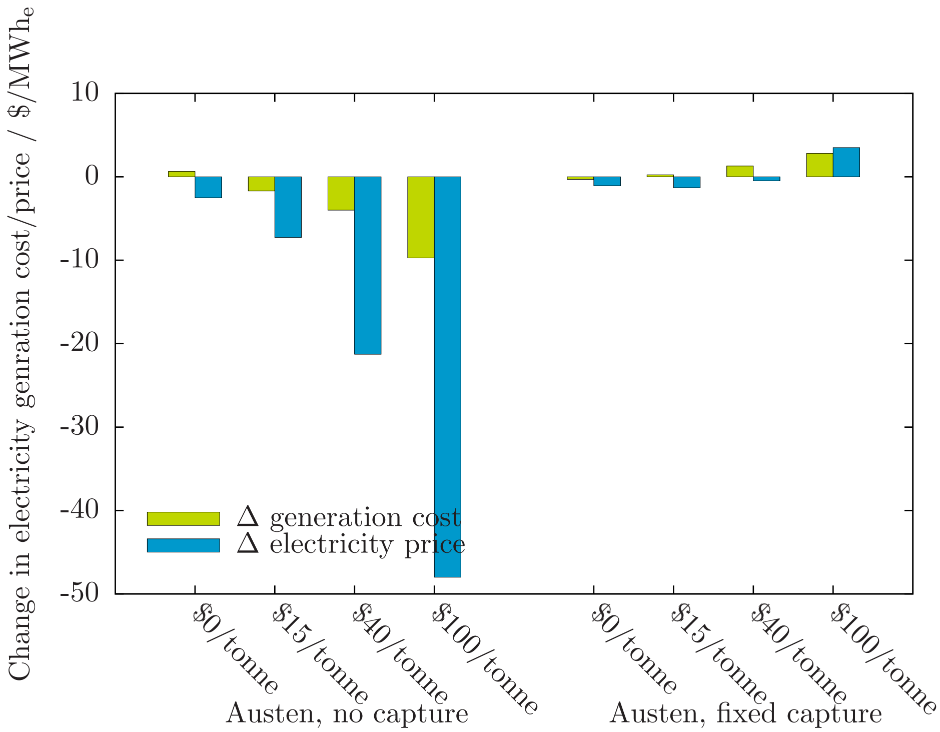

Figure 6.10: Difference in cost of generation and electricity price with no capture and fixed capture scenarios

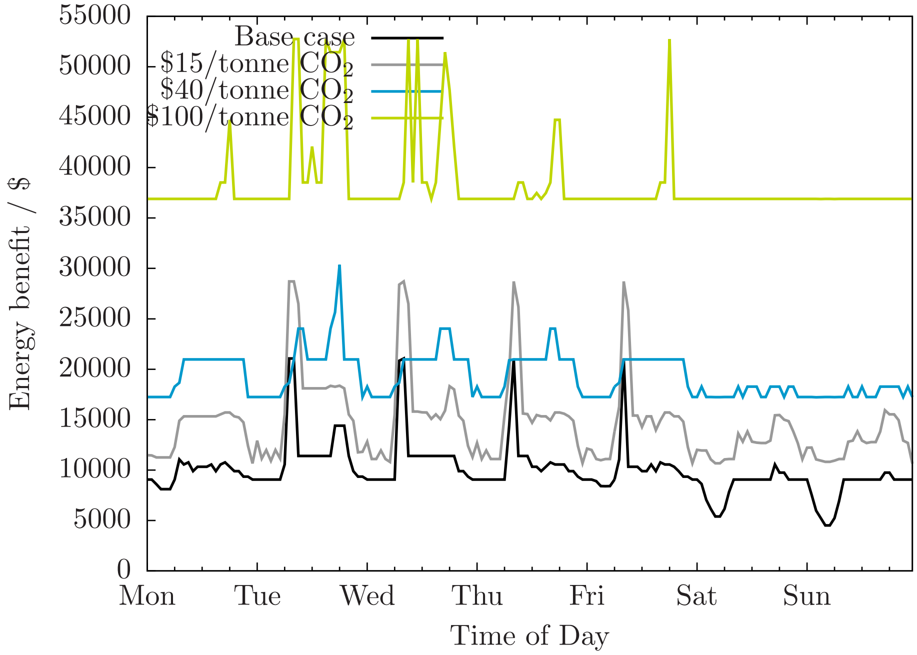

Figure 6.11: Energy benefit for 487 MW_e unit with flexible CO_2 capture at various carbon prices

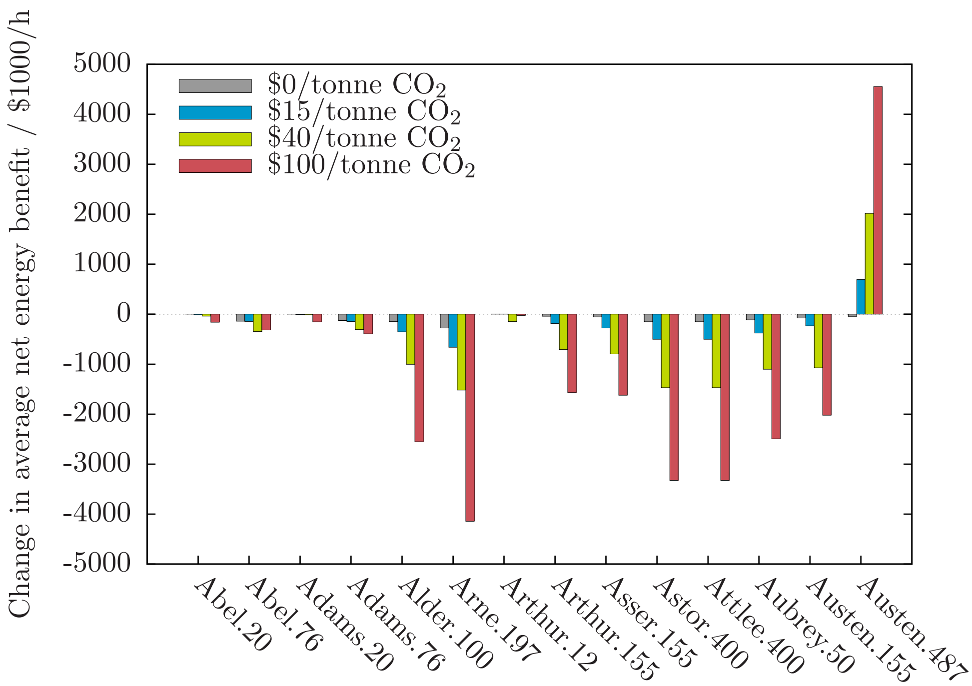

Figure 6.12: Change in net energy benefit different types of generating units at various CO_2 prices

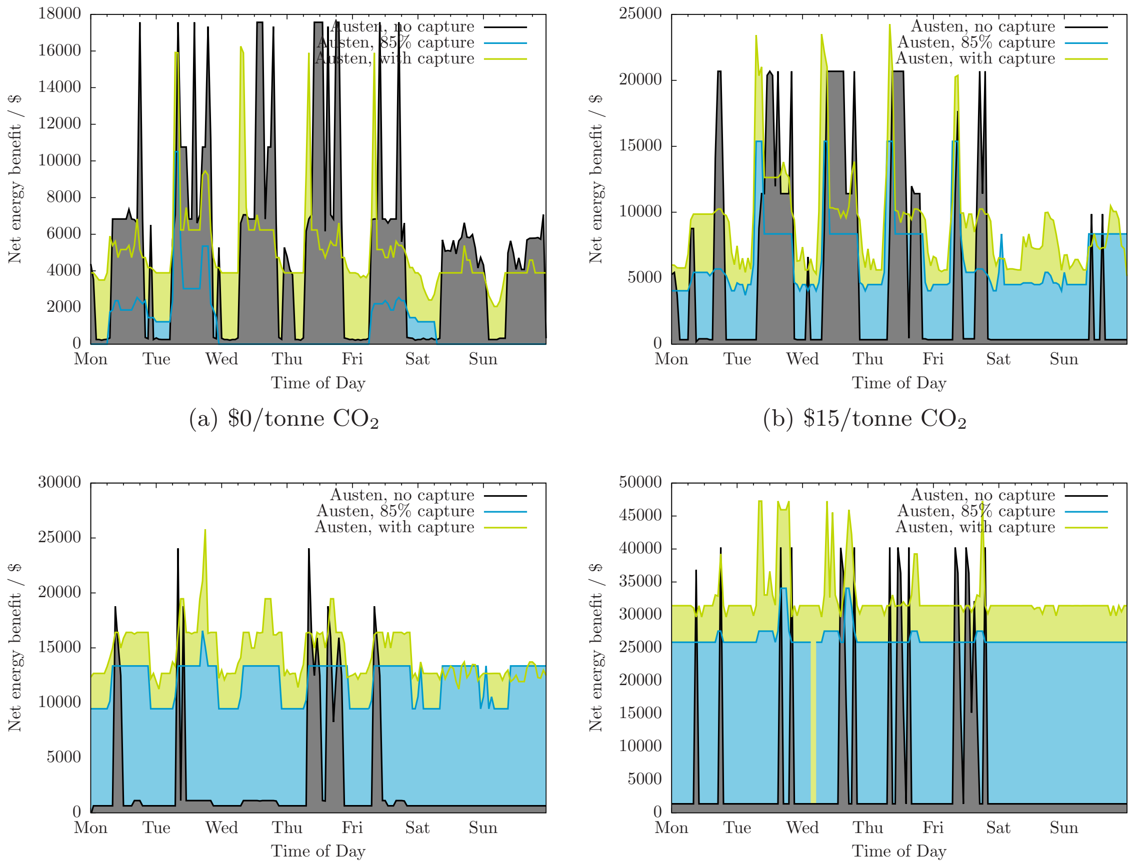

(a) \$0/tonne CO_2

(b) \$15/tonne CO_2

(c) \$40/tonne CO_2

(d) \$100/tonne CO_2

Figure 6.13: Net energy benefit for units at Austen

6.4.5 Transmission losses

Figure 5.28 summarizes the transission losses that are observed in the system for the period of interest. The losses are comparable to what is observed for the *fixed capture* and other scenarios.

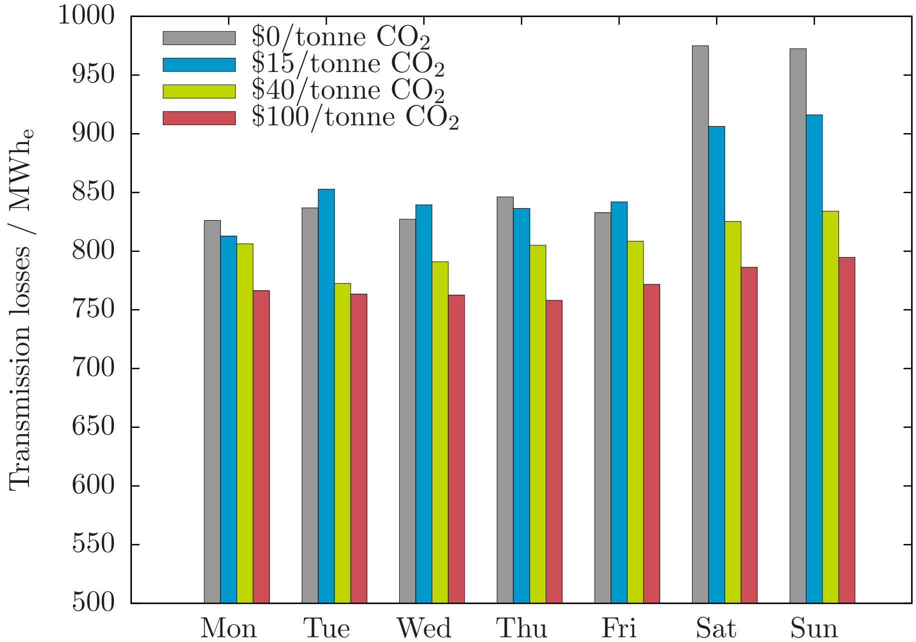

Figure 6.14: Daily aggregate transmission losses for IEEE RTS '96 with capture at various CO_2 prices

6.4.6 Congestion

It was observed in the *fixed capture* scenario that there is never a time period in which the power flow exceed the maximum continuous rating of a transmission line (see Figure 5.29). This is not the case in the *flexible capture* scenario where, as shown in Figure 6.15 for the \$15/tonne CO_2 case, the power flow along the Alder–Alger line does exceed the Maximum Continuous Rating. Note that the exceedance is still within the long-time emergency (24 hour) rating of the power line so there may not be a cause for immediate concern.

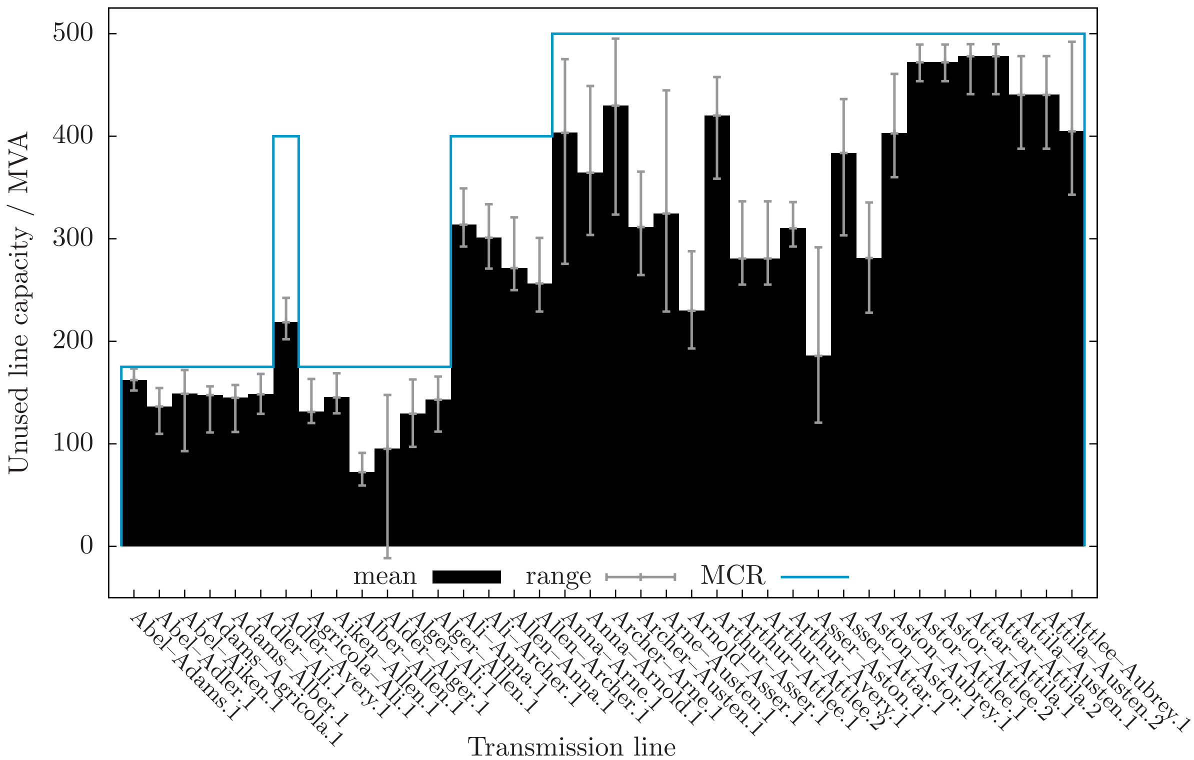

Figure 6.15: Mean, maximum, and minimum power flows along each transmission line for IEEE RTS '96 with capture: \$15/tonne CO_2

6.5 Conclusion

From the perspective of electricity system as a whole, flexible versus fixed capture has, at best, a moderate impact:

- GHG emissions are a bit higher,
- the average cost of generation and electricity prices are, especially on a relative basis, unchanged, and
- transmission losses are comparable.

That being said, the advantages noted in Chapter 5 related to the benefits accrued by the system with the presence of fixed CO_2 capture apply to flexible CO_2 capture as well.

From the perspective of a generator, though, flexible CO_2 capture is a compelling choice. Table 6.4 summarizes the improvement in net energy benefit realized by having generating unit with flexible CO_2 capture relative to one without capture or with capture fixed at 85% for carbon prices of \$0, \$15, \$40, and \$100/tonne CO_2. There appears to be significant economic benefit to pursuing CO_2 capture processes that are flexible and studies that do not include flexible operation of the CO_2 capture process within the scope of the analysis could be significantly underestimting the benefits of this technology as a GHG mitigation strategy.

Table 6.4: Comparison of net energy benefits for 500 MW_e units at Austen

Carbon Price	Improvement in net energy benefit vs *no capture* %	vs *fixed* capture %
\$0/tonne CO_2	-5	444
\$15/tonne CO_2	82	41
\$40/tonne CO_2	490	21
\$100/tonne CO_2	490	25

The benefits to a generating unit from having a flexible CCS process are due to the unit's ability to quickly increase power output by reducing the fraction of CO_2 that is recovered. It is proposed that the dynamics of a CO_2 capture process would be comparable to FGD (Flue Gas Desulphurization) and that the dynamic performance of an FGD would lend itself to a quick turndown.[10] Quickly reducing the steam extracted from the IP/LP crossover would not adversely impact the operation of the steam cycle and any concerns would be related to the controllability of the CO_2 capture process.

Chapter 7

Conclusions and Future Work

7.1 Conclusions

7.1.1 Utility of explicitly considering the operation of electricity system

The thesis is that understanding the effectiveness of GHG mitigation strategies on electricity systems requires detailed consideration of the operation of the electricity system in question. The premise for this is two-fold. Firstly, in cases where the detailed operation of the electricity system is not within the scope of an investigation, one must estimate key parameters (*e.g.*, capacity factor, unit heat rate) and this is difficult to do credibly. Secondly, without considering the detailed operation of the electricity system, information critical to the efficient design of GHG regulation and the electricity systems themselves is not available (*e.g.*, net energy benefit, congestion). To assess the validity of this thesis, an electricity system simulator is developed and implemented in GAMS for the IEEE RTS '96 and is used to assess the effectiveness of different GHG mitigation strategies.

A key enabling element that sets this work apart from previous published studies is the development of a short-term generation scheduling model containing a detailed representation of a generating unit with a flexible CO_2 capture process and its implementation in GAMS.

Essential to understanding the performance of an electricity system under different scenarios is being able to predict the dispatch of the generating units. Once the power output of the units in each time period is determined, the other parameters of interest fall out: capacity factor, unit heat rate, CO_2 emissions rate, electricity price, whether or not there is congestion, *etc.*. In the results from the electricity system simulator, significant variation is observed in unit dispatch from time period to time period, from day to day, from weekday to weekend, for different stringency of CO_2 regulation, and for different configurations of the electricity system (*i.e.*, with or without CO_2 capture).

Consider Table 7.1 which summarizes the capacity factor for two different types of units. It is expected that, in the face of increasing stringency of GHG regulation, units with higher GHG intensity would see their capacity factor increase and *vice versa*:

Table 7.1: Change in capacity factor in different scenarios

Scenario	Capacity factor			
	\$0/tonne CO_2	\$15/tonne CO_2	\$40/tonne CO_2	\$100/tonne CO_2
Load balancing				
Austen, 350/500 MW_e	0.83	0.81	0.63	0.40
Arne, 197 MW_e	0.28	0.33	0.53	0.73
Fixed CO_2 capture				
Austen, 350/500 MW_e	0.38	1.00	1.00	1.00
Arne, 197 MW_e	0.42	0.29	0.44	0.55

- In the load balancing scenario, this expectation is realized for the 197 MW_e units at Arne and the 350 MW_e unit at Austen. However, in the fixed CO_2 capture scenario, the capacity factor of the 197 MW_e units at Arne decreases from 0.42 to 0.29 as the CO_2 price increases from \$0/tonne CO_2 to \$15/tonne CO_2.

- In both scenarios shown in Table 7.1, the capacity factor of the 197 MW_e units at Arne increases as CO_2 price increases from \$15/tonne CO_2 through to \$100/tonne CO_2. However, the increase in the load balancing scenario is more pronounced.

The assumption that the capacity factor of generating units with GHG regulation is the same as the capacity factor of units pre-regulation would be invalid for the IEEE RTS '96. And, shortcut methods for calculating dispatch may be inadequate; it is shown in Chapter 2 and again in Chapter 5 that the dispatch order of units does not follow a strict merit-order approach. While it is straightforward to explain in hindsight why, for example, the capacity factor of this unit goes from 0.42 (\$0/tonne CO_2, fixed CO_2 capture) to 0.29 (\$15/tonne CO_2, fixed CO_2 capture) or why the capacity factor of the 350 MW_e unit at Austen goes from 0.83 (\$0/tonne CO_2, load balancing) to 0.38 (\$0/tonne CO_2, fixed CO_2 capture), predicting these changes in advance would not have been. These findings support the thesis that detailed consideration of the operation of the electricity system is important.

Beyond just capacity factor, the approach used in this work:

- Reduces the number of parameter values that need to be estimated.

- Provides outputs that are meaningful to a broader range of stakeholders.

- Allows technical and non-technical mitigation actions to be directly compared.

- Allows one to consider the difference that the location makes.

7.1.2 Effectiveness of CCS at mitigating GHG emissions

Some mitigation of GHG emissions is possible with no incremental capital investment. For example, a decrease in CO_2 emissions of 1.5% is observed in the load balancing scenario for the case of a \$15/tonne CO_2 carbon price. With CCS added to the system, the overall emissions from the system is reduced an additional 26.4% at the same carbon price of \$15/tonne CO_2. It is not remarkable that a system with CCS has lower emissions than a system without; it may be surprising, though, that installing CCS on 27% of the coal capacity and 10% of the total capacity could enable the mitigation of such a relatively large proportion of the system's emissions.

It is also interesting to contrast the economic impact of CCS on the system performance, comparing the scenarios with and without CO_2 capture installed on the 350 MW_e unit at Austen. With CCS in the system, the average cost of generation and electricity price are lower than they would otherwise been. It is also observed that, increasing stringency of carbon regulation reduces the net energy benefit of high-intensity coal-fired generating units except when fitted with CO_2 capture; the coal-fired generating unit with CO_2 capture saw its profitability grow as carbon prices increased.

It appears, then, that in addition to confirming the utility of CCS in reducing GHG emissions, this work indicates that there are significant economic benefits to deploying CCS and that these economic benefits increase with the stringency of GHG regulation.

7.2 Future Work

7.2.1 Applying approach to current electricity system

The IEEE RTS '96 served as a basis for the development of the electricity system simulator and for the assessment of the different CO_2 mitigation strategies considered in this work. As every electricity system is unique and the economic input data used in this study are dated, it would be interesting to apply to approach to a current electricity system.

7.2.2 Applying approach to current electricity system

One of the objectives of the work is to assess the potential advantage conferred by a generating unit with flexible CCS as opposed to one where the power plant output and CO_2 recovery rate are constant. And, it was demonstrated that flexibiltiy has the potential to confer a significant economic advantage to the generating unit at which it is employed. The benefits of flexibility hinge, though, on the generating unit being able to rapidly turndown the rate of CO_2 capture, thereby quickly increasing the unit's net power output. A next step is to confirm that the CO_2 capture process is capable of the requisite dynamic performance to capture the benefits.

7.2.3 Coupling of short- and long-run models

Given a set of electricity systems, the approach described in this work could be used to compare and contrast their respective performance in the *short-run*: the time-scale in which structural changes to the electricity system are not possible. A major limitation of this approach is that the candidate electricity systems need to be identified exogenously as changes of a capital nature, even those that could be implemented in relatively short-order, are out of scope. For example, adding CO_2 capture to the 350 MW_e unit at Austen seems reasonable but it is not established that this is the optimal deployment of CCS in the system.

The medium- to long-term electricity system planning approach [47, 25, 21] assesses the performance of the mitigation action in the *long-run* and could be used to synthesize candidate electricity systems. As these models consider electricity system operation in a rudimentary way, they can propose electricity systems that are suboptimal or, in the limit, inoperable.

There is significant scope for future work to couple the short- and long-run approaches to yield a framework that would propose an optimal investment strategy for an electricity system with environmental constraints where the electricity system is, at all times, robust to supply/demand, technical constraints, and standards for reliability. There would be a major computational challenge to overcome. While straightforward to directly couple the electricity system simulator and, for example, the electricity system planning model of Hashim [21], a GAMS implementation of this MINLP model would not be soluble on commodity computer hardware.

7.2.4 Assessing different GHG regulatory frameworks

Imposing a price on CO_2 emissions is a simple method of regulating GHG emissions. There are other approaches that have gained favour notably the cap-and-trade system that is implemented in the European Union. Incorporating the regulatory approach of limiting GHG emissions would extend the utility of the electricity system simulator and also introduce an interesting challenge.

In the deregulated electricity market after which the electricity system simulator is based, to a first approximation, the system operator dispatches generating units based upon the marginal cost of producing each quantity of power. In the case where GHGs are regulated via a price on carbon, the change in marginal cost of generation is built into the bid price. No changes to the structure of the underlying MINLP models is required.

In a electricity system simulator where GHG emissions are capped, a different approach for incorporating GHG regulation into the unit dispatch would be necessary. Potential options include:

- The development of an appropriate bid strategy for the affected generating units.

Such a strategy would need to consider the varying and uncertain requirement to constrain GHG emissions in any future time period. If a unit's bid price is too low, it may be dispatched to a greater extent then desired and, hence, cause the emissions cap to be exceeded. If a unit's bid price is too high, it will unnecessarily restrict its participation in the market.

- A rethink of the manner in which the electricity system operator dispatches units.

  At present, each bid that generators provide to the electricity system operator contains two pieces of information: the quantity of power being offered and the associated price. This could be extended such that the bid information also contained the emissions associated with the quantity of power being offered. The system operator would be responsible for ensuring that emissions caps were respected and would select bids accordingly.

Appendix A

Bid sorting for maximizing social welfare

It was stated in Section 1.3.4 that, as a matter of course, the system operator in a deregulated market sorts the received supply and demand bids prior to performing dispatch. Sorting the supply bids in order of increasing price in the manner shown in Figure 1.11 creates an aggregate supply curve for the market. Similarly, an aggregate demand curve is created by sorting the demand bids in decreasing order of price. In a perfectly behaving market, the intersection of the supply and demand curves is the equilibrium point for the market: there is no more incentive for the additional supply or demand of the commodity. Using the equilibrium price, the maximum social welfare is experienced.

In this construction, from the system operators stand, the key to maximizing social welfare is in the sorting of the bids. By illustration, Figures A.1 and A.2 depict situations in which the sort order is for demand bids is not strictly correct. In Figure A.1, the position of is swapped; in Figure A.2, it is Generator and Generator whose rank is changed. Visual comparison with Figure 1.11 easily shows that the social welfare is less in each of these two new cases.

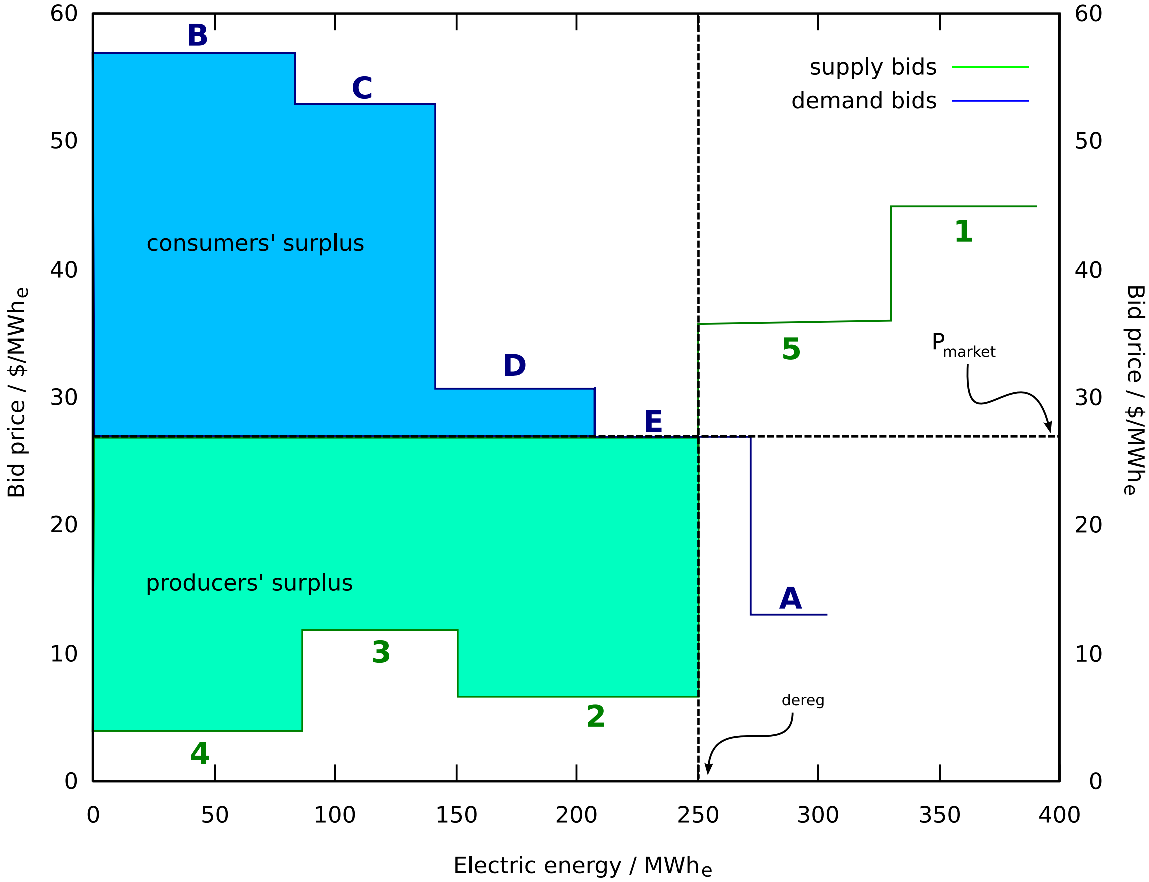

Figure A.1: Supply-demand curve for deregulated electricity market: Generator 2 and 3 bids are swapped relative to properly-sorted order

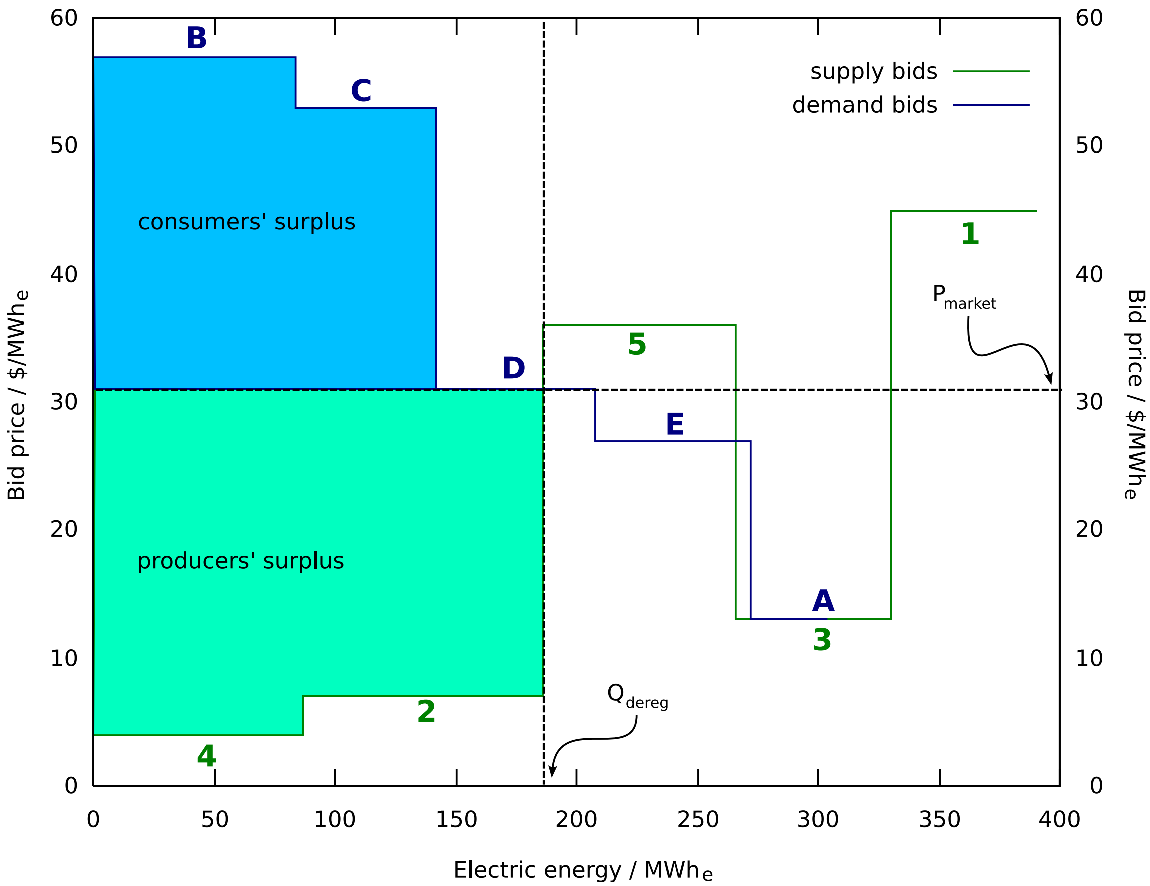

Figure A.2: Supply-demand curve for deregulated electricity market: Generator 4 and 5 bids are swapped relative to properly-sorted order

Appendix B

Calculation of demand in each time period

Table B.1 contains the load factors for each hour, day, and for the week of interest. The demand at bus k in time period t, P^D_{kt}, is given by:

$$P^D_{kt} = P^{max}_k \cdot x^w_t \cdot x^d_t \cdot x^h_t \tag{B.1}$$

Sample calculation Demand at Alder from 9:00 a.m. to 10:00 a.m. Saturday morning:

$$\begin{aligned} P^D_{kt} &= P^{max}_k \cdot x^w_t \cdot x^d_t \cdot x^h_t \\ &= (137.5\,\mathsf{MW_e}) \cdot (0.862) \cdot (0.77) \cdot (0.88) \\ &= 80.3\,\mathsf{MW_e} \end{aligned}$$

Table B.1: Selected demand factors for IEEE RTS '96

Week		Day		Hour		
				Time	Weekday	Weekend
1	0.862	Mon	0.93	00:00	0.67	0.78
		Tue	1.00	01:00	0.63	0.72
		Wed	0.98	02:00	0.60	0.68
		Thu	0.96	03:00	0.59	0.66
		Fri	0.94	04:00	0.59	0.64
		Sat	0.77	05:00	0.59	0.64
		Sun	0.75	06:00	0.74	0.66
				07:00	0.86	0.70
				08:00	0.95	0.80
				09:00	0.96	0.88
				10:00	0.96	0.90
				11:00	0.95	0.91
				12:00	0.95	0.90
				13:00	0.95	0.88
				14:00	0.93	0.87
				15:00	0.94	0.87
				16:00	0.99	0.91
				17:00	1.00	1.00
				18:00	1.00	0.99
				19:00	0.96	0.97
				20:00	0.91	0.94
				21:00	0.83	0.92
				22:00	0.73	0.87
				23:00	0.63	0.81

Appendix C

IEEE Reliability Test System 1996 unit parameters

Table C.1: IEEE RTS '96 fuel costs

Fuel	Cost \$/MMBtu
Nuclear	0.60
Coal	1.20
#2 Fuel Oil	3.00
#6 Fuel Oil	2.30

Table C.2: IEEE RTS '96 net plant heat rates

Fuel	Capacity MW_e	Net plant heat rate / Btu/kWh			
		Bid #1	Bid #2	Bid #3	Bid #4
#6 Fuel Oil	12	16017	12500	11900	12000
#2 Fuel Oil	20	15063	15000	14500	14499
Coal	76	17107	12637	11900	12000
#6 Fuel Oil	100	12999	10700	10087	10000
Coal	155	11244	10053	9718	9600
#6 Fuel Oil	197	10750	9850	9644	9600
Coal	350	10200	9600	9500	9500
Nuclear	400	12751	10825	10170	10000

Table C.3: IEEE RTS '96 CO_2 emissions intensity

Fuel	Emissions
	lb CO_2/MMBtu
Nuclear	0
Coal	210
Fuel Oil #2	160
Fuel Oil #6	170

Table C.4: IEEE RTS '96 incremental heat rates

Fuel	Capacity	Incremental heat rate /			
	MW_e	Btu/kWh			
		Bid #1	Bid #2	Bid #3	Bid #4
#6 Fuel Oil	12	10179	10330	11668	13219
#2 Fuel Oil	20	9859	10139	14272	14427
Coal	76	9548	9966	11576	13311
#6 Fuel Oil	100	8089	8708	9420	9877
Coal	155	8265	8541	8900	9381
#6 Fuel Oil	197	8348	8833	9225	9620
Coal	350	8402	8896	9244	9768
Nuclear	400	8848	8965	9210	9438

Table C.5: IEEE RTS '96 cold start unit heat input

Fuel	Capacity	Heat input
	MW_e	MMBtu
#6 Fuel Oil	12	68
#2 Fuel Oil	20	5
Coal	76	596
#6 Fuel Oil	100	566
Coal	155	953
#6 Fuel Oil	197	775
Coal	350	4468
Nuclear	400	0

Table C.6: Generator ramp rates reported in IEEE RTS 1996

Type	Size	Ramp rate		
	MW_e	MW_e/min	MW_e/h	%
Oil/Steam	12	1	60	8.3
Oil/CT	20	3	180	15.0
Hydro	50	∞	∞	∞
Coal/Steam	75	2	120	2.7
Oil/Steam	100	7	420	7.0
Coal/Steam	155	3	180	1.9
Oil/Steam	197	3	180	1.5
Coal/Steam	350	4	240	1.1
Nuclear	400	20	1200	5.0

Table C.7: Minimum generator up- and downtimes

Type	Size	τ^{on}	τ^{off}
	MW_e	h	h
Oil/Steam	12	4	2
Oil/CT	20	1	1
Hydro	50	0	0
Coal/Steam	76	8	4
Oil/Steam	100	8	8
Coal/Steam	155	8	8
Oil/Steam	197	12	10
Coal/Steam	350	24	48
Nuclear	400	1	1

Appendix D

Exact linearization of non-linear term

Consider a constraint of the form:

$$mx \leq b \tag{D.1}$$

where x is a continuous variable and m is a binary variable. The following procedure can be used to eactly linearize this constraint:

1. Define the continuous variable χ and substitute the non-linear term mx with it in the model:
$$\chi \leq b \tag{D.2}$$
2. Define a constraint limiting the maximum value of χ:
$$\chi \leq x \tag{D.3}$$
3. Define the constant M^{χ} such that $M \geq \max(x)$.
4. Define constraints limiting χ in terms of M^{χ}.
$$x - M^{\chi}(1-m) \leq \chi \leq M^{\chi}m \tag{D.4}$$

The complete set of contraints are:

$$\chi \leq x \tag{D.5}$$
$$x - M^{\chi}(1-m) \leq \chi \tag{D.6}$$
$$\chi \geq M^{\chi}m \tag{D.7}$$

Consider the signficance of the constraints for the possible values of m:

1. $m = 0$:

$$\begin{aligned} \chi &\leq x \\ \chi &\geq x - M \\ \chi &\leq 0 \end{aligned}$$

   By definition, $M \geq x$. Therefore, the last constraint must be active in the optimal solution and, hence, $\chi = 0$.

2. $m = 1$:

$$\begin{aligned} \chi &\leq x \\ \chi &\geq x \\ \chi &\leq M \end{aligned}$$

   By definition, $M \geq x$. Therefore, the first and second constraints must be active in the optimal solution and, hence, $\chi = x$.

Appendix E

Electricity system model source code

E.1 GAMS implementation of Ward and Hale loadflow problem

```
SET k busses (includes neutral bus) /1*7/;
ALIAS(k,i,m);

SET kVR(k) busses with voltage regulation /1,2/;

SET j(k,m) branches
    / 1.(4,6,7), (4,6,7).1
      2.(3,5),   (3,5).2
      3.4,       4.3
      4.(6,7),   (6,7).4
      5.6,       6.5
      6.7,       7.6
      /;

SET jTR(k,m) branches with off-nominal transformer ratios
    / 6.5
      4.3
      /;

SCALAR Pi / 3.14 /;

PARAMETER VTR(k,m) off-nominal transformer ratios
          / 6.5 1.0250
            4.3 1.1000
            /;

PARAMETER Vset(kVR) voltage set-point at busses with regulation
```

```
          / 1 1.05
            2 1.10
            /;

PARAMETER R(k,m) "Transmission line resistance, pu"
          / (1.4, 4.1) 0.080
            (1.6, 6.1) 0.123
            (1.7, 7.1) 0.000
            (2.3, 3.2) 0.723
            (2.5, 5.2) 0.282
            (3.4, 4.3) 0.000
            (4.6, 6.4) 0.097
            (4.7, 7.4) 0.000
            (5.6, 6.5) 0.000
            (6.7, 7.6) 0.000
            /;

PARAMETERS X(k,m) "Transmission line reactance, pu"
          / (1.4, 4.1)   0.370
            (1.6, 6.1)   0.518
            (1.7, 7.1) -29.500
            (2.3, 3.2)   1.050
            (2.5, 5.2)   0.640
            (3.4, 4.3)   0.133
            (4.6, 6.4)   0.407
            (4.7, 7.4) -34.100
            (5.6, 6.5)   0.300
            (6.7, 7.6) -28.500
            /;

PARAMETER G(k,m) "conductance of branch k-m";
PARAMETER B(k,m) "susceptance of branches k-m";
PARAMETER YG(k,m) "real component branch k-m admittances";
PARAMETER YB(k,m) "imaginary component branch k-m admittances";

* Calculate branch conductances
G(j) = R(j) / (power(R(j),2) + power(X(j),2));

* Calculate branch susceptances
B(j) = -X(j) / (power(R(j),2) + power(X(j),2));

* Calculate self-admittances
YG(k,k)$(ord(k) lt card(k)) = sum(i, G(i,k));
YB(k,k)$(ord(k) lt card(k)) = sum(i, B(i,k));

* Make adjustments to self-admittances for off-nominal transformer ratios
loop(jTR(k,m),
        YG(k,k) = YG(k,k) + (power(VTR(jTR), 2) - 1) * G(jTR);
        YB(k,k) = YB(k,k) + (power(VTR(jTR), 2) - 1) * B(jTR);
);
```

```
* Calculate mutual-admittances
YG(j(k,m))$(ord(k) lt card(k) and ord(m) lt card(m)) = -G(j);
YB(j(k,m))$(ord(k) lt card(k) and ord(m) lt card(m)) = -B(j);

* Make adjustments to mutual-admittances for off-nominal transformer ratios
loop(jTR(k,m),
        YG(jTR) = YG(jTR) - (VTR(jTR) - 1) * G(jTR);
        YG(m,k) = YG(m,k) - (VTR(jTR) - 1) * G(m,k);
        YB(jTR) = YB(jTR) - (VTR(jTR) - 1) * B(jTR);
        YB(m,k) = YB(m,k) - (VTR(jTR) - 1) * B(m,k);
);

VARIABLES
        z       "objective function"
        Ps(k)   "net real power injected at the kth bus, MW"
        Qs(k)   "net reactive power injected at the kth bus, MVar"
        Ia(k)   "real component of current"
        Ib(k)   "imaginary component of current"
        Ve(k)   "real component of voltage"
        Vf(k)   "imaginary component of voltage"
;

POSITIVE VARIABLES
        Vmag(k) "voltage magnitude"
;

EQUATIONS
        obj      "objective function defined"
        IaDef(k) "real component of current definition"
        IbDef(k) "imaginary component of current definition"
        PDef(k)  "real power definition"
        QDef(k)  "reactive power definition"
        VDef(k)  "voltage magnitude definition"
;

obj..      z =E= sum(k$(ord(k) lt card(k)), power((Vmag(k) - 1), 2));
IaDef(k)$(ord(k) lt card(k)).. Ia(k) =E= sum(m, YG(k,m)*Ve(m) - YB(k,m)*Vf(m));
IbDef(k)$(ord(k) lt card(k)).. Ib(k) =E= sum(m, YG(k,m)*Vf(m) + YB(k,m)*Ve(m));
PDef(k)$(ord(k) lt card(k))..  Ps(k) =E= Ia(k)*Ve(k) + Ib(k)*Vf(k);
QDef(k)$(ord(k) lt card(k))..  Qs(k) =E= Ia(k)*Vf(k) - Ib(k)*Ve(k);
VDef(k)$(ord(k) lt card(k))..  power(Vmag(k), 2) =E= power(Ve(k), 2)
                               + power(Vf(k), 2);

* fix voltage magnitude at busses with regulation
Vmag.fx(kVR) = Vset(kVR);

* fix phase angle at slack bus to zero
Vf.fx("1") = 0;
```

```
* specify net real power availability
Ps.fx("2") =  0.50;
Ps.fx("3") = -0.55;
Ps.fx("4") =  0.00;
Ps.fx("5") = -0.30;
Ps.fx("6") = -0.50;

* specify net reactive power availability
Qs.fx("3") = -0.13;
Qs.fx("4") =  0.00;
Qs.fx("5") = -0.18;
Qs.fx("6") = -0.05;

* provide initial values for voltages at non-generator busses
Ve.l(k)$(ord(k) lt card(k)) = 1.0;
Vf.l(k)$(ord(k) ne 1 and ord(k) lt card(k)) = 0.0;

MODEL loadflow /ALL/;

option nlp=minos;
option limrow=50;
SOLVE loadflow USING NLP MINIMIZING z;

* Compute terminal specifications and power flows
PARAMETERS
        theta(k) phase angle
        TP(k,m)  "real power transmission along line k-m, MW"
        TQ(k,m) "reactive power transmission along line k-m, MW"
;

theta(k)$(ord(k) lt card(k)) = arctan(Vf.l(k)/Ve.l(k))*(180/Pi);
TP(j(k,m)) = -YG(j)*(Ve.l(k)*(Ve.l(k) - Ve.l(m)) + Vf.l(k)*(Vf.l(k) - Vf.l(m)))
        - YB(j)*(-Ve.l(k)*(Vf.l(k) - Vf.l(m)) + Vf.l(k)*(Ve.l(k) - Ve.l(m)));

TQ(j(k,m)) = -YG(j)*(-Ve.l(k)*(Vf.l(k) - Vf.l(m)) + Vf.l(k)*(Ve.l(k) - Ve.l(m)))
        + YB(j)*(Ve.l(k)*(Ve.l(k) - Ve.l(m)) + Vf.l(k)*(Vf.l(k) - Vf.l(m)));


* Make adjustments for lines with off-nominal transformer ratios
loop(jTR(k,m),
        TP(jTR) = -YG(jTR)*(
                            Ve.l(k)*(VTR(jTR)*Ve.l(k) - Ve.l(m)) +
                            Vf.l(k)*(VTR(jTR)*Vf.l(k) - Vf.l(m)))
                 - YB(jTR)*(
                            -Ve.l(k)*(VTR(jTR)*Vf.l(k) - Vf.l(m)) +
                            Vf.l(k)*(VTR(jTR)*Ve.l(k) - Ve.l(m)));

        TQ(jTR) = -YG(jTR)*(
                            -Ve.l(k)*(VTR(jTR)*Vf.l(k) - Vf.l(m)) +
                            Vf.l(k)*(VTR(jTR)*Ve.l(k) - Ve.l(m)))
```

```
         + YB(jTR)*(
                    Ve.l(k)*(VTR(jTR)*Ve.l(k) - Ve.l(m)) +
                    Vf.l(k)*(VTR(jTR)*Vf.l(k) - Vf.l(m)));

TP(m,k) = -YG(jTR)*(
                    Ve.l(m)*((1/VTR(jTR))*Ve.l(m) - Ve.l(k)) +
                    Vf.l(m)*((1/VTR(jTR))*Vf.l(m) - Vf.l(k)))
         + YB(jTR)*(
                    Ve.l(m)*((1/VTR(jTR))*Vf.l(m) - Vf.l(k)) -
                    Vf.l(m)*((1/VTR(jTR))*Ve.l(m) - Ve.l(k)));

TQ(m,k) = YG(jTR)*(
                    Ve.l(m)*((1/VTR(jTR))*Vf.l(m) - Vf.l(k)) -
                    Vf.l(m)*((1/VTR(jTR))*Ve.l(m) - Ve.l(k)))
         +  YB(jTR)*(
```

E.2 PSAT implementation of Ward and Hale loadflow problem

```
Bus.con = [ ...
  1  400  1  0  2  1;
  2  400  1  0  2  1;
  3  400  1  0  2  1;
  4  400  1  0  2  1;
  5  400  1  0  2  1;
  6  400  1  0  2  1;
 ];

Line.con = [ ...
  1  4  100  400  60  0  0      0.080 0.370 0.028  0.0     0  0  0  0  1;
  1  6  100  400  60  0  0      0.123 0.518 0.040  0.0     0  0  0  0  1;
  2  3  100  400  60  0  0      0.723 1.050 0.0    0.0     0  0  0  0  1;
  2  5  100  400  60  0  0      0.282 0.640 0.0    0.0     0  0  0  0  1;
  3  4  100  400  60  0  0      0.000 0.133 0.0    1.100   0  0  0  0  1;
  4  6  100  400  60  0  0      0.097 0.407 0.031  0.0     0  0  0  0  1;
  5  6  100  400  60  0  0      0.000 0.300 0.0    1.025   0  0  0  0  1;
 ];

SW.con = [ ...
  1  100  400  1.05  0  1.5  -1.5  1.1 0.9  1  1  1;
 ];

PV.con = [ ...
  2  100  400  0.50 1.10  1.5  -1.5  1.1  0.9  1  1;
 ];

PQ.con = [ ...
  3  100  400  0.55  0.13  1.1  0.9  0  1;
  4  100  400  0.00  0.00  1.1  0.9  0  1;
  5  100  400  0.30  0.18  1.1  0.9  0  1;
  6  100  400  0.50  0.05  1.1  0.9  0  1;
 ];

Bus.names = {...
  'Bus1'; 'Bus2'; 'Bus3'; 'Bus4'; 'Bus5';
  'Bus6'};
```

E.3 GAMS implementation of IEEE RTS '96 loadflow problem

```
SET k "busses (includes neutral bus)"
*       1     2      3        4        5      6      7      8
    / Abel, Adams, Adler, Agricola, Aiken, Alber, Alder, Alger,

*       9     10    11     12     13     14      15      16
      Ali, Allen, Anna, Archer, Arne, Arnold, Arthur, Asser,

*      17     18     19      20     21      22      23      24      25
      Aston, Astor, Attar, Attila, Attlee, Aubrey, Austen, Avery, Neutral/
;
ALIAS(k,i,m);

SET slack(k) "slack bus"
    / Attlee
      /
;

SET kSH(k) "busses with shunt admittance to ground"
    / Alber
      /
    ;

SET kVR(k) "busses with voltage regulation"
    / Abel, Adams, Alder, Arne, Arnold, Arthur,
      Asser, Astor, Attlee, Aubrey, Austen
      /
;

PARAMETER Vset(kVR) "busses with voltage regulation"
    / Abel      1.035
      Adams     1.035
      Alder     1.025
      Arne      1.020
      Arnold    0.980
      Arthur    1.014
      Asser     1.017
      Astor     1.050
      Attlee    1.050
      Aubrey    1.050
      Austen    1.050
      /
;

SET Nj branch ID /1*2/;
SET j(k,m,Nj) "branches linking regions"
    / Abel.(Adams, Adler, Aiken).1,    (Adams, Adler, Aiken).Abel.1
```

```
      Adams.(Agricola, Alber).1,       (Agricola, Alber).Adams.1
      Adler.(Ali, Avery).1,            (Ali, Avery).Adler.1
      Agricola.Ali.1,                  Ali.Agricola.1
      Aiken.Allen.1,                   Allen.Aiken.1
      Alber.(Allen,Neutral).1,         (Allen,Neutral).Alber.1
      Alder.Alger.1,                   Alger.Alder.1
      Alger.(Ali, Allen).1,            (Ali, Allen).Alger.1
      Ali.(Anna, Archer).1,            (Anna, Archer).Ali.1
      Allen.(Anna, Archer).1,          (Anna, Archer).Allen.1
      Anna.(Arne, Arnold).1,           (Arne, Arnold).Anna.1
      Archer.(Arne, Austen).1,         (Arne, Austen).Archer.1
      Arne.Austen.1,                   Austen.Arne.1
      Arnold.Asser.1,                  Asser. Arnold.1
      Arthur.(Asser, Avery).1,         (Asser, Avery).Arthur.1
      Arthur.Attlee.(1,2),             Attlee.Arthur.(1,2)
      Asser.(Aston, Attar).1,          (Aston, Attar).Asser.1
      Aston.(Astor, Aubrey).1,         (Astor, Aubrey).Aston.1
      Astor.Attlee.(1,2),              Attlee.Astor.(1,2)
      Attar.Attila.(1,2),              Attila.Attar.(1,2)
      Attila.Austen.(1,2),             Austen.Attila.(1,2)
      Attlee.Aubrey.1,                 Aubrey.Attlee.1
      /
;

SET jTR(k,m,Nj) "branches with off-nominal transformer ratios"
    / Adler.Avery.1
      Ali.Anna.1
      Ali.Archer.1
      Allen.Anna.1
      Allen.Archer.1
      /;

PARAMETER nTR(k,m) "off-nominal transformer ratios"
    / Adler.Avery   1.015
      Ali.Anna      1.03
      Ali.Archer    1.03
      Allen.Anna    1.015
      Allen.Archer  1.015
      /;

SET Nu "unit ID" /1*6/;
SET u(k,Nu) "generating units"
    / Abel.(1*4)
      Adams.(1*4)
      Alder.(1*3)
      Arne.(1*3)
      Arnold.1
      Arthur.(1*6)
      Asser.1
      Astor.1
```

```
      Attlee.1
      Aubrey.(1*6)
      Austen.(1*3)
      /
;

PARAMETER Pd(k) "real power demand at each bus, MW"
    / Abel     108
      Adams     97
      Adler    180
      Agricola  74
      Aiken     71
      Alber    136
      Alder    125
      Alger    171
      Ali      175
      Allen    195
      Arne     265
      Arnold   194
      Arthur   317
      Asser    100
      Astor    333
      Attar    181
      Attila   128
      /
;

PARAMETER Qd(k) "reactive power demand at each bus, MVar"
    / Abel      22
      Adams     20
      Adler     37
      Agricola  15
      Aiken     14
      Alber     28
      Alder     25
      Alger     35
      Ali       36
      Allen     40
      Arne      54
      Arnold    39
      Arthur    64
      Asser     20
      Astor     68
      Attar     37
      Attila    26
      /
;

PARAMETER Pinit(k,Nu) "unit initial real power output, MW"
    / Abel.(1,2)    10
```

```
      Abel.(3,4)    76
      Adams.(1,2)   10
      Adams.(3,4)   76
      Alder.(1*3)   80
      Arne.(1*3)    95.1
      Arnold.1       0
      Arthur.(1*5)  12
      Arthur.6     155
      Asser.1      155
      Astor.1      400
      Attlee.1     400
      Aubrey.(1*6)  50
      Austen.(1,2) 155
      Austen.3     350
      /
;

PARAMETER Qinit(k,Nu) "unit initial reactive power output, MVAr"
    / Abel.(1,2)     0
      Abel.(3,4)    14.1
      Adams.(1,2)    0
      Adams.(3,4)    7
      Alder.(1*3)   17.2
      Arne.(1*3)    40.7
      Arnold.1      13.7
      Arthur.(1*5)   0
      Arthur.6       0.05
      Asser.1       25.22
      Astor.1      137.7
      Attlee.1     108.2
      Aubrey.(1*6)  -4.96
      Austen.(1,2)  31.79
      Austen.3      71.78
      /
;

PARAMETER R(k,m,Nj) "Transmission line resistance, pu"
    / (Abel.Adams.1,         Adams.Abel.1)         0.003
      (Abel.Adler.1,         Adler.Abel.1)         0.055
      (Abel.Aiken.1,         Aiken.Abel.1)         0.022
      (Adams.Agricola.1,     Agricola.Adams.1)     0.033
      (Adams.Alber.1,        Alber.Adams.1)        0.050
      (Adler.Ali.1,          Ali.Adler.1)          0.031
      (Adler.Avery.1,        Avery.Adler.1)        0.002
      (Agricola.Ali.1,       Ali.Agricola.1)       0.027
      (Aiken.Allen.1,        Allen.Aiken.1)        0.023
      (Alber.Allen.1,        Allen.Alber.1)        0.014
*       (Alber.Neutral.1,      Neutral.Alber.1)      1.000
      (Alder.Alger.1,        Alger.Alder.1)        0.016
      (Alger.Ali.1,          Ali.Alger.1)          0.043
```

```
      (Alger.Allen.1,        Allen.Alger.1)        0.043
      (Ali.Anna.1,           Anna.Ali.1)           0.002
      (Ali.Archer.1,         Archer.Ali.1)         0.002
      (Allen.Anna.1,         Anna.Allen.1)         0.002
      (Allen.Archer.1,       Archer.Allen.1)       0.002
      (Anna.Arne.1,          Arne.Anna.1)          0.006
      (Anna.Arnold.1,        Arnold.Anna.1)        0.005
      (Archer.Arne.1,        Arne.Archer.1)        0.006
      (Archer.Austen.1,      Austen.Archer.1)      0.012
      (Arne.Austen.1,        Austen.Arne.1)        0.011
      (Arnold.Asser.1,       Asser. Arnold.1)      0.005
      (Arthur.Asser.1,       Asser.Arthur.1)       0.002
      (Arthur.Attlee.(1,2),  Attlee.Arthur.(1,2))  0.006
      (Arthur.Avery.1,       Avery.Arthur.1)       0.007
      (Asser.Aston.1,        Aston.Asser.1)        0.003
      (Asser.Attar.1,        Attar.Asser.1)        0.003
      (Aston.Astor.1,        Astor.Aston.1)        0.002
      (Aston.Aubrey.1,       Aubrey.Aston.1)       0.014
      (Astor.Attlee.(1,2),   Attlee.Astor.(1,2))   0.003
      (Attar.Attila.(1,2),   Attila.Attar.(1,2))   0.005
      (Attila.Austen.(1,2),  Austen.Attila.(1,2))  0.003
      (Attlee.Aubrey.1,      Aubrey.Attlee.1)      0.009
      /
;

PARAMETER X(k,m,Nj) "Transmission line reactance, pu"
    / (Abel.Adams.1,         Adams.Abel.1)         0.014
      (Abel.Adler.1,         Adler.Abel.1)         0.211
      (Abel.Aiken.1,         Aiken.Abel.1)         0.085
      (Adams.Agricola.1,     Agricola.Adams.1)     0.127
      (Adams.Alber.1,        Alber.Adams.1)        0.192
      (Adler.Ali.1,          Ali.Adler.1)          0.119
      (Adler.Avery.1,        Avery.Adler.1)        0.084
      (Agricola.Ali.1,       Ali.Agricola.1)       0.104
      (Aiken.Allen.1,        Allen.Aiken.1)        0.088
      (Alber.Allen.1,        Allen.Alber.1)        0.061
*      (Alber.Neutral.1,      Neutral.Alber.1)      1.000
      (Alder.Alger.1,        Alger.Alder.1)        0.061
      (Alger.Ali.1,          Ali.Alger.1)          0.165
      (Alger.Allen.1,        Allen.Alger.1)        0.165
      (Ali.Anna.1,           Anna.Ali.1)           0.084
      (Ali.Archer.1,         Archer.Ali.1)         0.084
      (Allen.Anna.1,         Anna.Allen.1)         0.084
      (Allen.Archer.1,       Archer.Allen.1)       0.084
      (Anna.Arne.1,          Arne.Anna.1)          0.048
      (Anna.Arnold.1,        Arnold.Anna.1)        0.042
      (Archer.Arne.1,        Arne.Archer.1)        0.048
      (Archer.Austen.1,      Austen.Archer.1)      0.097
      (Arne.Austen.1,        Austen.Arne.1)        0.087
      (Arnold.Asser.1,       Asser. Arnold.1)      0.059
```

```
      (Arthur.Asser.1,       Asser.Arthur.1)       0.017
      (Arthur.Attlee.(1,2),  Attlee.Arthur.(1,2))  0.049
      (Arthur.Avery.1,       Avery.Arthur.1)       0.052
      (Asser.Aston.1,        Aston.Asser.1)        0.026
      (Asser.Attar.1,        Attar.Asser.1)        0.023
      (Aston.Astor.1,        Astor.Aston.1)        0.014
      (Aston.Aubrey.1,       Aubrey.Aston.1)       0.105
      (Astor.Attlee.(1,2),   Attlee.Astor.(1,2))   0.026
      (Attar.Attila.(1,2),   Attila.Attar.(1,2))   0.040
      (Attila.Austen.(1,2),  Austen.Attila.(1,2))  0.022
      (Attlee.Aubrey.1,      Aubrey.Attlee.1)      0.068
      /
;

PARAMETER Bc(k,m,Nj) "Transmission line charging susceptance, pu"
    / (Abel.Adams.1,         Adams.Abel.1)         0.461
      (Abel.Adler.1,         Adler.Abel.1)         0.057
      (Abel.Aiken.1,         Aiken.Abel.1)         0.023
      (Adams.Agricola.1,     Agricola.Adams.1)     0.034
      (Adams.Alber.1,        Alber.Adams.1)        0.052
      (Adler.Ali.1,          Ali.Adler.1)          0.032
      (Adler.Avery.1,        Avery.Adler.1)        0.000
      (Agricola.Ali.1,       Ali.Agricola.1)       0.028
      (Aiken.Allen.1,        Allen.Aiken.1)        0.024
      (Alber.Allen.1,        Allen.Alber.1)        2.459
*      (Alber.Neutral.1,      Neutral.Alber.1)       N/A
      (Alder.Alger.1,        Alger.Alder.1)        0.017
      (Alger.Ali.1,          Ali.Alger.1)          0.045
      (Alger.Allen.1,        Allen.Alger.1)        0.045
      (Ali.Anna.1,           Anna.Ali.1)           0.000
      (Ali.Archer.1,         Archer.Ali.1)         0.000
      (Allen.Anna.1,         Anna.Allen.1)         0.000
      (Allen.Archer.1,       Archer.Allen.1)       0.000
      (Anna.Arne.1,          Arne.Anna.1)          0.100
      (Anna.Arnold.1,        Arnold.Anna.1)        0.088
      (Archer.Arne.1,        Arne.Archer.1)        0.100
      (Archer.Austen.1,      Austen.Archer.1)      0.203
      (Arne.Austen.1,        Austen.Arne.1)        0.182
      (Arnold.Asser.1,       Asser. Arnold.1)      0.082
      (Arthur.Asser.1,       Asser.Arthur.1)       0.036
      (Arthur.Attlee.(1,2),  Attlee.Arthur.(1,2))  0.103
      (Arthur.Avery.1,       Avery.Arthur.1)       0.109
      (Asser.Aston.1,        Aston.Asser.1)        0.055
      (Asser.Attar.1,        Attar.Asser.1)        0.049
      (Aston.Astor.1,        Astor.Aston.1)        0.030
      (Aston.Aubrey.1,       Aubrey.Aston.1)       0.221
      (Astor.Attlee.(1,2),   Attlee.Astor.(1,2))   0.055
      (Attar.Attila.(1,2),   Attila.Attar.(1,2))   0.083
      (Attila.Austen.(1,2),  Austen.Attila.(1,2))  0.046
      (Attlee.Aubrey.1,      Aubrey.Attlee.1)      0.142
```

```
      /
;

PARAMETER G(k,m,Nj) "conductance of branch k-m";
PARAMETER B(k,m,Nj) "susceptance of branches k-m";
PARAMETER YG(k,m)   "real component of admittance between nodes k and m";
PARAMETER YB(k,m)   "imaginary component of admittance between nodes k-m";

* Calculate branch conductances
G(j(k,m,Nj))$(not (sameas(k,"Neutral") or sameas(m,"Neutral"))) =
        R(j) / (power(R(j),2) + power(X(j),2));

G("Alber","Neutral","1") = 0.0;
G("Neutral","Alber","1") = 0.0;

* Calculate branch susceptances
B(j(k,m,Nj))$(not (sameas(k,"Neutral") or sameas(m,"Neutral"))) =
        -X(j) / (power(R(j),2) + power(X(j),2));

B("Alber","Neutral","1") = 0.0;
B("Neutral","Alber","1") = 0.0;

* Calculate self-admittances
YG(k,k)$(ord(k) lt card(k)) = sum((i,Nj), G(i,k,Nj));
YB(k,k)$(ord(k) lt card(k)) = sum((i,Nj), B(i,k,Nj));

* Make adjustments to self-admittances for off-nominal transformer ratios
loop(jTR(k,m,Nj),
        YG(k,k) = YG(k,k) + (power(nTR(k,m), 2) - 1) * G(jTR);
        YB(k,k) = YB(k,k) + (power(nTR(k,m), 2) - 1) * B(jTR);
);

* Calculate mutual-admittances
loop(j(k,m,"1"),
        YG(k,m)$(ord(k) lt card(k) and ord(m) lt card(m)) = sum(Nj, -G(k,m,Nj));
        YB(k,m)$(ord(k) lt card(k) and ord(m) lt card(m)) = sum(Nj, -B(k,m,Nj));
);

* Make adjustments to mutual-admittances for off-nominal transformer ratios
loop(jTR(k,m,Nj),
        YG(k,m) = YG(k,m) - (nTR(k,m) - 1) * G(jTR);
        YG(m,k) = YG(m,k) - (nTR(k,m) - 1) * G(m,k,Nj);
        YB(k,m) = YB(k,m) - (nTR(k,m) - 1) * B(jTR);
        YB(m,k) = YB(m,k) - (nTR(k,m) - 1) * B(m,k,Nj);
);

VARIABLES
        z       "objective function"
        Ps(k)   "net real power injected at the kth bus, MW"
        Qs(k)   "net reactive power injected at the kth bus, MVar"
```

```
        Ia(k)   "real component of current"
        Ib(k)   "imaginary component of current"
        Ve(k)   "real component of voltage"
        Vf(k)   "imaginary component of voltage"
;

POSITIVE VARIABLES
        Vmag(k) "voltage magnitude"
;

EQUATIONS
        obj        "objective function defined"
        IaDef(k)   "real component of current definition"
        IbDef(k)   "imaginary component of current definition"
        PDef(k)    "real power definition"
        QDef(k)    "reactive power definition"
        QsDef(k)   "reactive power definition at busses with shunt admittance"
        VDef(k)    "voltage magnitude definition"
;

obj..      z =E= sum(k$(ord(k) lt card(k)), power((Vmag(k) - 1), 2));
IaDef(k)$(ord(k) lt card(k)).. Ia(k) =E= sum(m, YG(k,m)*Ve(m) - YB(k,m)*Vf(m));
IbDef(k)$(ord(k) lt card(k)).. Ib(k) =E= sum(m, YG(k,m)*Vf(m) + YB(k,m)*Ve(m));
PDef(k)$(ord(k) lt card(k))..  Ps(k)/100 =E= Ia(k)*Ve(k) + Ib(k)*Vf(k);
QDef(k)$(ord(k) lt card(k))..  Qs(k)/100 =E= Ia(k)*Vf(k) - Ib(k)*Ve(k);
QsDef(k)$kSH(k)..              Qs(k) =E= sum(Nu, Qinit(k,Nu)) - Qd(k)
                                         + 100*power(Vmag(k), 2);
VDef(k)$(ord(k) lt card(k))..  power(Vmag(k), 2) =E= power(Ve(k), 2)
                                                     + power(Vf(k), 2);

* fix voltage magnitude at busses with regulation
Vmag.fx(kVR) = Vset(kVR);

* fix phase angle at slack bus to zero
Vf.fx(slack) = 0;

* specify net real power availability
Ps.fx(k)$(not slack(k)) =  sum(Nu, Pinit(k,Nu)) - Pd(k);

* specify net reactive power availability
Qs.fx(k)$(not (kVR(k) or kSH(k))) =  sum(Nu, Qinit(k,Nu)) - Qd(k);

* provide initial values for voltages
Ve.l(k)$(ord(k) lt card(k)) = 1.0;
Vf.l(k)$(ord(k) ne 1 and ord(k) lt card(k)) = 0.0;
Vmag.l(k)$(ord(k) lt card(k)) = 1.0;

*==============================================================
* S O L V E   L O A D   F L O W
*==============================================================
```

```
MODEL loadflow /ALL/;

option nlp=minos;
option limrow=50;
SOLVE loadflow USING NLP MINIMIZING z;

YB(k,k)$(ord(k) lt card(k)) = YB(k,k) + sum((i,Nj), + Bc(i,k,Nj)/2);
```

E.4 PSAT implementation of IEEE RTS '96 loadflow problem

```
  6  138  1  0  1  1;
  7  138  1  0  1  1;
  8  138  1  0  1  1;
  9  138  1  0  1  1;
 10  138  1  0  1  1;
 11  230  1  0  1  1;
 12  230  1  0  1  1;
 13  230  1  0  1  1;
 14  230  1  0  1  1;
 15  230  1  0  1  1;
 16  230  1  0  1  1;
 17  230  1  0  1  1;
 18  230  1  0  1  1;
 19  230  1  0  1  1;
 20  230  1  0  1  1;
 21  230  1  0  1  1;
 22  230  1  0  1  1;
 23  230  1  0  1  1;
 24  230  1  0  1  1;
 ];

Line.con = [ ...
  1  2  100  138  60  0  0  0.003  0.014  0.461  0.0     0  0  0  0  1;
  1  3  100  138  60  0  0  0.055  0.211  0.057  0.0     0  0  0  0  1;
  1  5  100  138  60  0  0  0.022  0.085  0.023  0.0     0  0  0  0  1;
  2  4  100  138  60  0  0  0.033  0.127  0.034  0.0     0  0  0  0  1;
  2  6  100  138  60  0  0  0.050  0.192  0.052  0.0     0  0  0  0  1;
  3  9  100  138  60  0  0  0.031  0.119  0.032  0.0     0  0  0  0  1;
 24  3  100  230  60  0  5/3  0.002  0.084  0.000  1.015   0  0  0  0  1;
  4  9  100  138  60  0  0  0.027  0.104  0.028  0.0     0  0  0  0  1;
  5 10  100  138  60  0  0  0.023  0.088  0.024  0.0     0  0  0  0  1;
  6 10  100  138  60  0  0  0.014  0.061  2.459  0.0     0  0  0  0  1;
  7  8  100  138  60  0  0  0.016  0.061  0.017  0.0     0  0  0  0  1;
  8  9  100  138  60  0  0  0.043  0.165  0.045  0.0     0  0  0  0  1;
  8 10  100  138  60  0  0  0.043  0.165  0.045  0.0     0  0  0  0  1;
 11  9  100  230  60  0  5/3  0.002  0.084  0.000  1.030    0  0  0  0  1;
 12  9  100  230  60  0  5/3  0.002  0.084  0.000  1.030    0  0  0  0  1;
 11 10  100  230  60  0  5/3  0.002  0.084  0.000  1.015   0  0  0  0  1;
 12 10  100  230  60  0  5/3  0.002  0.084  0.000  1.015   0  0  0  0  1;
 11 13  100  230  60  0  0  0.006  0.048  0.100  0.0     0  0  0  0  1;
 11 14  100  230  60  0  0  0.005  0.042  0.088  0.0     0  0  0  0  1;
 12 13  100  230  60  0  0  0.006  0.048  0.100  0.0     0  0  0  0  1;
 12 23  100  230  60  0  0  0.012  0.097  0.203  0.0     0  0  0  0  1;
 13 23  100  230  60  0  0  0.011  0.087  0.182  0.0     0  0  0  0  1;
 14 16  100  230  60  0  0  0.005  0.059  0.082  0.0     0  0  0  0  1;
 15 16  100  230  60  0  0  0.002  0.017  0.036  0.0     0  0  0  0  1;
```

```
% 15 21  100  230  60  0  0  0.006  0.049  0.103  0.0     0  0  0  0  1;
 15 21  100  230  60  0  0  0.003  0.0245  0.206  0.0     0  0  0  0  1;
 15 24  100  230  60  0  0  0.007  0.052  0.109  0.0     0  0  0  0  1;
 16 17  100  230  60  0  0  0.003  0.026  0.055  0.0     0  0  0  0  1;
 16 19  100  230  60  0  0  0.003  0.023  0.049  0.0     0  0  0  0  1;
 17 18  100  230  60  0  0  0.002  0.014  0.030  0.0     0  0  0  0  1;
 17 22  100  230  60  0  0  0.014  0.105  0.221  0.0     0  0  0  0  1;
% 18 21  100  230  60  0  0  0.003  0.026  0.055  0.0     0  0  0  0  1;
 18 21  100  230  60  0  0  0.0015  0.013  0.110  0.0     0  0  0  0  1;
% 19 20  100  230  60  0  0  0.005  0.040  0.083  0.0     0  0  0  0  1;
 19 20  100  230  60  0  0  0.0025  0.020  0.166  0.0     0  0  0  0  1;
% 20 23  100  230  60  0  0  0.003  0.022  0.046  0.0     0  0  0  0  1;
 20 23  100  230  60  0  0  0.0015  0.011  0.092  0.0     0  0  0  0  1;
 21 22  100  230  60  0  0  0.009  0.068  0.142  0.0     0  0  0  0  1;
 ];

SW.con = [ ...
 21  100  230  1.05  0  1.5  -1.5  1.1 0.9  1  1  1;
 ];

PV.con = [ ...
  1  100  138   0.64  1.035  1.5  -1.5  1.1  0.9  1  1;
  2  100  138   0.75  1.035  1.5  -1.5  1.1  0.9  1  1;
  7  100  138   1.15  1.025  1.5  -1.5  1.1  0.9  1  1;
 13  100  230   0.203 1.020  1.5  -1.5  1.1  0.9  1  1;
 14  100  230  -1.94  0.980  1.5  -1.5  1.1  0.9  1  1;
 15  100  230  -1.02  1.014  1.5  -1.5  1.1  0.9  1  1;
 16  100  230   0.55  1.017  1.5  -1.5  1.1  0.9  1  1;
 18  100  230   0.67  1.050  1.5  -1.5  1.1  0.9  1  1;
 22  100  230   3.00  1.050  1.5  -1.5  1.1  0.9  1  1;
 23  100  230   6.60  1.050  1.5  -1.5  1.1  0.9  1  1;
 ];

PQ.con = [ ...
  3  100  138  1.80  0.37  1.1  0.9  0  1;
  4  100  138  0.74  0.15  1.1  0.9  0  1;
  5  100  138  0.71  0.14  1.1  0.9  0  1;
  6  100  138  1.36  0.28  1.1  0.9  0  1;
  8  100  138  1.71  0.35  1.1  0.9  0  1;
  9  100  138  1.75  0.36  1.1  0.9  0  1;
 10  100  138  1.95  0.40  1.1  0.9  0  1;
 11  100  230  0.00  0.00  1.1  0.9  0  1;
 12  100  230  0.00  0.00  1.1  0.9  0  1;
 17  100  230  0.00  0.00  1.1  0.9  0  1;
 19  100  230  1.81  0.37  1.1  0.9  0  1;
 20  100  230  1.28  0.26  1.1  0.9  0  1;
 24  100  230  0.00  0.00  1.1  0.9  0  1;
 ];

Shunt.con = [ ...
```

```
 6  100  138  60  0.00  1.00  1;
];

Bus.names = {...
 'Abel';  'Adams'; 'Adler'; 'Agricola'; 'Aiken';  'Alber';  'Alder';  'Alger';
 'Ali';   'Allen'; 'Anna';  'Archer';   'Arne';   'Arnold'; 'Arthur'; 'Asser';
 'Aston'; 'Astor'; 'Attar'; 'Attila';   'Attlee'; 'Aubrey'; 'Austen'; 'Avery'};
```

E.5 GAMS implementation of IEEE RTS '96 economic dispatch problem

```
* File: IEEE_RTS_1996_dispatch.gms
* --------------------------------
* This program performs the economic dispatch for the IEEE 1996 RTS
* (Reliability Test System) (Grigg et al. "The IEEE reliability test
* system - 1996", IEEE Transactions on Power Systems, Vol. 14, No. 3, August 1999):

SCALAR Pslack "price of imported power, $/MWh";
SCALAR L      "length of each time period, hours" /1.0/;

* SPECIFY BUS INFORMATION
* -----------------------
SET kn "busses (includes neutral bus)"
*       1      2     3        4       5      6      7      8
    / Abel, Adams, Adler, Agricola, Aiken, Alber, Alder, Alger,

*      9     10    11     12     13      14     15      16
      Ali, Allen, Anna, Archer, Arne, Arnold, Arthur, Asser,

*       17     18     19      20      21      22      23     24      25
      Aston, Astor, Attar, Attila, Attlee, Aubrey, Austen, Avery, Neutral/
;
ALIAS(kn,in,mn);

SET k(kn) "busses"
*       1      2     3        4       5      6      7      8
    / Abel, Adams, Adler, Agricola, Aiken, Alber, Alder, Alger,

*      9     10    11     12     13      14     15      16
      Ali, Allen, Anna, Archer, Arne, Arnold, Arthur, Asser,

*       17     18     19      20      21      22      23     24
      Aston, Astor, Attar, Attila, Attlee, Aubrey, Austen, Avery/
;
ALIAS(k,i,m);

SET slack(k) "slack bus"
    / Attlee
      /
;

SET kSH(k) "busses with shunt admittance to ground"
    / Alber
      /
;

SET kLD(k) "busses with loads"
```

```
    / Abel, Adams, Adler, Agricola, Aiken, Alber, Alder, Alger,
      Ali, Allen, Arne, Arnold, Arthur, Asser,
      Astor, Attar, Attila
      /
;

SET kVR(k) "busses with voltage regulation"
    / Abel, Adams, Alder, Arne, Arnold, Arthur,
      Asser, Astor, Attlee, Aubrey, Austen
      /
;

PARAMETER Vset(kVR) "voltage set-point of busses with voltage regulation"
          / Abel   1.035
            Adams  1.035
            Alder  1.025
            Arne   1.020
            Arnold 0.980
            Arthur 1.014
            Asser  1.017
            Astor  1.050
            Attlee 1.050
            Aubrey 1.050
            Austen 1.050
            /
;

PARAMETER VRon(kVR) "’1’ if at least on generator is on; ’0’ otherwise";

* SPECIFY BRANCH INFORMATION
* --------------------------
SET Nj "branch ID" /1*2/;
SET j(kn,mn,Nj) "branches linking regions"
    / Abel.(Adams, Adler, Aiken).1, (Adams, Adler, Aiken).Abel.1
      Adams.(Agricola, Alber).1,    (Agricola, Alber).Adams.1
      Adler.(Ali, Avery).1,         (Ali, Avery).Adler.1
      Agricola.Ali.1,                Ali.Agricola.1
      Aiken.Allen.1,                 Allen.Aiken.1
      Alber.(Allen,Neutral).1,      (Allen,Neutral).Alber.1
      Alder.Alger.1,                 Alger.Alder.1
      Alger.(Ali, Allen).1,         (Ali, Allen).Alger.1
      Ali.(Anna, Archer).1,         (Anna, Archer).Ali.1
      Allen.(Anna, Archer).1,       (Anna, Archer).Allen.1
      Anna.(Arne, Arnold).1,        (Arne, Arnold).Anna.1
      Archer.(Arne, Austen).1,      (Arne, Austen).Archer.1
      Arne.Austen.1,                 Austen.Arne.1
      Arnold.Asser.1,                Asser.Arnold.1
      Arthur.(Asser, Avery).1,      (Asser, Avery).Arthur.1
      Arthur.Attlee.(1,2),           Attlee.Arthur.(1,2)
      Asser.(Aston, Attar).1,       (Aston, Attar).Asser.1
```

```
      Aston.(Astor, Aubrey).1,      (Astor, Aubrey).Aston.1
      Astor.Attlee.(1,2),            Attlee.Astor.(1,2)
      Attar.Attila.(1,2),            Attila.Attar.(1,2)
      Attila.Austen.(1,2),           Austen.Attila.(1,2)
      Attlee.Aubrey.1,               Aubrey.Attlee.1
      /
;

SET jTR(k,m,Nj) "branches with off-nominal transformer ratios"
    / Adler.Avery.1
      Ali.Anna.1
      Ali.Archer.1
      Allen.Anna.1
      Allen.Archer.1
      /;

PARAMETER VTR(k,m) "off-nominal transformer ratios"
          / Adler.Avery  1.015
            Ali.Anna     1.03
            Ali.Archer   1.03
            Allen.Anna   1.015
            Allen.Archer 1.015
            /;

PARAMETER R(k,m,Nj) "Transmission line resistance, pu"
          / (Abel.Adams.1, Adams.Abel.1)               0.003
            (Abel.Adler.1, Adler.Abel.1)               0.055
            (Abel.Aiken.1, Aiken.Abel.1)               0.022
            (Adams.Agricola.1, Agricola.Adams.1)       0.033
            (Adams.Alber.1, Alber.Adams.1)             0.050
            (Adler.Ali.1, Ali.Adler.1)                 0.031
            (Adler.Avery.1, Avery.Adler.1)             0.002
            (Agricola.Ali.1, Ali.Agricola.1)           0.027
            (Aiken.Allen.1, Allen.Aiken.1)             0.023
            (Alber.Allen.1, Allen.Alber.1)             0.014
*           (Alber.Neutral.1, Neutral.Alber.1)         N/A
            (Alder.Alger.1, Alger.Alder.1)             0.016
            (Alger.Ali.1, Ali.Alger.1)                 0.043
            (Alger.Allen.1, Allen.Alger.1)             0.043
            (Ali.Anna.1, Anna.Ali.1)                   0.002
            (Ali.Archer.1, Archer.Ali.1)               0.002
            (Allen.Anna.1, Anna.Allen.1)               0.002
            (Allen.Archer.1, Archer.Allen.1)           0.002
            (Anna.Arne.1, Arne.Anna.1)                 0.006
            (Anna.Arnold.1, Arnold.Anna.1)             0.005
            (Archer.Arne.1, Arne.Archer.1)             0.006
            (Archer.Austen.1, Austen.Archer.1)         0.012
            (Arne.Austen.1, Austen.Arne.1)             0.011
            (Arnold.Asser.1, Asser. Arnold.1)          0.005
            (Arthur.Asser.1, Asser.Arthur.1)           0.002
```

```
            (Arthur.Avery.1, Avery.Arthur.1)           0.007
            (Arthur.Attlee.(1,2), Attlee.Arthur.(1,2)) 0.006
            (Asser.Aston.1, Aston.Asser.1)             0.003
            (Asser.Attar.1, Attar.Asser.1)             0.003
            (Aston.Astor.1, Astor.Aston.1)             0.002
            (Aston.Aubrey.1, Aubrey.Aston.1)           0.014
            (Astor.Attlee.(1,2), Attlee.Astor.(1,2))   0.003
            (Attar.Attila.(1,2), Attila.Attar.(1,2))   0.005
            (Attila.Austen.(1,2), Austen.Attila.(1,2)) 0.003
            (Attlee.Aubrey.1, Aubrey.Attlee.1)         0.009
            /
;

PARAMETER X(k,m,Nj) "Transmission line reactance, pu"
          / (Abel.Adams.1, Adams.Abel.1)               0.014
            (Abel.Adler.1, Adler.Abel.1)               0.211
            (Abel.Aiken.1, Aiken.Abel.1)               0.085
            (Adams.Agricola.1, Agricola.Adams.1)       0.127
            (Adams.Alber.1, Alber.Adams.1)             0.192
            (Adler.Ali.1, Ali.Adler.1)                 0.119
            (Adler.Avery.1, Avery.Adler.1)             0.084
            (Agricola.Ali.1, Ali.Agricola.1)           0.104
            (Aiken.Allen.1, Allen.Aiken.1)             0.088
            (Alber.Allen.1, Allen.Alber.1)             0.061
*           (Alber.Neutral.1, Neutral.Alber.1)         N/A
            (Alder.Alger.1, Alger.Alder.1)             0.061
            (Alger.Ali.1, Ali.Alger.1)                 0.165
            (Alger.Allen.1, Allen.Alger.1)             0.165
            (Ali.Anna.1, Anna.Ali.1)                   0.084
            (Ali.Archer.1, Archer.Ali.1)               0.084
            (Allen.Anna.1, Anna.Allen.1)               0.084
            (Allen.Archer.1, Archer.Allen.1)           0.084
            (Anna.Arne.1, Arne.Anna.1)                 0.048
            (Anna.Arnold.1, Arnold.Anna.1)             0.042
            (Archer.Arne.1, Arne.Archer.1)             0.048
            (Archer.Austen.1, Austen.Archer.1)         0.097
            (Arne.Austen.1, Austen.Arne.1)             0.087
            (Arnold.Asser.1, Asser. Arnold.1)          0.059
            (Arthur.Asser.1, Asser.Arthur.1)           0.017
            (Arthur.Attlee.(1,2), Attlee.Arthur.(1,2)) 0.049
            (Arthur.Avery.1, Avery.Arthur.1)           0.052
            (Asser.Aston.1, Aston.Asser.1)             0.026
            (Asser.Attar.1, Attar.Asser.1)             0.023
            (Aston.Astor.1, Astor.Aston.1)             0.014
            (Aston.Aubrey.1, Aubrey.Aston.1)           0.105
            (Astor.Attlee.(1,2), Attlee.Astor.(1,2))   0.026
            (Attar.Attila.(1,2), Attila.Attar.(1,2))   0.040
            (Attila.Austen.(1,2), Austen.Attila.(1,2)) 0.022
            (Attlee.Aubrey.1, Aubrey.Attlee.1)         0.068
            /
```

```
;

PARAMETER Bc(kn,mn,Nj) "Transmission line charging susceptance, pu"
          / (Abel.Adams.1, Adams.Abel.1)               0.461
            (Abel.Adler.1, Adler.Abel.1)               0.057
            (Abel.Aiken.1, Aiken.Abel.1)               0.023
            (Adams.Agricola.1, Agricola.Adams.1)       0.034
            (Adams.Alber.1, Alber.Adams.1)             0.052
            (Adler.Ali.1, Ali.Adler.1)                 0.032
            (Adler.Avery.1, Avery.Adler.1)             0.000
            (Agricola.Ali.1, Ali.Agricola.1)           0.028
            (Aiken.Allen.1, Allen.Aiken.1)             0.024
            (Alber.Allen.1, Allen.Alber.1)             2.459
*           (Alber.Neutral.1, Neutral.Alber.1)         N/A
            (Alder.Alger.1, Alger.Alder.1)             0.017
            (Alger.Ali.1, Ali.Alger.1)                 0.045
            (Alger.Allen.1, Allen.Alger.1)             0.045
            (Ali.Anna.1, Anna.Ali.1)                   0.000
            (Ali.Archer.1, Archer.Ali.1)               0.000
            (Allen.Anna.1, Anna.Allen.1)               0.000
            (Allen.Archer.1, Archer.Allen.1)           0.000
            (Anna.Arne.1, Arne.Anna.1)                 0.100
            (Anna.Arnold.1, Arnold.Anna.1)             0.088
            (Archer.Arne.1, Arne.Archer.1)             0.100
            (Archer.Austen.1, Austen.Archer.1)         0.203
            (Arne.Austen.1, Austen.Arne.1)             0.182
            (Arnold.Asser.1, Asser. Arnold.1)          0.082
            (Arthur.Asser.1, Asser.Arthur.1)           0.036
            (Arthur.Attlee.(1,2), Attlee.Arthur.(1,2)) 0.103
            (Arthur.Avery.1, Avery.Arthur.1)           0.109
            (Asser.Aston.1, Aston.Asser.1)             0.055
            (Asser.Attar.1, Attar.Asser.1)             0.049
            (Aston.Astor.1, Astor.Aston.1)             0.030
            (Aston.Aubrey.1, Aubrey.Aston.1)           0.221
            (Astor.Attlee.(1,2), Attlee.Astor.(1,2))   0.055
            (Attar.Attila.(1,2), Attila.Attar.(1,2))   0.083
            (Attila.Austen.(1,2), Austen.Attila.(1,2)) 0.046
            (Attlee.Aubrey.1, Aubrey.Attlee.1)         0.142
            /
;

PARAMETER TSmax(k,m,Nj) "Transmission line continuous rating limits, MVA"
          / (Abel.Adams.1, Adams.Abel.1)               175
            (Abel.Adler.1, Adler.Abel.1)               175
            (Abel.Aiken.1, Aiken.Abel.1)               175
            (Adams.Agricola.1, Agricola.Adams.1)       175
            (Adams.Alber.1, Alber.Adams.1)             175
            (Adler.Ali.1, Ali.Adler.1)                 175
            (Adler.Avery.1, Avery.Adler.1)             400
            (Agricola.Ali.1, Ali.Agricola.1)           175
```

```
            (Aiken.Allen.1, Allen.Aiken.1)             175
            (Alber.Allen.1, Allen.Alber.1)             175
            (Alder.Alger.1, Alger.Alder.1)             175
            (Alger.Ali.1, Ali.Alger.1)                 175
            (Alger.Allen.1, Allen.Alger.1)             175
            (Ali.Anna.1, Anna.Ali.1)                   400
            (Ali.Archer.1, Archer.Ali.1)               400
            (Allen.Anna.1, Anna.Allen.1)               400
            (Allen.Archer.1, Archer.Allen.1)           400
            (Anna.Arne.1, Arne.Anna.1)                 500
            (Anna.Arnold.1, Arnold.Anna.1)             500
            (Archer.Arne.1, Arne.Archer.1)             500
            (Archer.Austen.1, Austen.Archer.1)         500
            (Arne.Austen.1, Austen.Arne.1)             500
            (Arnold.Asser.1, Asser. Arnold.1)          500
            (Arthur.Asser.1, Asser.Arthur.1)           500
            (Arthur.Attlee.(1,2), Attlee.Arthur.(1,2)) 500
            (Arthur.Avery.1, Avery.Arthur.1)           500
            (Asser.Aston.1, Aston.Asser.1)             500
            (Asser.Attar.1, Attar.Asser.1)             500
            (Aston.Astor.1, Astor.Aston.1)             500
            (Aston.Aubrey.1, Aubrey.Aston.1)           500
            (Astor.Attlee.(1,2), Attlee.Astor.(1,2))   500
            (Attar.Attila.(1,2), Attila.Attar.(1,2))   500
            (Attila.Austen.(1,2), Austen.Attila.(1,2)) 500
            (Attlee.Aubrey.1, Aubrey.Attlee.1)         500
            /
;

PARAMETER G(kn,mn,Nj) "conductance of branch k-m";
PARAMETER B(kn,mn,Nj) "susceptance of branches k-m";
PARAMETER YG(k,m) "real component of admittance between nodes k and m";
PARAMETER YB(k,m) "imaginary component of admittance between nodes k-m";

* Calculate branch conductances
G(j(k,m,Nj)) = R(j) / (power(R(j),2) + power(X(j),2));
G("Alber","Neutral","1") = 0.0;
G("Neutral","Alber","1") = 0.0;

* Calculate branch susceptances
B(j(k,m,Nj)) = -X(j) / (power(R(j),2) + power(X(j),2));
B("Alber","Neutral","1") = 0.0;
B("Neutral","Alber","1") = 0.0;

* Calculate self-admittances
YG(k,k) = sum((in,Nj), G(in,k,Nj));
YB(k,k) = sum((in,Nj), B(in,k,Nj));

* Make adjustments to self-admittances for off-nominal transformer ratios
loop(jTR(k,m,Nj),
```

```
        YG(k,k) = YG(k,k) + (power(VTR(k,m), 2) - 1) * G(jTR);
        YB(k,k) = YB(k,k) + (power(VTR(k,m), 2) - 1) * B(jTR);
);

* Calculate mutual-admittances
loop(j(k,m,"1"),
        YG(k,m) = sum(Nj, -G(k,m,Nj));
        YB(k,m) = sum(Nj, -B(k,m,Nj));
);

* Make adjustments to mutual-admittances for off-nominal transformer ratios
loop(jTR(k,m,Nj),
        YG(k,m) = YG(k,m) - (VTR(k,m) - 1) * G(jTR);
        YG(m,k) = YG(m,k) - (VTR(k,m) - 1) * G(m,k,Nj);
        YB(k,m) = YB(k,m) - (VTR(k,m) - 1) * B(jTR);
        YB(m,k) = YB(m,k) - (VTR(k,m) - 1) * B(m,k,Nj);
);

* Make adjustments to self-admittances for lince-charging susceptances
YB(k,k) = YB(k,k) + sum((i,Nj), + Bc(i,k,Nj)/2);

* SPECIFY UNIT INFORMATION
* ------------------------
SET Nu unit ID /1*6/;
SET u(k,Nu) list of all generating units
    / Abel.(1,2)
      Abel.(3,4)
      Adams.(1,2)
      Adams.(3,4)
      Alder.(1*3)
      Arne.(1*3)
      Arnold.1
      Arthur.(1*5)
      Arthur.6
      Asser.1
      Astor.1
      Attlee.1
      Aubrey.(1*6)
      Austen.(1,2)
      Austen.3
      /
;
SETS
        U12(k,Nu) "Fuel oil type 6/Steam"              / Arthur.(1*5) /
        U20(k,NU) "Fuel oil type 2/Combustion turbine" / (Abel,Adams).(1,2)/
        U50(k,Nu) "Hydroelectric"                      / Aubrey.(1*6)/
        U76(k,Nu) "Coal/Steam turbine"                 / (Abel,Adams).(3,4)/
        U100(k,Nu) "Fuel oil type 6/Steam turbine"     / Alder.(1*3)/
        U155(k,Nu) "Coal/Steam turbine"                / Arthur.6, Asser.1,
                                                         Austen.(1,2) /
```

```
        U197(k,Nu) "Fuel oil type 6/Steam turbine"     / Arne.(1*3) /
        U350(k,Nu) "Coal/Steam turbine"                / Austen.3 /
        U400(k,Nu) "Nuclear/Steam turbine"             / (Astor,Attlee).1 /
        Sync(k,Nu) "Synchronous Condenser"             / Arnold.1 /
;

SET ud(k,Nu) "units with discrete performance data (IHR and HR vs P)";
ud(u) = U12(u) + U20(u) + U76(u) + U100(u) + U155(u) + U197(u) + U350(u)
      + U400(u);

* Maximum real power output
PARAMETER Pmax(k,Nu) "unit maximum real power output, MW";
Pmax(U12) =   12;
Pmax(U20) =   20;
Pmax(U50) =   50;
Pmax(U76) =   76;
Pmax(U100) = 100;
Pmax(U155) = 155;
Pmax(U197) = 197;
Pmax(U350) = 350;
Pmax(U400) = 400;
Pmax(Sync) =   0;

* Minimum real power output
PARAMETER Pmin(k,Nu) "generator minimum real power output, MVAr";
Pmin(U12) =   1.2;
Pmin(U20) =   2.0;
Pmin(U50) =   0.0;
Pmin(U76) =   7.6;
Pmin(U100) = 10.0;
Pmin(U155) = 15.5;
Pmin(U197) = 19.7;
Pmin(U350) = 35.0;
Pmin(U400) = 40.0;
Pmin(Sync) =  0.0;

* Maximum reactive power output
PARAMETER Qmax(k,Nu) "generator maximum reactive power output, MW";
Qmax(U12) =    6;
Qmax(U20) =   10;
Qmax(U50) =   16;
Qmax(U76) =   30;
Qmax(U100) =  60;
Qmax(U155) =  80;
Qmax(U197) =  80;
Qmax(U350) = 150;
Qmax(U400) = 200;
Qmax(Sync) = 200;

* Minimum reactive power output
```

```
PARAMETER Qmin(k,Nu) "generator minimum reactive power output, MVAr";
Qmin(U12) =    0;
Qmin(U20) =    0;
Qmin(U50) =  -10;
Qmin(U76) =  -25;
Qmin(U100) =   0;
Qmin(U155) = -50;
Qmin(U197) =   0;
Qmin(U350) = -25;
Qmin(U400) = -50;
Qmin(Sync) = -50;

* Base load real power output
PARAMETER Pbase(k,Nu) "generator base real power output, MW"
    / Abel.(1,2)    10
      Abel.(3,4)    76
      Adams.(1,2)   10
      Adams.(3,4)   76
      Alder.(1*3)   80
      Arne.(1*3)    95.1
      Arnold.1       0
      Arthur.(1*5)  12
      Arthur.6     155
      Asser.1      155
      Astor.1      400
      Attlee.1     400
      Aubrey.(1*6)  50
      Austen.(1,2) 155
      Austen.3     350
      /;

* Base load reactive power output
PARAMETER Qbase(k,Nu) "generator base reactive power output, MVAr"
    / Abel.(1,2)     0
      Abel.(3,4)    14.1
      Adams.(1,2)    0
      Adams.(3,4)    7
      Alder.(1*3)   17.2
      Arne.(1*3)    40.7
      Arnold.1      13.7
      Arthur.(1*5)   0
      Arthur.6       0.05
      Asser.1       25.22
      Astor.1      137.7
      Attlee.1     108.2
      Aubrey.(1*6)  -4.96
      Austen.(1,2)  31.79
      Austen.3      71.78
      /
;
```

```
* Unit ramp up and down rates
PARAMETER DeltaP(k,Nu) "generator ramp rate, MW/min";
DeltaP(U12) =   1;
DeltaP(U20) =   3;
DeltaP(U76) =   2;
DeltaP(U100) =  7;
DeltaP(U155) =  3;
DeltaP(U197) =  3;
DeltaP(U350) =  4;
DeltaP(U400) = 20;

PARAMETER TauStart(k,Nu) "generator cold start times, h";
TauStart(U12) =   4;
TauStart(U20) =   0;
TauStart(U50) =   0;
TauStart(U76) =  12;
TauStart(U100) =  7;
TauStart(U155) = 11;
TauStart(U197) =  7;
TauStart(U350) = 12;
TauStart(U400) = -1;

* Fuel costs
PARAMETER FC(k,Nu) "fuel costs, $/MMBtu (source: Billinton and Li, 1994)";
FC(U12) =  2.30;
FC(U20) =  3.00;
FC(U76) =  1.20;
FC(U100) = 2.30;
FC(U155) = 1.20;
FC(U197) = 2.30;
FC(U350) = 1.20;
FC(U400) = 0.60;

* CO2 emissions
PARAMETER EICO2(k,Nu) "CO2 emissions intensity, lb/MMBtu";
EICO2(U12) =  170;
EICO2(U20) =  160;
EICO2(U76) =  210;
EICO2(U100) = 170;
EICO2(U155) = 210;
EICO2(U197) = 170;
EICO2(U350) = 210;
EICO2(U400) = 0;

* SPECIFY BIDDING INFORMATION
* ---------------------------
SET Nb unit bids /1*4/;
ALIAS(Nb,bid);
```

```
* Supply quantities
PARAMETER PSbid(k,Nu,Nb) "real power supply bid quantities, MW";
PSbid(U12,"1") = 2.40;
PSbid(U12,"2") = 3.60;
PSbid(U12,"3") = 3.60;
PSbid(U12,"4") = 2.40;

PSbid(U20,"1") = 15.80;
PSbid(U20,"2") =  0.20;
PSbid(U20,"3") =  3.80;
PSbid(U20,"4") =  0.20;

PSbid(U50,"1") = 50.00;

PSbid(U76,"1") = 15.20;
PSbid(U76,"2") = 22.80;
PSbid(U76,"3") = 22.80;
PSbid(U76,"4") = 15.20;

PSbid(U100,"1") = 25.00;
PSbid(U100,"2") = 25.00;
PSbid(U100,"3") = 30.00;
PSbid(U100,"4") = 20.00;

PSbid(U155,"1") = 54.25;
PSbid(U155,"2") = 38.75;
PSbid(U155,"3") = 31.00;
PSbid(U155,"4") = 31.00;

PSbid(U197,"1") = 68.95;
PSbid(U197,"2") = 49.25;
PSbid(U197,"3") = 39.40;
PSbid(U197,"4") = 39.40;

PSbid(U350,"1") = 140.00;
PSbid(U350,"2") = 87.50;
PSbid(U350,"3") = 52.50;
PSbid(U350,"4") = 70.00;

PSbid(U400,"1") = 100.00;
PSbid(U400,"2") = 100.00;
PSbid(U400,"3") = 120.00;
PSbid(U400,"4") = 80.00;

* Supply bid reat rates
PARAMETER HRbid(k,Nu,Nb) "supply bid heat rates, Btu/kWh";
HRbid(U12,"1") = 16017;
HRbid(U12,"2") = 12500;
HRbid(U12,"3") = 11900;
HRbid(U12,"4") = 12000;
```

```
HRbid(U20,"1") = 15063;
HRbid(U20,"2") = 15000;
HRbid(U20,"3") = 14500;
HRbid(U20,"4") = 14499;

HRbid(U76,"1") = 17107;
HRbid(U76,"2") = 12637;
HRbid(U76,"3") = 11900;
HRbid(U76,"4") = 12000;

HRbid(U100,"1") = 12999;
HRbid(U100,"2") = 10700;
HRbid(U100,"3") = 10087;
HRbid(U100,"4") = 10000;

HRbid(U155,"1") = 11244;
HRbid(U155,"2") = 10053;
HRbid(U155,"3") =  9718;
HRbid(U155,"4") =  9600;

HRbid(U197,"1") = 10750;
HRbid(U197,"2") =  9850;
HRbid(U197,"3") =  9644;
HRbid(U197,"4") =  9600;

HRbid(U350,"1") = 10200;
HRbid(U350,"2") =  9600;
HRbid(U350,"3") =  9500;
HRbid(U350,"4") =  9500;

HRbid(U400,"1") = 12751;
HRbid(U400,"2") = 10825;
HRbid(U400,"3") = 10170;
HRbid(U400,"4") = 10000;

* Supply bid incremental heat rates
PARAMETER IHRbid(k,Nu,Nb) "supply bid incremental heat rates, Btu/kWh";
IHRbid(U12,"1") = 10179;
IHRbid(U12,"2") = 10330;
IHRbid(U12,"3") = 11668;
IHRbid(U12,"4") = 13219;

IHRbid(U20,"1") =  9859;
IHRbid(U20,"2") = 10139;
IHRbid(U20,"3") = 14272;
IHRbid(U20,"4") = 14427;

IHRbid(U76,"1") =  9548;
IHRbid(U76,"2") =  9966;
```

```
IHRbid(U76,"3") = 11576;
IHRbid(U76,"4") = 13311;

IHRbid(U100,"1") = 8089;
IHRbid(U100,"2") = 8708;
IHRbid(U100,"3") = 9420;
IHRbid(U100,"4") = 9877;

IHRbid(U155,"1") = 8265;
IHRbid(U155,"2") = 8541;
IHRbid(U155,"3") = 8900;
IHRbid(U155,"4") = 9381;

IHRbid(U197,"1") = 8348;
IHRbid(U197,"2") = 8833;
IHRbid(U197,"3") = 9225;
IHRbid(U197,"4") = 9620;

IHRbid(U350,"1") = 8402;
IHRbid(U350,"2") = 8896;
IHRbid(U350,"3") = 9244;
IHRbid(U350,"4") = 9768;

IHRbid(U400,"1") = 8848;
IHRbid(U400,"2") = 8965;
IHRbid(U400,"3") = 9210;
IHRbid(U400,"4") = 9438;

PARAMETER Pbid(k,Nu,Nb) "price of each offer to sell power, $/MWe";

* SPECIFY REAL AND REACTIVE POWER DEMAND INFORMATION
* --------------------------------------------------
PARAMETER
        Pd(k) "real power demand at kth bus, MW"
        / Abel    108
          Adams    97
          Adler   180
          Agricola 74
          Aiken    71
          Alber   136
          Alder   125
          Alger   171
          Ali     175
          Allen   195
          Arne    265
          Arnold  194
          Arthur  317
          Asser   100
          Astor   333
          Attar   181
```

```
          Attila  128
          /
;

PARAMETER
        Qd(k) "reactive power demand at each bus, MVar"
        / Abel     22
          Adams    20
          Adler    37
          Agricola 15
          Aiken    14
          Alber    28
          Alder    25
          Alger    35
          Ali      36
          Allen    40
          Arne     54
          Arnold   39
          Arthur   64
          Asser    20
          Astor    68
          Attar    37
          Attila   26
          /
;

* SPECIFY RESERVE POWER MARKET INFORMATION
* ------------------------------------------
SET mkt "markets into which generation units submit offers"
    / NRG "energy market"
      10SP "10-minute spinning reserve"
      10NS "10-minute non-spinning reserve"
      30NS "30-minute non-spinning reserve"
      /
;

SET rm(mkt)
    / 10SP "10-minute spinning reserve"
      10NS "10-minute non-spinning reserve"
      30NS "30-minute non-spinning reserve"
      /
;
ALIAS(rm,irm);

PARAMETER Rd(rm) "reserve market demand"
          / 10SP 200
            10NS 400
            30NS 600
            /
;
```

```
PARAMETER ReserveTime(rm) "time within which reserve unit must respond, minutes"
         / 10SP 10
           10NS 10
           30NS 30
           /
;

* DECLARE VARIABLES
* -----------------
VARIABLES
        z           "objective function, $"
        Pk(k)       "net real power injected at the kth bus, MW"
        Qk(k)       "net reactive power injected at the kth bus, MVAr"
        Qs(k,Nu)    "unit reactive power output, MVar"
        Ia(k)       "real component of current"
        Ib(k)       "imaginary component of current"
        theta(k)    "phase angle, radians"
;

POSITIVE VARIABLES
        Vmag(k)     "voltage magnitude"

        y(k,Nu,Nb)  "portion of unit bid that is used, MW"
        P(k,Nu)     "unit real power utilization, MW"
        Ps(k,Nu)    "unit real power injected into grid, MW"
        Pr(k,Nu,rm) "unit real power committed to reserve market rm, MW"
        xQsslack    "unsatisfied reactive power demand, MVAr"
        yQsslack    "unsatisfied reactive power demand, MVAr"

        Rs(rm)      "reserve market supply"
        Rslack(rm)  "shortfall in reserve market supply"
;

BINARY VARIABLES
        omega(k,Nu) "one if power plant is off, zero otherwise"
;

* VARIABLE BOUNDS AND INITIAL VALUES
* ----------------------------------
* specify unit real power bid upper bounds
y.up(u,Nb) = PSbid(u,Nb);

* specify unit real power upper bound
P.up(u) = Pmax(u);
Ps.up(u) = Pmax(u);
Pr.up(u,rm) = Pmax(u);

* specify unit reactive power upper and lower bounds
Qs.up(u) = Qmax(u);
```

```
Qs.lo(u) = Qmin(u);

* specify upper bound on Rslack
Rslack.up(rm) = Rd(rm);

* fix voltage magnitude at buses with regulation
Vmag.fx(kVR) = Vset(kVR);

* fix phase angle at slack bus to zero
theta.fx(slack) = 0;

* prevent nuclear power plants from participating in reserve market
Pr.fx(U400,rm) = 0;

* specify initial values for omega (may be overwritten if initial state exists)
omega.l(k,Nu) = 1$(Pbase(k,Nu) = 0 and Qbase(k,Nu) = 0);

* provide initial values for voltages and phase angles
Vmag.l(k) = 1.0;
theta.l(k) = 0;

* Set marginal cost of generation for each block of offered power, $/MWe
Pbid(ud,Nb) = IHRbid(ud,Nb)*FC(ud)/1000;

* Set price of imported power
Pslack = 1.1*smax((ud,Nb), Pbid(ud,Nb));

EQUATIONS
        zDef           "dispatch objective function defined"

        yDef(k,Nu)     "unit real power utilization disaggregation"
        PSupMax(k,Nu)  "maximum unit real power supply definition"
        PSupMin(k,Nu)  "minimum unit real power supply definition"

        PDef(k,Nu)     "unit real power utilization definition"
        QSupMax(k,Nu)  "maximum generator reactive power supply definition"
        QSupMin(k,Nu)  "minimum generator reactive power supply definition"
        PkDef(k)       "specify net real power availability"
        QkDef(k)       "net reactive power supply definition"

* Real and reactive power supply/demand balance
        IaDef(k)       "real component of current definition"
        IbDef(k)       "imaginary component of current definition"
        PVIDef(k)      "net real power definition"
        QVIDef(k)      "net reactive power definition"

* Reserve market
        Rs10SPDef(rm)  "10-minute spinning reserve market supply definition"
        Rs10NSDef(rm)  "10-minute non-spinning reserve market supply definition"
        Rs30NSDef(rm)  "30-minute non-spinning reserve market supply definition"
```

```
        RMDef(rm)      "reserve market definition"
        PrMax(k,Nu,rm) "reserve power limit based on generator ramp-rate"
;

*--------------------------------------------------------------------------------
* Objective function
*--------------------------------------------------------------------------------
zDef.. z =E= sum((ud,Nb), y(ud,Nb)*Pbid(ud,Nb)*L)
       + sum(k, Pslack*(xQsslack(k) + yQsslack(k)))
       + sum((rm), Pslack*Rslack(rm))
       ;

*--------------------------------------------------------------------------------
* Constraints
*--------------------------------------------------------------------------------
* specify unit real power utilization definition
yDef(ud).. P(ud) =E= sum(Nb, y(ud,Nb));

* Unit minimum and maximum real power output
PSupMax(u).. Ps(u) =L= (1 - omega(u))*Pmax(u);
PSupMin(u).. Ps(u) =G= (1 - omega(u))*Pmin(u);

* specify unit real power disaggregation
PDef(u).. P(u) =E= Ps(u) + sum(rm, Pr(u,rm));

* Unit minimum and maximum reactive power output
QSupMax(u).. Qs(u) =L= (1 - omega(u))*Qmax(u);
QSupMin(u).. Qs(u) =G= (1 - omega(u))*Qmin(u);

* specify bus net real power availability
PkDef(k).. Pk(k) =E= sum(Nu$u(k,Nu), Ps(k,Nu)) - Pd(k);

* specify net reactive power availability
QkDef(k).. Qk(k) =E= sum(Nu$u(k,Nu), Qs(k,Nu)) - Qd(k)
           + 100*power(Vmag(k), 2)$kSH(k)
           + xQsslack(k) - yQsslack(k)
           ;

* Exact power flow using trig functions
IaDef(k).. Ia(k) =E= sum(m, YG(k,m)*Vmag(m)*cos(theta(m))
             - YB(k,m)*Vmag(m)*sin(theta(m)));

IbDef(k).. Ib(k) =E= sum(m, YG(k,m)*Vmag(m)*sin(theta(m))
           + YB(k,m)*Vmag(m)*cos(theta(m)));

PVIDef(k).. Pk(k)/100 =E= Ia(k)*Vmag(k)*cos(theta(k))
            + Ib(k)*Vmag(k)*sin(theta(k));

QVIDef(k).. Qk(k)/100 =E= Ia(k)*Vmag(k)*sin(theta(k))
```

```
            - Ib(k)*Vmag(k)*cos(theta(k));

* Reserve power availabilty and requirement
Rs10SPDef(rm)$(sameas(rm,"10SP")).. Rs(rm) =E= sum(u, Pr(u,rm)*(1 - omega(u)));

Rs10NSDef(rm)$(sameas(rm,"10NS")).. Rs(rm) =E=
                                    Rs("10SP")
                                    + sum(u$(not TauStart(u)), Pr(u,rm)*omega(u));

Rs30NSDef(rm)$(sameas(rm,"30NS")).. Rs(rm) =E=
                                    Rs("10NS")
                                    + sum(u, Pr(u,rm)*(1 - omega(u)))
                                    + sum(u$(not TauStart(u)), Pr(u,rm)*omega(u));

RMDef(rm).. Rd(rm) =L= Rs(rm) + Rslack(rm);

* specify maximum reserve power for each discrete thermal unit
PrMax(ud,rm).. Pr(ud,rm) =L= DeltaP(ud)*ReserveTime(rm);

*=============================================================
* S O L V E   E C O N O M I C   D I S P A T C H
*=============================================================
option nlp=conopt;
option minlp=dicopt;
option limrow=30;

MODEL dispatch /
      zDef
      yDef, PDef, PkDef, QkDef
      PVIDef, QVIDef, IaDef, IbDef
      PSupMax, PSupMin, QSupMax, QSupMin
      Rs10SPDef, Rs10NSDef, Rs30NSDef, RMDef, PrMax
      /;

dispatch.optfile = 1;
```

Appendix F

Aspen Plus® Source Code

F.1 *Power plant*

```
; File:  power_plant_w_steam_extract.inp
; --------------------------------------
; This file simulates the part-load performance of a nominal 500 MW
; power plant.  Steam is extracted from the IP/LP crossover pipe,
; expanded through an auxiliary turbine, run through a condenser, and
; then reinjected into the cycle between the third and fourth
; feedwater preheaters.

;------------------------------------------------------------------------
; Report options
;------------------------------------------------------------------------
REPORT INPUT
STREAM-REPOR MOLEFLOW MASSFLOW PROPERTIES=ALL-SUBS

;------------------------------------------------------------------------
; Diagnostic specifications
;------------------------------------------------------------------------
DIAGNOSTICS
        HISTORY SIM-LEVEL=4 CONV-LEVEL=4
        MAX-PRINT SIM-LIMIT=9999

; This paragraph specifies time and error limits.
RUN-CONTROL MAX-TIME=84600 MAX-ERRORS=99999

; This paragraph will cause AspenPlus to include FORTRAN tracebacks in the
; history file.
SYS-OPTIONS TRACE=YES

; Indicate whether or not interactive simulation is desired.
SIMULATE INTERACTIVE=NO
```

```
;--------------------------------------------------------------------------
; Units
;--------------------------------------------------------------------------
IN-UNITS ENG POWER=KW
OUT-UNITS SI PRESSURE=kPa TEMPERATURE=C PDROP=kPa

;--------------------------------------------------------------------------
; Property Databanks
;--------------------------------------------------------------------------
DATABANKS ASPENPCD  / AQUEOUS  / SOLIDS  / INORGANIC  / PURE13
PROP-SOURCES ASPENPCD  / AQUEOUS  / SOLIDS  / INORGANIC / PURE13

;--------------------------------------------------------------------------
; Properties
;--------------------------------------------------------------------------

; Specify the property method to use in each section.
PROPERTIES PR-BM COAL
PROPERTIES STEAM-TA HP IP LP FPT FWP CNDR

PROP-SET ALL-SUBS VOLFLMX MASSVFRA MASSSFRA RHOMX MASSFLOW  &
        TEMP PRES UNITS='lb/cuft' SUBSTREAM=ALL
;  "Entire Stream Flows, Density, Phase Frac, T, P"

; This paragraph specifies the gross calorific value for each type of
; coal (Btu/lb) on a dry, mineral-matter free basis.
PROP-DATA HEAT
        IN-UNITS SI MASS-ENTHALPY="KJ/KG"
        PROP-LIST HCOMB
        PVAL COAL-IEA 27060        ; 11632
        PVAL COAL-PRB 27637        ; 11880
        PVAL COAL-USL 31768        ; 13656

PROP-SET VFLOW VOLFLMX

PROP-SET LPHASE MUMX RHOMX SIGMAMX VOLFLMX MASSFLMX PHASE=L &
         UNITS='KG/CUM' 'DYNE/CM'

PROP-SET VPHASE RHOMX VOLFLMX MASSFLMX PHASE=V UNITS='KG/CUM'

PROP-SET CPCVMX CPCVMX

DEF-STREAMS MIXCINC COAL
DEF-STREAMS CONVEN HP IP LP FPT FWP CNDR

;--------------------------------------------------------------------------
; Components
;--------------------------------------------------------------------------

COMPONENTS
```

```
; These components are involved in coal combustion.
        ; different types of coal
        COAL-IEA /
        COAL-PRB /
        COAL-USL /
        ASH /

        ; elements contained within coal
        C        C /
        H2        H2 /
        CL2         CL2 /
        HCL        HCL /
        S        S /
        H2O        H2O /

        ; components of air
        N2      N2 /
        O2        O2 /
        AR        AR /
        NE        NE /
        HE        HE-4 /
        CH4        CH4 /
        KR        KR /
        XE        XE /

        ; combustion products
        CO        CO /
        CO2     CO2 /
        NO        NO /
        NO2        NO2 /
        SO2        O2S /
        SO3        O3S

; This paragraph specifies the physical property method and model for each
; non-conventional component.

NC-COMPS COAL-IEA ULTANAL SULFANAL PROXANAL
NC-PROPS COAL-IEA ENTHALPY HCOALGEN 6 1 1 1 / DENSITY DCOALIGT

NC-COMPS COAL-PRB ULTANAL SULFANAL PROXANAL
NC-PROPS COAL-PRB ENTHALPY HCOALGEN 6 1 1 1 / DENSITY DCOALIGT

NC-COMPS COAL-USL ULTANAL SULFANAL PROXANAL
NC-PROPS COAL-USL ENTHALPY HCOALGEN 6 1 1 1 / DENSITY DCOALIGT

NC-COMPS ASH PROXANAL ULTANAL SULFANAL
NC-PROPS ASH ENTHALPY HCOALGEN / DENSITY DCOALIGT

;====================================================================
; BEGIN:  flowsheet specification
```

```
;======================================================================

; some globally defined blocks and streams
FLOWSHEET GLOBAL
        BLOCK "SHAFT"        IN="W_HP" "W_IP" "W_LP"        OUT="P_INTERN"

; globally defined streams
DEF-STREAMS WORK "P_INTERN"

; globally defined blocks
BLOCK SHAFT MIXER

;**********************************************************************
;                              COAL COMBUSTION
;**********************************************************************

;----------------------------------------------------------------------
; Flowsheet
;----------------------------------------------------------------------

FLOWSHEET COAL
    BLOCK DECOMP        IN=COAL-IN                      OUT=COAL-OUT "Q_DECOMP"
    BLOCK BURN                IN=COAL-OUT AIR "Q_DECOMP"        OUT=IN-BURN
    BLOCK HTRANS        IN=IN-BURN                      OUT=EXHAUST "Q_FURN"
    BLOCK SEPARATE        IN=EXHAUST                      OUT=FLUE-AHT SOLIDS
    BLOCK AIR-HEAT        IN=FLUE-AHT                      OUT=FLUE-SCR
    BLOCK SCRUB1        IN=FLUE-SCR                      OUT=WASTE1 IN-SCRUB
    BLOCK SCRUB2        IN=IN-SCRUB                      OUT=FLUE-GAS WASTE2

;----------------------------------------------------------------------
; Stream Specification
;----------------------------------------------------------------------

; specify the heat and work streams in the flowsheet
DEF-STREAMS HEAT "Q_DECOMP" "Q_FURN"

; The composition of air is taken from Cooper et al., p 653.
STREAM AIR TEMP=519 <F> PRES=101.3 <KPA> MOLE-FLOW=1.0
    MOLE-FRAC H2 .000050 / N2 78.090 / O2 20.940 / AR .930 /
        CO2 .0360 / NE .00180 / HE .000520 / CH4 .000170 /
        KR .00010 / NO2 .000030 / XE 8.0000E-06

STREAM COAL-IN
        SUBSTREAM NC TEMP=160 <F> PRES=101.30 <KPA> MASS-FLOW=10 <KG/SEC>
        MASS-FRAC COAL-IEA 0.0 / COAL-PRB 0.5 / COAL-USL 0.5

; PROXANAL                                ULTANAL
; water, moisture-included basis        ash (dry-basis)
; fixed carbon (dry-basis)                carbon (dry-basis)
; volatile matter (dry-basis)                hydrogen (dry-basis)
```

```
; ash (dry-basis)                       nitrogen (dry-basis)
;                                       chlorine (dry-basis)
;                                       sulfur (dry-basis)
;                                       oxygen (dry-basis)

; IEA tech specs coal...
        COMP-ATTR COAL-IEA ULTANAL ( 13.48 71.38 4.85 1.56 0.026 0.952 7.79 )
        COMP-ATTR COAL-IEA PROXANAL ( 9.50 86.52 0.0 13.48 )
        COMP-ATTR COAL-IEA SULFANAL ( 0.0 100 0.0 )

; Powder River basin coal
        COMP-ATTR COAL-PRB ULTANAL ( 7.1 69.4 4.9 1.0 0.000 0.4 17.2 )
        COMP-ATTR COAL-PRB PROXANAL ( 28.1 49.95 42.92 7.13 )
        COMP-ATTR COAL-PRB SULFANAL ( 0.0 100 0.0 )

; US low-sulphur coal
        COMP-ATTR COAL-USL ULTANAL ( 10.4 77.2 4.9 1.5 0.000 1.0 5.0 )
        COMP-ATTR COAL-USL PROXANAL ( 7.5 55.95 33.69 10.36 )
        COMP-ATTR COAL-USL SULFANAL ( 0.0 100 0.0 )

;-----------------------------------------------------------------------
; Block Section
;-----------------------------------------------------------------------

BLOCK DECOMP RYIELD
        PARAM TEMP=298.15 <K> PRES=0.0
        MASS-YIELD MIXED H2O .30 / NC ASH .10 / CISOLID C .10 / MIXED H2 .10 /
        N2 .10 / CL2 .10 / S .10 / O2 .10

        COMP-ATTR NC ASH PROXANAL ( 0.0 0.0 0.0 100 )
        COMP-ATTR NC ASH ULTANAL ( 100 0.0 0.0 0.0 0.0 0.0 0.0 )
        COMP-ATTR NC ASH SULFANAL ( 0.0 0.0 0.0 )

; This block decomposes the coal into a stream of its component elements.
CALCULATOR COAL-DEC
        DEFINE XC BLOCK-VAR BLOCK=DECOMP VARIABLE=YIELD SENTENCE=MASS-YIELD &
                ID1=CISOLID ID2=C
        DEFINE XH2 BLOCK-VAR BLOCK=DECOMP VARIABLE=YIELD SENTENCE=MASS-YIELD &
                ID1=MIXED ID2=H2
        DEFINE XN2 BLOCK-VAR BLOCK=DECOMP VARIABLE=YIELD SENTENCE=MASS-YIELD &
                ID1=MIXED ID2=N2
        DEFINE XCL2 BLOCK-VAR BLOCK=DECOMP VARIABLE=YIELD SENTENCE=MASS-YIELD &
                ID1=MIXED ID2=CL2
        DEFINE XS BLOCK-VAR BLOCK=DECOMP VARIABLE=YIELD SENTENCE=MASS-YIELD &
                ID1=MIXED ID2=S
        DEFINE XO2 BLOCK-VAR BLOCK=DECOMP VARIABLE=YIELD SENTENCE=MASS-YIELD &
                ID1=MIXED ID2=O2
        DEFINE XASH BLOCK-VAR BLOCK=DECOMP VARIABLE=YIELD SENTENCE=MASS-YIELD &
                ID1=NC ID2=ASH
        DEFINE XH2O BLOCK-VAR BLOCK=DECOMP VARIABLE=YIELD SENTENCE=MASS-YIELD &
```

```
                ID1=MIXED ID2=H2O

        DEFINE CIEA MASS-FLOW STREAM=COAL-IN SUBSTREAM=NC COMPONENT=COAL-IEA
        DEFINE CPRB MASS-FLOW STREAM=COAL-IN SUBSTREAM=NC COMPONENT=COAL-PRB
        DEFINE CUSL MASS-FLOW STREAM=COAL-IN SUBSTREAM=NC COMPONENT=COAL-USL

; ultimate analyses of the three coals
        VECTOR-DEF UIEA COMP-ATTR STREAM=COAL-IN SUBSTREAM=NC &
                COMPONENT=COAL-IEA ATTRIBUTE=ULTANAL
        VECTOR-DEF UPRB COMP-ATTR STREAM=COAL-IN SUBSTREAM=NC &
                COMPONENT=COAL-PRB ATTRIBUTE=ULTANAL
        VECTOR-DEF UUSL COMP-ATTR STREAM=COAL-IN SUBSTREAM=NC &
                COMPONENT=COAL-USL ATTRIBUTE=ULTANAL

; proximate analyses of the three coals
        VECTOR-DEF PIEA COMP-ATTR STREAM=COAL-IN SUBSTREAM=NC &
                COMPONENT=COAL-IEA ATTRIBUTE=PROXANAL
        VECTOR-DEF PPRB COMP-ATTR STREAM=COAL-IN SUBSTREAM=NC &
                COMPONENT=COAL-PRB ATTRIBUTE=PROXANAL
        VECTOR-DEF PUSL COMP-ATTR STREAM=COAL-IN SUBSTREAM=NC &
                COMPONENT=COAL-USL ATTRIBUTE=PROXANAL

; Stupid fucking Aspen Plus fortran interpreter can't handle lines >
; 72 characters so I have to break up the arithmetic into bite-sized pieces...

; COAL => total coal mass flowrate
F       COAL = CIEA + CPRB + CUSL

; THE VECTOR U___ CONTAINS THE MASS FRACTIONS OF THE COAL CONSTITUENTS
; ON A DRY-BASIS WHEREAS THE COAL FLOW RATE ON A WET-BASIS.  THE factor
; DRY___ is used to make this conversion.
;
; DRY___ => coal "dry" fraction (i.e. 1 - moisture fraction)
; P___(1) => coal moisture content, wt%
F       DRYIEA = (100 - PIEA(1)) / 100
F       DRYPRB = (100 - PPRB(1)) / 100
F       DRYUSL = (100 - PUSL(1)) / 100

F       ASH1 = (UIEA(1) / 100) * DRYIEA * CIEA
F       ASH2 = (UPRB(1) / 100) * DRYPRB * CPRB
F       ASH3 = (UUSL(1) / 100) * DRYUSL * CUSL
F       XASH = (ASH1 + ASH2 + ASH3) / COAL

F       C1 = (UIEA(2) / 100) * DRYIEA * CIEA
F       C2 = (UPRB(2) / 100) * DRYPRB * CPRB
F       C3 = (UUSL(2) / 100) * DRYUSL * CUSL
F       XC = (C1 + C2 + C3) / COAL

F       HYDRO1 = (UIEA(3) / 100) * DRYIEA * CIEA
F       HYDRO2 = (UPRB(3) / 100) * DRYPRB * CPRB
```

```
F       HYDRO3 = (UUSL(3) / 100) * DRYUSL * CUSL
F       XH2 = (HYDRO1 + HYDRO2 + HYDRO3) / COAL

F       FITRO1 = (UIEA(4) / 100) * DRYIEA * CIEA
F       FITRO2 = (UPRB(4) / 100) * DRYPRB * CPRB
F       FITRO3 = (UUSL(4) / 100) * DRYUSL * CUSL
F       XN2 = (FITRO1 + FITRO2 + FITRO3) / COAL

F       CHLOR1 = (UIEA(5) / 100) * DRYIEA * CIEA
F       CHLOR2 = (UPRB(5) / 100) * DRYPRB * CPRB
F       CHLOR3 = (UUSL(5) / 100) * DRYUSL * CUSL
F       XCL2 = (CHLOR1 + CHLOR2 + CHLOR3) / COAL

F       SULFR1 = (UIEA(6) / 100) * DRYIEA * CIEA
F       SULFR2 = (UPRB(6) / 100) * DRYPRB * CPRB
F       SULFR3 = (UUSL(6) / 100) * DRYUSL * CUSL
F       XS = (SULFR1 + SULFR2 + SULFR3) / COAL

F       OXYGN1 = (UIEA(7) / 100) * DRYIEA * CIEA
F       OXYGN2 = (UPRB(7) / 100) * DRYPRB * CPRB
F       OXYGN3 = (UUSL(7) / 100) * DRYUSL * CUSL
F       XO2 = (OXYGN1 + OXYGN2 + OXYGN3) / COAL

F       XH2O=(PIEA(1)*CIEA+PPRB(1)*CPRB+PUSL(1)*CUSL)/(COAL*100)

C       WRITE(NRPT, *) XH2O
C       WRITE(NRPT, *) XH2
C       WRITE(NRPT, *) XN2
C       WRITE(NRPT, *) XCL2
C       WRITE(NRPT, *) XS
C       WRITE(NRPT, *) XO2
C       WRITE(NRPT, *) XC
C       WRITE(NRPT, *) XASH

        EXECUTE BEFORE BLOCK DECOMP

BLOCK BURN RGIBBS
        PARAM PRES=101.3 <kPa>
        PROD H2O / C SS / H2 / N2 / CL2 / HCL / S / O2 / AR /
                CO / CO2 / NE / HE / CH4 / KR / XE / NO /
                NO2 / SO2 / SO3

; This block adjusts the air flow rate such that there is 20 mol %
; excess oxygen present during the coal combustion.
CALCULATOR AIR-FLOW
        DEFINE AIR STREAM-VAR STREAM=AIR SUBSTREAM=MIXED VARIABLE=MOLE-FLOW
        DEFINE O2COAL MOLE-FLOW STREAM=COAL-OUT SUBSTREAM=MIXED COMPONENT=O2
        DEFINE C MOLE-FLOW STREAM=COAL-OUT SUBSTREAM=CISOLID COMPONENT=C
        DEFINE N2 MOLE-FLOW STREAM=COAL-OUT SUBSTREAM=MIXED COMPONENT=N2
        DEFINE H2 MOLE-FLOW STREAM=COAL-OUT SUBSTREAM=MIXED COMPONENT=H2
```

```
        DEFINE S MOLE-FLOW STREAM=COAL-OUT SUBSTREAM=MIXED COMPONENT=S

F       XS = 0.21
; CMIXED IS THE MOLE FLOW OF CARBON IN THE COAL-OUT MIXED SUBSTREAM
F       AIR = ((C + 2*N2 + 0.5*H2 + S)* (1 + XS) - O2COAL) / 0.2094

        EXECUTE BEFORE BLOCK BURN

BLOCK HTRANS HEATER
        PARAM TEMP=320 <C> PRES=0.0 NPHASE=2 ; Neill and Gunter
;        PARAM TEMP=622 <F> PRES=0.0 NPHASE=2 ; Boiler design data

BLOCK SEPARATE SSPLIT
        FRAC MIXED FLUE-AHT 1.0
        FRAC CISOLID FLUE-AHT 0.0
        FRAC NC FLUE-AHT 0.0

; The air heater outlet temperature is taken from the Neil and Gunter
; study.
BLOCK AIR-HEAT HEATER
;        PARAM TEMP=134 <C>
        PARAM TEMP=247 <F>

BLOCK SCRUB1 SEP2
        FRAC STREAM=IN-SCRUB COMPS=N2 CO2 H2O FRACS=1 1 1
        FRAC STREAM=WASTE1 COMPS=H2 S O2 AR NE HE KR XE CO NO NO2 SO2 SO3 &
                          FRACS= 1 1  1  1  1  1  1  1  1  1   1   1   1

BLOCK SCRUB2 FLASH2
        PARAM TEMP=40 <C> PRES=0

;***********************************************************************
;                         HP turbine and FWP A
;***********************************************************************

;-----------------------------------------------------------------------
; Flowsheet
;-----------------------------------------------------------------------

FLOWSHEET HP
        BLOCK BOIL        IN=H2O-BOIL         OUT="ST_MAIN" "Q_BOIL"
        BLOCK "HP_SEP1"        IN="ST_MAIN"        OUT=ST-FPT1 ST-HPX
        BLOCK VALVE1        IN=ST-HPX        OUT=ST-HP
        BLOCK HP1        IN=ST-HP        OUT="HP_1X" "W_HP"
        BLOCK "HP_SEP2"        IN="HP_1X"        OUT=ST-REHT ST-FWPA
        BLOCK REHT        IN=ST-REHT        OUT=ST-IPX "Q_REHT"

;-----------------------------------------------------------------------
; Streams
;-----------------------------------------------------------------------
```

```
; specify the heat and work streams in the flowsheet
DEF-STREAMS HEAT "Q_BOIL" "Q_REHT"
DEF-STREAMS WORK "W_HP"

STREAM H2O-BOIL TEMP=487.91 PRES=2700 MASS-FLOW=3358670
        MOLE-FRAC H2O 1

;-----------------------------------------------------------------------
; Blocks
;-----------------------------------------------------------------------

BLOCK VALVE1 VALVE
        PARAM P-OUT=2236.19

; This design spec maintains constant volumetric flow rate into HP section
DESIGN-SPEC PRESOUT1
        DEFINE F STREAM-PROP STREAM=ST-HP PROPERTY=VFLOW

        SPEC "F" TO "1.155e6"
        TOL-SPEC "0.001e6"

        ; NB:  @ 50% plant load, the ST-HP pressure is 1080.68 psia
        VARY BLOCK-VAR BLOCK=VALVE1 SENTENCE=PARAM VARIABLE=P-OUT
;        LIMITS "900" "2365"
        LIMITS "0" "2365"

BLOCK "HP_SEP1" FSPLIT
        MASS-FLOW ST-FPT1 7000

BLOCK "HP_SEP2" FSPLIT
        MASS-FLOW ST-FWPA 334659

CALCULATOR "C_HP_SEP"
        DESCRIPTION "Specify HP steam extracted for feedwater preheating"

        DEFINE FREF STREAM-VAR STREAM=ST-HP VARIABLE=MASS-FLOW
        DEFINE FA BLOCK-VAR BLOCK="HP_SEP2" SENTENCE=MASS-FLOW VARIABLE=FLOW &
                ID1=ST-FWPA

F       FA = 0.1231 * FREF - 0.7894e5

        READ-VARS FREF
        WRITE-VARS FA

BLOCK REHT HEATER
        PARAM TEMP=1000

; This design spec maintains outlet temperature of 1000 F from VALVE2
DESIGN-SPEC TEMPOUT
        DEFINE T STREAM-VAR STREAM=ST-IP VARIABLE=TEMP
```

```
        SPEC "T" TO "1000"
        TOL-SPEC "0.5"

        VARY BLOCK-VAR BLOCK=REHT SENTENCE=PARAM VARIABLE=TEMP
        LIMITS "1000" "1100"

BLOCK BOIL HEATER
        PARAM TEMP=1000 PRES=2365

BLOCK HP1 COMPR
        PARAM TYPE=ISENTROPIC PRATIO=0.282 SEFF=0.904

CALCULATOR "C_HP1_P"
        DESCRIPTION "Specify the pressure ratio of HP1"

        DEFINE FLOW STREAM-VAR STREAM=ST-HP VARIABLE=MASS-FLOW
        DEFINE PRATIO BLOCK-VAR BLOCK=HP1 SENTENCE=PARAM VARIABLE=PRATIO

F       PRATIO = -0.4820e-02 * (FLOW/1E6) + 0.2944

        EXECUTE BEFORE HP1

;************************************************************************
;                    IP turbine and FWP B, C, and D
;************************************************************************

;------------------------------------------------------------------------
; Flowsheet
;------------------------------------------------------------------------

FLOWSHEET IP
        BLOCK VALVE2        IN=ST-IPX               OUT=ST-IP
        BLOCK "IP_SEP1"        IN=ST-IP               OUT="IP_02" "IP_03"
        BLOCK IP2        IN="IP_02"               OUT="IP_2X" "W_IP2"
        BLOCK "IP_SEP2"        IN="IP_2X"               OUT=ST-FWPC "IP_12"
        BLOCK IP1        IN="IP_12"               OUT=IP-1LP "W_IP1"
        BLOCK IP3        IN="IP_03"               OUT="IP_3X1" "W_IP3"
        BLOCK "IP_SEP3"        IN="IP_3X1"               OUT="IP_3X2" "IP_34"
        BLOCK IP4        IN="IP_34"               OUT="IP_4X" "W_IP4"
        BLOCK "IP_SEP4"        IN="IP_3X2"               OUT="ST-FPT2" "ST-FWPB"
        BLOCK "IP_SEP5"        IN="IP_4X"               OUT=IP-4LP ST-FWPD
        BLOCK "IP_COMB"        IN=IP-1LP IP-4LP        OUT=ST-LPX
        BLOCK "ST_EXTCT" IN=ST-LPX               OUT=ST-AUX ST-LP
        BLOCK "IP_SHAFT" IN="W_IP1" "W_IP2" "W_IP3" "W_IP4"        OUT="W_IP"

        ; Auxiliary turbine stuff
        BLOCK "AUX_TURB" IN=ST-AUX               OUT=ST-DHEAT "P_AUX"
        BLOCK DSUPRHTR        IN=ST-DHEAT               OUT=ST-REB
        BLOCK REBOILER        IN=ST-REB               OUT=H2O-REBP "Q_REB"
```

```
        BLOCK "REB_PUMP" IN=H2O-REBP                OUT=H2O-REB "P_REBP"

;-----------------------------------------------------------------------
; Streams
;-----------------------------------------------------------------------
DEF-STREAMS WORK "W_IP1" "W_IP2" "W_IP3" "W_IP4" "W_IP" "P_REBP" "P_AUX"

DEF-STREAMS HEAT "Q_REB"

;-----------------------------------------------------------------------
; Blocks
;-----------------------------------------------------------------------

BLOCK VALVE2 VALVE
        PARAM P-OUT=560.18

DESIGN-SPEC PRESOUT2
        DEFINE F STREAM-PROP STREAM=ST-IP PROPERTY=VFLOW

        SPEC "F" TO "4.531e6"
        TOL-SPEC "0.009e6"

        ; NB:  @ 50% plant load, the ST-IP pressure is 260 psia
        VARY BLOCK-VAR BLOCK=VALVE2 SENTENCE=PARAM VARIABLE=P-OUT
;        LIMITS "250" "600"
        LIMITS "0" "600"

BLOCK "IP_COMB" MIXER

BLOCK "IP_SEP1" FSPLIT
        FRAC "IP_02" 0.50

BLOCK "IP_SEP2" FSPLIT
        MASS-FLOW "ST-FWPC" 128853

BLOCK "IP_SEP3" FSPLIT
        MASS-FLOW "IP_3X2" 227662 ;sum of ST-FWPB and ST-FPT2

BLOCK "IP_SEP4" FSPLIT
        MASS-FLOW ST-FWPB 143920

BLOCK "IP_SEP5" FSPLIT
        MASS-FLOW ST-FWPD 136359

BLOCK "ST_EXTCT" FSPLIT
        FRAC ST-AUX 0.0

CALCULATOR "C_IP_SEP"
        DESCRIPTION "Specify IP steam extracted for feedwater preheating"
```

```
        DEFINE FREF STREAM-VAR STREAM=ST-IP VARIABLE=MASS-FLOW

        DEFINE FBP BLOCK-VAR BLOCK="IP_SEP3" SENTENCE=MASS-FLOW VARIABLE=FLOW &
                ID1="IP_3X2"
        DEFINE FB BLOCK-VAR BLOCK="IP_SEP4" SENTENCE=MASS-FLOW VARIABLE=FLOW &
                ID1=ST-FWPB
        DEFINE FD BLOCK-VAR BLOCK="IP_SEP5" SENTENCE=MASS-FLOW VARIABLE=FLOW &
                ID1=ST-FWPD

F       FB = 0.5389e-1 * FREF - 0.1685e5
F       FP = 0.2684e-1 * FREF + 0.1948e4
F       FBP = FB + FP
F       FC = 0.5095e-1 * FREF - 0.2440e5
F       FD = 0.5236e-1 * FREF - 0.2077e5


        READ-VARS FREF
        WRITE-VARS FB FBP FD

DESIGN-SPEC "C_IPSEP2"
        DEFINE Q BLOCK-VAR BLOCK="FWP_C-C" SENTENCE=RESULTS VARIABLE=NET-DUTY

        SPEC "Q" TO "0"
        TOL-SPEC "1e4"

        VARY BLOCK-VAR BLOCK="IP_SEP2" SENTENCE=MASS-FLOW VARIABLE=FLOW &
                ID1=ST-FWPC
        LIMITS "50000" "150000"

BLOCK IP1 COMPR
        PARAM TYPE=ISENTROPIC PRATIO=0.517 SEFF=0.902 NPHASE=2

BLOCK IP2 COMPR
        PARAM TYPE=ISENTROPIC PRATIO=0.233 SEFF=0.910 NPHASE=2

BLOCK IP3 COMPR
        PARAM TYPE=ISENTROPIC PRATIO=0.455 SEFF=0.895 NPHASE=2

BLOCK IP4 COMPR
        PARAM TYPE=ISENTROPIC PRATIO=0.265 SEFF=0.914 NPHASE=2

BLOCK "IP_SHAFT" MIXER

BLOCK "AUX_TURB" COMPR
        PARAM TYPE=ISENTROPIC PRATIO=0.3545 SEFF=0.90 MEFF=0.99 NPHASE=2

BLOCK DSUPRHTR HEATER
      PARAM PRES=0 VFRAC=1.0

BLOCK REBOILER HEATER
```

```
        IN-UNITS SI PRESSURE=kPa TEMPERATURE=C PDROP=kPa
        PARAM DELT=0 VFRAC=0

BLOCK "REB_PUMP" PUMP
        PARAM PRES=128 <psi>

;**********************************************************************
;                    LP turbine and FWP E, F, AND G
;**********************************************************************

;----------------------------------------------------------------------
; Flowsheet
;----------------------------------------------------------------------

FLOWSHEET LP
        BLOCK "LP_SEP1"        IN=ST-LP        OUT="LP_012" "LP_056"
        BLOCK "LP_SEP2"        IN="LP_012"        OUT="LP_01" "LP_02"
        BLOCK LP1        IN="LP_01"        OUT=ST-FWPF "W_LP1"
        BLOCK LP2        IN="LP_02"        OUT="LP_2X" "W_LP2"
        BLOCK "LP_SEP3"        IN="LP_2X"        OUT="LP_23" ST-2FWPG
        BLOCK LP3        IN="LP_23"        OUT="LP_3CR" "W_LP3"
        BLOCK "LP_SEP4"        IN="LP_056"        OUT="LP_05" "LP_06"
        BLOCK LP6        IN="LP_06"        OUT=ST-FWPE "W_LP6"
        BLOCK LP5        IN="LP_05"        OUT="LP_5X" "W_LP5"
        BLOCK "LP_SEP5"        IN="LP_5X"        OUT="LP_45" ST-5FWPG
        BLOCK LP4        IN="LP_45"        OUT="LP_4CR" "W_LP4"
        BLOCK "LP_COMB1"        IN="LP_3CR" "LP_4CR"        OUT=ST-CNDR
        BLOCK "LP_COMB2"        IN=ST-2FWPG ST-5FWPG        OUT=ST-FWPG
        BLOCK "LP_SHAFT"        IN="W_LP1" "W_LP2" "W_LP3" "W_LP4" &
                "W_LP5" "W_LP6"        OUT="W_LP"
;----------------------------------------------------------------------
; Streams
;----------------------------------------------------------------------

DEF-STREAMS WORK "W_LP1" "W_LP2" "W_LP3" "W_LP4" "W_LP5" "W_LP6" "W_LP"

; specify the material streams in the flowsheet

;----------------------------------------------------------------------
; Blocks
;----------------------------------------------------------------------

BLOCK "LP_COMB1" MIXER

BLOCK "LP_COMB2" MIXER

BLOCK "LP_SEP1" FSPLIT
        FRAC "LP_012" 0.50

BLOCK "LP_SEP2" FSPLIT
```

```
        MASS-FLOW "LP_01" 89306 ; flow of ST-FWPF

BLOCK "LP_SEP3" FSPLIT
        MASS-FLOW "ST-2FWPG" 63085 ; half of ST-FWPG

BLOCK "LP_SEP4" FSPLIT
        MASS-FLOW "LP_06" 135578 ; flow of ST-FWPE

BLOCK "LP_SEP5" FSPLIT
        MASS-FLOW "ST-5FWPG" 63086 ; other half of ST-FWPG

CALCULATOR "C_LP_SEP"
        DESCRIPTION "Specify LP steam extracted for feedwater preheating"

        DEFINE FREF STREAM-VAR STREAM=ST-LP VARIABLE=MASS-FLOW

        DEFINE FE BLOCK-VAR BLOCK="LP_SEP4" SENTENCE=MASS-FLOW VARIABLE=FLOW &
                ID1="LP_06"
        DEFINE FF BLOCK-VAR BLOCK="LP_SEP2" SENTENCE=MASS-FLOW VARIABLE=FLOW &
                ID1="LP_01"
        DEFINE FG2 BLOCK-VAR BLOCK="LP_SEP3" SENTENCE=MASS-FLOW VARIABLE=FLOW &
                ID1=ST-2FWPG
        DEFINE FG5 BLOCK-VAR BLOCK="LP_SEP5" SENTENCE=MASS-FLOW VARIABLE=FLOW &
                ID1=ST-5FWPG

F       FE = 0.6311e-1 * FREF - 0.2228e5
F       FF = 0.4162e-1 * FREF - 0.1475e5
F       FG = 0.6170e-1 * FREF - 0.2538e5
F       FG2 = FG / 2
F       FG5 = FG2

        READ-VARS FREF
        WRITE-VARS FE FF FG2 FG5

BLOCK LP1 COMPR
        PARAM TYPE=ISENTROPIC PRATIO=0.151 SEFF=0.910 NPHASE=2

BLOCK LP2 COMPR
        PARAM TYPE=ISENTROPIC PRATIO=0.068 SEFF=0.907 NPHASE=2

BLOCK LP3 COMPR
        PARAM TYPE=ISENTROPIC PRES=0.686 SEFF=0.640 NPHASE=2

BLOCK LP4 COMPR
        PARAM TYPE=ISENTROPIC PRES=0.686 SEFF=0.640 NPHASE=2

CALCULATOR "C_LP_P"
        DESCRIPTION "Set outlet pressure of LP3 and LP4 equal to the condenser"
        DEFINE PCOND BLOCK-VAR BLOCK=CONDENSE SENTENCE=PARAM VARIABLE=PRES
        DEFINE PLP3 BLOCK-VAR BLOCK=LP3 SENTENCE=PARAM VARIABLE=PRES
```

```
        DEFINE PLP4 BLOCK-VAR BLOCK=LP4 SENTENCE=PARAM VARIABLE=PRES

F       PLP3 = PCOND
F       PLP4 = PCOND

        EXECUTE BEFORE LP3

CALCULATOR "C_LP_EFF"
        DESCRIPTION "Use correlation to set LP3 and LP4 isentropic efficiency"

        DEFINE QOUT STREAM-PROP STREAM=ST-CNDR PROPERTY=VFLOW
        DEFINE SEFF3 BLOCK-VAR BLOCK=LP3 SENTENCE=PARAM VARIABLE=SEFF
        DEFINE SEFF4 BLOCK-VAR BLOCK=LP4 SENTENCE=PARAM VARIABLE=SEFF

F       ETA = -0.4016 * (QOUT/1e9) + 0.9867
F       SEFF3 = ETA
F       SEFF4 = ETA

        EXECUTE BEFORE CONDENSE
        READ-VARS QOUT
C        WRITE-VARS SEFF3 SEFF4

BLOCK LP5 COMPR
        PARAM TYPE=ISENTROPIC PRATIO=0.068 SEFF=0.907 NPHASE=2

BLOCK LP6 COMPR
        PARAM TYPE=ISENTROPIC PRATIO=0.435 SEFF=0.901 NPHASE=2

BLOCK "LP_SHAFT" MIXER


;*********************************************************************
;                        Feedwater pump turbine
;*********************************************************************

;---------------------------------------------------------------------
; Flowsheet
;---------------------------------------------------------------------

FLOWSHEET FPT
        BLOCK FPT1        IN=ST-FPT1        OUT="FPT_1X" "W_FPT1"
        BLOCK "FPT_COMB"        IN=ST-FPT2 "FPT_1X"        OUT="FPT_12"
        BLOCK FPT2        IN="FPT_12"        OUT=STFPT-CN "W_FPT2"
        BLOCK "FP_SHAFT"        IN="W_FPT1" "W_FPT2"        OUT="W_FPT"

;---------------------------------------------------------------------
; Streams
;---------------------------------------------------------------------

DEF-STREAMS WORK "W_FPT1" "W_FPT2" "W_FPT"
```

```
;----------------------------------------------------------------------
; Blocks
;----------------------------------------------------------------------

BLOCK "FPT_COMB" MIXER

BLOCK FPT1 COMPR
        PARAM TYPE=ISENTROPIC PRES=100 SEFF=0.153 NPHASE=2

BLOCK FPT2 COMPR
        PARAM TYPE=ISENTROPIC PRES=0.686 SEFF=0.795 NPHASE=2

CALCULATOR "C_FPT_P"
        DESCRIPTION "Specifies the outlet pressure of FPT1 and FPT2"

        DEFINE PREF STREAM-VAR STREAM=ST-FPT2 VARIABLE=PRES
        DEFINE PCOND BLOCK-VAR BLOCK=CONDENSE SENTENCE=PARAM VARIABLE=PRES
        DEFINE PFPT1 BLOCK-VAR BLOCK=FPT1 SENTENCE=PARAM VARIABLE=PRES
        DEFINE PFPT2 BLOCK-VAR BLOCK=FPT2 SENTENCE=PARAM VARIABLE=PRES

F       PFTP1 = PREF
F       PFTP2 = PCOND

        READ-VARS PREF PCOND
        WRITE-VARS PFPT1 PFPT2

BLOCK "FP_SHAFT" MIXER

;**********************************************************************
;                      Feed water preheater train
;**********************************************************************

;----------------------------------------------------------------------
; Flowsheet
;----------------------------------------------------------------------

FLOWSHEET FWP
        BLOCK "FWP_A-H"        IN=ST-FWPA Q-FWPA        OUT="STFWP_AB"
        BLOCK "FWP_A-C"        IN=H2O-FWPA        OUT=H2O-BOIL Q-FWPA

        BLOCK "FWP_B-H"        IN=ST-FWPB "STFWP_AB" Q-FWPB        OUT="STFWP_BC"
        BLOCK "FWP_B-C"        IN=H2O-FWPB        OUT=H2O-FWPA Q-FWPB

        ; dearator and pump
        BLOCK "FWP_C"        IN="STFWP_BC" ST-FWPC H2O-FWPC        OUT=H2-PUMP
        BLOCK FWPUMP2        IN=H2-PUMP "W_FPT"        OUT=IN-PUMP
        BLOCK "FWP_C-C"        IN=IN-PUMP        OUT=H2O-FWPB

        BLOCK "FWP_D-H"        IN=ST-FWPD Q-FWPD        OUT="STFWP_DE"
```

```
        BLOCK "FWP_D-C"        IN=H2O-FWPD H2O-REB        OUT=H2O-FWPC Q-FWPD

        BLOCK "FWP_E-H"        IN=ST-FWPE "STFWP_DE" Q-FWPE        OUT="STFWP_EF"
        BLOCK "FWP_E-C"        IN=H2O-FWPE        OUT=H2O-FWPD Q-FWPE

        BLOCK "FWP_F-H"        IN=ST-FWPF "STFWP_EF" Q-FWPF        OUT="STFWP_FG"
        BLOCK "FWP_F-C"        IN=H2O-FWPF        OUT=H2O-FWPE Q-FWPF

        BLOCK "FWP_G-H"        IN=ST-FWPG "STFWP_FG" Q-FWPG        OUT="STFWP_GC"
        BLOCK "FWP_G-C"        IN=H2O-FWPG        OUT=H2O-FWPF Q-FWPG

;------------------------------------------------------------------------
; Streams
;------------------------------------------------------------------------

; I need to define the heat streams in this flowsheet section
DEF-STREAMS HEAT Q-FWPA Q-FWPB Q-FWPD Q-FWPE Q-FWPF Q-FWPG

;------------------------------------------------------------------------
; Blocks
;------------------------------------------------------------------------

; feed water preheater "A"
BLOCK "FWP_A-H" HEATER
        PARAM PRES=0

BLOCK "FWP_A-C" HEATER
        PARAM TEMP=487.91

CALCULATOR "T_FWPA"
        DESCRIPTION "Calculate the cold-side outlet temperature for FWPA"

        DEFINE FFWPA STREAM-VAR STREAM=H2O-FWPA VARIABLE=MASS-FLOW
        DEFINE TFWPA BLOCK-VAR BLOCK="FWP_A-C" SENTENCE=PARAM VARIABLE=TEMP

F       TFWPA = 0.8546e2 * dlog(FFWPA) - 0.7963e3

        EXECUTE BEFORE "FWP_A-C"

; feed water preheater "B"
BLOCK "FWP_B-H" HEATER
        PARAM PRES=0

BLOCK "FWP_B-C" HEATER
        PARAM TEMP=400.56

CALCULATOR "T_FWPB"
        DESCRIPTION "Calculate the cold-side outlet temperature for FWPB"

        DEFINE FFWPB STREAM-VAR STREAM=H2O-FWPB VARIABLE=MASS-FLOW
```

```
        DEFINE TFWPB BLOCK-VAR BLOCK="FWP_B-C" SENTENCE=PARAM VARIABLE=TEMP
F       TFWPB = 0.6840e2 * dlog(FFWPB) - 0.6272e3

        EXECUTE BEFORE "FWP_B-C"

; feed water preheater "C" (dearator) and feed water pump
BLOCK "FWP_C" MIXER

BLOCK FWPUMP2 PUMP
;        PARAM PRES=2700

BLOCK "FWP_C-C" HEATER
        PARAM TEMP=351.19

CALCULATOR "T_FWPC"
        DESCRIPTION "Calculate the cold-side outlet temperature for FWPC"

        ; using the outlet mass flow rate is easier than having to sum
        ; the three input mass flow rates
        DEFINE FFWPC STREAM-VAR STREAM=IN-PUMP VARIABLE=MASS-FLOW
        DEFINE TFWPC BLOCK-VAR BLOCK="FWP_C-C" SENTENCE=PARAM VARIABLE=TEMP

F       TFWPC = 0.6468e2 * dlog(FFWPC) - 0.6212e3

        EXECUTE BEFORE "FWP_C-C"

; feed water preheater "D"
BLOCK "FWP_D-H" HEATER
        PARAM PRES=0

BLOCK "FWP_D-C" HEATER
        PARAM TEMP=293.20

CALCULATOR "T_FWPD"
        DESCRIPTION "Calculate the cold-side outlet temperature for FWPD"

        DEFINE FFWPD STREAM-VAR STREAM=H2O-FWPD VARIABLE=MASS-FLOW
        DEFINE FREB STREAM-VAR STREAM=H2O-REB VARIABLE=MASS-FLOW
        DEFINE TFWPD BLOCK-VAR BLOCK="FWP_D-C" SENTENCE=PARAM VARIABLE=TEMP

F       TFWPD = 0.5537e2 * dlog(FFWPD + FREB) - 0.5274e3

        EXECUTE BEFORE "FWP_D-C"

; feed water preheater "E"
BLOCK "FWP_E-H" HEATER
        PARAM PRES=0

BLOCK "FWP_E-C" HEATER
        PARAM TEMP=241.55
```

F.2 *Absorber* with packing

```
; File: absorber_packing_sqp.inp
; -----------------------------
; This file simulates the absorber of the MEA absorption process.
; RateSep, in rating mode and using random packing, is used to model
; the Absorber.  The design of the Absorber (i.e., selection of the
; diameter is achieved by solving an optimization problem with the SQP method.

;----------------------------------------------------------------------
; Report options
;----------------------------------------------------------------------

STREAM-REPOR MOLEFLOW MASSFLOW

;----------------------------------------------------------------------
; Diagnostic specifications
;----------------------------------------------------------------------

DIAGNOSTICS
        HISTORY SIM-LEVEL=4 CONV-LEVEL=4
        MAX-PRINT SIM-LIMIT=99999

; This paragraph specifies time and error limits.
RUN-CONTROL MAX-TIME=86400 MAX-ERRORS=1000

; This paragraph will case AspenPlus to include FORTRAN tracebacks in the
; history file.
SYS-OPTIONS TRACE=YES

;----------------------------------------------------------------------
; Units
;----------------------------------------------------------------------

IN-UNITS SI PRESSURE=kPa TEMPERATURE=C PDROP='N/sqm'

;----------------------------------------------------------------------
; Property Databanks
;----------------------------------------------------------------------

DATABANKS ASPENPCD / AQUEOUS / SOLIDS / INORGANIC / PURE13

PROP-SOURCES ASPENPCD / AQUEOUS / SOLIDS / INORGANIC / PURE13

;----------------------------------------------------------------------
; Properties
;----------------------------------------------------------------------

PROPERTIES ELECNRTL HENRY-COMPS=MEA-CO2 CHEMISTRY=MEA-CO2 TRUE-COMPS=YES
```

```
PROP-SET LPHASE MUMX RHOMX SIGMAMX VOLFLMX MASSFLMX PHASE=L &
         UNITS='KG/CUM' 'DYNE/CM'

PROP-SET VPHASE RHOMX VOLFLMX MASSFLMX PHASE=V UNITS='KG/CUM'

PROP-DATA HENRY-1
    IN-UNITS MET VOLUME-FLOW='cum/hr' ENTHALPY-FLO='Gcal/hr'  &
        HEAT-TRANS-C='kcal/hr-sqm-K' PRESSURE=bar TEMPERATURE=C  &
        VOLUME=cum DELTA-T=C HEAD=meter MOLE-DENSITY='kmol/cum'  &
        MASS-DENSITY='kg/cum' MOLE-ENTHALP='kcal/mol'  &
        MASS-ENTHALP='kcal/kg' HEAT=Gcal MOLE-CONC='mol/l'  &
        PDROP=bar
    PROP-LIST HENRY
    BPVAL CO2 H2O 159.1996745 -8477.711000 -21.95743000  &
        5.78074800E-3 -.1500000000 226.8500000 0.0

PROP-DATA NRTL-1
    IN-UNITS MET VOLUME-FLOW='cum/hr' ENTHALPY-FLO='Gcal/hr'  &
        HEAT-TRANS-C='kcal/hr-sqm-K' PRESSURE=bar TEMPERATURE=C  &
        VOLUME=cum DELTA-T=C HEAD=meter MOLE-DENSITY='kmol/cum'  &
        MASS-DENSITY='kg/cum' MOLE-ENTHALP='kcal/mol'  &
        MASS-ENTHALP='kcal/kg' HEAT=Gcal MOLE-CONC='mol/l'  &
        PDROP=bar
    PROP-LIST NRTL
    BPVAL H2O MEA 1.438498000 99.02104000 .2000000000 0.0 0.0  &
        0.0 25.00000000 150.0000000
    BPVAL MEA H2O -1.046602000 -337.5456000 .2000000000 0.0  &
        0.0 0.0 25.00000000 150.0000000
    BPVAL H2O CO2 10.06400000 -3268.135000 .2000000000 0.0 0.0  &
        0.0 0.0 200.0000000
    BPVAL CO2 H2O 10.06400000 -3268.135000 .2000000000 0.0 0.0  &
        0.0 0.0 200.0000000

PROP-DATA VLCLK-1
    IN-UNITS MET VOLUME-FLOW='cum/hr' ENTHALPY-FLO='Gcal/hr'  &
        HEAT-TRANS-C='kcal/hr-sqm-K' PRESSURE=bar TEMPERATURE=C  &
        VOLUME=cum DELTA-T=C HEAD=meter MOLE-DENSITY='kmol/cum'  &
        MASS-DENSITY='kg/cum' MOLE-ENTHALP='kcal/mol'  &
        MASS-ENTHALP='kcal/kg' HEAT=Gcal MOLE-CONC='mol/l'  &
        PDROP=bar
    PROP-LIST VLCLK
    BPVAL MEA+ OH- -390.9954000 1000.000000

PROP-DATA GMELCC-1
    IN-UNITS MET VOLUME-FLOW='cum/hr' ENTHALPY-FLO='Gcal/hr'  &
        HEAT-TRANS-C='kcal/hr-sqm-K' PRESSURE=bar TEMPERATURE=C  &
        VOLUME=cum DELTA-T=C HEAD=meter MOLE-DENSITY='kmol/cum'  &
        MASS-DENSITY='kg/cum' MOLE-ENTHALP='kcal/mol'  &
        MASS-ENTHALP='kcal/kg' HEAT=Gcal MOLE-CONC='mol/l'  &
        PDROP=bar
```

```
    PROP-LIST GMELCC
    PPVAL H2O ( MEA+ MEACOO- ) 9.887700000
    PPVAL ( MEA+ MEACOO- ) H2O -4.951100000
    PPVAL H2O ( MEA+ HCO3- ) 5.354100000
    PPVAL ( MEA+ HCO3- ) H2O -4.070500000
    PPVAL H2O ( H3O+ HCO3- ) 8.045000000
    PPVAL ( H3O+ HCO3- ) H2O -4.072000000
    PPVAL H2O ( H3O+ OH- ) 8.045000000
    PPVAL ( H3O+ OH- ) H2O -4.072000000
    PPVAL H2O ( H3O+ CO3-- ) 8.045000000
    PPVAL ( H3O+ CO3-- ) H2O -4.072000000
    PPVAL MEA ( MEA+ MEACOO- ) 15.00000000
    PPVAL ( MEA+ MEACOO- ) MEA -8.000000000
    PPVAL MEA ( MEA+ HCO3- ) 15.00000000
    PPVAL ( MEA+ HCO3- ) MEA -8.000000000
    PPVAL MEA ( MEA+ OH- ) 15.00000000
    PPVAL ( MEA+ OH- ) MEA -8.000000000
    PPVAL MEA ( MEA+ CO3-- ) 15.00000000
    PPVAL ( MEA+ CO3-- ) MEA -8.000000000
    PPVAL MEA ( H3O+ MEACOO- ) 15.00000000
    PPVAL ( H3O+ MEACOO- ) MEA -8.000000000
    PPVAL MEA ( H3O+ HCO3- ) 15.00000000
    PPVAL ( H3O+ HCO3- ) MEA -8.000000000
    PPVAL MEA ( H3O+ OH- ) 15.00000000
    PPVAL ( H3O+ OH- ) MEA -8.000000000
    PPVAL MEA ( H3O+ CO3-- ) 15.00000000
    PPVAL ( H3O+ CO3-- ) MEA -8.000000000
    PPVAL CO2 ( MEA+ MEACOO- ) 15.00000000
    PPVAL ( MEA+ MEACOO- ) CO2 -8.000000000
    PPVAL CO2 ( MEA+ HCO3- ) 15.00000000
    PPVAL ( MEA+ HCO3- ) CO2 -8.000000000
    PPVAL CO2 ( MEA+ OH- ) 15.00000000
    PPVAL ( MEA+ OH- ) CO2 -8.000000000
    PPVAL CO2 ( MEA+ CO3-- ) 15.00000000
    PPVAL ( MEA+ CO3-- ) CO2 -8.000000000
    PPVAL CO2 ( H3O+ MEACOO- ) 15.00000000
    PPVAL ( H3O+ MEACOO- ) CO2 -8.000000000
    PPVAL CO2 ( H3O+ HCO3- ) 15.00000000
    PPVAL ( H3O+ HCO3- ) CO2 -8.000000000
    PPVAL CO2 ( H3O+ OH- ) 15.00000000
    PPVAL ( H3O+ OH- ) CO2 -8.000000000
    PPVAL CO2 ( H3O+ CO3-- ) 15.00000000
    PPVAL ( H3O+ CO3-- ) CO2 -8.000000000

PROP-DATA GMELCD-1
    IN-UNITS MET VOLUME-FLOW='cum/hr' ENTHALPY-FLO='Gcal/hr'  &
        HEAT-TRANS-C='kcal/hr-sqm-K' PRESSURE=bar TEMPERATURE=C  &
        VOLUME=cum DELTA-T=C HEAD=meter MOLE-DENSITY='kmol/cum'  &
        MASS-DENSITY='kg/cum' MOLE-ENTHALP='kcal/mol'  &
        MASS-ENTHALP='kcal/kg' HEAT=Gcal MOLE-CONC='mol/l'  &
```

```
        PDROP=bar
    PROP-LIST GMELCD
    PPVAL H2O ( MEA+ MEACOO- ) 10.81300000
    PPVAL ( MEA+ MEACOO- ) H2O 0.0
    PPVAL H2O ( MEA+ HCO3- ) 965.2400000
    PPVAL ( MEA+ HCO3- ) H2O -11.06700000
    PPVAL MEA ( MEA+ MEACOO- ) 0.0
    PPVAL ( MEA+ MEACOO- ) MEA 0.0
    PPVAL MEA ( MEA+ HCO3- ) 0.0
    PPVAL ( MEA+ HCO3- ) MEA 0.0
    PPVAL MEA ( MEA+ OH- ) 0.0
    PPVAL ( MEA+ OH- ) MEA 0.0
    PPVAL MEA ( MEA+ CO3-- ) 0.0
    PPVAL ( MEA+ CO3-- ) MEA 0.0
    PPVAL MEA ( H3O+ MEACOO- ) 0.0
    PPVAL ( H3O+ MEACOO- ) MEA 0.0
    PPVAL MEA ( H3O+ HCO3- ) 0.0
    PPVAL ( H3O+ HCO3- ) MEA 0.0
    PPVAL MEA ( H3O+ OH- ) 0.0
    PPVAL ( H3O+ OH- ) MEA 0.0
    PPVAL MEA ( H3O+ CO3-- ) 0.0
    PPVAL ( H3O+ CO3-- ) MEA 0.0
    PPVAL CO2 ( MEA+ MEACOO- ) 0.0
    PPVAL ( MEA+ MEACOO- ) CO2 0.0
    PPVAL CO2 ( MEA+ HCO3- ) 0.0
    PPVAL ( MEA+ HCO3- ) CO2 0.0
    PPVAL CO2 ( MEA+ OH- ) 0.0
    PPVAL ( MEA+ OH- ) CO2 0.0
    PPVAL CO2 ( MEA+ CO3-- ) 0.0
    PPVAL ( MEA+ CO3-- ) CO2 0.0
    PPVAL CO2 ( H3O+ MEACOO- ) 0.0
    PPVAL ( H3O+ MEACOO- ) CO2 0.0
    PPVAL CO2 ( H3O+ HCO3- ) 0.0
    PPVAL ( H3O+ HCO3- ) CO2 0.0
    PPVAL CO2 ( H3O+ OH- ) 0.0
    PPVAL ( H3O+ OH- ) CO2 0.0
    PPVAL CO2 ( H3O+ CO3-- ) 0.0
    PPVAL ( H3O+ CO3-- ) CO2 0.0

PROP-DATA GMELCE-1
    IN-UNITS MET VOLUME-FLOW='cum/hr' ENTHALPY-FLO='Gcal/hr'  &
        HEAT-TRANS-C='kcal/hr-sqm-K' PRESSURE=bar TEMPERATURE=C  &
        VOLUME=cum DELTA-T=C HEAD=meter MOLE-DENSITY='kmol/cum'  &
        MASS-DENSITY='kg/cum' MOLE-ENTHALP='kcal/mol'  &
        MASS-ENTHALP='kcal/kg' HEAT=Gcal MOLE-CONC='mol/l'  &
        PDROP=bar
    PROP-LIST GMELCE
    PPVAL MEA ( MEA+ MEACOO- ) 0.0
    PPVAL ( MEA+ MEACOO- ) MEA 0.0
    PPVAL MEA ( MEA+ HCO3- ) 0.0
```

```
    PPVAL ( MEA+ HCO3- ) MEA 0.0
    PPVAL MEA ( MEA+ OH- ) 0.0
    PPVAL ( MEA+ OH- ) MEA 0.0
    PPVAL MEA ( MEA+ CO3-- ) 0.0
    PPVAL ( MEA+ CO3-- ) MEA 0.0
    PPVAL MEA ( H3O+ MEACOO- ) 0.0
    PPVAL ( H3O+ MEACOO- ) MEA 0.0
    PPVAL MEA ( H3O+ HCO3- ) 0.0
    PPVAL ( H3O+ HCO3- ) MEA 0.0
    PPVAL MEA ( H3O+ OH- ) 0.0
    PPVAL ( H3O+ OH- ) MEA 0.0
    PPVAL MEA ( H3O+ CO3-- ) 0.0
    PPVAL ( H3O+ CO3-- ) MEA 0.0
    PPVAL CO2 ( MEA+ MEACOO- ) 0.0
    PPVAL ( MEA+ MEACOO- ) CO2 0.0
    PPVAL CO2 ( MEA+ HCO3- ) 0.0
    PPVAL ( MEA+ HCO3- ) CO2 0.0
    PPVAL CO2 ( MEA+ OH- ) 0.0
    PPVAL ( MEA+ OH- ) CO2 0.0
    PPVAL CO2 ( MEA+ CO3-- ) 0.0
    PPVAL ( MEA+ CO3-- ) CO2 0.0
    PPVAL CO2 ( H3O+ MEACOO- ) 0.0
    PPVAL ( H3O+ MEACOO- ) CO2 0.0
    PPVAL CO2 ( H3O+ HCO3- ) 0.0
    PPVAL ( H3O+ HCO3- ) CO2 0.0
    PPVAL CO2 ( H3O+ OH- ) 0.0
    PPVAL ( H3O+ OH- ) CO2 0.0
    PPVAL CO2 ( H3O+ CO3-- ) 0.0
    PPVAL ( H3O+ CO3-- ) CO2 0.0

PROP-DATA GMELCN-1
    IN-UNITS MET VOLUME-FLOW=’cum/hr’ ENTHALPY-FLO=’Gcal/hr’  &
        HEAT-TRANS-C=’kcal/hr-sqm-K’ PRESSURE=bar TEMPERATURE=C  &
        VOLUME=cum DELTA-T=C HEAD=meter MOLE-DENSITY=’kmol/cum’  &
        MASS-DENSITY=’kg/cum’ MOLE-ENTHALP=’kcal/mol’  &
        MASS-ENTHALP=’kcal/kg’ HEAT=Gcal MOLE-CONC=’mol/l’  &
        PDROP=bar
    PROP-LIST GMELCN
    PPVAL MEA ( MEA+ MEACOO- ) .1000000000
    PPVAL MEA ( MEA+ HCO3- ) .1000000000
    PPVAL MEA ( MEA+ OH- ) .1000000000
    PPVAL MEA ( MEA+ CO3-- ) .1000000000
    PPVAL MEA ( H3O+ MEACOO- ) .1000000000
    PPVAL MEA ( H3O+ HCO3- ) .1000000000
    PPVAL MEA ( H3O+ OH- ) .1000000000
    PPVAL MEA ( H3O+ CO3-- ) .1000000000
    PPVAL CO2 ( MEA+ MEACOO- ) .1000000000
    PPVAL CO2 ( MEA+ HCO3- ) .1000000000
    PPVAL CO2 ( MEA+ OH- ) .1000000000
    PPVAL CO2 ( MEA+ CO3-- ) .1000000000
```

```
    PPVAL CO2 ( H3O+ MEACOO- ) .1000000000
    PPVAL CO2 ( H3O+ HCO3- ) .1000000000
    PPVAL CO2 ( H3O+ OH- ) .1000000000
    PPVAL CO2 ( H3O+ CO3-- ) .1000000000

;----------------------------------------------------------------------
; Components
;----------------------------------------------------------------------

COMPONENTS
    H2O H2O /
    MEA C2H7NO /
    CO2 CO2 /
    MEA+ C2H8NO+ /
    H3O+ H3O+ /
    MEACOO- C3H6NO3- /
    HCO3- HCO3- /
    OH- OH- /
    CO3-- CO3-2 /
    N2 N2

HENRY-COMPS MEA-CO2 CO2 N2

;----------------------------------------------------------------------
; Chemistry
;----------------------------------------------------------------------

CHEMISTRY MEA-CO2
    STOIC 1 H2O -2 / H3O+ 1 / OH- 1
    STOIC 2 CO2 -1 / H2O -2 / H3O+ 1 / HCO3- 1
    STOIC 3 HCO3- -1 / H2O -1 / H3O+ 1 / CO3-- 1
    STOIC 4 MEA+ -1 / H2O -1 / MEA 1 / H3O+ 1
    STOIC 5 MEACOO- -1 / H2O -1 / MEA 1 / HCO3- 1
    K-STOIC 1 A=132.89888 B=-13445.9 C=-22.4773 D=0
    K-STOIC 2 A=231.465439 B=-12092.1 C=-36.7816 D=0
    K-STOIC 3 A=216.05043 B=-12431.7 C=-35.4819 D=0
    K-STOIC 4 A=-3.038325 B=-7008.357 C=0 D=-.00313489
    K-STOIC 5 A=-.52135 B=-2545.53 C=0 D=0

;----------------------------------------------------------------------
; Flowsheet
;----------------------------------------------------------------------

FLOWSHEET MEA
        BLOCK FLUESPLT        IN=FLUE-SPL                OUT=FLUE-BLO FLUE-AUX
        BLOCK BLOWER        IN=FLUE-BLO                OUT=FLUE-DCC P-BLOW
        BLOCK "H2O_PUMP"        IN=H2O-PUMP        OUT=H2O-DCC P-H2OP
        BLOCK DCC        IN=FLUE-DCC H2O-DCC        OUT=FLUE-ABS H2O-OUT
        BLOCK ABSORBER        IN=FLUE-ABS LEAN-ABS        OUT=STACK RICH-PUM
```

```
;-----------------------------------------------------------------------
; Stream Specification
;-----------------------------------------------------------------------

; specify the heat and work streams in the flowsheet
DEF-STREAMS WORK P-BLOW P-H2OP

; The flue gas composition is estimated for 50/50 PRB/USLS coal mix with
; heat input as determined from steam cycle.  The temperature is the
; temperature at the air heater outlet taken from the boiler design data.
STREAM FLUE-SPL TEMP=40 <C> PRES=101.3 MASS-FLOW=2315713 <KG/HR>
        MOLE-FRAC N2 0.78991 / CO2 0.14627 / H2O 0.06381

; This represents 1/3 of the total flue gas.
;STREAM FLUE-BLO TEMP=40 <C> PRES=101.3 MASS-FLOW=771904 <KG/HR>
;        MOLE-FRAC N2 0.78991 / CO2 0.14627 / H2O 0.06381

; Cooling water temperature for Lake Erie is not given.  12C is summer
; mean temperature form IEA technical specifications document...
STREAM H2O-PUMP TEMP=12 PRES=101.3
        MOLE-FLOW H2O 70

; Note:  12.6 M MEA is 30 wt%
STREAM LEAN-ABS TEMP=40 PRES=101.3 MOLE-FLOW=10
        MOLE-FRAC MEA 0.126 / H2O 0.874 / CO2 0.03150

;-----------------------------------------------------------------------
; Block Specification
;-----------------------------------------------------------------------

;<FLUESPLT>
BLOCK FLUESPLT FSPLIT
        FRAC FLUE-BLO 0.3333
;</FLUESPLT>

;<BLOWER>
BLOCK BLOWER COMPR
        PARAM TYPE=ISENTROPIC SEFF=0.90 PRES=173.6 <kPa> NPHASE=2
;</BLOWER>

;<H2O_PUMP>
BLOCK "H2O_PUMP" PUMP
        PARAM PRES=173.6 <kPa>
;</H2O_PUMP>

; This block cools the flue gas stream with water.
BLOCK DCC FLASH2
        PARAM DUTY=0 PRES=-10 <kPa>

;<ABSORBER>
```

```
BLOCK ABSORBER RADFRAC
        PARAM NSTAGE=10 NPHASE=2 EFF=MURPHREE P-UPDATE=YES P-FIX=TOP &
                MAXOL=30 HYDRAULIC=YES

        COL-CONFIG CONDENSER=NONE REBOILER=NONE

        FEEDS FLUE-ABS 11 ABOVE-STAGE / LEAN-ABS 1 ABOVE-STAGE
        PRODUCTS STACK 1 V / RICH-PUM 10 L

        P-SPEC 1 101.3 / 10 163.6

        COL-SPECS 1 MOLE-RDV=1

; Specifies where to consider solution chemistry
        REAC-STAGES 1 10 MEA-CO2

; For rate-based analysis, the diameter is used as an initial guess
        PACK-RATE 1 1 10 RASCHIG PACK-MAT=METAL PACK-SIZE=75-MM &
                VENDOR=GENERIC PACK-HT=3 <METER> DIAM=11.2 DPMETH=ECKERT &
                P-UPDATE=YES

; Enables rate-based analysis (must also have TRAY-RATE or PACK-RATE sentence)
        RATESEP-ENAB CALC-MODE=RIG-RATE
        RATESEP-PARA INIT-EQUIL=YES RS-MAXIT=100

        PACK-RATE2 1 RATE-BASED=YES

        REPORT HYDANAL EXTHYD
        TRAY-REPORT2 COMP-EFF=YES STAGE-EFF=YES
;</ABSORBER>

;-----------------------------------------------------------------------
; Convergence options
;-----------------------------------------------------------------------

; This determines if results of previous convergence are used as starting
; point.
SIM-OPTIONS RESTART=YES

; This paragraph specifies convergence options.
CONV-OPTIONS
        PARAM SPEC-METHOD=SECANT TEAR-VAR=YES

CONVERGENCE COOL-FLU SECANT
        DESCRIPTION "Control convergence of design-spec COOL-FLU"

        SPEC COOL-FLU

CONVERGENCE CO2RECOV SECANT
        DESCRIPTION "Control convergence of design-spec CO2RECOV"
```

```
        SPEC CO2RECOV

CONVERGENCE MINFLEAN SQP
        DESCRIPTION "Converge BLOWERP and minimize lean MEA flowrate"

        OPTIMIZE MINFLEAN

        TEAR-VAR FOR-BLOCK=BLOWERP VAR-NAME=PBLOW LOWER=101.3 UPPER=300
        TEAR-VAR FOR-BLOCK=BLOWERP VAR-NAME=PPUMP LOWER=101.3 UPPER=300

;        PARAM MAXLSPASS=0 DERIVATIVE=CENTRAL EST-STEP=YES CONV-TEST=KKT1

; Absorber with optimum lean MEA flowrate
SEQUENCE ABSLOOP &
        MINFLEAN &
                BLOWER &
                COOL-FLU &
                         "H2O_PUMP" DCC &
                (RETURN COOL-FLU) &
                CO2RECOV &
                        ABSORBER &
                (RETURN CO2RECOV) &
                 BLOWERP WRITEOPT &
        (RETURN MINFLEAN)

; -------------------------------------------------------------
; Calculator:  BLOWERP
; -------------------------------------------------------------
; This block sets the pressure increase in the BLOWER equal to the pressure
; drop across the ABSORBER.
;
; In order to get the CALCULATOR block to introduce a convergence loop, the
; TEAR variable must be specified as a write variable, there should not be
; an EXECUTE sentence, and TEAR-VAR=YES must be specified in the
; CONV-OPTIONS paragraph.

CALCULATOR BLOWERP
        DEFINE PN BLOCK-VAR BLOCK=ABSORBER SENTENCE=PROFILE VARIABLE=PRES &
                ID1=2
        DEFINE DPDCC BLOCK-VAR BLOCK=DCC SENTENCE=PARAM VARIABLE=PRES

        DEFINE PBLOW BLOCK-VAR BLOCK=BLOWER SENTENCE=PARAM VARIABLE=PRES
        DEFINE PPUMP BLOCK-VAR BLOCK="H2O_PUMP" SENTENCE=PARAM VARIABLE=PRES

F       PBLOW = PN - DPDCC
F       PPUMP = PN - DPDCC

        READ-VARS PN DPDCC
        WRITE-VARS PBLOW PPUMP
```

```
        TEAR-VARS TEAR-VAR=PBLOW LOWER=101 UPPER=250

; --------------------------------------------------------------
; Calculator:  WRITEOPT
; --------------------------------------------------------------
; This block outputs the values of variables of interest during
; the MINFLEAN optimization block:
;    - ABSORBER diameter
;    - ABSORBER approach to vapour flooding
;    - BLOWER outlet pressure
;    - LEAN-ABS flowrate

CALCULATOR WRITEOPT
        DEFINE D BLOCK-VAR BLOCK=ABSORBER SENTENCE=PRATE-RESUL1 &
                VARIABLE=DIAM
         DEFINE V BLOCK-VAR BLOCK=ABSORBER SENTENCE=PRATE-RESULT &
                VARIABLE=FLOOD-FAC ID1=1
        DEFINE P BLOCK-VAR BLOCK=BLOWER SENTENCE=PARAM VARIABLE=PRES
        DEFINE F STREAM-VAR STREAM=LEAN-ABS VARIABLE=MOLE-FLOW

F       WRITE(NHSTRY, *) F, D, P, V

; --------------------------------------------------------------
; Design specification:  COOL-FLU
; --------------------------------------------------------------
; This block adjusts the flow rate of cooling water until the flue gas
; reaches the desired temperature.

DESIGN-SPEC COOL-FLU
        DEFINE TFLUE STREAM-VAR STREAM=FLUE-ABS VARIABLE=TEMP

        SPEC "TFLUE" TO "40"
        TOL-SPEC "0.5"

        VARY STREAM-VAR STREAM=H2O-PUMP VARIABLE=MOLE-FLOW
        LIMITS "0" "120"

; --------------------------------------------------------------
; Design specification:  CO2RECOV
; --------------------------------------------------------------
; This block sets the flow rate of LEAN-ABS such that the desired recovery
; of CO2 is achieved.
DESIGN-SPEC CO2RECOV
        DEFINE CO2IN MOLE-FLOW STREAM=FLUE-ABS COMPONENT=CO2
        DEFINE CO2OUT MOLE-FLOW STREAM=STACK COMPONENT=CO2

        SPEC "(CO2IN - CO2OUT) / CO2IN" TO "0.85"
        TOL-SPEC "0.005"
```

```
        VARY STREAM-VAR STREAM=LEAN-ABS VARIABLE=MOLE-FLOW
        LIMITS "1" "250"

; --------------------------------------------------------------
; Optimization:  MINFLEAN
; --------------------------------------------------------------
; This block adjusts the diameter and tray spacing of the Absorber in
; order to minimize the flow rate of lean solvent required subject to
; the named constraints
;   1. approach to entrainment flooding is less than or equal to 80%
;   2. approach to downcomer flooding is less than or equal to 50%
OPTIMIZATION MINFLEAN
        DEFINE FLEAN STREAM-VAR STREAM=LEAN-ABS VARIABLE=MOLE-FLOW

        MINIMIZE "FLEAN"

        CONSTRAINTS MAXFLOOD

        VARY BLOCK-VAR BLOCK=ABSORBER SENTENCE=PACK-RATE &
                VARIABLE=DIAM ID1=1
        LIMITS "1" "15"  MAX-STEP-SIZE=0.1


; --------------------------------------------------------------
; Constraint:  MAXFLOOD
; --------------------------------------------------------------
; This block specifies a maximum approach to entrainment flooding in
; the Absorber of 80%.
CONSTRAINT MAXFLOOD
             DEFINE EFA BLOCK-VAR BLOCK=ABSORBER SENTENCE=PRATE-RESULT &
                     VARIABLE=FLOOD-FAC ID1=1

        SPEC "EFA" LE "0.80"
        TOL-SPEC "0.005"
```

F.3 *Stripper* with packing

```
; File: stripper_packing_sqp_template.inp
; ---------------------------------------
; This file simulates the Stripper from the MEA absorption process.
; RateSep, in rating mode and using random packing, is used to model
; the Stripper.

; A flash is used to remove the vapour contained in the heat exchanger
; outlet.  Also, a design spec is used to establish the CO2 recovery.
;
; The design of the Stripper (i.e., selection of diameter, tray
; spacing, reflux ratio, bottoms-to-feed ratio, reboiler pressure) is
; achieved by solving an optimization problem using the SQP method.

; This is based upon stripper_sqp_v1.1.inp.

;-----------------------------------------------------------------------
; Report options
;-----------------------------------------------------------------------

STREAM-REPOR MOLEFLOW MASSFLOW

;-----------------------------------------------------------------------
; Diagnostic specifications
;-----------------------------------------------------------------------

DIAGNOSTICS
        HISTORY SIM-LEVEL=4 CONV-LEVEL=4
        MAX-PRINT SIM-LIMIT=99999

; This paragraph specifies time and error limits.
RUN-CONTROL MAX-TIME=99999 MAX-ERRORS=99999

; This paragraph will case AspenPlus to include FORTRAN tracebacks in the
; history file.
SYS-OPTIONS TRACE=YES

;-----------------------------------------------------------------------
; Units
;-----------------------------------------------------------------------

IN-UNITS SI PRESSURE=kPa TEMPERATURE=C PDROP='N/sqm'

;-----------------------------------------------------------------------
; Property Databanks
;-----------------------------------------------------------------------

DATABANKS ASPENPCD  / AQUEOUS  / SOLIDS  / INORGANIC  / PURE13
```

```
PROP-SOURCES ASPENPCD  / AQUEOUS  / SOLIDS  / INORGANIC / PURE13

;-----------------------------------------------------------------------
; Properties
;-----------------------------------------------------------------------

PROPERTIES ELECNRTL HENRY-COMPS=MEA-CO2 CHEMISTRY=MEA-CO2 TRUE-COMPS=YES

PROP-SET LPHASE MUMX RHOMX SIGMAMX VOLFLMX MASSFLMX PHASE=L &
         UNITS=’KG/CUM’ ’DYNE/CM’

PROP-SET VPHASE RHOMX VOLFLMX MASSFLMX PHASE=V UNITS=’KG/CUM’

PROP-DATA HENRY-1
    IN-UNITS MET VOLUME-FLOW=’cum/hr’ ENTHALPY-FLO=’Gcal/hr’  &
        HEAT-TRANS-C=’kcal/hr-sqm-K’ PRESSURE=bar TEMPERATURE=C  &
        VOLUME=cum DELTA-T=C HEAD=meter MOLE-DENSITY=’kmol/cum’  &
        MASS-DENSITY=’kg/cum’ MOLE-ENTHALP=’kcal/mol’  &
        MASS-ENTHALP=’kcal/kg’ HEAT=Gcal MOLE-CONC=’mol/l’  &
        PDROP=bar
    PROP-LIST HENRY
    BPVAL CO2 H2O 159.1996745 -8477.711000 -21.95743000  &
        5.78074800E-3 -.1500000000 226.8500000 0.0

PROP-DATA NRTL-1
    IN-UNITS MET VOLUME-FLOW=’cum/hr’ ENTHALPY-FLO=’Gcal/hr’  &
        HEAT-TRANS-C=’kcal/hr-sqm-K’ PRESSURE=bar TEMPERATURE=C  &
        VOLUME=cum DELTA-T=C HEAD=meter MOLE-DENSITY=’kmol/cum’  &
        MASS-DENSITY=’kg/cum’ MOLE-ENTHALP=’kcal/mol’  &
        MASS-ENTHALP=’kcal/kg’ HEAT=Gcal MOLE-CONC=’mol/l’  &
        PDROP=bar
    PROP-LIST NRTL
    BPVAL H2O MEA 1.438498000 99.02104000 .2000000000 0.0 0.0  &
        0.0 25.00000000 150.0000000
    BPVAL MEA H2O -1.046602000 -337.5456000 .2000000000 0.0  &
        0.0 0.0 25.00000000 150.0000000
    BPVAL H2O CO2 10.06400000 -3268.135000 .2000000000 0.0 0.0  &
        0.0 0.0 200.0000000
    BPVAL CO2 H2O 10.06400000 -3268.135000 .2000000000 0.0 0.0  &
        0.0 0.0 200.0000000

PROP-DATA VLCLK-1
    IN-UNITS MET VOLUME-FLOW=’cum/hr’ ENTHALPY-FLO=’Gcal/hr’  &
        HEAT-TRANS-C=’kcal/hr-sqm-K’ PRESSURE=bar TEMPERATURE=C  &
        VOLUME=cum DELTA-T=C HEAD=meter MOLE-DENSITY=’kmol/cum’  &
        MASS-DENSITY=’kg/cum’ MOLE-ENTHALP=’kcal/mol’  &
        MASS-ENTHALP=’kcal/kg’ HEAT=Gcal MOLE-CONC=’mol/l’  &
        PDROP=bar
    PROP-LIST VLCLK
    BPVAL MEA+ OH- -390.9954000 1000.000000
```

```
PROP-DATA GMELCC-1
    IN-UNITS MET VOLUME-FLOW=’cum/hr’ ENTHALPY-FLO=’Gcal/hr’  &
        HEAT-TRANS-C=’kcal/hr-sqm-K’ PRESSURE=bar TEMPERATURE=C  &
        VOLUME=cum DELTA-T=C HEAD=meter MOLE-DENSITY=’kmol/cum’  &
        MASS-DENSITY=’kg/cum’ MOLE-ENTHALP=’kcal/mol’  &
        MASS-ENTHALP=’kcal/kg’ HEAT=Gcal MOLE-CONC=’mol/l’  &
        PDROP=bar
    PROP-LIST GMELCC
    PPVAL H2O ( MEA+ MEACOO- ) 9.887700000
    PPVAL ( MEA+ MEACOO- ) H2O -4.951100000
    PPVAL H2O ( MEA+ HCO3- ) 5.354100000
    PPVAL ( MEA+ HCO3- ) H2O -4.070500000
    PPVAL H2O ( H3O+ HCO3- ) 8.045000000
    PPVAL ( H3O+ HCO3- ) H2O -4.072000000
    PPVAL H2O ( H3O+ OH- ) 8.045000000
    PPVAL ( H3O+ OH- ) H2O -4.072000000
    PPVAL H2O ( H3O+ CO3-- ) 8.045000000
    PPVAL ( H3O+ CO3-- ) H2O -4.072000000
    PPVAL MEA ( MEA+ MEACOO- ) 15.00000000
    PPVAL ( MEA+ MEACOO- ) MEA -8.000000000
    PPVAL MEA ( MEA+ HCO3- ) 15.00000000
    PPVAL ( MEA+ HCO3- ) MEA -8.000000000
    PPVAL MEA ( MEA+ OH- ) 15.00000000
    PPVAL ( MEA+ OH- ) MEA -8.000000000
    PPVAL MEA ( MEA+ CO3-- ) 15.00000000
    PPVAL ( MEA+ CO3-- ) MEA -8.000000000
    PPVAL MEA ( H3O+ MEACOO- ) 15.00000000
    PPVAL ( H3O+ MEACOO- ) MEA -8.000000000
    PPVAL MEA ( H3O+ HCO3- ) 15.00000000
    PPVAL ( H3O+ HCO3- ) MEA -8.000000000
    PPVAL MEA ( H3O+ OH- ) 15.00000000
    PPVAL ( H3O+ OH- ) MEA -8.000000000
    PPVAL MEA ( H3O+ CO3-- ) 15.00000000
    PPVAL ( H3O+ CO3-- ) MEA -8.000000000
    PPVAL CO2 ( MEA+ MEACOO- ) 15.00000000
    PPVAL ( MEA+ MEACOO- ) CO2 -8.000000000
    PPVAL CO2 ( MEA+ HCO3- ) 15.00000000
    PPVAL ( MEA+ HCO3- ) CO2 -8.000000000
    PPVAL CO2 ( MEA+ OH- ) 15.00000000
    PPVAL ( MEA+ OH- ) CO2 -8.000000000
    PPVAL CO2 ( MEA+ CO3-- ) 15.00000000
    PPVAL ( MEA+ CO3-- ) CO2 -8.000000000
    PPVAL CO2 ( H3O+ MEACOO- ) 15.00000000
    PPVAL ( H3O+ MEACOO- ) CO2 -8.000000000
    PPVAL CO2 ( H3O+ HCO3- ) 15.00000000
    PPVAL ( H3O+ HCO3- ) CO2 -8.000000000
    PPVAL CO2 ( H3O+ OH- ) 15.00000000
    PPVAL ( H3O+ OH- ) CO2 -8.000000000
    PPVAL CO2 ( H3O+ CO3-- ) 15.00000000
```

```
    PPVAL ( H3O+ CO3-- ) CO2 -8.000000000

PROP-DATA GMELCD-1
    IN-UNITS MET VOLUME-FLOW='cum/hr' ENTHALPY-FLO='Gcal/hr'  &
        HEAT-TRANS-C='kcal/hr-sqm-K' PRESSURE=bar TEMPERATURE=C  &
        VOLUME=cum DELTA-T=C HEAD=meter MOLE-DENSITY='kmol/cum'  &
        MASS-DENSITY='kg/cum' MOLE-ENTHALP='kcal/mol'  &
        MASS-ENTHALP='kcal/kg' HEAT=Gcal MOLE-CONC='mol/l'  &
        PDROP=bar
    PROP-LIST GMELCD
    PPVAL H2O ( MEA+ MEACOO- ) 10.81300000
    PPVAL ( MEA+ MEACOO- ) H2O 0.0
    PPVAL H2O ( MEA+ HCO3- ) 965.2400000
    PPVAL ( MEA+ HCO3- ) H2O -11.06700000
    PPVAL MEA ( MEA+ MEACOO- ) 0.0
    PPVAL ( MEA+ MEACOO- ) MEA 0.0
    PPVAL MEA ( MEA+ HCO3- ) 0.0
    PPVAL ( MEA+ HCO3- ) MEA 0.0
    PPVAL MEA ( MEA+ OH- ) 0.0
    PPVAL ( MEA+ OH- ) MEA 0.0
    PPVAL MEA ( MEA+ CO3-- ) 0.0
    PPVAL ( MEA+ CO3-- ) MEA 0.0
    PPVAL MEA ( H3O+ MEACOO- ) 0.0
    PPVAL ( H3O+ MEACOO- ) MEA 0.0
    PPVAL MEA ( H3O+ HCO3- ) 0.0
    PPVAL ( H3O+ HCO3- ) MEA 0.0
    PPVAL MEA ( H3O+ OH- ) 0.0
    PPVAL ( H3O+ OH- ) MEA 0.0
    PPVAL MEA ( H3O+ CO3-- ) 0.0
    PPVAL ( H3O+ CO3-- ) MEA 0.0
    PPVAL CO2 ( MEA+ MEACOO- ) 0.0
    PPVAL ( MEA+ MEACOO- ) CO2 0.0
    PPVAL CO2 ( MEA+ HCO3- ) 0.0
    PPVAL ( MEA+ HCO3- ) CO2 0.0
    PPVAL CO2 ( MEA+ OH- ) 0.0
    PPVAL ( MEA+ OH- ) CO2 0.0
    PPVAL CO2 ( MEA+ CO3-- ) 0.0
    PPVAL ( MEA+ CO3-- ) CO2 0.0
    PPVAL CO2 ( H3O+ MEACOO- ) 0.0
    PPVAL ( H3O+ MEACOO- ) CO2 0.0
    PPVAL CO2 ( H3O+ HCO3- ) 0.0
    PPVAL ( H3O+ HCO3- ) CO2 0.0
    PPVAL CO2 ( H3O+ OH- ) 0.0
    PPVAL ( H3O+ OH- ) CO2 0.0
    PPVAL CO2 ( H3O+ CO3-- ) 0.0
    PPVAL ( H3O+ CO3-- ) CO2 0.0

PROP-DATA GMELCE-1
    IN-UNITS MET VOLUME-FLOW='cum/hr' ENTHALPY-FLO='Gcal/hr'  &
        HEAT-TRANS-C='kcal/hr-sqm-K' PRESSURE=bar TEMPERATURE=C  &
```

```
        VOLUME=cum DELTA-T=C HEAD=meter MOLE-DENSITY='kmol/cum'  &
        MASS-DENSITY='kg/cum' MOLE-ENTHALP='kcal/mol'  &
        MASS-ENTHALP='kcal/kg' HEAT=Gcal MOLE-CONC='mol/l'  &
        PDROP=bar
    PROP-LIST GMELCE
    PPVAL MEA ( MEA+ MEACOO- ) 0.0
    PPVAL ( MEA+ MEACOO- ) MEA 0.0
    PPVAL MEA ( MEA+ HCO3- ) 0.0
    PPVAL ( MEA+ HCO3- ) MEA 0.0
    PPVAL MEA ( MEA+ OH- ) 0.0
    PPVAL ( MEA+ OH- ) MEA 0.0
    PPVAL MEA ( MEA+ CO3-- ) 0.0
    PPVAL ( MEA+ CO3-- ) MEA 0.0
    PPVAL MEA ( H3O+ MEACOO- ) 0.0
    PPVAL ( H3O+ MEACOO- ) MEA 0.0
    PPVAL MEA ( H3O+ HCO3- ) 0.0
    PPVAL ( H3O+ HCO3- ) MEA 0.0
    PPVAL MEA ( H3O+ OH- ) 0.0
    PPVAL ( H3O+ OH- ) MEA 0.0
    PPVAL MEA ( H3O+ CO3-- ) 0.0
    PPVAL ( H3O+ CO3-- ) MEA 0.0
    PPVAL CO2 ( MEA+ MEACOO- ) 0.0
    PPVAL ( MEA+ MEACOO- ) CO2 0.0
    PPVAL CO2 ( MEA+ HCO3- ) 0.0
    PPVAL ( MEA+ HCO3- ) CO2 0.0
    PPVAL CO2 ( MEA+ OH- ) 0.0
    PPVAL ( MEA+ OH- ) CO2 0.0
    PPVAL CO2 ( MEA+ CO3-- ) 0.0
    PPVAL ( MEA+ CO3-- ) CO2 0.0
    PPVAL CO2 ( H3O+ MEACOO- ) 0.0
    PPVAL ( H3O+ MEACOO- ) CO2 0.0
    PPVAL CO2 ( H3O+ HCO3- ) 0.0
    PPVAL ( H3O+ HCO3- ) CO2 0.0
    PPVAL CO2 ( H3O+ OH- ) 0.0
    PPVAL ( H3O+ OH- ) CO2 0.0
    PPVAL CO2 ( H3O+ CO3-- ) 0.0
    PPVAL ( H3O+ CO3-- ) CO2 0.0

PROP-DATA GMELCN-1
    IN-UNITS MET VOLUME-FLOW='cum/hr' ENTHALPY-FLO='Gcal/hr'  &
        HEAT-TRANS-C='kcal/hr-sqm-K' PRESSURE=bar TEMPERATURE=C  &
        VOLUME=cum DELTA-T=C HEAD=meter MOLE-DENSITY='kmol/cum'  &
        MASS-DENSITY='kg/cum' MOLE-ENTHALP='kcal/mol'  &
        MASS-ENTHALP='kcal/kg' HEAT=Gcal MOLE-CONC='mol/l'  &
        PDROP=bar
    PROP-LIST GMELCN
    PPVAL MEA ( MEA+ MEACOO- ) .1000000000
    PPVAL MEA ( MEA+ HCO3- ) .1000000000
    PPVAL MEA ( MEA+ OH- ) .1000000000
    PPVAL MEA ( MEA+ CO3-- ) .1000000000
```

```
    PPVAL MEA ( H3O+ MEACOO- ) .1000000000
    PPVAL MEA ( H3O+ HCO3- ) .1000000000
    PPVAL MEA ( H3O+ OH- ) .1000000000
    PPVAL MEA ( H3O+ CO3-- ) .1000000000
    PPVAL CO2 ( MEA+ MEACOO- ) .1000000000
    PPVAL CO2 ( MEA+ HCO3- ) .1000000000
    PPVAL CO2 ( MEA+ OH- ) .1000000000
    PPVAL CO2 ( MEA+ CO3-- ) .1000000000
    PPVAL CO2 ( H3O+ MEACOO- ) .1000000000
    PPVAL CO2 ( H3O+ HCO3- ) .1000000000
    PPVAL CO2 ( H3O+ OH- ) .1000000000
    PPVAL CO2 ( H3O+ CO3-- ) .1000000000

;----------------------------------------------------------------------
; Components
;----------------------------------------------------------------------

COMPONENTS
    H2O H2O /
    MEA C2H7NO /
    CO2 CO2 /
    MEA+ C2H8NO+ /
    H3O+ H3O+ /
    MEACOO- C3H6NO3- /
    HCO3- HCO3- /
    OH- OH- /
    CO3-- CO3-2 /
    N2 N2

HENRY-COMPS MEA-CO2 CO2 N2

;----------------------------------------------------------------------
; Chemistry
;----------------------------------------------------------------------

CHEMISTRY MEA-CO2
    STOIC 1 H2O -2 / H3O+ 1 / OH- 1
    STOIC 2 CO2 -1 / H2O -2 / H3O+ 1 / HCO3- 1
    STOIC 3 HCO3- -1 / H2O -1 / H3O+ 1 / CO3-- 1
    STOIC 4 MEA+ -1 / H2O -1 / MEA 1 / H3O+ 1
    STOIC 5 MEACOO- -1 / H2O -1 / MEA 1 / HCO3- 1
    K-STOIC 1 A=132.89888 B=-13445.9 C=-22.4773 D=0
    K-STOIC 2 A=231.465439 B=-12092.1 C=-36.7816 D=0
    K-STOIC 3 A=216.05043 B=-12431.7 C=-35.4819 D=0
    K-STOIC 4 A=-3.038325 B=-7008.357 C=0 D=-.00313489
    K-STOIC 5 A=-.52135 B=-2545.53 C=0 D=0

;----------------------------------------------------------------------
; Flowsheet
;----------------------------------------------------------------------
```

```
FLOWSHEET MEA
        BLOCK "RICH_PUM"        IN=RICH-PUM                OUT=RICH-HX P-RICHP
        BLOCK FLASH        IN=RICH-FLA                OUT=FLSH-CO2 RICH-STR
        BLOCK STRIPPER        IN=RICH-STR                OUT=STR-CO2 LEAN-HX
        BLOCK HEATX        IN=RICH-HX LEAN-HX        OUT=RICH-FLA LEAN-MIX
        BLOCK "CO2_COOL"        IN=FLSH-CO2 STR-CO2        OUT=CO2-COMP ST1
        BLOCK "CO2_COMP"        IN=CO2-COMP        OUT=CO2 ST2 ST3 ST4 P-COMP
        BLOCK POWER        IN= P-RICHP P-COMP        OUT=POWER

;-----------------------------------------------------------------------
; Stream Specification
;-----------------------------------------------------------------------

; specify the heat and work streams in the flowsheet
DEF-STREAMS WORK POWER P-RICHP P-COMP POWER

; Note:  T, F, and composition are obtained from packed-absorber
;        results (i.e., absorber_packing_sqp_x033r85a25An50Ah10.rep)
STREAM RICH-PUM TEMP=50.9669 PRES=107.6189
        MOLE-FLOW H2O 25.2757 / MEA 0.2569 / CO2 7.4843E-03 /
                N2 7.9348E-05 / HCO3- 0.1264 / MEACOO- 1.6962 /
                MEA+ 1.8448 / CO3-- 1.1088E-02 / H3O+ 3.8657E-09 /
                OH- 6.6203E-06

; Note:  F is obtained from absorber results
STREAM LEAN-HX VFRAC=0 PRES=178 MOLE-FLOW=28
        MOLE-FRAC H2O 0.874 / MEA 0.126 / CO2 0.0315

;-----------------------------------------------------------------------
; Block Specification
;-----------------------------------------------------------------------

;<RICH_PUM>
BLOCK "RICH_PUM" PUMP
        PARAM PRES=158 <kPa> DEFF=0.98
;</RICH_PUM>


BLOCK FLASH FLASH2
        PARAM PRES=0 DUTY=0

;<STRIPPER>
BLOCK STRIPPER RADFRAC
        PARAM NSTAGE=32 NPHASE=2 EFF=MURPHREE P-UPDATE=YES P-FIX=TOP &
                MAXOL=30 HYDRAULIC=YES

        COL-CONFIG CONDENSER=PARTIAL-V REBOILER=KETTLE

        FEEDS RICH-STR 2 ABOVE-STAGE
```

```
        PRODUCTS STR-CO2 1 V / LEAN-HX 32 L

        P-SPEC 1 158 / 32 178

        COL-SPECS MOLE-RDV=1 MOLE-RR=.50 B:F=.970
        DB:F-PARAMS

; Specifies where to consider solution chemistry
        REAC-STAGES 1 32 MEA-CO2

        PACK-RATE 1 2 31 RASCHIG PACK-MAT=METAL PACK-SIZE=75-MM &
                VENDOR=GENERIC PACK-HT=15 <METER> DIAM=7.6 <METER> &
                DPMETH=ECKERT P-UPDATE=YES

; Enables rate-based analysis (must also have TRAY-RATE sentence)
        RATESEP-ENAB CALC-MODE=RIG-RATE
        RATESEP-PARA INIT-EQUIL=YES RS-MAXIT=50
        PACK-RATE2 1 RATE-BASED=YES

        REPORT HYDANAL EXTHYD
;</STRIPPER>

; Shortcut heat exchanger calculation.
; 10 degree temperature approach at the hot stream outlet
; U = 1134 W / m^2 C (taken from Perry's for H2O-H2O liquid-liquid system)
BLOCK HEATX HEATX
        PARAM DELT-HOT=10
        FEEDS HOT=LEAN-HX COLD=RICH-HX
        PRODUCTS HOT=LEAN-MIX COLD=RICH-FLA
        HEAT-TR-COEF U=1134

BLOCK "CO2_COOL" FLASH2
        PARAM PRES=0 TEMP=25 <C>

BLOCK "CO2_COMP" MCOMPR
        PARAM NSTAGE=4 TYPE=ISENTROPIC PRES=110 <BAR> COMPR-NPHASE=1

        FEEDS CO2-COMP 1
        PRODUCTS ST2 1 L / ST3 2 L / ST4 3 L / CO2 4 / P-COMP GLOBAL
        COMPR-SPECS 1 SEFF=0.90 MEFF=0.99

        COOLER-SPECS 1 TEMP=25

BLOCK POWER MIXER

;----------------------------------------------------------------------
; Convergence Specifications
;----------------------------------------------------------------------

; This determines if results of previous convergence are used as starting
```

```
; point.
SIM-OPTIONS RESTART=YES

CONV-OPTIONS
        PARAM SPEC-METHOD=SECANT TEAR-VAR=YES

CONVERGENCE HXLOOP WEGSTEIN
        TEAR LEAN-HX

CONVERGENCE PRESSURE WEGSTEIN
        DESCRIPTION "Control convergence of tear variables in PUMPP"
        TEAR-VAR FOR-BLOCK=PUMPP VAR-NAME=PPUMP LOWER=101.3 UPPER=300

CONVERGENCE CO2RECOV SECANT
        SPEC CO2RECOV

CONVERGENCE MINDER8 SQP
        DESCRIPTION "Minimize Stripper power demand"

        OPTIMIZE MINDER8
        PARAM MAXIT=60

SEQUENCE STRLOOP &
        PRESSURE &
                "RICH_PUM" &
                HXLOOP &
                        HEATX FLASH &
                        MINDER8 &
                                STRIPPER "CO2_COOL" &
                                "CO2_COMP" POWER WRITEOPT &
                        (RETURN MINDER8) &
                (RETURN HXLOOP) &
        PUMPP &
        (RETURN PRESSURE)

DISABLE
        DESIGN-SPEC "STR_PRES"
        DESIGN-SPEC CO2RECOV
        CONVERGENCE CO2RECOV
;        CALCULATOR CO2SPEC
;        SEQUENCE STRLOOP2

; -------------------------------------------------------------
; Calculator:  PUMPP
; -------------------------------------------------------------
; This block sets the pressure increase in the RICH_PUM equal to the
; pressure at the STRIPPER inlet.
;
; In order to get the CALCULATOR block to introduce a convergence loop, the
; TEAR variable must be specified as a write variable, there should not be
```

```
; an EXECUTE sentence, and TEAR-VAR=YES must be specified in the
; CONV-OPTIONS paragraph.
CALCULATOR PUMPP
        DEFINE P2 BLOCK-VAR BLOCK=STRIPPER SENTENCE=PROFILE VARIABLE=PRES &
                ID1=2

        DEFINE PPUMP BLOCK-VAR BLOCK="RICH_PUM" SENTENCE=PARAM VARIABLE=PRES

F       PPUMP = P2

        READ-VARS P2
        WRITE-VARS PPUMP

        TEAR-VARS TEAR-VAR=PPUMP LOWER=101 UPPER=250

; ---------------------------------------------------------------
; Calculator:  WRITEOPT
; ---------------------------------------------------------------
; This block outputs the values of the manipulated variables from
; the MINFLEAN optimization block:  ABSORBER tray-spacing and diameter.

CALCULATOR WRITEOPT
C Z: objective value of the optimization
F       REAL*8 Z, FCO2

        DEFINE DIAM BLOCK-VAR BLOCK=STRIPPER SENTENCE=PACK-RATE &
                VARIABLE=DIAM ID1=1
        DEFINE BF BLOCK-VAR BLOCK=STRIPPER SENTENCE=COL-SPECS &
                VARIABLE=B:F
        DEFINE RR BLOCK-VAR BLOCK=STRIPPER SENTENCE=COL-SPECS &
                VARIABLE=MOLE-RR
        DEFINE PSET BLOCK-VAR BLOCK=STRIPPER SENTENCE=P-SPEC &
                VARIABLE=PRES ID1=1
        DEFINE PTOP BLOCK-VAR BLOCK=STRIPPER SENTENCE=PROFILE &
                VARIABLE=PRES ID1=1
        DEFINE PBOT BLOCK-VAR BLOCK=STRIPPER SENTENCE=PROFILE &
                VARIABLE=PRES ID1=32
        DEFINE QREB BLOCK-VAR BLOCK=STRIPPER SENTENCE=RESULTS &
                VARIABLE=REB-DUTY
        DEFINE PPUMP BLOCK-VAR BLOCK="RICH_PUM" SENTENCE=RESULTS &
                VARIABLE=BRAKE-POWER
        DEFINE PCOMP BLOCK-VAR BLOCK="CO2_COMP" SENTENCE=RESULTS &
                VARIABLE=BRAKE-POWER
        DEFINE FLCO2 MOLE-FLOW STREAM=FLSH-CO2 COMPONENT=CO2
        DEFINE STCO2 MOLE-FLOW STREAM=STR-CO2 COMPONENT=CO2

F       Z = 0.35*QREB + 0.98*(PPUMP + PCOMP)
F       FCO2 = FLCO2 + STCO2

F       WRITE(NHSTRY, *) DIAM, BF, RR, PTOP, PBOT, FCO2, Z
```

```
        READ-VARS DIAM BF RR PSET PTOP PBOT QREB PPUMP PCOMP &
                FLCO2 STCO2

; --------------------------------------------------------------
; Design specification:  STR_PRES
; --------------------------------------------------------------
; This block sets the Stripper reboiler pressure such that the reboiler
; temperature is 121C +- 1C.

DESIGN-SPEC "STR_PRES"
        DEFINE TN STREAM-VAR STREAM=LEAN-HX VARIABLE=TEMP

        SPEC "TN" TO "121"
        TOL-SPEC "1"

        VARY BLOCK-VAR BLOCK=STRIPPER SENTENCE=P-SPEC VARIABLE=PRES ID1=1
        LIMITS "101.3" "303.9"

; --------------------------------------------------------------
; Design specification:  CO2RECOV
; --------------------------------------------------------------
; This block sets the CO2 flow rate for the stream CO2 such that a CO2
; recovery of 85% is achieved.

DESIGN-SPEC CO2RECOV
        DEFINE FLCO2 MOLE-FLOW STREAM=FLSH-CO2 COMPONENT=CO2
        DEFINE STCO2 MOLE-FLOW STREAM=STR-CO2 COMPONENT=CO2

        SPEC "STCO2" TO "0.8847 - FLCO2"
        TOL-SPEC "0.01"

        VARY BLOCK-VAR BLOCK=STRIPPER SENTENCE=COL-SPECS VARIABLE=MOLE-RR
;        LIMITS "0.01" "0.99"
        LIMITS "0.01" "2.00"

; --------------------------------------------------------------
; Optimization:  MINDER8
; --------------------------------------------------------------
; This block adjusts the design (size and operation) of the Stripper
; in order to minimize the power demand (expressed in MWe) subject to
; the following constraints:
;   1. approach to entrainment flooding is less than or equal to 80%
;   2. reboiler temperature is less than or equal to 122C
;   3. CO2 captured is 85% of that initially present in flue gas

OPTIMIZATION MINDER8
        DEFINE QREB BLOCK-VAR BLOCK=STRIPPER SENTENCE=RESULTS &
                VARIABLE=REB-DUTY
        DEFINE PPUMP BLOCK-VAR BLOCK="RICH_PUM" SENTENCE=RESULTS &
```

```
                VARIABLE=BRAKE-POWER
        DEFINE PCOMP BLOCK-VAR BLOCK="CO2_COMP" SENTENCE=RESULTS &
                VARIABLE=BRAKE-POWER

        MINIMIZE "0.35*QREB + 0.98*(PPUMP + PCOMP)"

        CONSTRAINTS MAXFLOOD / MAXTREB / CO2RECOV

        VARY BLOCK-VAR BLOCK=STRIPPER SENTENCE=PACK-RATE &
                VARIABLE=DIAM ID1=1
        LIMITS "1" "15"  MAX-STEP-SIZE=0.1

        VARY BLOCK-VAR BLOCK=STRIPPER SENTENCE=COL-SPECS VARIABLE=B:F
        LIMITS "0.97" "0.99"

        VARY BLOCK-VAR BLOCK=STRIPPER SENTENCE=P-SPEC VARIABLE=PRES ID1=1
        LIMITS "101.3" "303.9"

        VARY BLOCK-VAR BLOCK=STRIPPER SENTENCE=COL-SPECS VARIABLE=MOLE-RR
        LIMITS "0.01" "1.00"

; ---------------------------------------------------------------
; Constraint:  MAXFLOOD
; ---------------------------------------------------------------
; This block specifies a maximum approach to entrainment flooding in
; the Stripper of 80%.
CONSTRAINT MAXFLOOD
             DEFINE EFA BLOCK-VAR BLOCK=STRIPPER SENTENCE=PRATE-RESULT &
                     VARIABLE=FLOOD-FAC ID1=1

        SPEC "EFA" LE "0.80"
        TOL-SPEC "0.005"

; ---------------------------------------------------------------
; Constraint:  MAXTREB
; ---------------------------------------------------------------
; This block specifies a maximum temperature in the Stripper reboiler
; of 122C.
CONSTRAINT MAXTREB
        DEFINE TN STREAM-VAR STREAM=LEAN-HX VARIABLE=TEMP

        SPEC "TN" LE "122"
        TOL-SPEC "0.5"

; ---------------------------------------------------------------
; Constraint:  CO2RECOV
; ---------------------------------------------------------------
; This block specifies the CO2 flow rate for the stream CO2 such that a CO2
; recovery of 85% is achieved.
```

```
CONSTRAINT CO2RECOV
        DEFINE FLCO2 MOLE-FLOW STREAM=FLSH-CO2 COMPONENT=CO2
        DEFINE STCO2 MOLE-FLOW STREAM=STR-CO2 COMPONENT=CO2

        SPEC "STCO2 + FLCO2" GE "0.8847"
        TOL-SPEC "0.01"
```

F.4 *Meaplant* design using optimization

```
; File:  meaplant_packing_minder8_template.inp
; -------------------------------------------
; This file simulates a capture process for recovering CO2 from flue gas
; using MEA absorption.  RateSep, in rating, mode is used to model the
; Absorber and the Stripper.

; The Absorber design (i.e., selection of diameter is taken from the
; results of the standalone Absorber simulation for a column with a
; packed hieght of 10 metres (5 segments per metre) and a lean solvent
; loading of 0.25.

; The Stripper design (i.e., selection of diameter, reflux ratio,
; bottoms-to-feed ratio, reboiler pressure) is taken from the results
; of the standalone Stripper simulation for a column with a packed
; height of 10 metres (2 segments per metre) and a lean solvent
; loading of 0.25.

; A flash is used to remove the vapour contained in the heat exchanger
; outlet.

;-----------------------------------------------------------------------
; Report options
;-----------------------------------------------------------------------

STREAM-REPOR MOLEFLOW MASSFLOW

;-----------------------------------------------------------------------
; Diagnostic specifications
;-----------------------------------------------------------------------

DIAGNOSTICS
        HISTORY SIM-LEVEL=4 CONV-LEVEL=4
        MAX-PRINT SIM-LIMIT=99999

; This paragraph specifies time and error limits.
RUN-CONTROL MAX-TIME=99999 MAX-ERRORS=86400

; This paragraph will case AspenPlus to include FORTRAN tracebacks in the
; history file.
SYS-OPTIONS TRACE=YES

;-----------------------------------------------------------------------
; Units
;-----------------------------------------------------------------------

IN-UNITS SI PRESSURE=kPa TEMPERATURE=C PDROP='N/sqm'

;-----------------------------------------------------------------------
```

```
; Property Databanks
;---------------------------------------------------------------------

DATABANKS ASPENPCD  / AQUEOUS  / SOLIDS  / INORGANIC  / PURE13

PROP-SOURCES ASPENPCD  / AQUEOUS  / SOLIDS  / INORGANIC / PURE13

;---------------------------------------------------------------------
; Properties
;---------------------------------------------------------------------

PROPERTIES ELECNRTL HENRY-COMPS=MEA-CO2 CHEMISTRY=MEA-CO2 TRUE-COMPS=YES

PROP-SET LPHASE MUMX RHOMX SIGMAMX VOLFLMX MASSFLMX PHASE=L &
         UNITS='KG/CUM' 'DYNE/CM'
PROP-SET VPHASE RHOMX VOLFLMX MASSFLMX PHASE=V UNITS='KG/CUM'

PROP-DATA HENRY-1
    IN-UNITS MET VOLUME-FLOW='cum/hr' ENTHALPY-FLO='Gcal/hr'  &
        HEAT-TRANS-C='kcal/hr-sqm-K' PRESSURE=bar TEMPERATURE=C  &
        VOLUME=cum DELTA-T=C HEAD=meter MOLE-DENSITY='kmol/cum'  &
        MASS-DENSITY='kg/cum' MOLE-ENTHALP='kcal/mol'  &
        MASS-ENTHALP='kcal/kg' HEAT=Gcal MOLE-CONC='mol/l'  &
        PDROP=bar
    PROP-LIST HENRY
    BPVAL CO2 H2O 159.1996745 -8477.711000 -21.95743000  &
        5.78074800E-3 -.1500000000 226.8500000 0.0

PROP-DATA NRTL-1
    IN-UNITS MET VOLUME-FLOW='cum/hr' ENTHALPY-FLO='Gcal/hr'  &
        HEAT-TRANS-C='kcal/hr-sqm-K' PRESSURE=bar TEMPERATURE=C  &
        VOLUME=cum DELTA-T=C HEAD=meter MOLE-DENSITY='kmol/cum'  &
        MASS-DENSITY='kg/cum' MOLE-ENTHALP='kcal/mol'  &
        MASS-ENTHALP='kcal/kg' HEAT=Gcal MOLE-CONC='mol/l'  &
        PDROP=bar
    PROP-LIST NRTL
    BPVAL H2O MEA 1.438498000 99.02104000 .2000000000 0.0 0.0  &
        0.0 25.00000000 150.0000000
    BPVAL MEA H2O -1.046602000 -337.5456000 .2000000000 0.0  &
        0.0 0.0 25.00000000 150.0000000
    BPVAL H2O CO2 10.06400000 -3268.135000 .2000000000 0.0 0.0  &
        0.0 0.0 200.0000000
    BPVAL CO2 H2O 10.06400000 -3268.135000 .2000000000 0.0 0.0  &
        0.0 0.0 200.0000000

PROP-DATA VLCLK-1
    IN-UNITS MET VOLUME-FLOW='cum/hr' ENTHALPY-FLO='Gcal/hr'  &
        HEAT-TRANS-C='kcal/hr-sqm-K' PRESSURE=bar TEMPERATURE=C  &
        VOLUME=cum DELTA-T=C HEAD=meter MOLE-DENSITY='kmol/cum'  &
        MASS-DENSITY='kg/cum' MOLE-ENTHALP='kcal/mol'  &
```

```
        MASS-ENTHALP='kcal/kg' HEAT=Gcal MOLE-CONC='mol/l'  &
        PDROP=bar
    PROP-LIST VLCLK
    BPVAL MEA+ OH- -390.9954000 1000.000000

PROP-DATA GMELCC-1
    IN-UNITS MET VOLUME-FLOW='cum/hr' ENTHALPY-FLO='Gcal/hr'  &
        HEAT-TRANS-C='kcal/hr-sqm-K' PRESSURE=bar TEMPERATURE=C  &
        VOLUME=cum DELTA-T=C HEAD=meter MOLE-DENSITY='kmol/cum'  &
        MASS-DENSITY='kg/cum' MOLE-ENTHALP='kcal/mol'  &
        MASS-ENTHALP='kcal/kg' HEAT=Gcal MOLE-CONC='mol/l'  &
        PDROP=bar
    PROP-LIST GMELCC
    PPVAL H2O ( MEA+ MEACOO- ) 9.887700000
    PPVAL ( MEA+ MEACOO- ) H2O -4.951100000
    PPVAL H2O ( MEA+ HCO3- ) 5.354100000
    PPVAL ( MEA+ HCO3- ) H2O -4.070500000
    PPVAL H2O ( H3O+ HCO3- ) 8.045000000
    PPVAL ( H3O+ HCO3- ) H2O -4.072000000
    PPVAL H2O ( H3O+ OH- ) 8.045000000
    PPVAL ( H3O+ OH- ) H2O -4.072000000
    PPVAL H2O ( H3O+ CO3-- ) 8.045000000
    PPVAL ( H3O+ CO3-- ) H2O -4.072000000
    PPVAL MEA ( MEA+ MEACOO- ) 15.00000000
    PPVAL ( MEA+ MEACOO- ) MEA -8.000000000
    PPVAL MEA ( MEA+ HCO3- ) 15.00000000
    PPVAL ( MEA+ HCO3- ) MEA -8.000000000
    PPVAL MEA ( MEA+ OH- ) 15.00000000
    PPVAL ( MEA+ OH- ) MEA -8.000000000
    PPVAL MEA ( MEA+ CO3-- ) 15.00000000
    PPVAL ( MEA+ CO3-- ) MEA -8.000000000
    PPVAL MEA ( H3O+ MEACOO- ) 15.00000000
    PPVAL ( H3O+ MEACOO- ) MEA -8.000000000
    PPVAL MEA ( H3O+ HCO3- ) 15.00000000
    PPVAL ( H3O+ HCO3- ) MEA -8.000000000
    PPVAL MEA ( H3O+ OH- ) 15.00000000
    PPVAL ( H3O+ OH- ) MEA -8.000000000
    PPVAL MEA ( H3O+ CO3-- ) 15.00000000
    PPVAL ( H3O+ CO3-- ) MEA -8.000000000
    PPVAL CO2 ( MEA+ MEACOO- ) 15.00000000
    PPVAL ( MEA+ MEACOO- ) CO2 -8.000000000
    PPVAL CO2 ( MEA+ HCO3- ) 15.00000000
    PPVAL ( MEA+ HCO3- ) CO2 -8.000000000
    PPVAL CO2 ( MEA+ OH- ) 15.00000000
    PPVAL ( MEA+ OH- ) CO2 -8.000000000
    PPVAL CO2 ( MEA+ CO3-- ) 15.00000000
    PPVAL ( MEA+ CO3-- ) CO2 -8.000000000
    PPVAL CO2 ( H3O+ MEACOO- ) 15.00000000
    PPVAL ( H3O+ MEACOO- ) CO2 -8.000000000
    PPVAL CO2 ( H3O+ HCO3- ) 15.00000000
```

```
    PPVAL ( H3O+ HCO3- ) CO2 -8.000000000
    PPVAL CO2 ( H3O+ OH- ) 15.00000000
    PPVAL ( H3O+ OH- ) CO2 -8.000000000
    PPVAL CO2 ( H3O+ CO3-- ) 15.00000000
    PPVAL ( H3O+ CO3-- ) CO2 -8.000000000

PROP-DATA GMELCD-1
    IN-UNITS MET VOLUME-FLOW='cum/hr' ENTHALPY-FLO='Gcal/hr'  &
        HEAT-TRANS-C='kcal/hr-sqm-K' PRESSURE=bar TEMPERATURE=C  &
        VOLUME=cum DELTA-T=C HEAD=meter MOLE-DENSITY='kmol/cum'  &
        MASS-DENSITY='kg/cum' MOLE-ENTHALP='kcal/mol'  &
        MASS-ENTHALP='kcal/kg' HEAT=Gcal MOLE-CONC='mol/l'  &
        PDROP=bar
    PROP-LIST GMELCD
    PPVAL H2O ( MEA+ MEACOO- ) 10.81300000
    PPVAL ( MEA+ MEACOO- ) H2O 0.0
    PPVAL H2O ( MEA+ HCO3- ) 965.2400000
    PPVAL ( MEA+ HCO3- ) H2O -11.06700000
    PPVAL MEA ( MEA+ MEACOO- ) 0.0
    PPVAL ( MEA+ MEACOO- ) MEA 0.0
    PPVAL MEA ( MEA+ HCO3- ) 0.0
    PPVAL ( MEA+ HCO3- ) MEA 0.0
    PPVAL MEA ( MEA+ OH- ) 0.0
    PPVAL ( MEA+ OH- ) MEA 0.0
    PPVAL MEA ( MEA+ CO3-- ) 0.0
    PPVAL ( MEA+ CO3-- ) MEA 0.0
    PPVAL MEA ( H3O+ MEACOO- ) 0.0
    PPVAL ( H3O+ MEACOO- ) MEA 0.0
    PPVAL MEA ( H3O+ HCO3- ) 0.0
    PPVAL ( H3O+ HCO3- ) MEA 0.0
    PPVAL MEA ( H3O+ OH- ) 0.0
    PPVAL ( H3O+ OH- ) MEA 0.0
    PPVAL MEA ( H3O+ CO3-- ) 0.0
    PPVAL ( H3O+ CO3-- ) MEA 0.0
    PPVAL CO2 ( MEA+ MEACOO- ) 0.0
    PPVAL ( MEA+ MEACOO- ) CO2 0.0
    PPVAL CO2 ( MEA+ HCO3- ) 0.0
    PPVAL ( MEA+ HCO3- ) CO2 0.0
    PPVAL CO2 ( MEA+ OH- ) 0.0
    PPVAL ( MEA+ OH- ) CO2 0.0
    PPVAL CO2 ( MEA+ CO3-- ) 0.0
    PPVAL ( MEA+ CO3-- ) CO2 0.0
    PPVAL CO2 ( H3O+ MEACOO- ) 0.0
    PPVAL ( H3O+ MEACOO- ) CO2 0.0
    PPVAL CO2 ( H3O+ HCO3- ) 0.0
    PPVAL ( H3O+ HCO3- ) CO2 0.0
    PPVAL CO2 ( H3O+ OH- ) 0.0
    PPVAL ( H3O+ OH- ) CO2 0.0
    PPVAL CO2 ( H3O+ CO3-- ) 0.0
    PPVAL ( H3O+ CO3-- ) CO2 0.0
```

```
PROP-DATA GMELCE-1
    IN-UNITS MET VOLUME-FLOW='cum/hr' ENTHALPY-FLO='Gcal/hr'  &
        HEAT-TRANS-C='kcal/hr-sqm-K' PRESSURE=bar TEMPERATURE=C  &
        VOLUME=cum DELTA-T=C HEAD=meter MOLE-DENSITY='kmol/cum'  &
        MASS-DENSITY='kg/cum' MOLE-ENTHALP='kcal/mol'  &
        MASS-ENTHALP='kcal/kg' HEAT=Gcal MOLE-CONC='mol/l'  &
        PDROP=bar
    PROP-LIST GMELCE
    PPVAL MEA ( MEA+ MEACOO- ) 0.0
    PPVAL ( MEA+ MEACOO- ) MEA 0.0
    PPVAL MEA ( MEA+ HCO3- ) 0.0
    PPVAL ( MEA+ HCO3- ) MEA 0.0
    PPVAL MEA ( MEA+ OH- ) 0.0
    PPVAL ( MEA+ OH- ) MEA 0.0
    PPVAL MEA ( MEA+ CO3-- ) 0.0
    PPVAL ( MEA+ CO3-- ) MEA 0.0
    PPVAL MEA ( H3O+ MEACOO- ) 0.0
    PPVAL ( H3O+ MEACOO- ) MEA 0.0
    PPVAL MEA ( H3O+ HCO3- ) 0.0
    PPVAL ( H3O+ HCO3- ) MEA 0.0
    PPVAL MEA ( H3O+ OH- ) 0.0
    PPVAL ( H3O+ OH- ) MEA 0.0
    PPVAL MEA ( H3O+ CO3-- ) 0.0
    PPVAL ( H3O+ CO3-- ) MEA 0.0
    PPVAL CO2 ( MEA+ MEACOO- ) 0.0
    PPVAL ( MEA+ MEACOO- ) CO2 0.0
    PPVAL CO2 ( MEA+ HCO3- ) 0.0
    PPVAL ( MEA+ HCO3- ) CO2 0.0
    PPVAL CO2 ( MEA+ OH- ) 0.0
    PPVAL ( MEA+ OH- ) CO2 0.0
    PPVAL CO2 ( MEA+ CO3-- ) 0.0
    PPVAL ( MEA+ CO3-- ) CO2 0.0
    PPVAL CO2 ( H3O+ MEACOO- ) 0.0
    PPVAL ( H3O+ MEACOO- ) CO2 0.0
    PPVAL CO2 ( H3O+ HCO3- ) 0.0
    PPVAL ( H3O+ HCO3- ) CO2 0.0
    PPVAL CO2 ( H3O+ OH- ) 0.0
    PPVAL ( H3O+ OH- ) CO2 0.0
    PPVAL CO2 ( H3O+ CO3-- ) 0.0
    PPVAL ( H3O+ CO3-- ) CO2 0.0

PROP-DATA GMELCN-1
    IN-UNITS MET VOLUME-FLOW='cum/hr' ENTHALPY-FLO='Gcal/hr'  &
        HEAT-TRANS-C='kcal/hr-sqm-K' PRESSURE=bar TEMPERATURE=C  &
        VOLUME=cum DELTA-T=C HEAD=meter MOLE-DENSITY='kmol/cum'  &
        MASS-DENSITY='kg/cum' MOLE-ENTHALP='kcal/mol'  &
        MASS-ENTHALP='kcal/kg' HEAT=Gcal MOLE-CONC='mol/l'  &
        PDROP=bar
    PROP-LIST GMELCN
```

```
    PPVAL MEA ( MEA+ MEACOO- ) .1000000000
    PPVAL MEA ( MEA+ HCO3- ) .1000000000
    PPVAL MEA ( MEA+ OH- ) .1000000000
    PPVAL MEA ( MEA+ CO3-- ) .1000000000
    PPVAL MEA ( H3O+ MEACOO- ) .1000000000
    PPVAL MEA ( H3O+ HCO3- ) .1000000000
    PPVAL MEA ( H3O+ OH- ) .1000000000
    PPVAL MEA ( H3O+ CO3-- ) .1000000000
    PPVAL CO2 ( MEA+ MEACOO- ) .1000000000
    PPVAL CO2 ( MEA+ HCO3- ) .1000000000
    PPVAL CO2 ( MEA+ OH- ) .1000000000
    PPVAL CO2 ( MEA+ CO3-- ) .1000000000
    PPVAL CO2 ( H3O+ MEACOO- ) .1000000000
    PPVAL CO2 ( H3O+ HCO3- ) .1000000000
    PPVAL CO2 ( H3O+ OH- ) .1000000000
    PPVAL CO2 ( H3O+ CO3-- ) .1000000000

;-----------------------------------------------------------------------
; Components
;-----------------------------------------------------------------------

COMPONENTS
    H2O H2O /
    MEA C2H7NO /
    CO2 CO2 /
    MEA+ C2H8NO+ /
    H3O+ H3O+ /
    MEACOO- C3H6NO3- /
    HCO3- HCO3- /
    OH- OH- /
    CO3-- CO3-2 /
    N2 N2

HENRY-COMPS MEA-CO2 CO2 N2

;-----------------------------------------------------------------------
; Chemistry
;-----------------------------------------------------------------------

CHEMISTRY MEA-CO2
    STOIC 1 H2O -2 / H3O+ 1 / OH- 1
    STOIC 2 CO2 -1 / H2O -2 / H3O+ 1 / HCO3- 1
    STOIC 3 HCO3- -1 / H2O -1 / H3O+ 1 / CO3-- 1
    STOIC 4 MEA+ -1 / H2O -1 / MEA 1 / H3O+ 1
    STOIC 5 MEACOO- -1 / H2O -1 / MEA 1 / HCO3- 1
    K-STOIC 1 A=132.89888 B=-13445.9 C=-22.4773 D=0
    K-STOIC 2 A=231.465439 B=-12092.1 C=-36.7816 D=0
    K-STOIC 3 A=216.05043 B=-12431.7 C=-35.4819 D=0
    K-STOIC 4 A=-3.038325 B=-7008.357 C=0 D=-.00313489
    K-STOIC 5 A=-.52135 B=-2545.53 C=0 D=0
```

```
;---------------------------------------------------------------------
; Flowsheet
;---------------------------------------------------------------------

FLOWSHEET ABSSEC
        BLOCK FLUESPLT   IN=FLUE-SPL          OUT=FLUE-BLO FLUE-AUX
        BLOCK BLOWER     IN=FLUE-BLO          OUT=FLUE-DCC P-BLOW
        BLOCK "H2O_PUMP" IN=H2O-PUMP          OUT=H2O-DCC P-H2OP
        BLOCK DCC        IN=FLUE-DCC H2O-DCC  OUT=FLUE-ABS H2O-OUT
        BLOCK ABSORBER   IN=FLUE-ABS LEAN-ABS OUT=STACK RICH-PUM

FLOWSHEET STRSEC
        BLOCK "RICH_PUM" IN=RICH-PUM          OUT=RICH-HX P-RICHP
        BLOCK FLASH      IN=RICH-FLA          OUT=FLSH-CO2 RICH-STR
        BLOCK STRIPPER   IN=RICH-STR          OUT=STR-CO2 LEAN-HX
        BLOCK HEATX      IN=RICH-HX LEAN-HX   OUT=RICH-FLA LEAN-MIX
        BLOCK "CO2_COOL" IN=FLSH-CO2 STR-CO2  OUT=CO2-COMP ST1
        BLOCK "CO2_COMP" IN=CO2-COMP          OUT=CO2 ST2 ST3 ST4 P-COMP
        BLOCK POWER      IN= P-RICHP P-COMP   OUT=POWER

FLOWSHEET GLOBAL
        BLOCK "MU_MIXER" IN=LEAN-MIX ST1 ST2 ST3 ST4 MAKE-UP OUT=LEAN-HT
        BLOCK "ABS_PRHT" IN=LEAN-HT           OUT=LEAN-ABS

;---------------------------------------------------------------------
; Stream Specification
;---------------------------------------------------------------------

; specify the heat and work streams in the flowsheet
DEF-STREAMS WORK P-BLOW P-H2OP POWER P-RICHP P-COMP POWER

; The flue gas composition is estimated for 50/50 PRB/USLS coal mix with
; heat input as determined from steam cycle.  The temperature is the
; temperature at the air heater outlet taken from the boiler design data.
STREAM FLUE-SPL TEMP=40 <C> PRES=101.3 MASS-FLOW=2315713 <KG/HR>
        MOLE-FRAC N2 0.78991 / CO2 0.14627 / H2O 0.06381

; Cooling water temperature for Lake Erie is not given.  12C is summer
; mean temperature form IEA technical specifications document...
STREAM H2O-PUMP TEMP=12 PRES=101.3
        MOLE-FLOW H2O 1

STREAM MAKE-UP TEMP=20 <C> PRES=101.3 <KPA> MOLE-FLOW=1.0
        MOLE-FRAC MEA 0.874 / MEA 0.126

; Note:  12.6 M MEA is 30 wt%
;        CO2 loading is 0.10
STREAM LEAN-ABS TEMP=40 PRES=101.3 MOLE-FLOW=30.9
        MOLE-FRAC MEA 0.126 / H2O 0.874 / CO2 .03150
```

```
; Note:  F is obtained from absorber results
STREAM LEAN-HX VFRAC=0 PRES=173 MOLE-FLOW=30.2
        MOLE-FRAC H2O 0.874 / MEA 0.126 / CO2 .03150

;-----------------------------------------------------------------------
; Block Specification
;-----------------------------------------------------------------------

;<FLUESPLT>
BLOCK FLUESPLT FSPLIT
        FRAC FLUE-BLO .33
;</FLUESPLT>

;<BLOWER>
BLOCK BLOWER COMPR
        PARAM TYPE=ISENTROPIC SEFF=0.90 MEFF=0.99 PRES=117.0 <kPa> NPHASE=2
;</BLOWER>

;<H2O_PUMP>
BLOCK "H2O_PUMP" PUMP
        PARAM PRES=117.0 <kPa>
;</H2O_PUMP>

; This block cools the flue gas stream with water.
BLOCK DCC FLASH2
        PARAM DUTY=0 PRES=-10 <kPa>

;<ABSORBER>
BLOCK ABSORBER RADFRAC
        PARAM NSTAGE=50 NPHASE=2 EFF=MURPHREE P-UPDATE=YES P-FIX=TOP &
                MAXOL=30 HYDRAULIC=YES

        COL-CONFIG CONDENSER=NONE REBOILER=NONE

        FEEDS FLUE-ABS 51 ABOVE-STAGE / LEAN-ABS 1 ABOVE-STAGE
        PRODUCTS STACK 1 V / RICH-PUM 50 L

        P-SPEC 1 101.3 / 50 106.9

        COL-SPECS 1 MOLE-RDV=1

; Specifies where to consider solution chemistry
        REAC-STAGES 1 50 MEA-CO2

; For rate-based analysis, the diameter is used as an initial guess
        PACK-RATE 1 1 50 RASCHIG PACK-MAT=METAL PACK-SIZE=75-MM &
                VENDOR=GENERIC PACK-HT=10 <METER> DIAM=11.2 DPMETH=ECKERT &
                P-UPDATE=YES
```

```
; Enables rate-based analysis (must also have TRAY-RATE or PACK-RATE sentence)
        RATESEP-ENAB CALC-MODE=RIG-RATE
        RATESEP-PARA INIT-EQUIL=YES RS-MAXIT=100

        PACK-RATE2 1 RATE-BASED=YES

        REPORT HYDANAL EXTHYD
        TRAY-REPORT2 COMP-EFF=YES STAGE-EFF=YES
;</ABSORBER>

;<RICH_PUM>
BLOCK "RICH_PUM" PUMP
        PARAM PRES=142.5 <kPa>
;</RICH_PUM>


BLOCK FLASH FLASH2
        PARAM PRES=0 DUTY=0

;<STRIPPER>
BLOCK STRIPPER RADFRAC
        PARAM NSTAGE=22 NPHASE=2 EFF=MURPHREE P-UPDATE=YES P-FIX=TOP &
                MAXOL=30 HYDRAULIC=YES

        COL-CONFIG CONDENSER=PARTIAL-V REBOILER=KETTLE

        FEEDS RICH-STR 2 ABOVE-STAGE
        PRODUCTS STR-CO2 1 V / LEAN-HX 22 L

        P-SPEC 1 141.0 / 22 144.93

        COL-SPECS MOLE-RDV=1 MOLE-RR=.46 B:F=.990
        DB:F-PARAMS

; Specifies where to consider solution chemistry
        REAC-STAGES 1 22 MEA-CO2

        PACK-RATE 1 2 21 RASCHIG PACK-MAT=METAL PACK-SIZE=75-MM &
                VENDOR=GENERIC PACK-HT=10 <METER> DIAM=7.6 <METER> &
                DPMETH=ECKERT P-UPDATE=YES

; Enables rate-based analysis (must also have TRAY-RATE sentence)
        RATESEP-ENAB CALC-MODE=RIG-RATE
        RATESEP-PARA INIT-EQUIL=YES RS-MAXIT=50
        PACK-RATE2 1 RATE-BASED=YES

        REPORT HYDANAL EXTHYD
;</STRIPPER>

; Shortcut heat exchanger calculation.
```

```
; 10 degree temperature approach at the hot stream outlet
; U = 1134 W / m^2 C (taken from Perry's for H2O-H2O liquid-liquid system)
BLOCK HEATX HEATX
        PARAM DELT-HOT=10
        FEEDS HOT=LEAN-HX COLD=RICH-HX
        PRODUCTS HOT=LEAN-MIX COLD=RICH-FLA
        HEAT-TR-COEF U=1134

BLOCK "CO2_COOL" FLASH2
        PARAM PRES=0 TEMP=25 <C>

BLOCK "CO2_COMP" MCOMPR
        PARAM NSTAGE=4 TYPE=ISENTROPIC PRES=110 <BAR> COMPR-NPHASE=1

        FEEDS CO2-COMP 1
        PRODUCTS ST2 1 L / ST3 2 L / ST4 3 L / CO2 4 / P-COMP GLOBAL
        COMPR-SPECS 1 SEFF=0.90 MEFF=0.99

        COOLER-SPECS 1 TEMP=25

BLOCK POWER MIXER

BLOCK "MU_MIXER" MIXER

BLOCK "ABS_PRHT" HEATER
        PARAM PRES=0 TEMP=40 <C>

;-----------------------------------------------------------------------
; Convergence Specifications
;-----------------------------------------------------------------------

; This determines if results of previous convergence are used as starting
; point.
SIM-OPTIONS RESTART=YES

CONV-OPTIONS
        PARAM SPEC-METHOD=SECANT TEAR-VAR=YES CHECK-SEQ=NO

CONVERGENCE COOL-FLU SECANT
        DESCRIPTION "Control convergence of design-spec COOL-FLU"
        SPEC COOL-FLU

CONVERGENCE ABSLOOP WEGSTEIN
        DESCRIPTION "Control convergence of tear stream LEAN-ABS"
        TEAR LEAN-ABS / ST1 / ST2 / ST3 / ST4

CONVERGENCE HXLOOP WEGSTEIN
        DESCRIPTION "Control convergence of tear stream LEAN-HX"
        TEAR LEAN-HX
        TEAR-VAR FOR-BLOCK=PUMPP VAR-NAME=PPUMP LOWER=101.3 UPPER=300
```

```
CONVERGENCE PRESSURE SQP
        DESCRIPTION "Converge BLOWER and H2O_PUMP pressure"

        BLOCK-OPTIONS CONV-LEVEL=5

        TEAR-VAR FOR-BLOCK=BLOWERP VAR-NAME=PBLOW LOWER=101.3 UPPER=300
        TEAR-VAR FOR-BLOCK=BLOWERP VAR-NAME=PPUMP LOWER=101.3 UPPER=300
        OPTIMIZE MINDER8

SEQUENCE CAPTURE &
        PRESSURE &
                MANIPLOG BLOWER &
                COOL-FLU &
                         "H2O_PUMP" DCC &
                (RETURN COOL-FLU) &
                ABSLOOP &
                        ABSORBER &
                        HXLOOP &
                                "RICH_PUM" HEATX FLASH STRIPPER PUMPP &
                        (RETURN HXLOOP) &
                        "CO2_COOL" "CO2_COMP" POWER &
                        MAKEUP "MU_MIXER" "ABS_PRHT" &
                (RETURN ABSLOOP) &
                OPTIMLOG BLOWERP &
        (RETURN PRESSURE)

DISABLE

; -------------------------------------------------------------
; Calculator:  BLOWERP
; -------------------------------------------------------------
; This block sets the pressure increase in the BLOWER equal to the pressure
; drop across the ABSORBER.
;
; In order to get the CALCULATOR block to introduce a convergence loop, the
; TEAR variable must be specified as a write variable, there should not be
; an EXECUTE sentence, and TEAR-VAR=YES must be specified in the
; CONV-OPTIONS paragraph.

CALCULATOR BLOWERP
        DEFINE PN BLOCK-VAR BLOCK=ABSORBER SENTENCE=PROFILE VARIABLE=PRES &
                ID1=50
        DEFINE DPDCC BLOCK-VAR BLOCK=DCC SENTENCE=PARAM VARIABLE=PRES

        DEFINE PBLOW BLOCK-VAR BLOCK=BLOWER SENTENCE=PARAM VARIABLE=PRES
        DEFINE PPUMP BLOCK-VAR BLOCK="H2O_PUMP" SENTENCE=PARAM VARIABLE=PRES

F       PBLOW = PN - DPDCC
F       PPUMP = PN - DPDCC
```

```
        READ-VARS PN DPDCC
        WRITE-VARS PBLOW PPUMP

        TEAR-VARS TEAR-VAR=PBLOW LOWER=101 UPPER=250

; -------------------------------------------------------------
; Design specification:  COOL-FLU
; -------------------------------------------------------------
; This block adjusts the flow rate of cooling water until the flue gas
; reaches the desired temperature.

DESIGN-SPEC COOL-FLU
        DEFINE TFLUE STREAM-VAR STREAM=FLUE-ABS VARIABLE=TEMP

        SPEC "TFLUE" TO "40"
        TOL-SPEC "0.5"

        VARY STREAM-VAR STREAM=H2O-PUMP VARIABLE=MOLE-FLOW
        LIMITS "0" "10"

; -------------------------------------------------------------
; Calculator:  PUMPP
; -------------------------------------------------------------
; This block sets the pressure increase in the RICH_PUM equal to the
; pressure at the STRIPPER inlet.
;
; In order to get the CALCULATOR block to introduce a convergence loop, the
; TEAR variable must be specified as a write variable, there should not be
; an EXECUTE sentence, and TEAR-VAR=YES must be specified in the
; CONV-OPTIONS paragraph.
CALCULATOR PUMPP
        DEFINE P2 BLOCK-VAR BLOCK=STRIPPER SENTENCE=PROFILE VARIABLE=PRES &
                ID1=2

        DEFINE PPUMP BLOCK-VAR BLOCK="RICH_PUM" SENTENCE=PARAM VARIABLE=PRES

F       PPUMP = P2

        READ-VARS P2
        WRITE-VARS PPUMP

        TEAR-VARS TEAR-VAR=PPUMP LOWER=101 UPPER=250

; -------------------------------------------------------------
; Balance block:  MAKEUP
; -------------------------------------------------------------
; This block calculates the composition and flow rate of stream
; MAKE-UP for the lean MEA recycle.
```

```
BALANCE MAKEUP
        PARAM EXECUTE=ALWAYS

        M-BAL 1 INLETS=FLUE-ABS MAKE-UP OUTLETS=STACK CO2 &
                 COMPS=H2O H3O+ OH- MEA MEA+ MEACOO-

        CALCULATE MAKE-UP FLOW=COMPS ENTHALPY=NO &
                 COMPS=H2O H3O+ OH- MEA MEA+ MEACOO-

; ---------------------------------------------------------------
; Calculator:  MANIPLOG
; ---------------------------------------------------------------
; This block outputs the values of the manipulated variables from
; the MINDR8 optimization block.

CALCULATOR MANIPLOG
        DEFINE PBLOW BLOCK-VAR BLOCK=BLOWER SENTENCE=PARAM VARIABLE=PRES
        DEFINE PPUMP BLOCK-VAR BLOCK="H2O_PUMP" SENTENCE=PARAM VARIABLE=PRES
        DEFINE FLEAN STREAM-VAR STREAM=LEAN-ABS VARIABLE=MOLE-FLOW
        DEFINE BF BLOCK-VAR BLOCK=STRIPPER SENTENCE=COL-SPECS &
                VARIABLE=B:F
        DEFINE RR BLOCK-VAR BLOCK=STRIPPER SENTENCE=COL-SPECS &
                VARIABLE=MOLE-RR
        DEFINE PTOP BLOCK-VAR BLOCK=STRIPPER SENTENCE=PROFILE &
                VARIABLE=PRES ID1=1

F       WRITE(NHSTRY, *) PBLOW, PPUMP, FLEAN, BF, RR, PTOP

        READ-VARS PBLOW PPUMP FLEAN BF RR PTOP

; ---------------------------------------------------------------
; Calculator:  OPTIMLOG
; ---------------------------------------------------------------
; This block outputs the values of variables of interest during
; the MINDER8 optimization block.  First, the decision variables:
;   - ABSORBER and STRIPPER tray-spacing and diameter
;   - STRIPPER bottoms-to-feed ratio, reflux ratio, condenser pressure
;   - LEAN-ABS flow rate
;
; Second, important state variables:
;   - ABSORBER and STRIPPER vapour and downcomer approach to flooding
;   -
;   - BLOWER outlet pressure
;   - LEAN-ABS flowrate

CALCULATOR OPTIMLOG
C RCO2: CO2 recovery
F       REAL*8 RCO2

        DEFINE FLEAN STREAM-VAR STREAM=LEAN-ABS VARIABLE=MOLE-FLOW
```

```
       DEFINE DABS BLOCK-VAR BLOCK=ABSORBER SENTENCE=PACK-RATE &
               VARIABLE=DIAM ID1=1
       DEFINE DSTR BLOCK-VAR BLOCK=STRIPPER SENTENCE=PACK-RATE &
               VARIABLE=DIAM ID1=1
       DEFINE BF BLOCK-VAR BLOCK=STRIPPER SENTENCE=COL-SPECS &
               VARIABLE=B:F
       DEFINE RR BLOCK-VAR BLOCK=STRIPPER SENTENCE=COL-SPECS &
               VARIABLE=MOLE-RR
       DEFINE PTOP BLOCK-VAR BLOCK=STRIPPER SENTENCE=PROFILE &
               VARIABLE=PRES ID1=1

       DEFINE FAABS BLOCK-VAR BLOCK=ABSORBER SENTENCE=PRATE-RESULT &
               VARIABLE=FLOOD-FAC ID1=1
       DEFINE FASTR BLOCK-VAR BLOCK=STRIPPER SENTENCE=PRATE-RESULT &
               VARIABLE=FLOOD-FAC ID1=1
       DEFINE TREB BLOCK-VAR BLOCK=STRIPPER SENTENCE=PROFILE &
               VARIABLE=TEMP ID1=22
       DEFINE CO2IN MOLE-FLOW STREAM=FLUE-BLO COMPONENT=CO2
       DEFINE CO2OUT MOLE-FLOW STREAM=CO2 COMPONENT=CO2

       DEFINE PH2O BLOCK-VAR BLOCK="H2O_PUMP" SENTENCE=RESULTS &
               VARIABLE=BRAKE-POWER
       DEFINE PBLOW BLOCK-VAR BLOCK="BLOWER" SENTENCE=RESULTS &
               VARIABLE=BRAKE-POWER
       DEFINE PRICH BLOCK-VAR BLOCK="RICH_PUM" SENTENCE=RESULTS &
               VARIABLE=BRAKE-POWER
       DEFINE PCOMP BLOCK-VAR BLOCK="CO2_COMP" SENTENCE=RESULTS &
               VARIABLE=BRAKE-POWER
       DEFINE QREB BLOCK-VAR BLOCK=STRIPPER SENTENCE=RESULTS &
               VARIABLE=REB-DUTY

       DEFINE CO2 MOLE-FLOW STREAM=LEAN-HX COMPONENT=CO2
       DEFINE HCO3 MOLE-FLOW STREAM=LEAN-HX COMPONENT=HCO3-
       DEFINE CO3 MOLE-FLOW STREAM=LEAN-HX COMPONENT=CO3--
       DEFINE MEACOO MOLE-FLOW STREAM=LEAN-HX COMPONENT=MEACOO-
       DEFINE MEA MOLE-FLOW STREAM=LEAN-HX COMPONENT=MEA
       DEFINE MEAP MOLE-FLOW STREAM=LEAN-HX COMPONENT=MEA+

F      FCO2 = CO2 + HCO3 + CO3 + MEACOO
F      FMEA = MEA + MEAP + MEACOO
F      ALPHA = FCO2 / FMEA

F      RCO2 = CO2OUT / CO2IN

F      WRITE(NHSTRY, *) FLEAN, ALPHA, DABS, DSTR, BF,
F   + RR, PTOP, FAABS, FASTR, TREB, RCO2, PH2O, PBLOW,
F   + PRICH, PCOMP, QREB

       READ-VARS FLEAN DABS DSTR BF RR PTOP FAABS &
               FASTR TREB CO2IN CO2OUT PH2O PBLOW PRICH PCOMP QREB
```

```
; ---------------------------------------------------------------
; Optimization:  MINDER8
; ---------------------------------------------------------------
; This block attempts to minimize the reduction in net power plant
; caused by the CO2 capture process by adjusting the operation of the
; Absorber and Stripper subject to the following constraints:

;   1. approach to entrainment flooding is less than or equal to 80%
;   2. approach to downcomer flooding is less than or equal to 50%
;   3. reboiler temperature is less than or equal to 122C
;   4. CO2 captured is 85% of that initially present in flue gas

OPTIMIZATION MINDER8
        DEFINE PLOW BLOCK-VAR BLOCK=BLOWER SENTENCE=RESULTS &
                VARIABLE=BRAKE-POWER
        DEFINE QREB BLOCK-VAR BLOCK=STRIPPER SENTENCE=RESULTS &
                VARIABLE=REB-DUTY
        DEFINE PPUMP BLOCK-VAR BLOCK="RICH_PUM" SENTENCE=RESULTS &
                VARIABLE=BRAKE-POWER
        DEFINE PCOMP BLOCK-VAR BLOCK="CO2_COMP" SENTENCE=RESULTS &
                VARIABLE=BRAKE-POWER

        MINIMIZE "0.35*QREB + (PPUMP + PCOMP + PBLOW)/0.98"

        CONSTRAINTS ABSFLOOD / STRFLOOD /
                MAXTREB / CO2RECOV

        VARY STREAM-VAR STREAM=LEAN-ABS VARIABLE=MOLE-FLOW
        LIMITS "1" "40"

;        VARY BLOCK-VAR BLOCK=ABSORBER SENTENCE=PACK-RATE &
;                VARIABLE=DIAM ID1=1
;        LIMITS "1" "15"  MAX-STEP-SIZE=0.1

;        VARY BLOCK-VAR BLOCK=STRIPPER SENTENCE=PACK-RATE &
;                VARIABLE=DIAM ID1=1
;        LIMITS "1" "15"  MAX-STEP-SIZE=0.1

        VARY BLOCK-VAR BLOCK=STRIPPER SENTENCE=COL-SPECS VARIABLE=B:F
        LIMITS "0.97" "0.99"

        VARY BLOCK-VAR BLOCK=STRIPPER SENTENCE=P-SPEC VARIABLE=PRES ID1=1
        LIMITS "101.3" "303.9"

        VARY BLOCK-VAR BLOCK=STRIPPER SENTENCE=COL-SPECS VARIABLE=MOLE-RR
        LIMITS "0.01" "1.00" MAX-STEP-SIZE=0.10

; ---------------------------------------------------------------
; Constraint:  ABSFLOOD
```

```
; --------------------------------------------------------------
; This block specifies a maximum approach to entrainment flooding in
; the Absorber of 80%.
CONSTRAINT ABSFLOOD
             DEFINE EFA BLOCK-VAR BLOCK=ABSORBER SENTENCE=PRATE-RESULT &
                     VARIABLE=FLOOD-FAC ID1=1

        SPEC "EFA" LE "0.80"
        TOL-SPEC "0.005"

; --------------------------------------------------------------
; Constraint:  STRFLOOD
; --------------------------------------------------------------
; This block specifies a maximum approach to entrainment flooding in
; the Stripper of 80%.
CONSTRAINT STRFLOOD
             DEFINE EFA BLOCK-VAR BLOCK=STRIPPER SENTENCE=PRATE-RESULT &
                     VARIABLE=FLOOD-FAC ID1=1

        SPEC "EFA" LE "0.80"
        TOL-SPEC "0.005"

; --------------------------------------------------------------
; Constraint:  MAXTREB
; --------------------------------------------------------------
; This block specifies a maximum temperature in the Stripper reboiler
; of 122C.
CONSTRAINT MAXTREB
        DEFINE TN STREAM-VAR STREAM=LEAN-HX VARIABLE=TEMP

        SPEC "TN" LE "122"
        TOL-SPEC "0.5"

; --------------------------------------------------------------
; Constraint:  CO2RECOV
; --------------------------------------------------------------
; This block specifies the CO2 flow rate for the stream CO2 such that a CO2
; recovery of 85% is achieved.

CONSTRAINT CO2RECOV
        DEFINE CO2IN MOLE-FLOW STREAM=FLUE-BLO COMPONENT=CO2
        DEFINE CO2OUT MOLE-FLOW STREAM=CO2 COMPONENT=CO2

        SPEC "CO2OUT / CO2IN" GE ".85"
        TOL-SPEC "0.01"
```

Bibliography

[1] K. H. Abdul-Rahman, S. M. Shahidehpour, M. Aganagle, and S. Mokhtari. A practical resource scheduling with OPF constraints. *IEEE Transactions on Power Systems*, 11(1):254–259, feb 1996.

[2] Keigo Akimoto, Hironori Kotsubo, Takayoshi Asami, Xiaochun Li, Motoo Uno, Toshimasa Tomoda, and Takashi Ohsumi. Evaluation of carbon sequestrations in Japan with a mathematical model. In J. Gale and Y. Kaya, editors, *Greenhouse Gas Control Technologies: Proceedings of the 6th International Conference on Greenhouse Gas Control Technologies*, volume 1, pages 115–119. Elsevier Science Ltd., October 2002. find page reference....

[3] Colin Alie. CO_2 capture with MEA: integrating the absorption process and steam cycle of an existing coal-fired power plant. Master's thesis, University of Waterloo, Waterloo, Ontario, Canada, 2004. Electronic version available at `http://etd.uwaterloo.ca/etd/calie2004.pdf`.

[4] Colin Alie and Peter Douglas. Scoping study on operating flexibility of power plants with CO_2 capture. Technical Report 2008/TR1, IEA Greenhouse Gas R&D Programme, September 2008.

[5] anon. Technology roadmap: Carbon capture and storage. Technical report, International Energy Agency, Paris, France, 2013. `http://www.iea.org/publications/freepublications/publication/TechnologyRoadmapCarbonCaptureandStorage.pdf`.

[6] Aspen Technology, Inc., Cambridge, MA, USA. *Aspen Plus Version 11.1 User Guide*, September 2001.

[7] Aspen Technology, Inc., Cambridge, MA, USA. *Aspen Plus Version 2004.1 Input Language Guide*, April 2005.

[8] R Barchas and R Davis. The Kerr-McGee/ABB Lummus Crest technology for the recovery of CO_2 from stack gases. *Energy Conversion and Management*, 33(5–8):333–340, 1992.

[9] Arthur Bergen and Vijay Vittal. *Power Systems Analysis*. Prentice-Hall, Inc., Upper Saddle River, New Jersey, second edition, 2000.

[10] Nick Booth. Personal communication, June 2006. Combustion & Emission Control, E.ON.

[11] M. J. Box. A new method of constrained optimization and a comparison with other methods. *Computer Journal*, 7–8:42–52, 1964–1965.

[12] Hannah Chalmers and Jon Gibbins. Initial evaluation of the impact of post-combustion capture of carbon dioxide on supercritical pulverised coal power plant part load performance. *Fuel*, 86:pp 2109–2123, 2007.

[13] A. A. Chowdhury and D. O. Koval. Generation reliability impacts of industry-ownded distributed generation sources. In *Proceedings of 38th IAS Annual Meeting*, pages 1321–1327, October 2003.

[14] C. David Cooper and F. C. Alley. *Air pollution control: a design approach*. Waveland Press, Inc., U.S.A., second edition, 1994.

[15] Arne Drud. Conopt - a large-scale grg code. *ORSA Journal on Computing*, 6:207–216, 1992.

[16] Joseph P. Pickett *et al.*, editor. *The American Heritage Dictionary of the English Language*. Houghton Mifflin Company, Boston, fourth edition, 2000. http://www.bartleby.com/61/.

[17] Raymond F. Ghajar and Roy Billinton. Economic costs of power interruptions: a consistent model and methodology. *Electrical Power and Energy Systems*, 28:29–35, 2006.

[18] STEAG Energy Services GmbH. EBSILON® Professional. WWW. `http://www.steag-systemtechnologies.com/ebsilon_professional+M52087573ab0.html`.

[19] Don W. Green, editor. *Perry's chemical engineers' handbook*. McGraw-Hill, seventh edition, 1997.

[20] C. Grigg, P. Wong, P. Albrecht, R. Allan ad M. Bhavaraju, R. Billinton, Q. Chen, C. Fong, S. Haddad, S. Kuruganty, W. Li, R. Mukerji, D. Patton, N. Rau, D. Reppen, A. Schneider, M. Shahidehpour, and C. Singh. The IEEE reliability test system — 1996. *IEEE Transactions on Power Systems*, 14(3):1010–1021, August 1999.

[21] Haslenda Hashim. *An optimal fleet-wide CO_2 mitigation strategy for a network of power plants*. PhD thesis, University of Waterloo, Waterloo, Ontario, Canada, February 2006.

[22] IESO. *Market Rules for the Ontario Electricity Market*, thirty-second edition, December 2008. `http://ieso.com/imoweb/pubs/GuideToDocsInBaseline.pdf`.

[23] International Energy Agency, Paris, France. *World Energy Outlook*, 2008.

[24] IPCC. *Climate Change 2001: Mitigation*. Cambridge University Press, 2001. Contribution of Working Group III to the Third Assessment Report of the Intergovernmental Panel on Climate Change.

[25] Timothy L. Johnson and David Keith. Fossil electricity and CO_2 sequestration: how natural gas prices, initial conditions and retrofits determine the cost of controlling CO_2 emissions. *Energy Policy*, 32:367–382, 2004.

[26] Amit Kanudia and Richard Loulou. *Extended MARKAL: A Brief User Manual for its Stochastic Programming and Multi-Region Features*. Groupe d'études et de recherche en analyse des décicions, March 1997.

[27] Amit Kanudia and Richard Loulou. Joint mitigation under the Kyoto protocol: A Canada-USA-India case study. *submitted to Energy Policy*, 1998.

[28] Amit Kanudia and Richard Loulou. Advanced bottom-up modelling for national and regional energy planning in response to climate change. *International Journal of Environment and Pollution*, 12(2/3):191–216, 1999.

[29] Amit Kanudia and P. R. Shakula. Modelling of uncertainties and price elastic demands in energy-environment planning for India. *Omega*, 26(3):409–423, June 1998.

[30] Harry Kooijman and Ross Taylor. *The ChemSep book*. Libri Books on Demand, 2000.

[31] Richad Loulou and Amit Kanudia. The Kyoto protocol, inter-provincial cooperation, and energy trading: A systems analysis with integrated MARKAL models. *Energy Studies Review*, 9(1):1–23, 1999.

[32] Richard Loulou and Amit Kanudia. Minimax regret strategies for greenhouse gas abatement: methodology and application. *Operations Research Letters*, 25(5):219–230, December 1999.

[33] Richard Loulou, Amit Kanudia, and Denis Lavigne. GHG abatement in central Canada with inter-provincial cooperation. *Energy Studies Review*, 8(2):120–129, 1996.

[34] Haili Ma and S. M. Shahidehpour. Unit commitment with transmission security and voltage constraints. *IEEE Transactions on Power Systems*, 14(2):757–764, may 1999.

[35] Douglas MacDonald, Loretta MacDonald, Afshin Matin, Jackie Mercer, Mark McGovern, David Moore, Lindsay Pratt, and Emily West. National inventory report 19902011: Greenhouse gas sources and sinks in canada. Canadas 2013 unfccc submission, Environment Canada, Canada, 2013.

[36] Carl Mariz, Larry Ward, Garfiled Ganong, and Rob Hargrave. Cost of CO_2 recovery and transmission for EOR from boiler stack gas. In Pierce Riemer and Alexander Wokaun, editors, *Greenhouse Gas Control Technologies: Proceedings of the 4th International Conference on Greenhouse Gas Control Technologies*. Elsevier Science Ltd., April 1999.

[37] Federico Milano. *Power System Analysis Toolbox: Quick Reference Manual for PSAT version 2.1.2*, June 2008. `http://www.power.uwaterloo.ca/~fmilano/psat.htm`.

[38] B. A. Murtagh and M. A. Saunders. Minos 5.0 user's guide. Technical Report SOL 83-20, Department of Operations Research, Standford University, 1983.

[39] Aroonsri Nuchitprasittichai and Selen Cremaschi. Optimization of CO_2 capture process with aqueous amines using response surface methodology. *Computers and Chemical Engineering*, 35:1521–1531, 2011.

[40] J. Guillermo Ordorica-Garcia. Evaluation of combined-cycle power plants for CO_2 avoidance. Master's thesis, University of Waterloo, Waterloo, Ontario, Canada, 2003.

[41] Geradino A. Pete. *Electric Power Systems Manual*. McGray-Hill, Inc., U.S.A., 1992.

[42] Anand B. Rao and Edward S. Rubin. A technical, economic, and environmental assessment of amine-based CO_2 capture technology for power plant greehouse gas control. *Environmental Science and Technology*, 36(20):4467–4475, 2002.

[43] David J. Singh. Simulation of CO_2 capture strategies for an existing coal fired power plant - MEA scrubbing versus O_2/CO_2 recycle combustion. Master's thesis, University of Waterloo, 2001.

[44] F. T. Sparrow and Brian H. Bowen. *Modelling electricity trade in southern Africa: user manual for the long-term model*. Purdue Univeristy, seventh edition, February 2001.

[45] Simon Taylor. The ranking of negative-cost emissions reduction measures. *Energy Policy*, 48:430–438, 2012.

[46] Paitoon Tontiwachwuthikul, Christine Chan, Weerapong Kritpiphat, David DeMontigny, David Skoropad, Don Gelowitz, Adisorm Aroonwilas, Frank Mourits, Malcolm Wilson, and Larry Ward. Large scale carbon dioxide production from coal-fired power stations for enhanced oil recovery: a new economic feasibility study. *Journal of Canadian Petroleum Technology*, 37(11):48–55, November 1998.

[47] Ralph Turvery and Dennis Anderson. *Electricity Economics: Essays and Case Studies*, chapter 8, pages 184–200. The Johns Hopkin University Press, Baltimore, 1977. Electricity Development in Turkey: A Case Study Using Linear Programming.

[48] W. N. Venables and D. M. Smith. *An Introduction to R.* R Core Team, 2012. `http://cran.r-project.org/doc/manuals/r-release/R-intro.pdf`.

[49] S. J. Wang, S. M. Shahidehpour, D. S. Kirschen, S. Mokhtari, and G. D. Irisarri. Short-term generation scheduling with transmission and environmental constraints using an augmented Lagrangian relaxation. *IEEE Transactions of Power Systems*, 10(3):1294–1301, August 1995.

[50] J. B. Ward and H. W. Hale. Digital computer solution of power-flow problems. *Transactions of the American Institute of Electrical Engineers*, PAS-75:398–404, jun 1956.

[51] Allen J. Wood and Bruce F. Wollenberg. *Power generation, operation, and control*. Wiley & Sons, New York, second edition, 1996.

[52] Hisham Zerriffi, Hadi Dowlatabadi, and Alex Farrell. Incorporating stress in electric power systems reliability models. *Energy Policy*, 35:61–75, 2007.